frontiers | Research Topics

Space physiology and medicine: reports and unique data obtained on small sample sizes

Edited by
Marc-Antoine Custaud, Kunihiko Tanaka, Pooneh Bagher, Jack J. W. A. van Loon, Elena S. Tomilovskaya, Brandon Richard Macias, Olga Vinogradova, Martina Heer, Alan R. Hargens, Alexander Chouker and Alain Maillet

Published in
Frontiers in Physiology

ISSN 1664-8714
ISBN 978-2-8325-7240-5
DOI 10.3389/978-2-8325-7240-5

Generative AI statement
Any alternative text (Alt text) provided alongside figures in the articles in this ebook has been generated by Frontiers with the support of artificial intelligence and reasonable efforts have been made to ensure accuracy, including review by the authors wherever possible. If you identify any issues, please contact us.

About Frontiers

Frontiers is more than just an open access publisher of scholarly articles: it is a pioneering approach to the world of academia, radically improving the way scholarly research is managed. The grand vision of Frontiers is a world where all people have an equal opportunity to seek, share and generate knowledge. Frontiers provides immediate and permanent online open access to all its publications, but this alone is not enough to realize our grand goals.

Frontiers journal series

The Frontiers journal series is a multi-tier and interdisciplinary set of open-access, online journals, promising a paradigm shift from the current review, selection and dissemination processes in academic publishing. All Frontiers journals are driven by researchers for researchers; therefore, they constitute a service to the scholarly community. At the same time, the *Frontiers journal series* operates on a revolutionary invention, the tiered publishing system, initially addressing specific communities of scholars, and gradually climbing up to broader public understanding, thus serving the interests of the lay society, too.

Dedication to quality

Each Frontiers article is a landmark of the highest quality, thanks to genuinely collaborative interactions between authors and review editors, who include some of the world's best academicians. Research must be certified by peers before entering a stream of knowledge that may eventually reach the public - and shape society; therefore, Frontiers only applies the most rigorous and unbiased reviews. Frontiers revolutionizes research publishing by freely delivering the most outstanding research, evaluated with no bias from both the academic and social point of view. By applying the most advanced information technologies, Frontiers is catapulting scholarly publishing into a new generation.

What are Frontiers Research Topics?

Frontiers Research Topics are very popular trademarks of the *Frontiers journals series*: they are collections of at least ten articles, all centered on a particular subject. With their unique mix of varied contributions from Original Research to Review Articles, Frontiers Research Topics unify the most influential researchers, the latest key findings and historical advances in a hot research area.

Find out more on how to host your own Frontiers Research Topic or contribute to one as an author by contacting the Frontiers editorial office: frontiersin.org/about/contact

Space physiology and medicine: reports and unique data obtained on small sample sizes

Topic editors

Marc-Antoine Custaud — Université d'Angers, France
Kunihiko Tanaka — Gifu University of Medical Science, Japan
Pooneh Bagher — University of Nebraska Medical Center, United States
Jack J. W. A. van Loon — VU Amsterdam, Netherlands
Elena S. Tomilovskaya — Institute of Biomedical Problems, Russian Academy of Sciences (RAS), Russia
Brandon Richard Macias — KBRwyle, United States
Olga Vinogradova — Institute of Biomedical Problems, Russian Academy of Sciences (RAS), Russia
Martina Heer — International University of Applied Sciences Bad Honnef, Germany
Alan R. Hargens — University of California, San Diego, United States
Alexander Chouker — LMU Munich University Hospital, Germany
Alain Maillet — MEDES-IMPS, France

Citation

Custaud, M.-A., Tanaka, K., Bagher, P., van Loon, J. J. W. A., Tomilovskaya, E. S., Macias, B. R., Vinogradova, O., Heer, M., Hargens, A. R., Chouker, A., Maillet, A., eds. (2025). *Space physiology and medicine: reports and unique data obtained on small sample sizes*. Lausanne: Frontiers Media SA. doi: 10.3389/978-2-8325-7240-5

Table of contents

frontiers | Frontiers in Physiology

TYPE Original Research
PUBLISHED 21 November 2023
DOI 10.3389/fphys.2023.1303938

OPEN ACCESS

EDITED BY
Alain Maillet,
MEDES-IMPS, France

REVIEWED BY
Gianfranco Bosco,
University of Rome Tor Vergata, Italy
Marc-Antoine Custaud,
Université d'Angers, France

*CORRESPONDENCE
Gilles Clément,
gilles.r.clement@nasa.gov

RECEIVED 28 September 2023
ACCEPTED 06 November 2023
PUBLISHED 21 November 2023

CITATION
Clément G, Macaulay TR, Moudy SC, Kuldavletova O and Wood SJ (2023), Back to the future—revisiting Skylab data on ocular counter-rolling and motion sickness.
Front. Physiol. 14:1303938.
doi: 10.3389/fphys.2023.1303938

Back to the future—revisiting Skylab data on ocular counter-rolling and motion sickness

Gilles Clément[1]*, Timothy R. Macaulay[1], Sarah C. Moudy[2], Olga Kuldavletova[3] and Scott J. Wood[4]

[1]KBR, Houston, TX, United States, [2]Aegis Aerospace, Houston, TX, United States, [3]INSERM U1075 COMETE, University of Caen Normandy, Caen, France, [4]Neuroscience Laboratory, NASA Johnson Space Center, Houston, TX, United States

In the early 1970s, nine astronauts participated in missions to the Skylab space station. During two preflight testing sessions at the Naval Aerospace Medical Research Laboratory in Pensacola, the amplitudes of their ocular counter-rolling (OCR) during body tilts were assessed to determine if their vestibular functions were within normal ranges. We recently re-evaluated this data to determine asymmetry of each astronaut's OCR response and their OCR slope from sigmoid fits during static leftward and rightward body tilts, which we then compared with their Coriolis sickness susceptibility index (CSSI) on the ground, their motion sickness symptom scores during 0 g maneuvers in parabolic flight, and the severity of the symptoms of space motion sickness (SMS) they reported during their spaceflights. We arranged the astronauts in rank order for SMS severity based on the SMS symptoms they reported during spaceflight and the amount of anti-motion sickness medication they used. As previously reported, the OCR amplitudes of these astronauts were within the normal range. We determined that the OCR amplitudes were not correlated with SMS severity ranking, CSSI, or motion sickness symptoms experienced during parabolic flight. Indices of asymmetry in the OCR reflex were generally small and poorly correlated with SMS scores; however, the only subject with a high index of asymmetry also ranked highly for SMS. Although OCR slope, CSSI, and motion sickness symptoms induced during parabolic flight were each only moderately correlated with SMS severity ranking (rho = 0.41–0.44), a combined index that included all three parameters with equal weighting was significantly correlated with SMS severity ranking (rho = 0.71, p = 0.015). These results demonstrate the challenge of predicting an individual's susceptibility to SMS by measuring a single test parameter in a terrestrial environment and from a limited sample size.

KEYWORDS

space motion sickness, ocular counter-rolling, Coriolis sickness, parabolic flight, asymmetry

Introduction

May 2023 marked the 50th anniversary of the first crewed Skylab mission (Skylab-2), which lasted 28 days (from 25 May 1973, to 22 June 1973). The second Skylab mission (Skylab-3) lasted 56 days (from 28 July 1973, to 25 September 1973), and the third (Skylab-4) lasted 84 days (from 16 November 1973, to 8 February 1974). Nine astronauts participated in

these missions, three per mission. Medical experiments were performed on these Skylab astronauts before, during, and after their missions to assess physiological responses of exposure to weightlessness, whereas crewmembers of the previous Apollo and Gemini mission were assessed only before and after their missions (Johnston, 1977).

Dr. Ashton Graybiel and his colleagues from the Naval Aerospace Medical Research Laboratory (NAMRL) in Pensacola, FL conducted an extensive investigation of each Skylab astronaut's vestibular system. In the so-called *Experiment M-131–Human Vestibular Function*, a rotating chair was used to study their vestibular function and their susceptibility to motion sickness on board Skylab (Miller and Graybiel, 1973; Graybiel et al., 1977; Lackner and DiZio, 2006). The preflight tests included a measure of ocular counter-rolling (OCR) during static body tilt to the right and the left to assess the sensitivity of the otolith organs' response to linear acceleration (Diamond and Markham, 1989). The Coriolis sickness susceptibility index (CSSI) test was also performed before flight. CSSI is calculated from the number of head movements in four cardinal directions the astronauts were able to complete while they were rotating in a chair at increasing velocity until they developed motion sickness (Miller and Graybiel, 1974). Each crewmember also reported motion sickness symptoms they experienced during 0 g parabolic maneuvers and reported the symptoms and the anti-motion sickness medications they took during different phases of the Skylab missions (Graybiel et al., 1975; Graybiel et al., 1977). Our retrospective analysis used the original OCR data set, which was recently identified in the archives of Drs. Jerry Homick and Millard Reschke at the NASA Johnson Space Center.

Structural differences in the right and left otolith organs can lead to slightly different sensitivities to vestibular sensing. Normal, healthy individuals in a 1 g gravitational environment use central processes to compensate for this naturally occurring peripheral vestibular asymmetry. Some authors have suggested that bilateral asymmetry in OCR is associated with susceptibility to motion sickness (Von Baumgarten and Thumler, 1979; Lackner et al., 1987; Markham and Diamond, 1993; Nooij et al., 2011; Sugawara et al., 2021). A recent study using inner ear magnetic resonance imaging determined that individuals who were highly susceptibility to motion sickness had larger morphological asymmetry of the bilateral vestibular organs (Harada et al., 2021).

Lackner et al. (1987) examined asymmetric otolith function in healthy subjects using the same device that was used in the Skylab studies (Figure 1) to determine if OCR asymmetry is associated with increased susceptibility to motion sickness during exposure to various levels of gravito-inertial acceleration. The average indices of OCR asymmetry in the highly susceptible group (42 of 71 subjects) were approximately twice that of the low and the moderate susceptible groups. Although the indices of OCR asymmetry did not predict susceptibility in all cases, this study suggested that otolith asymmetries for some individuals, which manifest as OCR during static roll tilt testing in 1g, may be associated with susceptibility to motion sickness in altered gravito-inertial environments. Therefore, we conducted this retrospective analysis to determine whether correlations existed between the Skylab astronauts' preflight OCR asymmetry during leftward and rightwards body tilts and the severity of their space motion sickness (SMS) symptoms during flight. A secondary objective was to examine how the new OCR parameters derived from a sigmoidal fit to the OCR data relate to other preflight susceptibility tests described above (CSSI and motion sickness symptoms during parabolic flight), and how these parameters relate to the SMS severity.

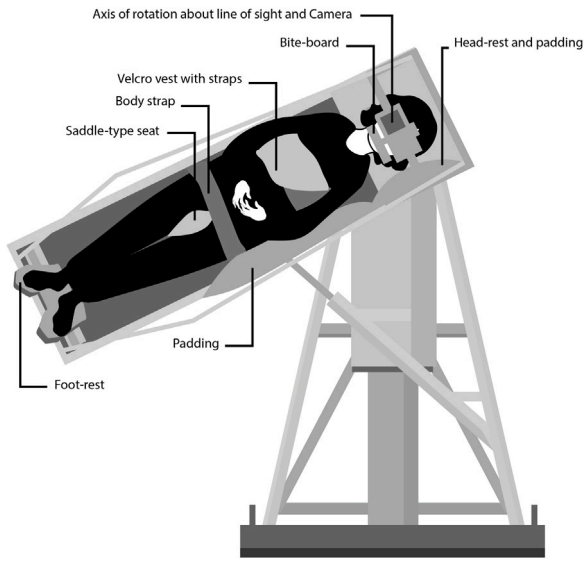

FIGURE 1
Diagram showing the counter-rolling test device at the Naval Aerospace Medical Research Laboratory in Pensacola, FL. The subjects were tilted up to 64 deg to the side around an axis that was aligned with their right or left eye. A camera placed on a platform in front of the subject's face took photographs of the eye for offline measurements of ocular counter-rolling. Credit: Olga Kuldavletova [adapted from Miller and Graybiel (1972)].

Methods

Participants

The nine Skylab astronauts were all male, aged 41.3 ± 2.0 years (mean ± SD), who were selected through extensive screening procedures (Santy, 1994). Seven of the astronauts flew for the first time on their Skylab mission, two astronauts had participated in a previous Apollo mission that included a Moon landing, and one of these two astronauts had also participated in a Gemini mission. Individual characteristics of the nine Skylab astronauts were reported in Johnson and Dietlein (1977).

All the Skylab astronauts elected to participate in *Experiment M-131—Human Vestibular Function*. This experiment was performed, like all the other medical experiments on board Skylab, in accordance with the ethical standards established by the 1964 Declaration of Helsinki. All subjects provided written, informed consent before participating in the study (Johnston, 1977).

Experimental protocol

The aim of the Skylab M-131 experiment was to measure vestibular responses in astronauts while they were weightless

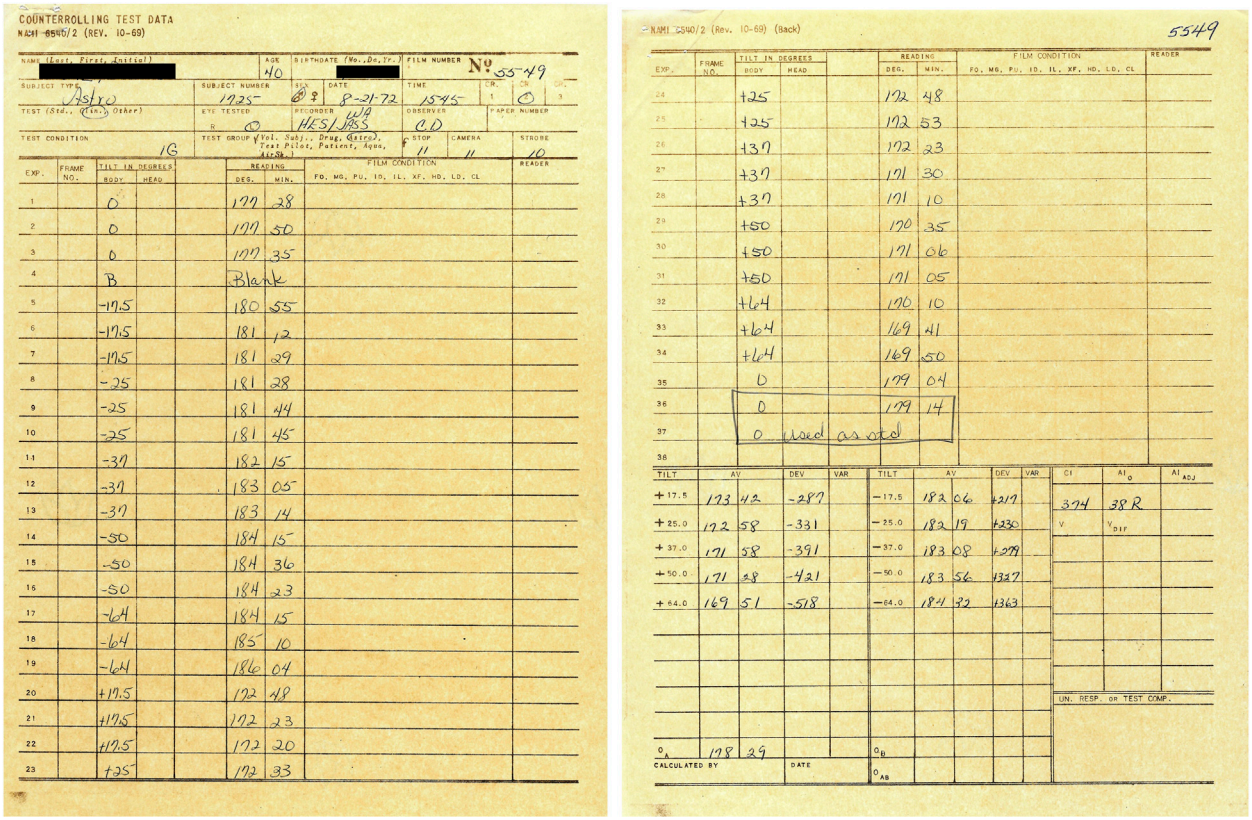

FIGURE 2
Example of worksheet used during collection of the ocular counter-rolling test data at the Naval Aerospace Medical Research Laboratory. The name and date of birth of the astronaut-subject have been masked.

during orbital flight and to compare these responses to measurements taken before and after flight. The parts of the M-131 experiment that related to susceptibility to motion sickness included a) evaluating the astronaut's susceptibility to a variety of motion sickness stressors, including maneuvers during 0 g in parabolic flight and Coriolis, cross-coupled angular accelerations during pitch and roll head movements while being rotated about an Earth-vertical axis; b) measuring the amplitude of OCR during static body tilt in roll relative to gravity; and c) grading the severity of SMS using diagnostic criteria (Miller and Graybiel, 1973; Graybiel et al., 1977).

Preflight functional tests of the astronauts' vestibular organs using caloric nystagmus and head rotation stimuli revealed no abnormalities. A postural equilibrium test that required the astronauts to maintain postural equilibrium on narrow metal rails with their eyes open or closed indicated that their responses were within the normal range (Homick and Reschke, 1977). Other than the activities indicated above, none of the Skylab astronauts underwent a specific vestibular training or vestibular desensitization program.

During tests to grade the astronauts' susceptibility to motion sickness on Earth, the astronauts sat in a chair that rotated at angular velocities up to 30 rpm and were asked to execute 90-deg head movements (front, back, left, and right). The CSSI was then determined for each subject by multiplying an E-factor related to the rotation velocity and the number of head movements required to provoke a severe malaise (Miller and Graybiel, 1970). CSSI scores above 15 are generally considered to be in the low susceptibility range (Miller and Graybiel, 1974). The severity of motion sickness symptoms during 0 g parabolic maneuvers were also reported (Graybiel et al., 1977). Symptoms category included nausea, epigastric discomfort, skin color, cold sweating, increased salivation, drowsiness, and headache (Graybiel et al., 1968).

OCR was evaluated at the NAMRL from August 1972 to April 1973. Subjects assumed a semi-standing position in the counter-rolling test device, with their weight distributed between a saddle-type seat arrangement and an adjustable foot-rest platform (Figure 1). Their heads were maintained in place using a locked headrest and bite-board assembly. A camera recording system was placed on a platform in front of their face. The subjects were shifted sideways until the center of the pupil of their right or left eye was aligned with the optic axis of the camera and the rotation axis of the test device. Subjects were tilted 17.5, 25, 39, 50, and 64 deg from upright, alternately to the right and to the left (Miller, 1962). No OCR measurements were performed post-flight.

Four trials were performed during two sessions. During the first session, either the right or the left eye was recorded during body tilt to the right and to the left. The other eye was tested the following day. An example of the datasheet used during one session is shown in Figure 2. Three photographs of the eye were taken at each body tilt angle for subsequent analysis of eye position based on natural iris landmarks. The recorded positions of the eye roll during the initial

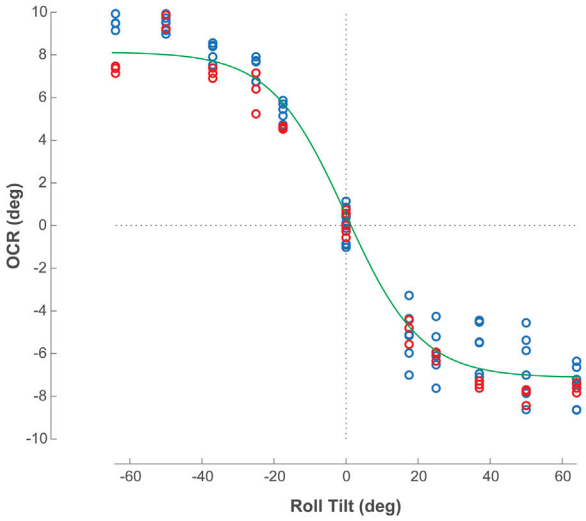

FIGURE 3
Amplitude of ocular counter-rolling (OCR) of a typical Skylab astronaut during actual body tilts to the right and to the left. Body tilt to the right (positive values) generated a counterrotation of the eye to the left (negative values). Multiple measurements of OCR were taken for each eye at each body tilt position. Red symbols: measures of OCR of the right eye; blue symbols: measures of OCR of the left eye. Source: Naval Aerospace Medical Research Laboratory, Pensacola, FL. The sigmoidal curve fit (green line) using all OCR values was based on a three-parameter model to obtain leftward and rightward OCR and the slope around the upright orientation (Roll Tilt = 0°).

and the terminal upright body positions were used as the baseline (zero) position to which all other OCR measurements were related (Miller, 1962). Because the OCR of the right and the left eye were assessed on separate days, it was not possible to measure ocular torsional disconjugacy, which appears to be associated with a history of SMS (Markham and Diamond, 1993).

OCR index was previously calculated by Graybiel et al. (1977) as half the maximum eye roll amplitude when tilted right and left. However, this measure does not account for the variations in OCR amplitude across various roll tilt angles nor the sensitivity of the reflex to tilts near the upright orientation. Using the original OCR data collected at the NAMRL, we calculated OCR parameters in each astronaut. Data obtained from trials of each eye at all angles of roll tilt were combined and fit with a sigmoid function in MATLAB (version R2022b, The MathWorks, Inc.) using three free parameters: maximum OCR during rightward tilt, maximum OCR during leftward tilt, and slope at the zero crossing (i.e., OCR slope, see sample in Figure 3). Similar to the method used by Lackner et al. (1987), the otolith asymmetry ratio was then computed by taking the ratio of the larger to the smaller ocular counter-rolling responses for left tilts and right tilts, subtracting 1, and then multiplying by 100.

The occurrence and frequency of SMS the Skylab astronauts experienced and their use of medication to counter the symptoms of SMS have been previously reported (Graybiel et al., 1975; 1977). Studies have commonly reported high degrees of inter-subject variability in SMS (Davis et al., 1988; Reschke et al., 2017). To examine how the preflight motion sickness susceptibility and OCR indices related to SMS data in this limited sample set, we rank ordered the astronauts according to SMS susceptibility based on the sum of symptom points reported by Graybiel et al. (1977) across mission phases (before docking, after docking, and during flight days 1–3). If astronauts had the same number of symptom points, the number of SMS medications they took were used to assign the ranking. Relationships between the various parameters were analyzed using non-parameter Spearman rank correlation (SPSS Statistics, v29, IBM Corp.).

Results

The nine Skylab astronauts' preflight CSSI, OCR indices, and symptom scores during 0 g parabolic flight have been previously published by Graybiel et al. (1977) and are shown in Table 1. Six of the astronauts had CSSI scores that indicated low susceptibility: five had scores in the top 80% of normal responses, and one (Subject H) had scores in the top 90% (Miller and Graybiel, 1974). Symptoms reported during 0 g maneuvers in parabolic flight ranged between 2 and 16, again most of this cohort were in the low susceptibility range.

As previously reported (Graybiel et al., 1975; Graybiel et al., 1977), none of the Skylab-2 crewmembers experienced SMS. Astronaut E of the Skylab-3 crew experienced motion sickness within an hour of transition into orbit (before and after docking). All three Skylab-3 astronauts experienced motion sickness during the first 3 days of spaceflight. These astronauts obtained relief by avoiding head and body movements and by a using a combination of Scopolamine (0.35 mg) and Dexedrine (5.0 mg). All three astronauts of the Slylab-4 crew took prophylactic medication before entering the Skylab station and continued to do so on flight days 2 and 3. This medication included a combination of Scopolamine (0.35 mg) and Dexedrine (5.0 mg) or a combination of Promethazine (25 mg) and Ephedrine (50 mg). Astronaut I did not get sick while on board, whereas the other two Skylab-4 astronauts got moderately sick during the first 3 days of spaceflight (Table 1). On and after the sixth day of spaceflight none of all nine astronauts experienced SMS, including when moving their head while on the Skylab rotating chair that generated Coriolis, cross-coupled angular accelerations (Graybiel et al., 1977).

The amplitudes of the OCR in the nine Skylab astronauts were clearly related to the angle of head tilt (i.e., the magnitude of the acceleration vector in the plane of the utricles) and the amplitude of the eye torsional movement. The amplitude of this otolith-mediated eye movement was approximately 10% of the maximum head tilt (Figure 3). Previous tests conducted in 550 normal subjects reported a mean OCR index of 5.73 deg (Graybiel, 1970). Six of the Skylab astronauts (A, C, E, F, H, I) had OCR index values that were lower than normal. However, five of the Skylab astronauts (C, D, E, G, H) had higher OCR amplitudes when tilted to the right, whereas four of the Skylab astronauts (A, B, F, I) had higher OCR amplitudes when tilted to the left (Figure 3; Table 1).

The new OCR parameters from the sigmoidal fits include the amplitude in each direction and its slope around the upright orientation. The average amplitude from the sigmoidal fits were significantly correlated with the OCR index previously reported by Graybiel et al. (1977) (rho = 0.945, $p < 0.001$). Therefore, we only included the original OCR index in this analysis. As described above,

TABLE 1 Values for Coriolis sickness susceptibility index (CSSI), motion sickness symptoms during 0 g maneuvers in parabolic flight, ocular counter-rolling (OCR) index, OCR asymmetry, OCR slope and space motion sickness (SMS) for the 9 Skylab astronauts (A-I).

		Skylab-2			Skylab-3			Skylab-4		
		A	B	C	D	E	F	G	H	I
CSSI[a]		10.2	19.8	8.2	23.1	19.2	26.4	7.5	52.8	8.9
Parabolic 0 g symptoms[a]		4	2	4	15	4	4	16	8	8
OCR Index (deg)[a]		2.63	6.23	5.00	6.08	5.53	2.63	8.23	4.23	4.35
OCR Asymmetry		13.9	25.4	15.0	21.1	54.0	17.5	9.5	4.5	19.5
OCR Slope (from sigmoid fit)		0.034	0.025	0.033	0.028	0.027	0.035	0.034	0.048	0.016
SMS Symptoms[a]	Predock	0	0	0	0	1	0	1	3	0
	Postdock	0	0	0	0	1	0	1	2	0
	FD1	0	0	0	2	3	3	0	1	0
	FD2	0	0	0	2	1	2	1	1	0
	FD3	0	0	0	0	1	1	1	1	0
SMS Medication[a]	Predock	0	0	1				2	2	2
	Postdock	0	0					3	3	3
	FD1	0	0							
	FD2	0	0		2	2	2	3	2	3
	FD3	0	0			3		1	2	1
SMS Rank		1	1	3	5	8	7	6	9	4

Predock: inside the Apollo module before docking with Skylab; Postdock: inside the Apollo module after docking with Skylab. FD = flight day in Skylab; SMS Symptoms: 1 = slight, 2 = moderate, 3 = severe. The values in the SMS medication rows represent the number of anti-motion sickness medication taken by each astronaut.
[a]Shaded cells indicate original data published in Graybiel et al. (1977).

the OCR amplitudes in the left and the right eye from the sigmoidal fits were used to calculate OCR asymmetry using the same convention used by Lackner et al. (1987). Interestingly, OCR asymmetry was negatively correlated with OCR slope from the sigmoidal fits (rho = −0.77, p = 0.008). The OCR asymmetry measures were small and not significantly correlated with any of the measures of motion sickness susceptibility. Eight of the 9 astronauts had OCR asymmetries ≤25, consistent with the low susceptibility groups reported by Lackner et al. (1987). The only Skylab astronaut with an OCR asymmetry consistent with the high susceptibility group also had a high SMS rank (8 of 9). The OCR slope from the sigmoidal fit was moderately correlated with SMS ranking (Figure 4A, rho = 0.41, p = 0.14).

The correlations between SMS ranking and motion sickness symptoms during 0 g in parabolic flight or CSSI were also moderate but non-significant (Figures 4B, C; Table 2). Given the OCR slope, motion sickness symptoms during 0 g parabolic flight, and CSSI scores were moderately but not significantly correlated with SMS rank, each of these variables were then transformed using a two-step approach described by Templeton (2011). This process involved 1) fractional ranking of each variable, and 2) transformation using an inverse distribution function with a normalized mean and standard deviation so that the three parameters (OCR slope, CSSI, and motion sickness symptoms during parabolic flight) could be averaged to compute a composite motion sickness index. The resulting motion sickness index, which comprises the contributions of all three variables, significantly correlated with SMS ranking (Figure 4D; Table 2, rho = 0.72, p = 0.015).

Discussion

This reanalysis of the Skylab data allowed us to investigate relationships between OCR parameters measured during static roll tilt and other preflight susceptibility tests and the Skylab astronauts' SMS ranking. Given the limitations of the small sample size, caution should be exercised when interpreting these results. However, the inability to identify a significant association between SMS susceptibility and a single measure obtained in a terrestrial environment is consistent with the results of previous studies of larger cohorts (Reschke, 1990). As Lackner et al. (1987) pointed out, otolith asymmetry reflected by the static roll tilt may contribute to SMS but is likely not the only cause of SMS. A significant relationship to SMS ranking was only found after combining the OCR slope, CSSI scores, and motion sickness symptoms induced by parabolic flight, which presumably represent a multitude of contributing factors.

It is important to point out that an association between SMS and otolith asymmetry cannot be ruled out completely because underlying otolith asymmetry that is centrally compensated for in terrestrial conditions (Von Baumgarten and Thumler, 1979) might not be detected during static roll tilt in 1 g. Markham and

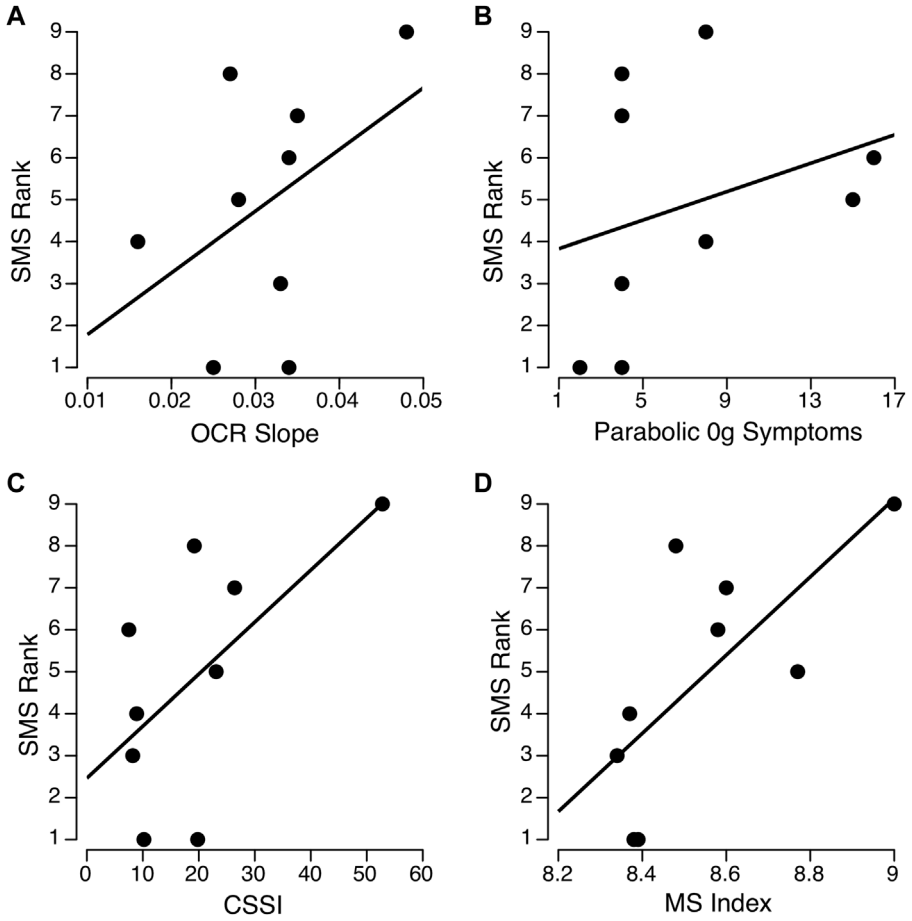

FIGURE 4
Relationships between ocular counter-rolling (OCR) slope **(A)** motion sickness symptoms during parabolic flight **(B)**, Coriolis sickness susceptibility index (CSSI) **(C)**, and composite motion sickness (MS) index **(D)** with Space Motion Sickness (SMS) ranking for the nine Skylab astronauts. The parabolic and CSSI scores were obtained from Graybiel et al. (1977). Spearman's rho was between 0.41 and 0.44 across the three separate measures **(A–C)** and 0.71 (p = 0.015) for the composite MS index **(D)**.

Diamond (1993) reported that ocular torsional disconjugacy was related to motion sickness susceptibility, but only during exposure to altered gravito-inertial states during parabolic flight. Subjects who experienced motion sickness after altered g-exposure from sustained centrifugation on Earth, i.e., after a transition from 3 g to 1g, were more likely to experience SMS (Nooij et al., 2007). However, the authors noted that subjects who are susceptible to motion sickness during centrifugation had only a marginally higher degree of OCR asymmetry than subjects who were not susceptible (Nooij et al., 2011). Consistent with our composite motion sickness index, a combination of utricular and semicircular canal parameters better predicted the subjects who are susceptible motion sickness during centrifugation.

OCR is considered to reflect mainly utricular responses to interaural acceleration accompanied with lateral head tilt (Clarke et al., 2003; Otero-Milan et al., 2017). One limitation of the OCR test during body tilt is that it is a bilateral otolith stimulation, i.e., the gravitational acceleration stimulus is equivalent for both the right and left otolith organs. At present the best practical approaches for testing unilateral otolith function are measuring OCR during unilateral centrifugation (Clarke et al., 2003; Wuyts et al., 2003), assessing ocular vestibular evoked myogenic potentials (VEMP) to test utricular function, and measuring cervical VEMP as an indicator of saccule function (Manzari et al., 2012).

Evidence indicates that OCR during static body tilt or lateral centrifugation decreases after spaceflight, particularly after long-duration space missions (Hallgren et al., 2016; Reschke et al., 2018; Schoenmaeker et al., 2022). Six of the Skylab astronauts' preflight OCR amplitudes were lower than of the normal population. The low OCR amplitudes and OCR asymmetry values limited our ability to find and an association between the M-131 data and the SMS ranking.

If central asymmetry in otolith function is unmasked by exposure to weightlessness, then asymmetry may be detected after flight. Clarke and Schonfeld (2015) showed that OCR asymmetry, subjective visual vertical during unilateral centrifugation, and cervical VEMP (which reflects saccular function) increased after spaceflight relative to preflight baseline values and returned to baseline levels within 10 days. On landing day, the response from one vestibular labyrinth was equivalent to preflight values, whereas the other labyrinth had considerable discrepancy. Unfortunately, the OCR test during body tilt used in

TABLE 2 Results of the non-parametric correlation analysis (* indicates $p < 0.05$).

		OCR index	OCR asym	OCR slope	CSSI	Parabolic	MS index
OCR index	rho						
	sig (1-tail)						
OCR asym	rho	0.32					
	sig (1-tail)	0.20					
OCR slope	rho	−0.51	−0.77 *				
	sig (1-tail)	0.08	0.008				
CSSI	rho	−0.37	0.05	0.37			
	sig (1-tail)	0.17	0.45	0.17			
Parabolic	rho	0.26	−0.42	0.15	−0.16		
	sig (1-tail)	0.25	0.13	0.35	0.34		
SMS rank	rho	−0.09	−0.16	0.41	0.44	0.41	0.71 *
	sig (1-tail)	0.41	0.34	0.14	0.12	0.14	0.015

The light shaded areas are plotted in Figure 4.
OCR, ocular counter-rolling; asym: asymmetry; CSSI, Coriolis sickness susceptibility index; SMS, space motion sickness; Parabolic, motion sickness symptoms during 0 g maneuvers in parabolic flight.

the Skylab M-131 experiment cannot discriminate such asymmetry between the vestibular organs.

Although Lackner et al. (1987) cautioned that OCR asymmetry was insufficient to predict an individual's susceptibility to motion sickness during parabolic flight, they demonstrated group mean differences in OCR asymmetries could predict motion sickness. Previous attempts to predict an individual's SMS from their preflight susceptibility to motion sickness have also been elusive, although group differences suggest some relationships. For example, Homick et al. (1987) found that 67% of SMS susceptible crewmembers had CSSI scores below the mean (i.e., were more susceptible to CSSI) whereas only 40% of non-susceptible crewmembers were below the mean. The authors concluded that a single ground-based test parameter or procedure was inadequate to predict SMS susceptibility and recommended the use of a composite or weighted score. The association between SMS ranking and our Spearman correlation rho values for OCR slope, CSSI, or motion sickness symptoms during parabolic flight were greater than 0.4 but were non-significant. However, the composite motion sickness index that averaged the three parameters did result in a significant association to SMS rank in this limited sample set.

OCR is an important measure of otolith utricular function. It is possible, however, that asymmetry in saccular responses is more closely associated with motion sickness susceptibility than is asymmetry in utricular responses. After assessing both ocular VEMP (which reflects utricular function) and cervical VEMP (which reflects saccular function), Singh et al. (2014) reported that individual susceptibility to motion sickness is associated not only with asymmetry of utricular functional but also with asymmetry of saccular functional.

Because OCR gain is very low, it is inadequate to compensate for head tilt. By contrast the modulation of neck, trunk, and muscle musculature by the otolith-spinal pathways is very important for postural control. Lackner and Dizio (2006) suggested that individuals could centrally compensate for asymmetric OCR using these otolith-spinal pathways. Central compensatory effects could also occur in individuals with unbalanced peripheral inputs from the otolith organs, which could be due to differences in otoconial mass between the paired otolith organs.

Given that a combination of many motion types can cause motion sickness in real-life situations, predicting susceptibility to motion sickness from laboratory experiments has some limitations. SMS remains a persistent problem during spaceflight missions, both when astronauts enter the weightless environment and when they return to Earth after long-duration missions. The Skylab M-131 experiment clearly showed that astronauts were no longer susceptible to motion sickness when exposed to Coriolis, cross-coupling stimulation on or after the sixth day of their spaceflight. On return to Earth, they were less susceptible to this type of stimulation than they were before flight and remained so for several weeks (Lackner and Dizio, 2006). Therefore, further research is needed to better understand motion sickness susceptibility and vestibular adaptation.

Data availability statement

The original contributions presented in the study are included in the article/supplementary materials, further inquiries can be directed to the corresponding author.

Ethics statement

The studies involving humans were approved by NASA Institutional Review Board. The studies were conducted in accordance with the local legislation and institutional

requirements. The participants provided their written informed consent to participate in this study.

Author contributions

GC: Conceptualization, Formal Analysis, Investigation, Methodology, Writing–original draft, Writing–review and editing. TM: Conceptualization, Formal Analysis, Methodology, Writing–review and editing. SM: Conceptualization, Formal Analysis, Methodology, Writing–review and editing. OK: Conceptualization, Formal Analysis, Methodology, Writing–review and editing. SW: Conceptualization, Formal Analysis, Funding acquisition, Methodology, Resources, Writing–review and editing, Investigation.

Funding

The authors declare financial support was received for the research, authorship, and/or publication of this article. The National Aeronautics and Space Administration (NASA) provided funding for this study.

Acknowledgments

The authors thank Kerry George and Yiri De Dios for editing the manuscript.

Conflict of interest

Authors GC and TM were employed by the company KBR. Author SM was employed by the company Aegis Aerospace.

The remaining authors declare that the research was conducted in the absence of any commercial or financial relationships that could be construed as a potential conflict of interest.

Publisher's note

References

Clarke, A., Schönfeld, U., and Helling, K. (2003). Unilateral examination of utricle and saccule function. *J. Vestib. Res.* 13, 215–225. doi:10.3233/VES-2003-134-606

Clarke, A. H., and Schonfeld, U. (2015). Modification of unilateral otolith responses following spaceflight. *Exp. Brain Res.* 233 (12), 3613–3624. doi:10.1007/s00221-015-4428-0

Davis, J. R., Vanderploeg, J. M., Santy, P. A., Jennings, R. T., and Stewart, D. F. (1988). Space motion sickness during 24 flights of the space shuttle. *Aviat. Space Environ. Med.* 59 (12), 1185–1189.

Diamond, S. G., and Markham, C. H. (1989). Ocular counter-rolling as a test of otolith function. *Acta. Otolaryngol. Suppl.* 468, 267–270. doi:10.3109/00016488909139059

Graybiel, A. (1970). Susceptibility to acute motion sickness in blind persons. *Aerosp. Med.* 44, 593–608.

Graybiel, A., Miller, E. F., II, and Homick, J. L. (1975). Individual differences in susceptibility to motion sickness among six Skylab astronauts. *Acta. Astronaut.* 2, 155–174. doi:10.1016/0094-5765(75)90051-x

Graybiel, A., Miller, E. F., and Homick, J. L. (1977). "Experiment M131: human vestibular function," in *Biomedical results from Skylab*. Editors R. S. Johnston and L. F. Dietlein (NASA: Washington DC: NASA SP-377), 74–103.

Graybiel, A., Woods, C., Miller, E., and Kramer, D. (1968). Diagnostic criteria for grading the severity of acute motion sickness. *Aerosp. Med.* 39, 453–455.

Hallgren, E., Kornilova, L., Fransen, E., Glukhikh, D., Moore, S. T., Clément, G., et al. (2016). Decreased otolith-mediated vestibular response in 25 astronauts induced by long-duration spaceflight. *J. Neurophysiol.* 115 (6), 3045–3051. doi:10.1152/jn.00065.2016

Harada, T., Sugawara, T., Ito, T., Wada, Y., Fukunaga, M., Sadato, N., et al. (2021). Vestibular morphological asymmetry associated with motion sickness susceptibility. *Front. Neurosci.* 15, 763040. doi:10.3389/fnins.2021.763040

Homick, J. L., and Reschke, M. F. (1977). Postural equilibrium following exposure to weightless space flight. *Acta. Otolaryngol.* 83 (5–6), 455–464. doi:10.3109/00016487709128871

Homick, J. L., Reschke, M. F., and Vanderploeg, J. M. (1987). "Prediction of susceptibility to space motion sickness," in *Results of the life sciences DSOs conducted aboard the space shuttle 1981-1986*. Editors M. W. Bungo, T. M. Bagian, M. A. Bowman, and B. M. Levitan (Houston: NASA TM 58280), 153–158.

Johnston, R. S. (1977). "Skylab medial program overview," in *Biomedical results from Skylab*. Editors R. S. Johnston and L. F. Dietlein (NASA: Washington DC: NASA SP-377), 3–19.

Johnston, R. S., and Dietlein, L. F. (1977). *Biomedical results from Skylab*. Washington DC: NASA-SP 377, NASA. Available at: https://ntrs.nasa.gov/citations/19770026836.

Lackner, J. R., and Dizio, P. (2006). Space motion sickness. *Exp. Brain Res.* 175, 377–399. doi:10.1007/s00221-006-0697-y

Lackner, J. R., Graybiel, A., Johnson, W. H., and Money, K. E. (1987). Asymmetric otolith function and increased susceptibility to motion sickness during exposure to variations in gravitoinertial acceleration level. *Aviat. Space Environ. Med.* 58, 652–657.

Manzari, L., Burgess, A. M., and Curthoys, I. S. (2012). Ocular and cervical vestibular evoked myogenic potentials in response to bone-conducted vibration in patients with probable inferior vestibular neuritis. *J. Laryngol. Otol.* 126 (7), 683–691. doi:10.1017/S0022215112000692

Markham, C. H., and Diamond, S. G. (1993). A predictive test for space motion sickness. *J. Vestib. Res.* 3, 289–295. doi:10.3233/VES-1993-3309

Miller, E. F., and Graybiel, A. (1973). Experimental M-131--human vestibular function. *Aerosp. Med.* 44, 593–608.

Miller, E. F., II. (1962). Counterrolling of the human eyes produced by head tilt with respect to gravity. *Acta. Otolaryngol. Stockh.* 54, 479–501. doi:10.3109/00016486209126967

Miller, E. F., II, and Graybiel, A. (1970). A provocative test for grading susceptibility to motion sickness yielding a single numerical score. *Acta. Otolaryngol. Stockh.* 274, 1–20.

Miller, E. F., II, and Graybiel, A. (1972). *Ocular counterrolling measured during eight hours of sustained body tilt*. Pensacola, FL: Naval Aerospace Medical Research Laboratory.

Miller, E. F., II, and Graybiel, A. (1974). Comparison of five levels of motion sickness severity as the basis for grading susceptibility. *Aerosp. Med.* 45, 602–609.

Nooij, S., Vanspauwen, R., Bos, J., and Wuyts, F. (2011). A re-investigation of the role of utricular asymmetries in space motion sickness. *J. Vestib. Res.* 21, 141–151. doi:10.3233/VES-2011-0400

Nooij, S. A., Bos, J., Groen, E., Bles, W., and Ockels, W. (2007). Space sickness on earth. *Microgravity Sci. Technol.* 19, 113–117. doi:10.1007/bf02919464

Otero-Millan, J., Trevino, C., Winnick, A., Zee, D. S., Carey, J. P., and Kheradmand, A. (2017). The video ocular counter-roll (vOCR): a clinical test to detect loss of otolith-ocular function. *Acta. Otolaryngol.* 137, 593–597. doi:10.1080/00016489.2016.1269364

Reschke, M. F. (1990). "Statistical prediction of space motion sickness," in *Motion and space motion sickness*. Editor G. H. Crampton GH (Boca Raton: CRC Press), 263–315.

Reschke, M. F., Good, E. F., and Clément, G. (2017). Neurovestibular symptoms in astronauts immediately after *space shuttle* and *international space station* missions. *Otolaryngol. Head. Neck Surg.* 1, 1–8. doi:10.1177/2473974X17738767

Reschke, M. F., Wood, S. J., and Clément, G. (2018). Ocular counter rolling in astronauts after short- and long-duration spaceflight. *Sci. Rep.* 8, 7747. doi:10.1038/s41598-018-26159-0

Santy, P. A. (1994). *Choosing the right stuff: the psychological selection of astronauts and cosmonauts*. Praeger: Wesport CT.

Schoenmaeker, C., De Laet, C., Kornilova, L., Glukhikh, D., Moore, S., MacDougall, H., et al. (2022). Ocular counter-roll is less affected in experienced versus novice space crew after long-duration spaceflight. *npj Microgravity* 8, 27. doi:10.1038/s41526-022-00208-5

Singh, N. K., Pandey, P., and Mahesh, S. (2014). Assessment of otolith function using cervical and ocular vestibular evoked myogenic potentials in individuals with motion sickness. *Ergonomics* 57, 1907–1918. doi:10.1080/00140139.2014.952683

Sugawara, T., Wada, Y., Ito, T., and Sakai, H. (2021). Bilateral asymmetry in ocular counter-rolling reflex is associated with individual motion sickness susceptibility. *Front. Neurol.* 12, 759764. doi:10.3389/fneur.2021.759764

Templeton, G. F. (2011). A two-step approach for transforming continuous variables to normal: implications and recommendations for IS research. *Commun. Assoc. Inf. Syst.* 28, 4. doi:10.17705/1cais.02804

Von Baumgarten, R. J., and Thumler, R. (1979). A model for vestibular function in altered gravitational states. *Life Sci. Space Res.* 17, 161–170. doi:10.1016/b978-0-08-023416-8.50025-8

Wuyts, F. L., Hoppenbrouwers, M., Pauwels, G., and Van de Heyning, P. H. (2003). Utricular sensitivity and preponderance assessed by the unilateral centrifugation test. *J. Vestib. Res.* 13, 227–234. doi:10.3233/ves-2003-134-607

frontiers | Frontiers in Physiology

TYPE Data Report
PUBLISHED 01 December 2023
DOI 10.3389/fphys.2023.1285802

OPEN ACCESS

EDITED BY
Marc-Antoine Custaud,
Université d'Angers, France

REVIEWED BY
Jean-Luc Morel,
Centre National de la Recherche Scientifique (CNRS), France
Ronan Padraic Murphy,
Dublin City University, Ireland

*CORRESPONDENCE
O. V. Popova,
olya.popovaolga2710@yandex.ru

RECEIVED 30 August 2023
ACCEPTED 24 November 2023
PUBLISHED 01 December 2023

CITATION
Pastushkova LH, Goncharova AG, Rusanov VB, Nosovsky AM, Kashirina DN, Popova OV and Larina IM (2023), Correlation between proteome changes and synchrony of cardiac electrical excitation under 3-day «dry immersion» conditions.
Front. Physiol. 14:1285802.
doi: 10.3389/fphys.2023.1285802

Correlation between proteome changes and synchrony of cardiac electrical excitation under 3-day «dry immersion» conditions

L. H. Pastushkova, A. G. Goncharova, V. B. Rusanov, A. M. Nosovsky, D. N. Kashirina, O. V. Popova* and I. M. Larina

State Scientific Center of the Russian Federation, Institute of Medical and Biological Problems Russian Academy of Sciences, Moscow, Russia

KEYWORDS

proteome, cardiovascular system (CVS), protrombin, dry immersion, calmodulin

Introduction

Cardiac mechano-electrical feedback is the effect of cardiac muscle contraction on its electrical activity (Quinn et al., 2014). Mechano-electrical feedback is a contour of regulation of cardiac muscle function. Mechanical heterogeneity or mechanical ventricular dyssynchrony of the heart is accompanied by electrical remodeling and an increase in myocardial electrical heterogeneity (Kamkin and Iu, 2012; Jeyaraj et al., 2007). The magnitude of mechanical load on cardiac muscle significantly affects not only the nature of mechanical activity of cardiomyocytes, but also their electrical activity. The risk of heart rhythm disturbances development as a reflection of total processes of myocardial electrical excitation desynchronization in practically healthy subjects from the group of special contingent (cosmonauts, volunteer testers) makes the study of blood proteomic composition peculiarities relevant to regulation of myocardial repolarization and depolarization processes. The common prevalence of atrial fibrillation in active astronauts is ≈5%, similar to the general population but at a younger age. Risk factors for atrial fibrillation are left atrial enlargement, increased number of premature atrial complexes, and certain electrocardiogram parameters: P waveform duration, RMS voltage at the last 20 ms of the P waveform with signal averaging, and P waveform amplitud.

According to Khine H.W. et al. in thirty astronauts who flew in space missions of 6 months' duration, transient changes in the structure of the left atrium and changes in atrial electrophysiology, which increase the risk of atrial fibrillation, were detected. However, no definite signs of increased supraventricular arrhythmias and no detectable episodes of AF were found (Khine et al., 2018).

It is known that subjects in the state of dry immersion (DI) register the same reactions as astronauts in the first week on the ISS (Tomilovskaya et al., 2018). DI contributes to the development of rapid gravitational deconditioning of the somatosensory, cardiovascular, and other systems (Navasiolava et al., 2011; Tomilovskaya et al., 2021).

It has been noted that 7-day DI causes changes in autonomic regulation and changes in myocardial state, which are manifested in the growth of sympathetic regulation activity, decrease in the functional reserve of regulatory systems, decrease in systolic blood pressure and deterioration of myocardial electrophysiological characteristics. All these shifts are signs of adaptive restructuring of regulatory mechanisms, which leads, among other things, to a decrease in orthostatic stability (Larina et al., 2011).

In the experiment with 21-day DI it was shown that model conditions sharply changed hemodynamic and baroreflex response both at rest and during special tests (Borovik et al., 2020).

However, studies of blood proteome dynamics reflecting myocardial electrical excitation using the DI model in women have never been performed. Taking into account that excitation processes are regulated by anatomically localized structures in the atrial walls and other (see anatomy) structures, we believe that changes in distensibility on the one hand, and in electrolyte balance on the other hand, are reflected in the proteomic composition.

Therefore, the aim of the work was to search for the relationship between proteome changes and some indices of myocardial electrical excitation under conditions of 3-day DI.

Materials and methods

The experiment with female DI (NAJADA-2020) was conducted at the Institute of Biomedical Problems of the Russian Academy of Sciences from September 7 to 30 November 2020. Six healthy women (age 30.17 ± 5.5 years) participated in the experiment. Each participant had two menstrual cycles (MC) during the study period, including the pre-immersion period and the post-experiment follow-up period. The mean duration of MC was 28.4 ± 2.8 days. In order to unify the influence of hormonal status on the investigated clinical-instrumental and laboratory parameters, the start of baseline studies was timed to the first day of the second cycle. The start of immersion in all participants was on the 7th day of the cycle and its completion was on the 10th day.

The conducted studies were approved by the Bioethical Commission of the Institute of Medical and Biological Problems of the Russian Academy of Sciences (protocol No. 544 of 16 July 2020) and were in full compliance with the principles of the 1964 Helsinki Declaration of Human Rights. Each study participant voluntarily signed an informed consent after the potential risks, tasks, and nature of the upcoming study were explained to her (Pastushkova et al., 2012).

Background examinations were performed on day 5 of the cycle (2 days before immersion), and post-immersion examinations on day 12 (the second day after leaving the immersion). Thus, all blood samples were collected during the follicular phase of the menstrual cycle.

The capillary blood (40 μL) was extracted by puncturing the phalanx of the finger using an automatic scarifier. Sampling was performed with an automatic micropipette with further transfer to filter paper, which was dried and later stored at −20°C. Sample preparation included the following steps: recovery, incubation, trypsin inactivation, deoxycholate precipitation and extraction.

The obtained mixture of tryptic peptides was analyzed by liquid chromatography-mass spectrometry based on a Dionex Ultimate3000 nano HPLC system (Thermo Fisher Scientific, USA) and a timsTOF Pro mass spectrometer (Bruker Daltonics, USA). The mass spectrometric analysis was carried out by parallel accumulation sequential fragmentation (PASEF) data acquisition method. It was measured in the m/z range from 100 to 1700 Th. Ionic mobility were in the range of 0.60–1.60 V - s/cm^2. Functional annotation of proteins was performed using the String web resource (https://string-db.org) (Pastushkova et al., 2023).

To assess bioelectrical processes in myocardium, an electrocardiogram (ECG) was recorded in the supine position for 5 min in 3 standard leads from the limbs, followed by analysis of microvibrations characterizing electrophysiological properties of myocardium by the method of dispersion mapping (ECG DC) (Ivanov and Sula et al., 2009).

ECG was recorded and analyzed using the hardware-software complex "Cardiovisor" (Russia). To obtain signals of low-amplitude fluctuations of the ECG complex, several consecutive cardiac cycles were synchronized in 30-second segments of a 5-minute recording.

The variance characteristics were calculated for 9 groups (G1-G9), which reflect the degree of severity and localization of electrophysiological disturbances in the atrial and ventricular myocardium during the phases of de- and repolarization (G1 - right atrial depolarization, G2 - left atrial depolarization, G3 - end of right ventricular depolarization, G4 - end of left ventricular depolarization, G5 - right ventricular repolarization, G6 - left ventricular repolarization, G7 - symmetry of ventricular depolarization, G8 - intraventricular blockades, G9 - electrical symmetry of leads).

The total value of all groups of dispersion deviations is the integral "index of microalternations" (IM), which varies from 0% to 100%. The greater its values, the greater the deviations from the norm. Values not exceeding 15% are considered normal. The amplitude of microvariations of the T wave (T-tooth alternation) was also calculated.

To analyze the data set characterizing bioelectrical processes in the myocardium, we used the methods of cluster, discriminant and factor analysis. The *t*-test (p-value <0.05) has been used to detect significant protein concentration differences between the experiment points. The whole calculations were performed with the help of STATISTICA 12 statistical program package.

Results

ECG DC, in our opinion, is one of the most informative techniques used to screen the functional state of the heart muscle during DI. Changes in dispersion characteristics can be detected earlier than in standard ECG analysis.

The variance mapping scores were analyzed using factor analysis. The obtained factor loading pattern revealed the most significant factor in the analyzed sample (describing 65% of the total variance) - "synchrony of myocardial electrical excitation," which was formed by indicators with the corresponding correlation coefficients: IM (−0.7), T-tooth alternation (−0.7) and G9 (−0.9), reflecting synchrony of depolarization and repolarization in the corresponding heart sections.

All dry blood spot (DBS) samples were analyzed using the PASEF method implemented on timsTOF Pro instruments. Altogether 1256 different proteins were identified in the samples (Pastushkova et al., 2023). Two proteins CAN1_HUMAN and THRB_HUMAN, significantly correlating with ECG dispersion mapping, which reflects electrical processes in the myocardium, were identified when analyzing the protein composition of blood spots of volunteers (Table 1).

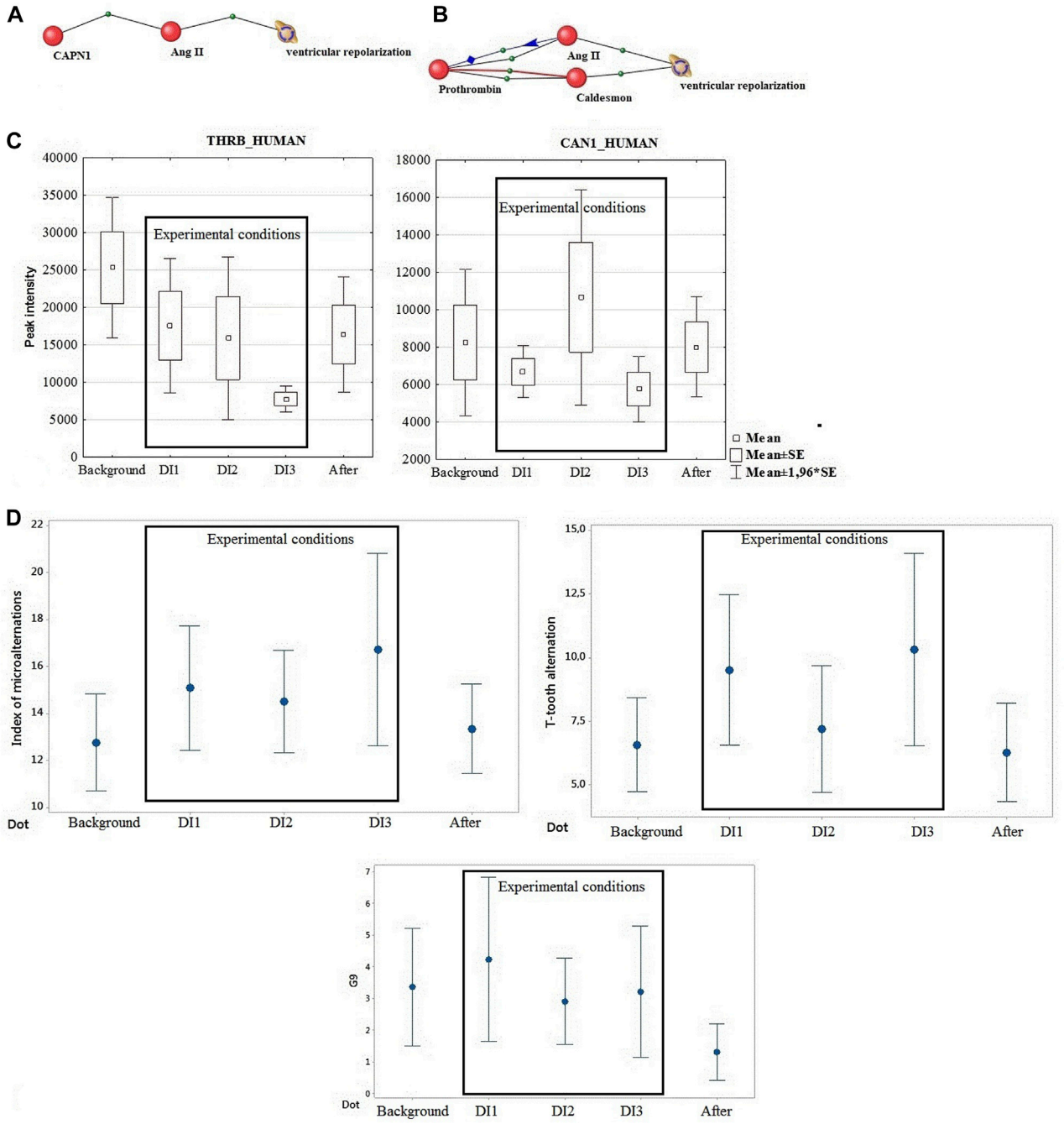

FIGURE 1
(A) Calpain binding via one mediator protein to the process of ventricular repolarization. **(B)** Connection of prothrombin protein through two mediators (angiontensin 2 and caldesmon) with the process of ventricular repolarization Blue line – regulation, Red line-involvement, Black line – association. **(C)** Directionality of calpain and prothrombin dynamics under the influence of DI. **(D)** Dynamics of DC ECG parameters (IM, T-tooth alternation, G9).

Factor analysis in this study did not reveal a significant effect of 3-day dry immersion on biological processes of atrial repolarization and depolarization.

For this purpose, an attempt was made to graphically depict the biological relationship between calpain1 and the process of cardiac ventricular repolarization using AndVisio software (Figure 1A) (Ivanisenko et al., 2015). It turned out that calpain 1 through one protein mediator angiotensin 2 regulates the process of ventricular repolarization.

Repolarization is the phase during which the original resting potential of the nerve cell membrane is restored after the passage of a nerve impulse. Ventricular repolarization can be significantly altered by many factors. In the context of this work, it is a change in the mechanoelectrical feedback loop during thoracocranial

TABLE 1 ECG DC indices included in the factor "synchronization of myocardial electrical excitation" and their correlations with CAN1_HUMAN (calpain) and THRB_HUMAN (prothrombin) proteins.

Variable	SS Effect	Df Effect	MS Effect	SS Error	dF Error	MS Error	F	p
CAN1_HUMAN	2.492143	1	2.492143	12.9127	28	0.461169	5.403975	0.027566
THRB_HUMAN	4.038610	1	4.038610	24.3395	28	0.869267	4.645995	0.039870

Protein annotation was performed by investigating the physiological processes that are regulated with the participation of calpain and prothrombin (Dewitt and Hallett et al., 2020).

redistribution of blood and reduction of cardiac output accompanied by myocardial structural rearrangement.

Calpains are known to be a family of cysteine proteases directly activated by Ca2+ and regulated by the endogenous specific inhibitor calpastatin. Among them, calpain-1 and calpain-2 are the most abundant and well-known isoforms (Sorimachi et al., 2011). Calpain-1 - calcium-regulated non-lysosomal thiol-protease which catalyzes limited proteolysis of substrates involved in cytoskeletal remodeling and signal transduction. Overexpression of calpain-1 in cardiomyocytes leads to increased global calpain activity and cardiac remodeling even in the absence of significant changes in intracellular Ca2+ (Galvez et al., 2007). The calpain/calpastatin system is involved in the development of maladaptive hypertrophy triggered by numerous pathologic stimuli (Wang et al., 2018; Aluja et al., 2019) and as indicated in several studies, leads to platelet aggregation, myocardial ischemia, and ultimately heart failure (Zatz and Starling et al., 2005; Wang et al., 2021). It was shown that in ventricular cardiomyocytes of newborn rats angiotensin II increased the expression of calpain 1 (Cao et al., 2022).

Prothrombin, one of the most important factors of the blood coagulation system, which showed a connection with ventricular repolarization, tended to decrease by the end of the experiment. It has been shown that experiments on modeling microgravity conditions do not cause activation of coagulation, although an increase in the peak and rate of thrombin formation was observed after the end of the experiments (Cvirn et al., 2015; Waha et al., 2015). Accordingly, prothrombin may be associated with observable phenotypic and functional changes post DI. Figure 1B shows the relationship of prothrombin protein through the mediator angiontensin 2 and the second mediator caldesmon with the process of ventricular repolarization.

During this study, the dynamics of calpain 1 and prothrombin changes were identical. This fact led us to focus on common mediators for the effects of these two proteins. The significant change in the mediator of both proteins, angiotensin II, is noteworthy (Figures 1A, B). These data are consistent with the changes in angiotensin levels and hemodynamic changes known from literature data under DI conditions of different duration (Pastushkova et al., 2012).

There is increasing evidence that angiotensin II (Ang II) is associated with the occurrence of ventricular arrhythmias. However, little is known about the electrophysiological effects of Ang II on ventricular repolarization. It is known that the fast component of the K(+) delayed rectifier current (I(Kr)) plays a critical role in cardiac repolarization, and Ang II via the protein kinase C pathway-associated AT(1) receptors in ventricular myocytes exerts an inhibitory effect on I(Kr)/hERG currents. This is thought to be a potential mechanism that elevated levels of Ang II are involved in the occurrence of arrhythmias in cardiac hypertrophy and heart failure (Wang et al., 2008).

The second intermediary (Figure 1B) is the actin- and myosin-binding protein Caldesmon (CALD1 gene). This protein is implicated in the regulation of actomyosin interactions in smooth muscle and non-muscle cells. Caldesmon promotes actin binding of tropomyosin, which enhances the stabilization of actin filament structure. It inhibits actomyosin ATPase in muscle tissues by binding to F-actin. The effect is reduced by calcium-calmodulin and increased by tropomyosin. It was shown that saldesmon cooperates with actin, myosin, two molecules of tropomyosin and with calmodulin (Huber et al., 1993).

Discussion

Disturbance of synchronization of electrical excitation of the heart as a reflection of the state of the circuit of mechano-electrical regulation of the heart under conditions of hemodynamic influence of DI was investigated for the first time. Proteomic regulation of atrial and ventricular depolarization and repolarization processes and ECG DC parameters were evaluated. Factor analysis excluded a reliable influence of DI on biological processes of atrial repolarization and depolarization.

Ventricular repolarization disorders in the population are frequent, asymptomatic, and have multiple causes. Ventricular repolarization disorders are based on congenital individual features of electrophysiological processes in the myocardium, leading to early repolarization of its subepicardial layers, such as: 1. Additional conduction pathways.2. Uneven course of the processes of de- and repolarization of the ventricles. 3. Dysfunction of the autonomic nervous system. 4. Electrolyte disturbances (hypercalcemic theory) (Shulenin et al., 2007).

In DI conditions, in which the state of synchronization of electrical excitation of the heart was assessed, such factors were changes in the structure of cardiac muscle and volume of heart chambers in DI (Westby et al., 2015; Perhonen et al., 2001).

Studying the changes in the cardiovascular system during DI showed the gradual engagement of electrical (an increase in the amplitude of the QRS complex) and then energetometabolic (a decrease in the heart rate and alteration of the water-electrolyte balance) processes in the myocardium; the most pronounced changes were detected on the 5th day of DI (Ivanov et al., 2011). The correlation between changes in hydro-electrolyte balance and its regulation and modifications of electrophysiologic propagation of myocardial excitation, increase in dispersion of intrinsic small oscillations of cardiac potential were described. Changes in hydro-electrolyte balance could cause protein and energy shifts that were reflected, especially, in the rate of ventricular repolarization. The significant (more than 2-fold) growth of the

centralization index at the end of SI indicates that the inclusion of the central regulation mechanisms in the processes of adaptation was an appropriate response aimed at compensating the primary changes in the water-electrolyte balance and hemodynamics (Larina et al., 2011). The multi-factor genesis of changes in ventricular repolarization requires more profound studies of proteomic and electrolyte parameters which affect the regulation of the functional state of the heart under simulated and real extreme conditions.

Thus, for the first time the regulation of synchronization of electrical excitation of the heart under conditions of 3 days DI with the participation of women was evaluated at the level of changes in the proteomic composition of blood. Factor analysis in this study excluded a significant effect of dry immersion for 3 days on biological processes of atrial repolarization and depolarization. By bioinformatic analysis of ANDvisio proteomics data from the total list of blood proteins in DI, two proteins related to the biological process of ventricular repolarization through two mediators (angiotensin II and caldesmon) were identified. These data correlate with the results of the DC ECG on changes in ventricular repolarization in all participants during DI. The multifactorial genesis of changes in ventricular repolarization requires further in-depth studies of proteomic and electrolyte circuits of cardiac regulation during DI of different durations to confirm this hypothesis, including gender differences.

Data availability statement

The datasets presented in this study can be found in online repositories. The names of the repository/repositories and accession number(s) can be found below: http://www.proteomexchange.org/, PXD027654.

Ethics statement

The studies involving humans were approved by Bioethical Commission of the Institute of Medical and Biological Problems of the Russian Academy of Sciences (protocol No. 544 of 16 July 2020) . The studies were conducted in accordance with the local legislation and institutional requirements. The participants provided their written informed consent to participate in this study.

Author contributions

LP: Conceptualization, Writing–original draft. AG: Conceptualization, Writing–original draft. VR: Conceptualization, Writing–original draft. AN: Data curation, Formal Analysis, Writing–review and editing. DK: Methodology, Software, Visualization, Writing–review and editing. OP: Formal Analysis, Methodology, Software, Writing–review and editing. IL: Conceptualization, Writing–review and editing.

Funding

The author(s) declare financial support was received for the research, authorship, and/or publication of this article. This research was funded by the Russian Science Foundation grant No. 22-74-00069, https://rscf.ru/project/22-74-00069/.

Conflict of interest

The authors declare that the research was conducted in the absence of any commercial or financial relationships that could be construed as a potential conflict of interest.

Publisher's note

References

Aluja, D., Inserte, J., Penela, P., Ramos, P., Ribas, C., Iñiguez, M. Á., et al. (2019). Calpains mediate isoproterenol-induced hypertrophy through modulation of GRK2. *Basic Res. Cardiol.* 114, 21. doi:10.1007/s00395-019-0730-5

Borovik, A. S., Orlova, E. A., Tomilovskaya, E. S., Tarasova, O. S., and Vinogradova, O. L. (2020). Phase coupling between baroreflex oscillations of blood pressure and heart rate changes in 21-day dry immersion. *Front. Physiol.* 11, 455. doi:10.3389/fphys.2020.00455

Cao, Y., Wang, Q., Liu, C., Wang, W., Lai, S., Zou, H., et al. (2022). Capn4 aggravates angiotensin II-induced cardiac hypertrophy by activating the IGF-AKT signalling pathway. *J. Biochem.* 171, 53–61. doi:10.1093/jb/mvab100

Cvirn, G., Waha, J. E., Ledinski, G., Schlagenhauf, A., Leschnik, B., Koestenberger, M., et al. (2015). Bed rest does not induce hypercoagulability. *Eur. J. Clin. Invest.* 45 (1), 63–69. doi:10.1111/eci.12383

Dewitt, S., and Hallett, M. B. (2020). Calpain activation by Ca2+ and its role in phagocytosis. *Adv. Exp. Med. Biol.* 1246, 129–151. doi:10.1007/978-3-030-40406-2_8

Galvez, A. S., Diwan, A., Odley, A. M., Hahn, H. S., Osinska, H., Melendez, J. G., et al. (2007). Cardiomyocyte degeneration with calpain deficiency reveals a critical role in protein homeostasis. *Circ. Res.* 100, 1071–1078. doi:10.1161/01.RES.0000261938.28365.11

Huber, P. A., Redwood, C. S., Avent, N. D., Tanner, M. J., and Marston, S. B. (1993). Identification of functioning regulatory sites and a new myosin binding site in the C-terminal 288 amino acids of caldesmon expressed from a human clone. *J. Muscle Res. Cell Motil.* 14, 385–391. doi:10.1007/BF00121289

Ivanisenko, V. A., Saik, O. V., Ivanisenko, N. V., Tiys, E. S., Ivanisenko, T. V., Demenkov, P. S., et al. (2015). ANDSystem: an Associative Network Discovery System for automated literature mining in the field of biology. *BMC Syst. Biol.* 9 Suppl 2, S2. doi:10.1186/1752-0509-9-S2-S2

Ivanov, G. G., Baevsky, R. M., Bersenev, E. Y., et al. (2011). ECG dispersion mapping indices during exposure to 5-day "dry" immersion *Aviakosmicheskaya i ekologicheskaya meditsina. Med* 45 (6), 44–47.

Ivanov, G. G., and Sula, A. S. (2009). Dispersive ECG mapping: theoretical foundations and clinical practice. *Mosc. Tekhnos.*,

Jeyaraj, D., Wilson, L. D., Zhong, J., Flask, C., Saffitz, J. E., Deschênes, I., et al. (2007). Mechanoelectrical feedback as novel mechanism of cardiac electrical remodeling. *Circulation* 2007, 3145–3155. doi:10.1161/CIRCULATIONAHA.107.688317

Kamkin, A. G., and Iu, M. E. (2012). Mechanically gated cardiac ion channels and their regulation by cytokines. *Usp. Fiziol. Nauk.* 43 (4), 3–44.

Khine, H. W., Steding-Ehrenborg, K., Hastings, J. L., Kowal, J., Daniels, J. D., Page, R. L., et al. (2018). Effects of prolonged spaceflight on atrial size, atrial electrophysiology, and risk of atrial fibrillation. *Circ. Arrhythm. Electrophysiol.* 11, e005959. doi:10.1161/CIRCEP.117.005959

Larina, I. M., Baevsky, R. M., Pastushkova, L. H., Novoselova, N. M., et al. (2011). Relationship between changes in water-electrolyte balance and reactions of the cardiovascular system in the experiment with 7-day "dry immersion. *Hum. Physiol.* 5, 100–107.

Navasiolava, N. M., Custaud, M. A., Tomilovskaya, E. S., Larina, I. M., Mano, T., Gauquelin-Koch, G., et al. (2011). Long-term dry immersion: review and prospects. *Eur. J. Appl. Physiol.* 111, 1235–1260. doi:10.1007/s00421-010-1750-x

Pastushkova, L. H., Goncharova, A. G., Rusanov, V. B., Kashirina, D. N., Brzhozovskiy, A. G., Popova, O. V., et al. (2023). Connection of dried blood spot proteomic composition dynamics and heart rate variability in 3-day female dry immersion. *Microgravity Sci. Technol.* 35, 19. doi:10.1007/s12217-023-10047-y

Pastushkova, L. H., Pakharukova, N. A., Novoselova, N. M., Dobrokhotov, I. V., Valeeva, O. A., Kusto, M.-A., et al. (2012). Direct proteomic profiling of human urine and blood serum in experiment with 5-day "dry" immersion Aerospace and Environmental Medicine. *Med.* 46.

Perhonen, M. A., Zuckerman, J. H., and Levine, B. D. (2001). Deterioration of left ventricular chamber performance after bed rest: "cardiovascular deconditioning" or hypovolemia? *Circulation* 103, 1851–1857. doi:10.1161/01.cir.103.14.1851

Quinn, T. A., Kohl, P., and Ravens, U. (2014). Cardiac mechano-electric coupling research: fifty years of progress and scientific innovation. *Prog. Biophys. Mol. Biol.* 115, 71–75. doi:10.1016/j.pbiomolbio.2014.06.007

Shulenin, S. N., Boitsov, S. A., and Bobrov, A. L. (2007). Clinical significance of early ventricular repolarization syndrome, algorithm of patient examination. *Arrhythmology Bull.* (50), 33–39.

Sorimachi, H., Hata, S., and Ono, Y. (2011). Impact of genetic insights into calpain biology. *J. Biochem.* 150, 23–37. doi:10.1093/jb/mvr070

Tomilovskaya, E., Amirova, L., Nosikova, I., Rukavishnikov, I., Chernogorov, R., Lebedeva, S., et al. (2021). The first female dry immersion (NAIAD-2020): design and specifics of a 3-day study. *Front. Physiol.* 12, 661959. doi:10.3389/fphys.2021.661959

Tomilovskaya, E., Shigueva, T., Sayenko, D., Rukavishnikov, I., and Kozlovskaya, I. (2019). Dry immersion as a ground-based model of microgravity physiological effects. *Front. Physiol.* 10, 284. doi:10.3389/fphys.2019.00284

Waha, J. E., Goswami, N., Schlagenhauf, A., Leschnik, B., Koestenberger, M., Reibnegger, G., et al. (2015). Effects of exercise and nutrition on the coagulation system during bedrest immobilization. *Med. Baltim.* 94 (38), e1555. doi:10.1097/MD.0000000000001555

Wang, J., Ciampa, G., Zheng, D., Shi, Q., Chen, B., Abel, E. D., et al. (2021). Calpain-2 specifically cleaves Junctophilin-2 at the same site as Calpain-1 but with less efficacy. *Biochem. J.* 478, 3539–3553. doi:10.1042/BCJ20210629

Wang, Y., Chen, B., Huang, C. K., Guo, A., Wu, J., Zhang, X., et al. (2018). Targeting calpain for heart failure therapy: implications from multiple murine models. *JACC Basic Transl. Sci.* 3, 503–517. doi:10.1016/j.jacbts.2018.05.004

Wang, Y. H., Shi, C. X., Dong, F., Sheng, J. W., and Xu, Y. F. (2008). Inhibition of the rapid component of the delayed rectifier potassium current in ventricular myocytes by angiotensin II via the AT1 receptor. *Br. J. Pharmacol.* 154, 429–439. doi:10.1038/bjp.2008.95

Westby, C. M., Martin, D. S., Lee, S. M., Stenger, M. B., and Platts, S. H. (2015). Left ventricular remodeling during and after 60 days of sedentary head-down bed rest. *J. Appl. Physiol.* 2016, 956–964. doi:10.1152/japplphysiol.00676.2015

Zatz, M., and Starling, A. (2005). Calpains and disease. *N. Engl. J. Med.* 352, 2413–2423. doi:10.1056/NEJMra043361

frontiers | Frontiers in Physiology

TYPE Brief Research Report
PUBLISHED 18 April 2024
DOI 10.3389/fphys.2024.1369788

OPEN ACCESS

EDITED BY
Marc-Antoine Custaud,
Université d'Angers, France

REVIEWED BY
Nastassia Navasiolava,
Centre Hospitalier Universitaire d'Angers, France
Barbara La Scaleia,
Santa Lucia Foundation (IRCCS), Italy

*CORRESPONDENCE
Sarah C. Moudy,
sarah.c.moudy@nasa.gov

RECEIVED 12 January 2024
ACCEPTED 02 April 2024
PUBLISHED 18 April 2024

CITATION
Moudy SC, Peters BT, Clark TK, Schubert MC and Wood SJ (2024), Development of a ground-based sensorimotor disorientation analog to replicate astronaut postflight experience. *Front. Physiol.* 15:1369788. doi: 10.3389/fphys.2024.1369788

Development of a ground-based sensorimotor disorientation analog to replicate astronaut postflight experience

Sarah C. Moudy[1]*, Brian T. Peters[2], Torin K. Clark[3], Michael C. Schubert[4] and Scott J. Wood[5]

[1]Aegis Aerospace, Houston, TX, United States, [2]KBR, Houston, TX, United States, [3]Bioastronautics Laboratory, Smead Aerospace Engineering Sciences Department, University of Colorado Boulder, Boulder, CO, United States, [4]Laboratory of Vestibular NeuroAdaptation, Department of Otolaryngology Head and Neck Surgery, Johns Hopkins University School of Medicine, Baltimore, MD, United States, [5]NASA Johnson Space Center, Houston, TX, United States

The perceptual and motor coordination problems experienced following return from spaceflight reflect the sensory adaptation to altered gravity. The purpose of this study was to develop a ground-based analog that replicates similar sensorimotor impairment using a standard measures test battery and subjective feedback from experienced crewmembers. This Sensorimotor Disorientation Analog (SDA) included varying levels of sensorimotor disorientation through combined vestibular, visual, and proprioceptive disruptions. The SDA was evaluated on five previously flown astronauts to compare with their postflight experience and functional motor performance immediately (Return (R)+0 days) and +24 h (R+1) after landing. The SDA consisted of galvanic vestibular stimulation (GVS), visual disruption goggles, and a weighted suit to alter proprioceptive feedback and replicate perceived heaviness postflight. Astronauts reported that GVS alone replicated ~50–90% of their postflight performance with the weighted suit fine-tuning the experience to replicate an additional 10%–40% of their experience. Astronauts did not report feeling that the disruption goggles represented either the visual disruptions or illusory sensations that they experienced, nor did they impact motor performance in postflight tasks similarly. Based on these results, we recommend an SDA including the GVS and the weighted suit. These results provide a more realistic and portable SDA framework to provide transient spaceflight-relevant sensorimotor disruptions for use in countermeasure testing and as a pre-flight training tool.

KEYWORDS

spaceflight analog, sensorimotor system, functional performance, disorientation, vestibular system

1 Introduction

Upon return to Earth's gravity following prolonged microgravity exposure, astronauts experience re-entry motion sickness (Reschke et al., 2017), perceptual illusions (Harm et al., 2015), and alterations to functional performance including postural stability (Wood et al., 2015) and locomotion (Mulavara et al., 2018; Clément et al., 2022). Sensorimotor disruptions following long-duration stays on the International Space Station (ISS) have had prominent effects on functional performance immediately upon landing (Reschke et al.,

2020) and +24 h after landing (Miller et al., 2018; Mulavara et al., 2018). The sensorimotor system includes the vestibular, proprioceptive, and visual systems that are critical for postural stability and gait. Not surprisingly, the postflight effects include visual orientation illusions (Oman, 2003), vestibular-mediated gain changes (Reschke et al., 2018) and changes in proprioception leading to perceived heaviness of limbs (Ross, 1998).

Simulating the postflight sensorimotor disruptions after long duration missions is exceedingly challenging on Earth. Spaceflight ground analogs such as bed rest and dry/wet immersion simulate the response to microgravity for various physiological systems (Pandiarajan and Hargens, 2020). Another spaceflight analog, centrifugation, simulates artificial gravity and can elicit vestibular adaptive changes similar to G-transitional effects following spaceflight (Bles et al., 1997; Nooij and Bos, 2007; Groen et al., 2008). Each of these spaceflight analogs provide the ability to capture large experimental datasets to test spaceflight countermeasures. However, these analogs are costly, require large facilities and significant time and effort, and most do not necessarily capture the relevant sensorimotor mechanisms. One spaceflight analog specific to sensorimotor mechanisms was developed by Dixon and Clark (2020) using a 12-h "wheelchair head immobilization paradigm" that did elicit illusory sensations and significant performance decrements in tasks sensitive to vestibular function such as tandem walk with eyes closed. However, this analog still requires significant time and effort to implement and produced limited proprioceptive and visual disruptions. A portable simple alternative that can mimic postflight sensorimotor disorientation could aid in defining sensorimotor performance thresholds and allow for faster countermeasure viability testing. Disorientation of the sensorimotor system in 1G through the same mechanisms as exposure to microgravity is difficult to replicate, however, we can replicate the motor output that is seen postflight by altering the vestibular, proprioceptive, and visual systems concurrently.

Previous studies have utilized galvanic vestibular stimulation (GVS) as a means to disrupt vestibular input and mimic astronaut postflight performance. A pseudorandom GVS profile with peaks up to 5 mA was found to significantly degrade postural stability during a computerized dynamic posturography task with eyes open and eyes closed (MacDougall et al., 2006) and performance in a locomotor obstacle course task (Moore et al., 2006). These studies found performance decrements with GVS were similar to those observed in short duration mission astronauts immediately postflight. GVS is also a portable system that can be worn while ambulating and is temporary with quick dissipation of the disruption. Thus, GVS can be a useful tool in replicating post-spaceflight task performance.

Proprioceptive functions are altered with exposure to microgravity (Macaulay et al., 2021). Vibration-induced limb position caused a greater extension perception during 1.8G parabolic flights relative to 1G (Lackner and DiZio, 1992). Lackner and DiZio (1992) proposed that these proprioceptive illusions were due to a central reinterpretation of muscle spindle stretch activity relative to gravity cues. It is possible that applying increased body-loading in 1G could elicit perceived alterations in limb position sensing. Applied loads could also mimic the subjective heaviness felt postflight by astronauts and decrements associated with reduced muscular fitness and fatigue that impact motor output and limb position sensing. Ryder et al. (2013) developed an analog to simulate spaceflight decrements in muscular fitness by applying loads upwards of 120% body weight across all body segments finding reductions in task performance as loads increased. This study found task performance was comparable to that of six astronauts after short duration shuttle missions. Distally applied loads at the ankle have also been shown to increase overall metabolic rate (Browning et al., 2007) where muscle fatigue can influence limb position sensing (Walsh et al., 2004). At the wrist, distally applied loads can increase limb position sensing error when the arm is swung (Shibata et al., 2012) and when in static unsupported condition (Winter et al., 2005). Taken together, applied body loading at the chest and distally at the wrists and ankles could elicit similar motor performance decrements as returning astronauts experience postflight.

Visual disruptions are experienced postflight including illusory sensations and reduced dynamic visual acuity (Bloomberg and Mulavara, 2003). Illusory sensations are thought to occur due to postflight readaptation of the otolith organs due to microgravity exposure where head tilt cues are reinterpreted as linear translation. This readaptation results in perceived translation of the environment or body when tilting the head after return from spaceflight which can impact postural and dynamic stability (Merfeld, 2003; Harm et al., 2015; Reschke et al., 2017). Dynamic visual acuity decreases postflight (Peters et al., 2011) and is postulated to occur due to changes in gaze stabilization mechanisms where compensatory eye movements, mediated by the vestibular system, are altered (Bloomberg and Mulavara, 2003). It was also proposed that lower-limb kinematics were altered to compensate for the changes in gaze stabilization. This visual-motor relationship, independent of cause-effect, suggests that visual distortion type challenges (e.g., Welch et al., 2009) could impact motor performance and that this could aid in replicating postflight performance.

The purpose of this exploratory study was to validate a novel post-spaceflight Sensorimotor Disorientation Analog (SDA) for replicating the postflight subjective experience in previously flown astronauts. Each of these crewmembers had participated in a sensorimotor test battery following long-duration spaceflight occurring immediately after landing (Return (R)+0 days) and 1-day after landing (R+1) (Clément et al., 2022). Therefore, both subjective feedback and comparison of performance on this test battery served as the criteria to validate the SDA.

2 Methods

2.1 Participants

The test procedures were approved through the NASA Institutional Review Board and in accordance with the Declaration of Helsinki. Five United States Orbital Segment (USOS) Astronauts (4 female, 1 male; Age: 45 ± 8 years (Mean ± SD)) who had previously flown on the ISS (average mission duration: 249 days) provided written informed consent to participate in this study. All astronauts had previously participated in sensorimotor field testing (Clément et al., 2022) immediately post-landing (1.7 ± 0.8 h) and 1-day after landing (26.9 ± 5.2 h) on their most recent return. The average time

10.3389/fphys.2024.1369788

TABLE 1 Starting and final levels of disorientation for each element of the sensorimotor disorientation analog at each time point.

Level	GVS (peak mA) (S)	Weighted suit (%BW)	Visual disruption (BAC)
Investigator Defined Initial Starting Levels of Disorientation			
Low (i.e., aiming to replicate R+1)	2.0	20	.07–.10+
High (i.e., aiming to replicate R+0)	3.0	40	.12–.15+
Final Levels of Disorientation from Crew Feedback			
Low (i.e., aiming to replicate R+1)	2.0	15	None
High (i.e., aiming to replicate R+0)	3.0	30	None

S = standard profile; BW = bodyweight; BAC = blood alcohol content,

since their most recent return was 377 days (range: 95–904 days). The astronauts who participated in this study were selected based on their availability with the preference of those who had more recently returned from spaceflight in order to aid in recall. The tasks performed for this study were the same tasks completed during field testing in order to aid in recall of their experience and performance at the R+0 and R+1 time points. One astronaut did not perform field testing on R+0 but was able to perform at R+1. Feedback from this astronaut was only gathered for the R+1 time point.

2.2 Sensorimotor disorientation analog

The SDA consisted of three elements: GVS, visual disorientation prism goggles, and a weighted suit. Two levels of disorientation were defined as low, attempting to replicate R+1, and high, attempting to replicate R+0. The initial investigator defined starting levels for each element of the SDA are included in Table 1.

A custom GVS generator was used to deliver a bilateral bipolar stimulus. The current was delivered via two 3" diameter circular electrodes placed over the mastoid processes. An electrode pad with a layer of electrode gel was placed between the skin and the electrode. The electrodes were secured to the head via elastic straps that did not restrict head movement. The stimulus was generated from accelerometer data captured during capsule wave motions to create a random sum-of-sines profile with frequencies between 0 and 0.3 Hz (Wood, 2002; Clement and Wood, 2014). Three standard (S) profiles were generated with peak amplitudes reaching 1 mA, 2 mA, and 3 mA. Additionally, three boosted (B) profiles were generated that multiplied the standard signal to the power of 1.2 while maintaining the peak amplitude thresholds (Figure 1). Each profile contained ten, 3-min portions of non-repeating signal, for a total of 30 min, however, the GVS was only active when performing the field tasks. The six profiles were sorted by increasing levels of disorientation as defined by average peak amplitudes of the signal as follows: 1 mA S, 2 mA S, 1 mA B, 3 mA S, 2 mA B, 3 mA B.

Fatal Vision Alcohol Impairment Goggles (Innocorp, ltd., Verona, WI) were used to alter visual input. The goggles had varying levels of visual disorientation based on estimated ranges of blood alcohol content (BAC) including: 0.07–0.10+, 0.12–0.15+, and 0.17–0.20+. Prior to testing the visual disruption goggles, astronauts were told that the goggles would not replicate the actual visual disruptions or illusory sensations they experienced, if any, rather that these goggles were meant to reduce visual dependency such that task performance was similar to how postflight visual disruptions or illusory sensations could have impacted their postflight performance.

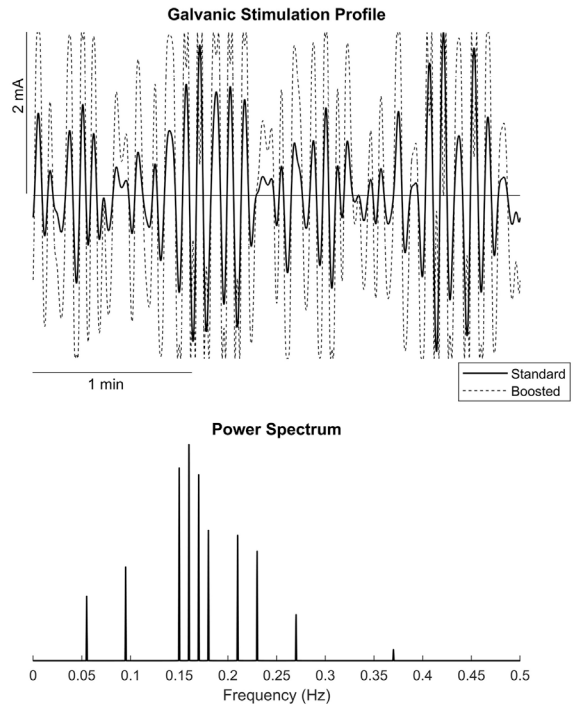

FIGURE 1
(A) example Standard and Boosted galvanic vestibular stimulation profiles, **(B)** power spectrum of the stimulation profiles.

The weighted suit was comprised of the custom-made weighted vest (Ryder et al., 2013) and commercial off-the-shelf ankle and wrist straps. The vest portion only of the Ryder et al. (2013) custom-made suit was utilized for initial set-up, however, the hips and upper and lower arm and leg pieces were available to be included in testing dependent on astronaut feedback. Weights were distributed anthropometrically and symmetrically based on the relative percent weight of each body segment with respect to the overall body weight as follows: 7.3% for each wrist, 15.9% of each ankle, and 26.8% for the chest and back individually. The levels of disruption

can be incrementally increased or decreased by overall percent bodyweight, with initial investigator defined starting levels noted in Table 1 for all elements.

2.3 Data collection procedure

Upon arrival, the astronauts were shown videos of their performance during field testing at both R+0 and R+1 to enable recall of their experience. Astronauts then performed the same field test tasks with no SDA to provide a baseline of performance. These tasks included a sit-to-stand with walk-and-turn and tandem walk. The sit-to-stand with walk-and-turn included standing from a chair, walking to and around a cone placed 400 cm away while navigating an 30 cm tall obstacle placed 130 cm away from the chair. The tandem walk was performed with both eyes open, and eyes closed including 10–12 heel-to-toe steps with arms crossed. These tasks are described in full in Clément et al. (2022).

Iterative testing of the SDA was performed such that the elements (GVS, vision goggles, weighted suit) were examined separately and combined as depicted in Figure 2. This approach helped determine if a singular or multiple elements of the SDA were needed to sufficiently replicate the postflight experience and performance. To note, the weighted suit alone for the high level was not performed with the tasks due to time constraints, however, subjective feedback was still captured. Throughout testing, video cameras were used to capture verbal feedback and task performance. After each block and performance of field test tasks, astronauts were asked the following questions:

- "What time point do you believe your performance and/or experience with this SDA level best reflects?"
- When applicable, "Do you believe the combination of [elements] is the same, worse, or better than with the [element] alone?"

Specific questions for each element were also asked including:

- "Is the weight and distribution of the weight similar to your postflight heaviness?"
- "Does the weight impact your ability to perform the tasks similar to postflight?"
- "Did you experience any asymmetrical heaviness postflight?"
- "Do the vision goggles impact your performance similar to your postflight performance?"

Motor performance changes were quantified via the tandem walk task. No data was gathered from the sit-to-stand with walk-and-turn task that would allow for comparison to postflight performance, rather the task was used solely to enable recall of their experience. Scoring was performed on the tandem walks when the astronaut was wearing the final preferred SDA as determined by their experience for both low and high levels. Two independent scorers examined the videos to determine percent correct steps. As in Clément et al. (2022), an incorrect step was defined as any of the following: 1) a cross-over step; 2) the stepping foot touches the ground more than once per step; 3) a wide swing of the stepping foot typically accompanied by a lateral trunk bend; 4) a step duration greater than 3 s; or 5) a heel-toe gap larger than 10 cm at the completion of the step. The average value of percent correct steps across scorers was used for each trial.

3 Results

In summary, the final SDA based on astronaut feedback included the GVS at the proposed starting levels and the weighted suit which was reduced to 15% and 30% body weight for the low (R+1) and high (R+0) levels respectively (Table 1). These levels were decided based on the majority consensus (GVS) or average of preferred level (weighted suit). The visual disruption goggles were removed from SDA.

These conclusions were based upon the following feedback from astronauts. All five astronauts believed the 2 mA S profile best reflected their overall experience and performance at the R+1 time point. For the R+0 time point, three of four astronauts chose the 3 mA S profile and one astronaut selected the "boosted" 2 mA profile. Four of the five astronauts (all female) subjectively reported that GVS alone replicated ~80–90% of their postflight experience and performance with one astronaut (male) stating only 50% replicative. Two astronauts stated the GVS level for both time points was task specific such that complex tasks sensitive to vestibular function, such as tandem walk eyes closed, were more affected by GVS.

For the weighted suit element of the SDA, the final bodyweight percentage ranged from 25%–40% for the high level (R+0) and 10%–20% for the low level (R+1). The astronaut who concluded testing with 40% bodyweight for the high level (R+0) stated this was too high, however, due to time constraints this astronaut was unable to test 30% bodyweight. Overall, all the astronauts believed the weighted suit alone replicated between 5%–40% of their postflight experience and should be used alongside the GVS. All astronauts stated they did not experience asymmetrical heaviness, therefore, only a uniform application of weight was used. Three of five astronauts stated the ankle weights were useful in replicating postflight proprioceptive disruption as it reduced their ability to determine foot placement during tandem walk and disrupted the standard swing phase mechanics during the sit-to-stand with walk-and-turn. The vest aided in overall subjective heaviness; however, it was noted by the astronauts that the vest partially aided in stability during upright standing and walking tasks as the weight is around the center of mass. A few additional suggestions on weight distribution were to add light head weights to further influence head mechanics (n = 1) and distribute weight across upper and lower arms (n = 1).

Two astronauts did experience illusory sensations postflight (non-specific) and all five astronauts stated they used vision to compensate for vestibular disruptions. Four of the five astronauts did not believe the visual disruption goggles represented either the illusory sensations or other visual disruptions that they experienced postflight. Specifically, these 4 astronauts reported that the lowest BAC level of the goggles was too disruptive. Two of the four astronauts did not perform the tasks with the goggles as they either did not want to proceed after donning the goggles and standing or they were on a time constraint and wanted to focus on the other aspects of the SDA they deemed more replicative. The

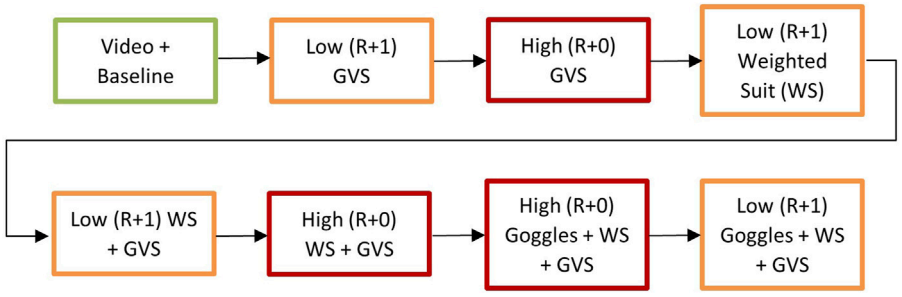

FIGURE 2
Testing procedure for each element of the Sensorimotor Disorientation Analog (SDA) with the low level (attempting to replicate R+1) outlined in orange and the high level (attempting to replicate R+0) outlined in red. Green outline represent the pre-SDA procedures. GVS = galvanic vestibular stimulation, WS = weighted suit.

other two astronauts did not believe the goggles impacted their performance in postflight tasks similarly. One astronaut did believe the goggles aided in fine-tuning the SDA to achieve an additional 5% of their postflight experience. This astronaut felt the 0.07–0.10+ BAC replicated R+1 and 0.12–0.15+ BAC replicated R+0.

Changes in motor performance while wearing the astronauts' preferred SDA is summarized in Table 2 using percent correct steps during tandem walk. The preferred SDA for four of the five astronauts included only the GVS and weighted suit whereas the fifth astronaut also included the visual disruption goggles. In comparison to published postflight data inclusive of the astronauts in this study (Clement et al., 2022), the SDA elicited on average 10% and 6.5% less correct steps for the low level (R+1) with eyes open and closed, respectively (Table 2). Individually, each astronaut ranged from 2.4%–40% correct steps different than their respective postflight R+1 data for eyes open and 0%–22.5% correct steps different for eyes closed. Eyes closed performance for the high level (R+0) had 2.3% less correct steps when wearing the SDA compared to postflight and, individually ranged from 1.7%–17.5% corrects steps different. Conversely, performance was better with 19.8% more correct steps while wearing the SDA for eyes open at the high level (R+0), and individually ranged from 10% correct steps worse with the SDA or between 5.7%–45% corrects steps better with the SDA.

4 Discussion

The results of this study demonstrated that combining a GVS sum-of-sines profile with a weighted suit was able to approximately replicate, based upon subjective comparisons, astronaut immediate and +24 h postflight experience and motor performance during dynamic locomotor tasks. While no analog can fully replicate the adaptations that occur due to spaceflight, the SDA proposed in this study provides a framework for a portable spaceflight analog.

GVS alone was the best at replicating postflight experience after long duration missions. This is consistent with previous studies that utilized only GVS to successfully replicate short duration postflight postural stability and dynamic task performance (MacDougall et al., 2006; Moore et al., 2006). One astronaut noted that postflight vestibular disruptions were greater when head movements were performed including head movement relative to the body (e.g., head pitch to view obstacle on the ground) and relative to space (e.g., sit-to-stand with head locked to trunk). Moore et al. (2006) examined a head-coupled GVS profile using head yaw velocity and vertical linear acceleration to elicit proportional galvanic stimulus. These results found that the head-coupled GVS significantly disrupted performance yet produced less disruption to motor performance than a pseudorandom GVS profile similar to that used in this study. The head-coupled GVS profile utilized only yaw motion, where head pitch and roll have been reported to cause illusory sensations of exaggerated translational motion postflight (Reschke and Clément, 2018). It is also possible that the proportional relationship between head movement and galvanic stimulus was not disruptive enough to replicate astronaut's postflight experiences. Further research is needed to determine the validity of head-coupled GVS profiles to better reflect postflight experience.

The weighted suit received overall positive feedback on replicating subjective heaviness and eliciting certain proprioceptive disruptions that are experienced following spaceflight (Ross, 1998). However, the suit was only helpful in replicating postflight experience in combination with the GVS as the visual and vestibular systems were able to compensate for the added weight. One astronaut in this study noted that the weighted suit helped to stabilize them while performing the tandem walk. Applied loads to body segments is known to impair postural limits of stability (Holbein and Chaffin, 1997), however, loading of small weights has been used therapeutically to improve postural alignment (Widener et al., 2020). It is possible that the location of the weights, specifically at the chest, may have aided in stability. Conversely, the distally applied loads at the ankle were noted by astronauts to subjectively impair task performance similar to postflight experience.

While we did not examine limb position sensing error, we did quantify motor performance during the tandem walk task as a result of the preferred combined SDA. Overall, tandem walk performance with the SDA was within 10% correct steps (~1 step) of the average postflight performance from previous research except for eyes open at the high level (R+0) where performance was better with 19.8% more correct steps (~2 steps) with the SDA. Postflight task performance soon after landing is highly variable, especially when able to utilize vision. This is seen in the Clément et al. (2022) data (Table 2) where the full possible range of postflight performance (0%–100% correct steps) was captured on R+0 for tandem walk eyes open. This range of performance was similarly

TABLE 2 Percent correct steps for tandem walk with eyes open and closed while wearing the Sensorimotor Disorientation Analog (SDA) at the high and low levels and postflight data retrieved from Clement et al. (2022) at the R+0 and R+1 time points.

	High Level/R+0		Low Level/R+1	
	Eyes open (%)	Eyes closed (%)	Eyes open (%)	Eyes closed (%)
SDA (R+0: n = 4, R+1: n = 5) (Mean, [Min, Max])	53.3 [18–75]	7.6 [0–19]	74.4 [56–100]	18.8 [12–30]
Clement et al. (2022) (n = 19) (Mean, [Min, Max])	33.5 [0–100]	9.9 [0–33]	84.6 [9–100]	25.3 [0–58]

Clement et al. (2022) data retrieved from supplementary file. Average of the mean data for repeat and first flight was used.

replicated by the SDA resulting in a range of performance from 18%–75% correct steps. The final preferred SDAs across astronauts were similar, although not exact. This suggests that motor output in response to the SDA can vary by person which is consistent with postflight readaptation response.

The visual disruption goggles were utilized as a means to reduce visual dependency and, therefore, alter motor output. However, even with this pre-emptive statement, the negative feedback received about the goggles suggests that replicating the sensory experience is important. On closer examination of the one astronaut that did include the visual disruption goggles in their final preferred SDA, tandem walk scores decreased relative to without the visual disruption goggles (SDA low level (R+1): 100%–65%; high level (R+0): 92%–18% correct steps). With the goggles, SDA performance for the high level (R+0) more closely resembled their actual postflight performance. However, for the low level (R+1) their SDA performance was much worse than their actual postflight performance where performance without the goggles more accurately represented postflight. Visual dependency was calculated for all astronauts in this study from the difference in preflight tandem walk scores between eyes open and closed. The absolute differences ranged from 11%–34% correct steps with the astronaut who included the visual disruption goggles in their final preferred SDA had a 12.5% correct step difference. This suggests they are on the lower end of visual dependency compared to the others in this study. Finally, when examining individual differences in tandem walk scores between the SDA and postflight performance, eyes open had larger differences up to 45% correct steps different in comparison to eyes closed with up to 18.9% correct steps different. Taken together, this suggests that a visual disruption could improve the SDA, however, it is unclear when a visual disruption should be included. If a visual disruption is to be used, it is clear that the disruption should better replicate the postflight sensory experience such as eliciting an exaggerated movement of the surrounding environment relative to the voluntary real head movement and/or including a time delay of movement of the surrounding environment (Harm and Parker, 1993). Further research is needed to provide similar illusory sensations more accurately such as through virtual or augmented reality.

While the results from this study were compiled from a small sample of astronauts, the subjective feedback from those who relatively recently experienced these difficult to describe sensations is invaluable. One limitation of this study is that not all test conditions (e.g., visual goggles alone) were tested. It is possible that the test sequence could have influenced the subjective evaluations. Therefore, the proposed SDA is presented as a starting framework for a portable analog that requires further validation. Without prompting, three of the five astronauts suggested that the non-head-coupled GVS profile alone could be a useful preflight training tool for first time flyers. The portable SDA allows for out-of-lab field testing and provides a relatively quick reversible disorientation (Dilda et al., 2014). The SDA may be useful in future investigations on spaceflight countermeasure testing and understanding adaptation and compensatory mechanisms of the broader vestibular loss community.

Data availability statement

The original contributions presented in the study are included in the article/Supplementary material, further inquiries can be directed to the corresponding author.

Ethics statement

The studies involving humans were approved by National Aeronautics and Space Administration Institutional Review Board. The studies were conducted in accordance with the local legislation and institutional requirements. The participants provided their written informed consent to participate in this study.

Author contributions

SM: Conceptualization, Data curation, Formal Analysis, Investigation, Methodology, Project administration, Visualization, Writing–original draft, Writing–review and editing. BP: Conceptualization, Writing–review and editing. TC: Conceptualization, Writing–review and editing. MS: Conceptualization, Writing–review and editing. SW: Conceptualization, Methodology, Supervision, Writing–review and editing.

Funding

The author(s) declare that financial support was received for the research, authorship, and/or publication of this article. Funding was provided by the National Aeronautics and Space Administration (NASA). The data reported here were from the NASA Human Research Program Directed Research (#15099) “Development of Sensorimotor Fitness for Duty Assessments Using Ground Analogs.”

Acknowledgments

The authors would like to thank the astronauts for their time and effort. The authors would also like to thank Marissa Rosenberg for her collaboration in conceiving the SDA, Aaron Allred for developing the GVS waveform profiles, and Erin Caldwell, Aaron Allred, and Yiri De Dios for their support in data collection.

Conflict of interest

SM was employed by Aegis Aerospace, Houston, TX, United States. BP was employed by KBR, Houston, TX.

The remaining authors declare that the research was conducted in the absence of any commercial or financial relationships that could be construed as a potential conflict of interest.

The author(s) declared that they were an editorial board member of Frontiers, at the time of submission. This had no impact on the peer review process and the final decision.

Publisher's note

All claims expressed in this article are solely those of the authors and do not necessarily represent those of their affiliated organizations, or those of the publisher, the editors and the reviewers. Any product that may be evaluated in this article, or claim that may be made by its manufacturer, is not guaranteed or endorsed by the publisher.

References

Bles, W., De Graaf, B., Bos, J. E., Groen, E., and Krol, J. R. (1997). A sustained hyper-g load as a tool to simulate space sickness. *J. Gravitational Physiology* 4, P1–P4.

Bloomberg, J. J., and Mulavara, A. P. (2003). Changes in walking strategies after spaceflight. *IEEE Eng. Med. Biol. Mag.* 22, 58–62. doi:10.1109/memb.2003.1195697

Browning, R. C., Modica, J. R., Kram, R., and Goswami, A. (2007). The effects of adding mass to the legs on the energetics and biomechanics of walking. *Med. Sci. Sports Exerc.* 39, 515–525. doi:10.1249/mss.0b013e31802b3562

Clément, G., Moudy, S. C., Macaulay, T. R., Bishop, M. O., and Wood, S. J. (2022). Mission-critical tasks for assessing risks from vestibular and sensorimotor adaptation during space exploration. *Front. Physiology* 13, 1029161. doi:10.3389/fphys.2022.1029161

Clement, G., and Wood, S. J. (2014). Rocking or rolling--perception of ambiguous motion after returning from space. *PLoS One* 9, e111107. doi:10.1371/journal.pone.0111107

Dilda, V., Morris, T. R., Yungher, D. A., Macdougall, H. G., and Moore, S. T. (2014). Central adaptation to repeated galvanic vestibular stimulation: implications for pre-flight astronaut training. *PLoS One* 9, e112131. doi:10.1371/journal.pone.0112131

Dixon, J. B., and Clark, T. K. (2020). Sensorimotor impairment from a new analog of spaceflight-altered neurovestibular cues. *J. Neurophysiol.* 123, 209–223. doi:10.1152/jn.00156.2019

Groen, E. L., Nooij, S. A., and Bos, J. E. (2008). Ground-based research on vestibular adaptation to g-level transitions. *Proc. Symposium Life Space Life Earth* 663.

Harm, D. L., and Parker, D. E. (1993). Perceived self-orientation and self-motion in microgravity, after landing and during preflight adaptation training. *J. Vestib. Res.* 3, 297–305. doi:10.3233/ves-1993-3310

Harm, D. L., Reschke, M. F., and Wood, S. J. (2015). "Spatial orientation and motion perception in microgravity," in *The cambridge handbook of applied perception research*. Editors R. R. HOFFMAN, P. A. HANCOCK, M. W. SCERBO, R. PARASURAMAN, and J. L. SZALMA (Cambridge, U.K.: Cambridge University Press).

Holbein, M. A., and Chaffin, D. B. (1997). Stability limits in extreme postures: effects of load positioning, foot placement, and strength. *Hum. Factors* 39, 456–468. doi:10.1518/001872097778827160

Lackner, J. R., and Dizio, P. (1992). Gravitoinertial force level affects the appreciation of limb position during muscle vibration. *Brain Res.* 592, 175–180. doi:10.1016/0006-8993(92)91673-3

Macaulay, T. R., Peters, B. T., Wood, S. J., Clement, G. R., Oddsson, L., and Bloomberg, J. J. (2021). Developing proprioceptive countermeasures to mitigate postural and locomotor control deficits after long-duration spaceflight. *Front. Syst. Neurosci.* 15, 658985. doi:10.3389/fnsys.2021.658985

Macdougall, H. G., Moore, S. T., Curthoys, I. S., and Black, F. O. (2006). Modeling postural instability with Galvanic vestibular stimulation. *Exp. Brain Res.* 172, 208–220. doi:10.1007/s00221-005-0329-y

Merfeld, D. M. (2003). Rotation otolith tilt-translation reinterpretation (ROTTR) hypothesis: a new hypothesis to explain neurovestibular spaceflight adaptation. *J. Vestib. Res.* 13, 309–320. doi:10.3233/ves-2003-134-615

Miller, C. A., Kofman, I. S., Brady, R. R., May-Phillips, T. R., Batson, C. D., Lawrence, E. L., et al. (2018). Functional task and balance performance in bed rest subjects and astronauts. *Aerosp. Med. Hum. Perform.* 89, 805–815. doi:10.3357/AMHP.5039.2018

Moore, S. T., Macdougall, H. G., Peters, B. T., Bloomberg, J. J., Curthoys, I. S., and Cohen, H. S. (2006). Modeling locomotor dysfunction following spaceflight with Galvanic vestibular stimulation. *Exp. Brain Res.* 174, 647–659. doi:10.1007/s00221-006-0528-1

Mulavara, A. P., Peters, B. T., Miller, C. A., Kofman, I. S., Reschke, M. F., Taylor, L. C., et al. (2018). Physiological and functional alterations after spaceflight and bed rest. *Med. Sci. Sports Exerc* 50, 1961–1980. doi:10.1249/MSS.0000000000001615

Nooij, S. A., and Bos, J. E. (2007). Sickness induced by head movements after different centrifugal G x-loads and durations. *J. Vestib. Res.* 17, 323–332. doi:10.3233/ves-2007-175-612

Oman, C. M. (2003). *Human visual orientation in weightlessness. Levels of perception*. New York: Springer.

Pandiarajan, M., and Hargens, A. R. (2020). Ground-based analogs for human spaceflight. *Front. Physiology* 11, 716. doi:10.3389/fphys.2020.00716

Peters, B. T., Miller, C. A., Brady, R. A., Richards, J. T., Mulavara, A. P., and Bloomberg, J. J. (2011). Dynamic visual acuity during walking after long-duration spaceflight. *Aviat. Space Environ. Med.* 82, 463–466. doi:10.3357/asem.2928.2011

Reschke, M. F., and Clément, G. (2018). Verbal reports of neurovestibular symptoms in astronauts after short-duration space flight. *Acta Astronaut.* 152, 229–234. doi:10.1016/j.actaastro.2018.08.028

Reschke, M. F., Good, E. F., and Clément, G. R. (2017). Neurovestibular symptoms in astronauts immediately after space shuttle and international space station missions. *OTO open* 1, 2473974X17738767. doi:10.1177/2473974X17738767

Reschke, M. F., Kozlovskaya, I. B., Lysova, N., Kitov, V., Rukavishnikov, I., Kofman, I. S., et al. (2020). Joint Russian-USA Field Test: implications for deconditioned crew following long duration spaceflight. *Aerosp. Environ. Med.* 54, 94–100. doi:10.21687/0233-528x-2020-54-6-94-100

Reschke, M. F., Wood, S. J., and Clément, G. R. (2018). Effect of spaceflight on the spatial orientation of the vestibulo-ocular reflex during eccentric roll rotation: a case report. *J. Vestib. Res.* 27, 243–249. doi:10.3233/VES-170631

Ross, H. E. (1998). Astronaut's perception of heaviness and limb position. *Hum. Perform. extreme Environ.* 3, 34–36.

Ryder, J. W., Buxton, R. E., Goetchius, E., Scott-Pandorf, M., Hackney, K. J., Fiedler, J., et al. (2013). Influence of muscle strength to weight ratio on functional task performance. *Eur. J. Appl. Physiol.* 113, 911–921. doi:10.1007/s00421-012-2500-z

Shibata, H., Gyoba, J., and Takeshima, Y. (2012). Perception of the end position of a limb loaded with a weight. *Atten. Percept. Psychophys.* 74, 225–238. doi:10.3758/s13414-011-0232-5

Walsh, L. D., Hesse, C. W., Morgan, D. L., and Proske, U. (2004). Human forearm position sense after fatigue of elbow flexor muscles. *J. Physiology* 558, 705–715. doi:10.1113/jphysiol.2004.062703

Welch, R. B., Hoover, M., and Southward, E. F. (2009). Cognitive performance during prismatic displacement as a partial analogue of "space fog". *Aviat. space, Environ. Med.* 80, 771–780. doi:10.3357/asem.2415.2009

Widener, G. L., Conley, N., Whiteford, S., Gee, J., Harrell, A., Gibson-Horn, C., et al. (2020). Changes in standing stability with balance-based torso-weighting with cerebellar ataxia: a pilot study. *Physiother. Res. Int.* 25, e1814. doi:10.1002/pri.1814

Winter, J., Allen, T. J., and Proske, U. (2005). Muscle spindle signals combine with the sense of effort to indicate limb position. *J. physiology* 568, 1035–1046. doi:10.1113/jphysiol.2005.092619

Wood, S. J. (2002). Human otolith-ocular reflexes during off-vertical axis rotation: effect of frequency on tilt-translation ambiguity and motion sickness. *Elsevier Neurosci. Lett.* 323, 41–44. doi:10.1016/s0304-3940(02)00118-0

Wood, S. J., Paloski, W. H., and Clark, J. B. (2015). Assessing sensorimotor function following ISS with computerized dynamic posturography. *Aerosp. Med. Hum. Perform.* 86, A45–A53. doi:10.3357/AMHP.EC07.2015

frontiers | Frontiers in Physiology

TYPE Original Research
PUBLISHED 27 May 2024
DOI 10.3389/fphys.2024.1374309

OPEN ACCESS

EDITED BY
Marc-Antoine Custaud,
Université d'Angers, France

REVIEWED BY
Ronan Padraic Murphy,
Dublin City University, Ireland
Marc Kermorgant,
INSERM U1048 Institut des Maladies Métaboliques et Cardiovasculaires, France

*CORRESPONDENCE
Adel B. Elmoselhi,
amoselhi@sharjah.ac.ae

RECEIVED 21 January 2024
ACCEPTED 13 May 2024
PUBLISHED 27 May 2024

CITATION
Elmoselhi AB, Shankhwar V, Qaisar R, Hamoudi R, Brix B, Salon A and Goswami N (2024), Retinal vascular changes and arterial stiffness during 8-month isolation and confinement: the SIRIUS-21 space analog mission.
Front. Physiol. 15:1374309.
doi: 10.3389/fphys.2024.1374309

Retinal vascular changes and arterial stiffness during 8-month isolation and confinement: the SIRIUS-21 space analog mission

Adel B. Elmoselhi[1,2]*, Vishwajeet Shankhwar[3], Rizwan Qaisar[1,2], Rifat Hamoudi[1,2,4], Bianca Brix[5], Adam Salon[5,6] and Nandu Goswami[3,5]

[1]College of Medicine, University of Sharjah, Sharjah, United Arab Emirates, [2]Research Institute for Medical and Health Sciences, University of Sharjah, Sharjah, United Arab Emirates, [3]Mohammed Bin Rashid University of Medicine and Health Sciences (MBRU), Dubai, United Arab Emirates, [4]Division of Surgery and Interventional Science, University College London, London, United Kingdom, [5]Division of Physiology and Pathophysiology, Otto Loewi Research Center for Vascular Biology, Immunology, and Inflammation, Medical University of Graz, Graz, Austria, [6]Faculty of Health and Social Sciences, Inland Norway University of Applied Sciences, Lillehammer, Norway

Introduction: Isolation and confinement are significant stressors during space travel that can impact crewmembers' physical and mental health. Space travel has been shown to accelerate vascular aging and increase the risk of cardiovascular and cerebrovascular disorders. However, the effect of prolonged isolation and confinement on microvascular function has not yet been thoroughly investigated.

Methods: Retinal vascular imaging was conducted on four crewmembers during- and post-8-month SIRIUS-21 space analog mission. Central retinal arteriolar equivalent (CRAE), central retinal venular equivalent (CRVE), and arteriovenous ratio (AVR) were measured. Pulse wave velocity (PWV), an indicator of arterial stiffness, was also measured.

Results: Data from 4 participants was analyzed. These participants had a mean age of 34.75 ± 5.44 years, height of 170.00 ± 2.00 cm, weight of 74.50 ± 12.53 kg, and average BMI of 25.47 ± 3.94 kg/m^2. During- and post-isolation, average CRVE showed an upward trend (Pearson's r 0.784, R-square 0.62), suggesting a dilation of retinal venules, while AVR showed a downward trend (Pearson's r −0.238, R-square 0.057), which is suggestive of a higher risk of cardiovascular and cerebrovascular dysfunctions. But neither of these trends were statistically significant. Additionally, the average PWV showed an upward trend during- and after-isolation across all crew members.

Conclusion: Isolation and confinement appear to contribute towards retinal vascular damage and arterial stiffness. This cautiously suggests an increased risk of cardiovascular and cerebrovascular disorders due to the contribution of the isolation in space flight. Further studies are needed to confirm and expand on these results as we prepare for future manned missions to the Moon and Mars.

KEYWORDS

isolation and confinement, cardiovascular and cerebrovascular disorders, SIRIUS-21, space flight, retinal vasculature, analog mission

Introduction

Space travel exposes crew members to various stressors such as microgravity, radiation as well as isolation and confinement. Consequently, there are multiple deleterious effects of these stressors on several organs systems of the space travelers, including cardiovascular and cerebrovascular disorders. However, the causes and mechanisms underlying those disorders in isolation, confined and extreme environments (ICE) are not fully understood. To dissect out the effect of these stressors on vascular health, we studied the effect of long-term isolation and confinement on the changes of retinal blood vessels and arterial stiffness, during- and post-8-month Scientific International Research in Unique terrestrial Station (SIRIUS) analog mission.

Isolation and confinement, in general, are inherent stressors that can significantly perturb human physiology, as they are associated with increased activation of stress pathways (Pagel and Chouker, 2016). Among various physiological systems, the human vasculature is particularly vulnerable to the effects of neuronal and hormonal stress (Schakman et al., 2013; Cacioppo et al., 2015). SIRIUS-21 space analog mission offered an excellent opportunity to investigate the impact of these stressors on human vasculature in a controlled environment, which mimicked the isolation of spaceflight. Previous studies have demonstrated that confinement and isolation during the MARS-500 mission resulted in pathological structural changes in peripheral vasculature (Arbeille et al., 2014). However, the effects of isolation and confinement on microvascular functions and arterial stiffness in long-duration missions have not been fully explored.

The purpose of this study is to investigate the changes in microvascular functions and arterial stiffness that occur during an 8-month SIRIUS analog mission and how long it took the variables to return to baseline values following the isolation. We used non-invasive clinical diagnostic methods such as the Pulse Wave Velocity (PWV) to assess vascular stiffness and measured the retinal microvasculature changes, including the Central Retinal Arteriolar Equivalent (CRAE), the Central Retinal Venular Equivalent (CRVE), and the arteriovenous ratio (AVR) during- and after-isolation. The vascular retinal measurements reflect cardiovascular and cerebrovascular microvasculature beds. In particular, decreases in AVR predict development of cerebral atrophy, stroke and other cardiovascular events in adults (French et al., 2022).

The findings of this study help us better understand the effects of ICE on microvasculature. This research is important as we plan for ambitious manned missions to the Moon and Mars. Similarly, the knowledge gained from such studies can be important in developing effective countermeasures to mitigate negative effects of isolation and confinement on human physiology.

Materials and methods

Study design and population

The study was conducted jointly by Roscosmos, NASA, and Mohammed Bin Rashid Space Centre (MBRSC), Dubai at the refurbished isolation facility located at the Institute of Biomedical Problems (IBMP) in Moscow, Russia between 4 November 2021, until 3 July 2022. The current study was one of multiple projects in an international large study named SIRIUS-21. The investigation of the effects of 8-month of confinement initially started with a group of six crewmembers. Following 33 days from the beginning of the mission, one of the crewmembers withdrew because of an unexpected health issue following a minor arm injury during exercise. However, the mission was completed with the remaining crew (three men and two women) including Russian, American and Arab background participants. The recruitment and the inclusion and exclusion criteria with healthy young and middle age healthy individuals, which were selected by IBMP leadership scientific team, in collaboration with NASA and MBRSC. During the 8-month confinement period, the crew members resided in a cylindrical module with a volume of 500 m^3, engaging in experimental scientific activities that involved moderate physical exertion (Schneider et al., 2013). They lived in conditions similar to those on Earth, though within a restricted space. Throughout the duration, the subjects maintained limited yet regular contact with the control center. Out of the nine measurement time points conducted during the mission (DM), seven were found reliable and analyzed on days 68–69 (DM3), day 93–95 (DM 4), day 109–111 (DM 5), day 154–156 (DM6), day 180–182 (DM7), day 222–224 (DM8), day 238–239 (DM9). Additionally, two post-mission (PM) time points were measured on 4–7 (PM1), and day 13–14 (PM2) as shown in Table 2.

Assessment of vascular stiffness

Rates of the movement of the pressure waves were used to assess pulse wave velocity (PWV) using Vicorder device. The device measures the velocity of waves transmitted between two points across the walls of the large carotid and femoral arteries. Operating in connection with a laptop software program, the device analyzes the waveform, delivering the speed measurement in meters per second (m/s). After a period of 20 min in a supine position to ensure relaxation, the assessment of PWV was undertaken. The detailed guidelines for using the Vicorder device have reported earlier (McGreevy et al., 2013).

Non-invasive retinal vessel's assessment

Retinal images were collected serially with a non-mydriatic hand-held retinal camera (Optomed, Finland) according to the study protocol. Trained graders from crew members have performed vessel measurements on the optic disc–centered image of the right eye. For detailed processing of retinal images see methods in Saloň et al. (2023). The image analysis was done using the IVAN software (University of Wisconsin, Madison, WI). This approach has previously been used in other population-based studies (Chandra et al., 2019).

Ethics statement and informed consent

The study incorporated human participants and received thorough evaluation and endorsement from the Bioethical

TABLE 1 Demographics of the four crew members completed the mission.

S. No	Sex	Age (years)	Height (cm)	Weight (kg)	BMI
CM-1	F	33	168	67	23.7
CM-2	F	30	172	67	22.6
CM-3	M	44	172	96	32.4
CM-4	M	32	168	68	24.1

CM, crew member; F, female; M, male; BMI, Body Mass Index (kg/m^2).

Commission at the Institute of Biomedical Problems of the Russian Academy of Sciences (Protocol No. 539 of 17 March 2020). The study fully adhered to the tenets outlined in the Declaration of Helsinki.

Each study participant voluntarily signed an informed consent after they were comprehensively briefed on the potential risks, advantages, and objectives of the forthcoming research.

Results

The present study was conducted with a total of 5 adult participants. However, due to data artifacts in 1 participant, the analysis and presentation below only involved 4 participants. These participants had a mean age of 34.75 ± 5.44 years, height of 170.00 ± 2.00 cm, weight of 74.50 ± 12.53 kg, and average BMI of 25.47 ± 3.94 kg/m^2, as shown in Table 1.

Retinal arteriolar and venular diameters

Figure 1A shows the Central Retinal Arteriolar Equivalent (CRAE) in seven time points during mission/isolation (DM) and two times points post mission/isolation (PM) for four crew members separately and their means measured. The mean of all CRAE (μm) time points shows an upward trend with a slope of 0.661 ± 0.83, Pearson's r 0.332 and R-square 0.11 (Figure 1B). Similarly, the CRVE values (μm) are shown in Figure 1C during mission/isolation and post mission/isolation. Figure 1D shows a steeper upward elevation of CRVE with the slope of 1.676 ± 0.59, stronger correlation with Pearson's r 0.784, and a higher R square 0.62 compared to CRAE.

Retinal arteriovenous ratio

Figure 1E shows the AVR at all seven time points during the mission/isolation (DM) and two time points post mission/isolation (PM) for four crew members separately as well as their average. Figure 1F shows the average AVR across all time points, which exhibits a downward trend with a slope of −0.00294 ± 0.005. In addition, the figure shows Pearson's r of–0.238 and R-square of 0.057 which indicate a weak negative correlation between time and AVR, which means that as time goes on, there is a slight decrease in AVR. The actual values for the AVR during- and post-mission/isolation as well as their average are in Table 2. We used linear regression analysis as is depicted in Table 3. It appears that only crew member # 2 showed a statistically significant decrease trend over time, while the other crew members and the average did not show statistically significant trends. The t-value for crew member #2 is −0.624, which is significant at a 5% significance level (p-value = 0.036).

Assessment of vascular stiffness

The arterial stiffness was measured using pulse wave velocity (PWV) of the four crew members and their average, as shown in Figure 2A, during mission/isolation. However, a few data were not counted in the study due to the presence of artifact in them. Thus, fewer measurements were included in calculation. Figure 2B shows the average of all PWV (m/s) time points with an upward trend with a positive linear relationship between independent variable during mission and post mission with intercept = −1.081, slope 0.914.

Discussion

Our study focused on its effect of 8-month isolation and confinement on small retinal vessels as well as vascular stiffness of larger vessels. Our results indicate a decreasing trend (although not statistically significance) of the average retinal arteriolar-to-venular diameter ratio (AVR) due to retinal venular dilation during and post isolation, suggesting an increased risk of several health conditions, including cardiovascular disease, stroke, hypertension, and, potentially, dementia. Additionally, we observed an increasing trend (again not statistically significance) in pulse wave velocity, indicating a tendency toward vascular stiffness and a higher risk for cardiovascular diseases.

The vascular dysfunction tendency observed in our study is consistent with a previous study of isolation and confinement in the MARS-500 mission conducted in the same facility. Using echography in this study, Arbeille et al. (2014), have shown that the retinal vessel intima media thickness, but not the diameters, were significantly increased (14%–28%, $p < 0.05$) during isolation and immediately post-isolation in all six crew members. Monitoring changes in the retinal blood vessels is critical for the early detection and management of various cardiovascular and cerebrovascular disorders. An excellent meta-analysis has previously reported the predictive value of retinal vessel diameters for incident stroke in multiple large cohort studies (Streese et al., 2020). A follow-up period of 5–12 years documented a total of 945 stroke incidents (4.5%), revealing that wider venular diameters were associated with a higher incidence of stroke. The data indicated that for every 20 μm

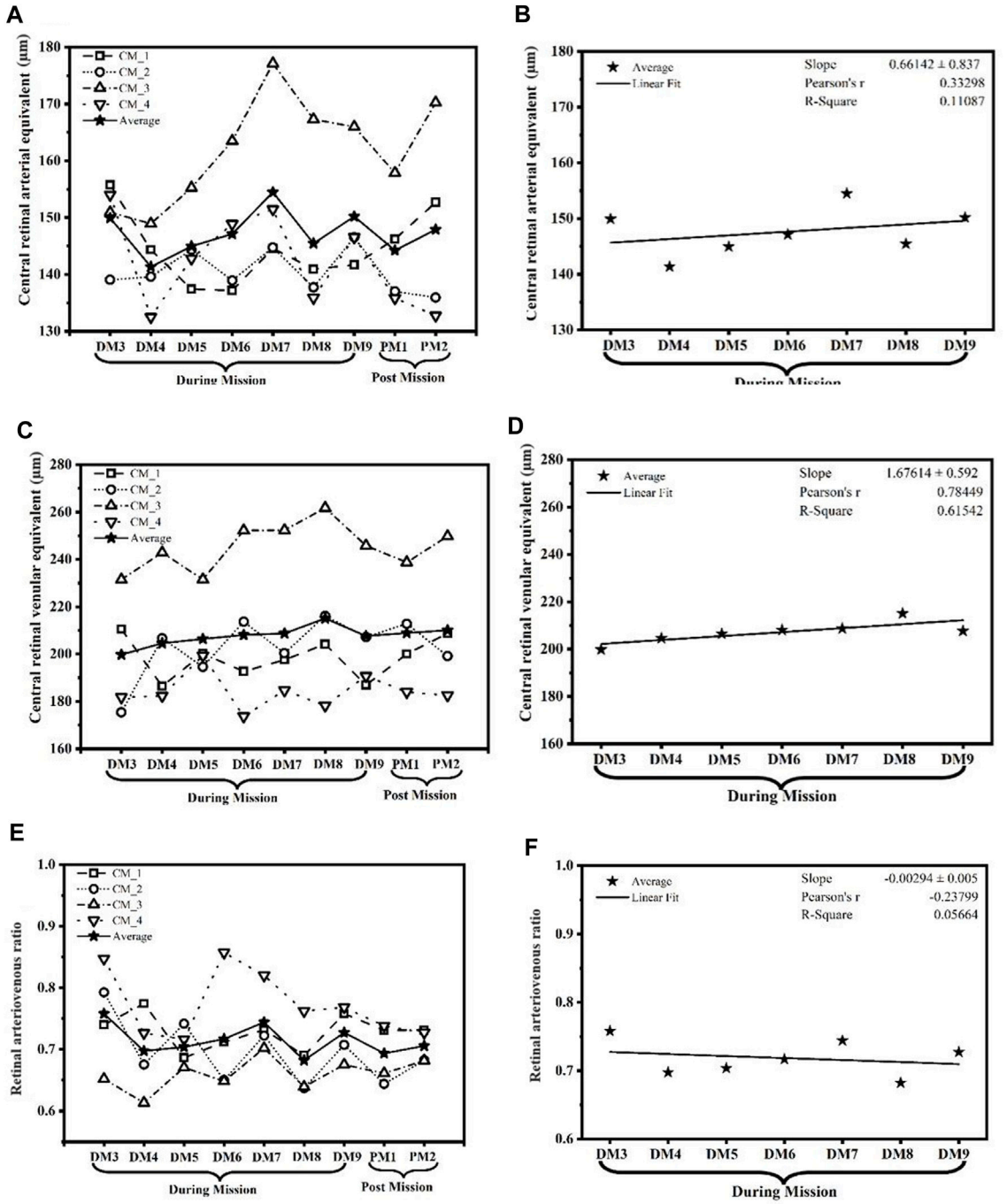

FIGURE 1
The graph showcases the temporal changes and potential tendencies in **(A,B)** central retinal arteriolar equivalent (CRAE) in µm; **(C,D)** central retinal venular equivalent (CRVE) in µm; and **(E,F)** arteriovenous ratio (AVR). These parameters were measured across the duration of the SIRIUS-21 mission, illustrating potential trends that signify the impact of isolation and confinement on retinal vasculature. (CM, Crew member; DM, During mission; PM, Post mission).

increase in venular diameter, the risk of stroke increased by 15%, with no significant correlation to arteriolar diameter, according to the Rotterdam Scan Study (McGeechan et al., 2009). This study concluded that venular dilation warrants further attention, as it could provide new insights into the pathophysiology of cerebral small vessel disease, echoing the suggestions made by our findings. Relevant to the limited physical activity in the isolated and confined conditions experienced by our participants, a wider CRVE (Central Retinal Vein Equivalent) was observed in sedentary individuals at risk compared to healthy ones, a finding supported by several other studies that described the impact of exercise on retinal vessel diameters (Hanssen et al., 2011; Streese et al., 2019). Consequently, an optimized and enhanced physical exercise program may be necessary in isolated environments during

TABLE 2 The arterio-venular ratio of the retinal images analysis in each crew member and their averages in various time points during and post mission/isolation.

Participant	DM3	DM4	DM5	DM 6	DM7	DM8	DM9	PM1	PM2
CM-1	0.739946	0.774305	0.6864	0.711838	0.731762	0.690208	0.75794	0.730906	0.731276
CM-2	0.792701	0.675404	0.741695	0.650148	0.722413	0.637196	0.707341	0.643787	0.682582
CM-3	0.65206	0.613222	0.670512	0.64823	0.702036	0.639206	0.675268	0.66115	0.681595
CM-4	0.847261	0.726646	0.716217	0.857117	0.820063	0.762225	0.768329	0.738282	0.727212
Average	0.757992	0.697394	0.703706	0.716833	0.744069	0.682209	0.727219	0.693531	0.705666

CM, crew member; DM, during mission; PM, post mission.

TABLE 3 Linear regression analysis of retinal images. Only CM_2 (crew member 2) shows a statistically significant decreasing trend over time (p-value = 0.0359), while the other crew members and the average do not show statistically significant trends.

Participant	Slope	Intercept	Correlation coefficient	T-value	p-value
CM-1	−0.000246904	0.7320885	−0.035427704	−0.06478998	0.949792461
CM-2	−0.002688155	0.7460516	−0.183576128	−0.62356398	*0.035865034
CM-3	0.001642172	0.6477883	0.057988743	0.188463818	0.856356767
CM-4	0.004338102	0.4583304	0.478190867	1.428220161	0.195829728
Average	0.000429559	0.7023972	0.122088976	0.469355064	0.649776546

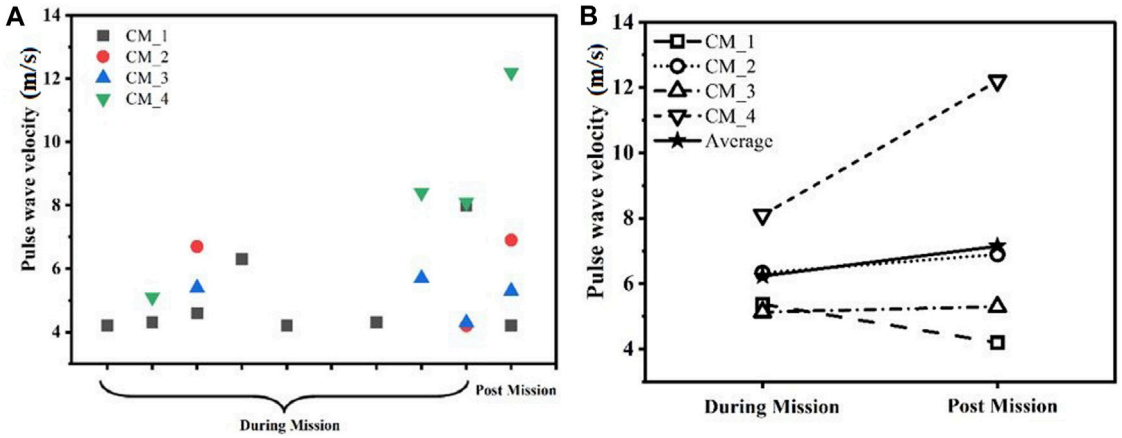

FIGURE 2
The graph showcases the **(A)** changes and **(B)** potential tendencies in pulse wave velocity (PWV). PWV (m/s) was measured across the duration of the SIRIUS-21 mission. (CM, Crew member; DM, During mission; PM, Post mission).

prolonged spaceflight. Additionally, CRVE widening has been associated with inflammatory states related to obesity, diabetes, and dyslipidemia, all of which may correlate with our findings but require further future investigations (Ikram et al., 2004; Liu et al., 2021). Although challenging to fully explain, the tendency for CRAE dilation rather than narrowing, potentially induced by stress in our isolated environment, is notable. This is especially significant since previous reports have linked CRAE narrowing with hypertension and endothelial dysfunction, both precursors to atherosclerosis and increased cardiovascular disease risk (Chew et al., 2012). For instance, a 16-year follow-up study among several others provided evidence that CRAE narrowing and CRVE widening were associated with a higher incidence of heart failure in both men and women (Chandra et al., 2019). The exact relationships between various retinal vascular parameters (CRAE, CRVE, and AVR) and the increased risk of cardiovascular disorders are not fully understood and required further investigations. However, in line with our findings, a decrease in the Arteriovenous Ratio (AVR) has consistently been observed in the majority of studies as a useful parameter for stratifying cardiovascular risk in patients (French et al., 2022).

Several cellular and molecular mechanisms have been shown to result in changes in retinal arteriolar and venular caliber (CRAE and CRVE) and arteriolar-to-venular ratio (AVR), especially during aging,

and increased cardiovascular risk. These mechanisms include increased endothelin levels, reactive oxygen species, inflammation, insulin resistance, visceral adiposity, blood pressure, as well as decreased nitric oxide (NO) and other vasodilators, and endothelial progenitor cells (EPCs) (Wong et al., 2001; Gu et al., 2016; Hanssen et al., 2022).

Arterial stiffness has been shown to occur after a 6-month stay on the International Space Station. In both male and female astronauts, post-flight data showed up to 17%–30% changes in β-stiffness index (p = 0.006) as compared to preflight data (Hughson et al., 2016). Beside the effect of microgravity on inducing arterial stiffness in this study, a portion of this stiffness could be due to the stress induced by isolation and confinement, which would be consistent with the trend in our study that needs to be verified further in future and larger studies.

The limitation of our study is the smaller sample size, which is a common challenge in space-related studies. Therefore, further studies involving more participants are needed to confirm our results and achieve statistical significance, and to possibly elucidate the underlying mechanisms. In addition, some artifact data points were noticed due to, most likely, errors and unexperienced crew members in conducting the measurements. Thus, we considered only the reliable data points to draw most accurate conclusion.

Taken together, our results suggest that during 8-month isolation period of the SIRIUS analog mission, there is a trend of lower AVR and increased CRVE, which predicts a higher tendency for crew members to experience cerebrovascular and cardiovascular events in the future. The steeper upward elevation of CRVE with the slope of 1.676 ± 0.59, stronger correlation with Pearson's r 0.784 compared to CRAE. These results revealed a stronger connection between CRVE and time points relative to the CRAE. This aspect of our conclusion should be interpreted with caution until further studies can verify it. Furthermore, our findings indicate a potential increase in vascular stiffness during and after the 8-month isolation period. This trend of higher arterial stiffness at the end of the mission may also place these analog participants at higher risk of cardiovascular diseases. Overall, our findings underscore the importance of investigating the effects of isolation and confinement on vasculature and highlight the need for continued research in this area as we work towards the goal of manned missions to Mars and beyond.

Data availability statement

The original contributions presented in the study are included in the article/Supplementary material, further inquiries can be directed to the corresponding author.

Ethics statement

The studies involving humans were approved by the BIOMEDICINE ETHICS COMMITTEE of the RF SRC–Institute of Biomedical Problems, Russian Academy of Sciences/Physiology Section of the Russian Bioethics Committee, Russian Federation National Commission for UNESCO, under Protocol No. 539 on 17 March 2020. The studies were conducted in accordance with the local legislation and institutional requirements. The participants provided their written informed consent to participate in this study.

Author contributions

AE: Conceptualization, Formal Analysis, Funding acquisition, Project administration, Supervision, Writing–original draft. VS: Data curation, Formal Analysis, Software, Writing–review and editing. RQ: Validation, Visualization, Writing–review and editing. RH: Validation, Visualization, Writing–review and editing. BB: Data curation, Methodology, Validation, Visualization, Writing–review and editing. AS: Data curation, Formal Analysis, Software, Writing–review and editing. NG: Conceptualization, Formal Analysis, Resources, Supervision, Writing–original draft.

Funding

The author(s) declare that financial support was received for the research, authorship, and/or publication of this article. This study was supported by MBRSC (Mohammed Bin Rashid Space Centre), Dubai, UAE, contract number: CO- 21- 0034. Project PI, ABE.

Acknowledgments

We would like to sincerely thank the whole team at the Institute of Biomedical Problems (IBMP) facilities and all the crewmembers of SIRIUS 21 space analog mission.

Conflict of interest

The authors declare that the research was conducted in the absence of any commercial or financial relationships that could be construed as a potential conflict of interest.

Publisher's note

References

Arbeille, P., Provost, R., Vincent, N., and Aubert, A. (2014). Adaptation of the main peripheral artery and vein to long term confinement (Mars 500). *PLoS One* 9 (1), e83063. doi:10.1371/journal.pone.0083063

Cacioppo, J. T., Cacioppo, S., Capitanio, J. P., and Cole, S. W. (2015). The neuroendocrinology of social isolation. *Annu. Rev. Psychol.* 66, 733–767. doi:10.1146/annurev-psych-010814-015240

Chandra, A., Seidelmann, S. B., Claggett, B. L., Klein, B. E., Klein, R., Shah, A. M., et al. (2019). The association of retinal vessel calibres with heart failure and long-term alterations in cardiac structure and function: the Atherosclerosis Risk in Communities (ARIC) Study. *Eur. J. Heart Fail* 21, 1207–1215. doi:10.1002/ejhf.1564

Chew, S. K. H., Xie, J., and Wang, J. J. (2012). Retinal arteriolar diameter and the prevalence and incidence of hypertension: a systematic review and meta-analysis of their association. *Curr. Hypertens. Rep.* 14, 144–151. doi:10.1007/s11906-012-0252-0

French, C., Cubbidge, R. P., and Heitmar, R. (2022). The application of arterio-venous ratio (AVR) cut-off values in clinic to stratify cardiovascular risk in patients. *Ophthalmic Physiol. Opt.* 42, 666–674. doi:10.1111/opo.12967

Gu, Y. M., Petit, T., Wei, F. F., Thijs, L., Jacobs, L., Zhang, Z. Y., et al. (2016). Renal glomerular dysfunction in relation to retinal arteriolar narrowing and high pulse pressure in seniors. *Hypertens. Res.* 39, 138–143. doi:10.1038/hr.2015.125

Hanssen, H., Nickel, T., Drexel, V., Hertel, G., Emslander, I., Sisic, Z., et al. (2011). Exercise-induced alterations of retinal vessel diameters and cardiovascular risk reduction in obesity. *Atherosclerosis* 216 (2), 433–439. doi:10.1016/j.atherosclerosis.2011.02.009

Hanssen, H., Streese, L., and Vilser, W. (2022). Retinal vessel diameters and function in cardiovascular risk and disease. *Prog. Retin Eye Res.* 91, 101095. doi:10.1016/j.preteyeres.2022.101095

Hughson, R. L., Robertson, A. D., Arbeille, P., Shoemaker, J. K., Rush, J. W., Fraser, K. S., et al. (2016). Increased postflight carotid artery stiffness and inflight insulin resistance resulting from 6-mo spaceflight in male and female astronauts. *Am. J. Physiol. Heart Circ. Physiol.* 310 (5), H628–H638. doi:10.1152/ajpheart.00802.2015

Ikram, M. K., de Jong, F. J., Vingerling, J. R., Witteman, J. C., Hofman, A., Breteler, M. M., et al. (2004). Are retinal arteriolar or venular diameters associated with markers for cardiovascular disorders? The Rotterdam Study. *Invest. Ophthalmol. Vis. Sci.* 45 (7), 2129–2134. doi:10.1167/iovs.03-1390

Liu, M., Lovern, C., Lycett, K., He, M., Wake, M., Wong, T. Y., et al. (2021). The association between markers of inflammation and retinal microvascular parameters: a systematic review and meta-analysis. *Atherosclerosis* 336, 12–22. doi:10.1016/j.atherosclerosis.2021.09.025

McGeechan, K., Liew, G., Macaskill, P., Irwig, L., Klein, R., Klein, B. E., et al. (2009). Prediction of incident stroke events based on retinal vessel caliber: a systematic review and individual-participant meta-analysis. *Am. J. Epidemiol.* 170 (11), 1323–1332. doi:10.1093/aje/kwp306

McGreevy, C., Barry, M., Bennett, K., and Williams, D. (2013). Repeatability of the measurement of aortic pulse wave velocity (aPWV) in the clinical assessment of arterial stiffness in community-dwelling older patients using the Vicorder(®) device. *Scand. J. Clin. Lab. Invest.* 73 (4), 269–273. doi:10.3109/00365513.2013.770162

Pagel, J. I., and Chouker, A. (2016). Effects of isolation and confinement on humans-implications for manned space explorations. *J. Appl. Physiol. (1985)* 120 (12), 1449–1457. doi:10.1152/japplphysiol.00928.2015

Saloň, A., Steuber, B., Neshev, R., Schmid-Zalaudek, K., De Boever, P., Bergmann, E., et al. (2023). Vascular responses following light therapy: a pilot study with healthy volunteers. *J. Clin. Med.* 12, 2229. doi:10.3390/jcm12062229

Schakman, O., Kalista, S., Barbé, C., Loumaye, A., and Thissen, J. P. (2013). Glucocorticoid-induced skeletal muscle atrophy. *Int. J. Biochem. Cell Biol.* 45 (10), 2163–2172. doi:10.1016/j.biocel.2013.05.036

Schneider, S., Abeln, V., Popova, J., Fomina, E., Jacubowski, A., Meeusen, R., et al. (2013). The influence of exercise on prefrontal cortex activity and cognitive performance during a simulated space flight to Mars (MARS500). *Behav. Brain Res.* 236 (1), 1–7. doi:10.1016/j.bbr.2012.08.022

Streese, L., Guerini, C., Bühlmayer, L., Lona, G., Hauser, C., Bade, S., et al. (2020). Physical activity and exercise improve retinal microvascular health as a biomarker of cardiovascular risk: a systematic review. *Atherosclerosis* 315, 33–42. doi:10.1016/j.atherosclerosis.2020.09.017

Streese, L., Suades, R., Cosentino, F., and Hanssen, H. (2019). Exercise-induced improvement of microvascular phenotype and reprogramming of p66Shc DNA methylation. *Eur. Heart J.* 40 (48), 3948–3949. doi:10.1093/eurheartj/ehz830

Wong, T. Y., Klein, R., Couper, D. J., Cooper, L. S., Shahar, E., Hubbard, L. D., et al. (2001). Retinal microvascular abnormalities and incident stroke: the atherosclerosis risk in communities study. *Lancet* 358 (9288), 1134–1140. doi:10.1016/S0140-6736(01)06253-5

frontiers | Frontiers in Physiology

TYPE Brief Research Report
PUBLISHED 14 June 2024
DOI 10.3389/fphys.2024.1360353

OPEN ACCESS

EDITED BY
Elena S. Tomilovskaya,
Russian Academy of Sciences (RAS), Russia

REVIEWED BY
Catherine M. Davis,
Uniformed Services University of the Health Sciences, United States
Giuseppe Barisano,
Stanford University, United States

*CORRESPONDENCE
Ford Burles,
cfburles@ucalgary.ca

RECEIVED 22 December 2023
ACCEPTED 21 May 2024
PUBLISHED 14 June 2024

CITATION
Burles F, Willson M, Townes P, Yang A and Iaria G (2024), Preliminary evidence of high prevalence of cerebral microbleeds in astronauts with spaceflight experience. *Front. Physiol.* 15:1360353. doi: 10.3389/fphys.2024.1360353

Preliminary evidence of high prevalence of cerebral microbleeds in astronauts with spaceflight experience

Ford Burles[1,2]*, Morgan Willson[3], Parker Townes[1,2], Allison Yang[1,2] and Giuseppe Iaria[1,2]

[1]Canadian Space Health Research Network, Calgary, AB, Canada, [2]Neurolab, Department of Psychology, University of Calgary, Calgary, AB, Canada, [3]Departments of Radiology and Clinical Neurosciences, Cumming School of Medicine, University of Calgary, Calgary, AB, Canada

Long-duration spaceflight poses a variety of health risks to astronauts, largely resulting from extended exposure to microgravity and radiation. Here, we assessed the prevalence and incidence of cerebral microbleeds in sixteen astronauts before and after a typical 6-month mission on board the International Space Station Cerebral microbleeds are microhemorrhages in the brain, which are typically interpreted as early evidence of small vessel disease and have been associated with cognitive impairment. We identified evidence of higher-than-expected microbleed prevalence in astronauts with prior spaceflight experience. However, we did not identify a statistically significant increase in microbleed burden up to 7 months after spaceflight. Altogether, these preliminary findings suggest that spaceflight exposure may increase microbleed burden, but this influence may be indirect or occur over time courses that exceed 1 year. For health monitoring purposes, it may be valuable to acquire neuroimaging data that are able to detect the occurrence of microbleeds in astronauts following their spaceflight missions.

KEYWORDS

susceptibility weighted imaging (SWI), MRI, cerebral amyloid angiopathy (CAA), cerebrovascular, brain structure

Introduction

Forthcoming manned lunar missions, as well as prospective manned missions to Mars, underscore the importance of a deep understanding of both the short and long-term effects of spaceflight on astronauts's health and wellbeing. Two salient environmental features present in spaceflight, microgravity and radiation exposure, are both known to produce medically-relevant changes to astronaut health. For instance, microgravity-induced bone density losses (Stavnichuk et al., 2020), muscle atrophy (Comfort et al., 2021), neuro-ophthalmic damage (Lee et al., 2020), and radiation-related cancer risks (Azzam et al., 2012) are all well-known health risks astronauts face during and following a spaceflight.

In addition to these risks, both prolonged microgravity exposure and increased exposure to ionizing radiation can produce a suite of changes to cardiovascular structure and function. Microgravity produces a cephalic fluid shift, diminished postflight orthostatic tolerance, cardiac arrhythmias (Anzai et al., 2014), arterial stiffening (Hughson et al., 2016), and potentially increases in intracranial pressure (Lawley et al., 2017), among other effects (Demontis et al., 2017). Increased exposure to

ionizing radiation has also been shown to increase the risk of cardiovascular disease, by exacerbating atherosclerotic processes (Koutroumpakis et al., 2022), producing structural damage to blood vessels (Kuzichkin et al., 2022) and exacerbating microgravity-related thrombosis risks (Marshall-Goebel et al., 2019).

More recently, researchers have identified cerebral microbleeds (CMBs) as potential indicators of damage resulting from the cerebrovascular risks associated with spaceflight (Hähnel, 2020; Miller et al., 2022). Cerebral microbleeds are microhemorrhages (<10 mm in diameter) in the brain, producing covert lesions, and are visible as small hypointense foci on T_2*-weighted gradient-recalled echo (GRE) and similar MRI sequences (Puy et al., 2021). Cerebral microbleeds represent powerful markers to identify the type and magnitude of small vessel disease, and are associated with an increased risk of cognitive impairment (Poels et al., 2012), stroke (Akoudad et al., 2015), and mortality (Akoudad et al., 2013). Importantly, they are considered early disease markers, often appearing in otherwise asymptomatic individuals before evidence of more serious morbidity (Igase et al., 2009).

Scientific investigation of small vessel disease typically focuses on the presence, quantity, and spatial location of cerebral microbleeds. With respect to location, cerebral microbleeds are typically localised as either "lobar" or "non-lobar" (Gregoire et al., 2009). Lobar microbleeds are located in one of the lobes of the cerebral cortex itself, including both the cortical grey matter as well as the adjacent subcortical white matter. Non-lobar microbleeds include both "deep" cerebral microbleeds (located in subcortical grey matter, i.e., the thalamus and basal ganglia, along with nearby white matter structures, e.g., the internal and external capsules and the corpus callosum) as well as "infratentorial" microbleeds located in the brainstem and cerebellum. Clinically, lobar and non-lobar cerebral microbleeds have been shown to have different primary underlying causes, with lobar microbleeds more related to Cerebral Amyloid Angiopathy (CAA), and non-lobar microbleeds more associated with hypertension and arteriosclerosis (Puy et al., 2021). There is also evidence that exposure to ionizing radiation, as present in many radiation therapies, such as those for cancer treatment, facilitates the development of cerebral microbleeds (Morrison et al., 2019).

Given the variety of risk factors present in spaceflight environments that may produce cerebrovascular damage, and the utility of cerebral microbleeds as early indicators of such damage, we set out to evaluate the presence of these biomarkers in a sample of astronauts before and after a typical mission onboard the International Space Station (ISS). In particular, we investigated if astronauts exhibit more cerebral microbleeds after spaceflight as compared to before spaceflight, and determined whether or not previous spaceflight exposure was associated with the presence of cerebral microbleeds cross-sectionally.

Methods

Participants

We collected MRI data from 16 astronauts (seven female, aged *M*(*SD*) 45.72 (5.70) years old at first assessment), of which six had previous spaceflight experience (with mission durations of *M*(*SD*) 113.13 (74.38) days). Of these six individuals with previous spaceflight experience, their previous missions occurred *M*(*SD*) 2812 (822) days (*i.e.*, averaging over 7 years) before our initial data collection. Data were collected at three time points, one before and two after typical missions onboard the ISS (lasting *M*(*SD*) 200.31 (44.01) days): the first data collection was performed about 7 months prior launch (*M*(*SD*) 213.63 (118.35) days), the second "early postflight" was performed about 2 weeks after landing (*M*(*SD*) 12.44 (1.82) days), and the third "late post flight" on 14 of the 16 subjects was performed about 7 months after landing (*M*(*SD*) 221.07 (44.58) days). This study was approved by the institutional review boards of NASA's Johnson Space Center and the University of Calgary. All participants provided written informed consent, and NASA has reviewed this manuscript and ensured it is compliant with the privacy standards of the NASA Astronaut Office.

MRI data collection

At each of the three time points, we collected susceptibility-weighted images (SWI) using a 32-channel head coil on a 3T Siemens Verio MRI (running Syngo B19). SWI sequences are commonly used to identity cerebral microbleeds, and are more sensitive than T2*-weighted acquisitions (Shams et al., 2015). This gradient echo sequence had a 20.9 ms echo time, 2.9 ms repetition time, 20° flip angle, a pixel bandwidth of 121 Hz, and an in-plane acceleration factor of 3. Derived Siemens SWI images were produced by the acquisition software. Derived SWI slices had an axial-plane resolution of 0.625 × 0.625 mm and a left-right FOV of 288 voxels, and an anterior-posterior FOV of 384 voxels, with 72 slices spaced 2 mm apart.

Microbleed identification

To identify microbleeds from the SWI images, we utilized heterogeneous methods and three raters with varying degrees of proficiency. Our expert rater, MW, has 10 years of experience as a board certified neuroradiologist in clinical and academic practice. Student raters, PT and AY were naive to microbleed identification prior to this project. FB ensured that raters were blinded to any data identifiers and administered a two-step CMB identification procedure. The first step was intended to have raters identify candidate CMBs across the entire dataset, and the second step was to generate explicit confirmation on the absence or presence of deduplicated and unified candidates across different timepoints and all raters. For the first step, the expert rater performed microbleed identification utilizing exhaustive manual identification. Student raters utilized a semi automated approach (Bian et al., 2013; Morrison et al., 2018) in which CMB candidates are identified automatically, and each student rater then manually pruned candidates to remove what they believed were false positive identifications.

After the first step was completed, FB deduplicated microbleeds identified by the raters, and unified identified microbleeds across different timepoints. This required moving the collected SWI

volumes at different time points into alignment with one another using a rigid body registration in *antspyx* version 0.3.8. To ensure the appearance or disappearance of microbleeds from time point to time point was not due to rater error, FB then presented each unique microbleed candidate identified by any rater alongside the same volume in other timepoints from the same subject, and asked raters to identify the presence or absence of the microbleed candidate at each timepoint. Candidates were presented to raters in axial 64 × 64 patches, and raters were able to view three slices above and below the candidate centroid. At this stage, raters were presented with 21 unique candidates across three timepoints, requiring them to explicitly affirm or deny the presence of a microbleed in 63 images. Expert rater MW and student rater PT positively flagged the same 51 candidates and negatively flagged the remaining 12, resulting in a Cohen's Kappa of 1. Student rater AY positively flagged the same 51 candidates, as well as an additional 2, resulting in a Cohen's Kappa of 0.89 between AY and the other raters. Reported results are majority consensus, which are equivalent to the expert rater's judgement.

Analyses

We used paired-samples *t*-tests to compare microbleed counts, as well as microbleed presence (a boolean version of the microbleed count) between each adjacent time point. Other factors of interest that may influence the presence or quantity of microbleeds, i.e., previous spaceflight experience and age at time of preflight testing, were assessed with independent samples *t*-tests and bivariate correlation, respectively. For context, literature-derived microbleed incidences were compared against our sample incidences utilizing binomial tests. Due to the well-known sensitivity differences between different MRI field strength (Stehling et al., 2008; Conijn et al., 2011) and acquisition parameters (i.e., T_2^* GRE vs. SWI) (Goos et al., 2011; Shams et al., 2015), we restricted our literature comparisons to the studies using similar acquisition paradigms (Yates et al., 2014), i.e., SWI data collected at 3T, and did not include comparisons with literature values derived from larger studies with different acquisition paradigms (Poels et al., 2010).

Results

Microbleeds identified by majority consensus across our dataset are reported in Figure 1 and depicted in the Appendix Figure A1. We did not detect any microbleeds in the majority (i.e. 62.5%) of our participants at preflight timepoints. However we did detect 15 microbleeds in the remaining six (out of 16) participants at preflight, with individual counts ranging from a single to six microbleeds. At the early postflight time point, approximately 2 weeks after landing, we detected 17 microbleeds: three new microbleeds appearing in one participant and one microbleed in a different participant resolving. Finally, at our final time point, approximately 7 months after landing, we identified a total of 19 unique microbleeds, with novel microbleeds appearing in two subjects. All microbleeds identified in our dataset were lobar cerebral microbleeds; neither deep nor infratentorial microbleeds were detected. These lobar microbleeds were located most commonly in the frontal (60%) and temporal lobes (35%), with a single microbleed identified in the parietal lobe.

Generally, we did not detect any statistically significant increase in the presence or count of microbleeds after a typical stay onboard the ISS. Total microbleed count nominally increased from preflight to early postflight ($\Delta = 2$, $t_{15} = 0.620$, $p = .544$, $d = 0.155$), and from early postflight to late postflight ($\Delta = 2$, $t_{15} = 1.472$, $p = .165$, $d = 0.393$). We did not identify any instances of astronauts developing their first microbleed after spaceflight, and all novel microbleed identification was in individuals who exhibited microbleeds at our preflight assessment.

Astronauts with previous spaceflight experience demonstrated a nonsignificant trend towards being more likely to have a higher total microbleed count ($t_{14} = 1.945$, $p = .072$, $d = 1.004$), but no significant difference in simple microbleed presence ($t_{14} = 0.764$, $p = .458$, $d = 0.524$). However, astronauts with previous spaceflight experience were older than astronauts without previous experience ($MD = 9.01$ years, $t_{14} = 4.827$, $p < .001$, $d = 2.493$). Age is a known factor associated with an increased prevalence of cerebral microbleeds (Poels et al., 2010). In our dataset, astronaut age was not significantly associated with the presence ($r = .304$, $p = .253$) or amount ($r = .297$, $p = .264$) of microbleeds, but these effects trended in the directions expected by the previous literature. Reference prevalence estimates in healthy individuals using similar acquisition paradigms is limited. However, Yates and others (Yates et al., 2014) enumerated three studies that collected data in healthy controls utilizing SWI at 3T. These studies reported microbleed prevalences of 8.7% (Gao et al., 2008), 14% (Haller et al., 2010), and 19% (Yates et al., 2011) in samples of 23, 35, and 84 individuals, respectively. Mean group ages in these studies ranged from 63.7 to 74.6 years old, making them notably older than our astronaut group at a mean age of 45.72 years. Microbleed prevalence at our preflight time point in all sixteen astronaut participants, at 37.5%, trends higher than these three estimates ($p = .002$, $p = .017$, and $p = .101$, respectively). In the six astronauts with previous spaceflight experience (aged $M(SD)$ 51.35 (2.089) years), microbleed prevalence at preflight timepoints was quite high, at 50%, trending above the literature estimates in older healthy samples ($p = .011$, $p = .039$, $p = .087$, respectively). The astronauts without previous spaceflight experience showed much lower prevalence, at 30%, a difference that did not significantly differ from literature values at this sample size ($p = .050$, $p = .151$, $p = .414$, respectively).

Discussion

Astronauts are exposed to a variety of health threats during spaceflight. Here, we investigated the prevalence and incidence of cerebral microbleeds, small microhemorrhages indicative of cerebrovascular damage. We did not find strong evidence that spaceflight produced an increase in the incidence of cerebral microbleeds up to approximately 7 months after a typical mission onboard the ISS. We did, however, identify an increased prevalence of cerebral microbleeds in astronauts as compared to the non-astronauts samples reported in the literature, particularly in those astronauts with previous spaceflight experience. Interestingly, all 20 unique microbleeds that we identified were lobar grey and white

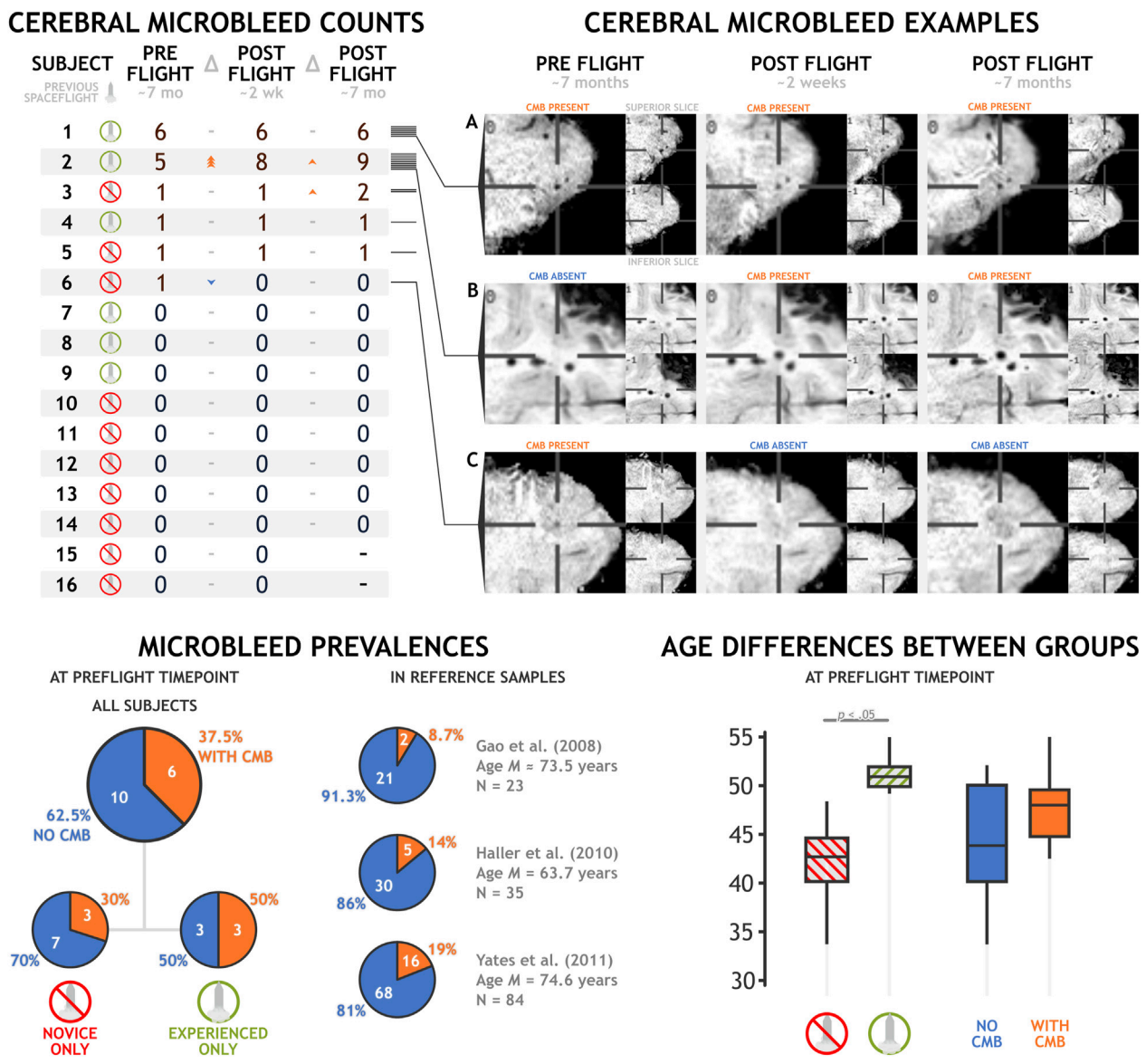

FIGURE 1
Cerebral microbleed counts and examples in a sample of 16 astronauts before and after a typical spaceflight mission. Exemplar **(A)** depicts a cerebral microbleed that remains present across preflight and postflight time points. **(B)** depicts a microbleed that manifested between the preflight and postflight time points. **(C)** depicts the only microbleed that appeared to resolve between preflight and postflight time points.

matter bleeds, and we did not identify any deep or infratentorial microbleeds.

Strictly lobar microbleeds are a radiological feature typically associated with cerebral amyloid angiopathy (CAA), a cerebrovascular disease characterized by amyloid-β peptide deposition (Jung et al., 2020). CAA can be caused by the same amyloid protein that is associated with Alzheimer's disease, but can also be present in individuals without a history of dementia (Cozza et al., 2023). The presence and quantity of cerebral microbleeds we have detected here is not direct and conclusive evidence of CAA, as conclusive diagnoses are typically done via autopsy (Charidimou et al., 2022). However, other research by Zu Eulenburg and others (Zu Eulenburg et al., 2021) in cosmonauts following typical missions onboard the ISS has identified increased levels of a handful of blood-based biomarkers of brain injury and neurodegeneration. These findings highlighted varying increases in levels of neurofilament light chain, tau, and Amyloid β 40 and 42 proteins at different points up to 3 weeks after cosmonauts returned from their missions. Zu Elenburg and others interpreted these findings as evidence of postflight reparatory processes following spaceflight-related brain injury.

An additional neurological feature associated with small vessel disease is the volume of perivascular spaces (PVS) - small fluid-filled regions adjacent to cerebral vasculature that facilitate fluid drainage and waste exchange (Wardlaw et al., 2020). Much like the presence of CMBs, enlarged PVS are considered markers of small vessel disease (Gyanwali et al., 2019). Recent studies in astronauts have identified that ISS missions were associated with an increase in PVS

(Barisano et al., 2022), but astronauts with prior spaceflight experience appeared to be resilient to this effect (Hupfeld et al., 2022). In contrast to the observed pattern of cerebral microbleed prevalences, changes in PVS appear to be affected by spaceflight in a more acute manner, and most saliently in novice astronauts (Hupfeld et al., 2022). It is possible that both enlarged PVS and cerebral microbleeds are caused by a common feature of spaceflight, with PVS changes more acutely sensitive and the microbleeds manifesting later.

However, our findings did not reveal salient increases in the number of microbleeds between preflight and postflight in our sample, undermining the interpretation that spaceflight plays a causal role in increasing microbleed prevalence. It is possible that the postflight time frame of approximately 7 months was of insufficient duration for microbleeds to manifest after spaceflight exposure. For instance, a study investigating the time course of cerebral microbleed burden after radiation therapy found that microbleed count increased by 18% per year following treatment (Morrison et al., 2019). The highest microbleed burden reported in this study in an individual approximately 15 years after radiation therapy, suggesting the most salient microbleed burden should not be expected to follow immediately after radiation exposure, as an example of a mechanism that may be driving the effect we have observed. In our sample, astronauts with prior spaceflight experience landed from their last mission an average of over 7 years prior to testing, giving ample time for microbleeds to manifest. This process may not explain the presence of microbleeds in our participants without previous spaceflight experience, as their cumulative radiation exposure is likely lower than that of the astronauts with such experience. However, CMB incidence has been seen following exposure to other "extreme environments", such as following high altitude cerebral edema (Kallenberg et al., 2008), and related markers of neurological damage may be present in air force pilots (Lim et al., 2012), all reinforcing the possibility that multiple causal factors may be driving these effects.

In conclusion, our study did not provide evidence of increased incidence of cerebral microbleeds up to 7 months following a low earth orbit spaceflight. However, we have identified preliminary evidence that prior spaceflight experience is associated with abnormally high cerebral microbleed prevalence. This is particularly concerning for astronaut health considering the fact that astronauts typically display strong "healthy participant" effects, and are generally expected to show lower morbidity and mortality than the general population (Reynolds and Day, 2019; Reynolds et al., 2021). It does, however, support previous researchers' suggestions that spaceflight may produce neurological damage (Zu Eulenburg et al., 2021), and parallels the "rapid aging" paradigms supported by astronaut musculoskeletal degeneration (Vernikos and Schneider, 2010), as we observed microbleed burdens in otherwise healthy astronauts that met or exceeded those in healthy controls decades their senior. Future research will need to more clearly establish the prevalence, mechanisms, and time course of this potential cerebral microbleed burden in astronauts. As with many studies in astronaut populations, our sample size is small, and larger studies are needed to validate the effects we have reported to ensure they are not spurious or misattributed. Future work will also need to ensure that astronaut and comparison samples have similar ages, as spaceflight veterancy was confounded with age in our sample, preventing us from asserting a causal association between prior spaceflight experience and microbleed incidence. Unfortunately, NASA's current Lifetime Surveillance of Astronaut Health Program MRI protocol does not include sequences appropriate for microbleed identification. Inclusion of an SWI (or manufacturer-equivalent), Quantitative Susceptibility Mapping (QSM), or a more innovative sequence (Sun et al., 2020) may be important to implement to monitor astronaut health and properly evaluate the cerebrovascular risk associated with spaceflight.

Data availability statement

The datasets presented in this article are not readily available to protect participant privacy. Requests to access secondary data should be directed to FB, cfburles@ucalgary.ca.

Ethics statement

The studies involving humans were approved by University of Calgary Conjoint Health Research Ethics Board and the NASA Institutional Review Board. The studies were conducted in accordance with the local legislation and institutional requirements. The participants provided their written informed consent to participate in this study.

Author contributions

FB: Writing–review and editing, Writing–original draft, Visualization, Supervision, Software, Methodology, Investigation, Funding acquisition, Formal Analysis, Data curation, Conceptualization. MW: Writing–review and editing, Investigation, Formal Analysis. PT: Writing–review and editing, Investigation, Formal Analysis. AY: Writing–review and editing, Investigation, Formal Analysis. GI: Writing–review and editing, Supervision, Resources, Project administration, Investigation, Funding acquisition, Conceptualization.

Funding

The author(s) declare that financial support was received for the research, authorship, and/or publication of this article. This research was supported by the Canadian Space Agency–"Wayfinding" Project.

Conflict of interest

The authors declare that the research was conducted in the absence of any commercial or financial relationships that could be construed as a potential conflict of interest.

The author(s) declared that they were an editorial board member of Frontiers, at the time of submission. This had no impact on the peer review process and the final decision.

Publisher's note

References

Akoudad, S., Ikram, M. A., Koudstaal, P. J., Hofman, A., van der Lugt, A., and Vernooij, M. W. (2013). Cerebral microbleeds and the risk of mortality in the general population. *Eur. J. Epidemiol.* 28 (10), 815–821. doi:10.1007/s10654-013-9854-3

Akoudad, S., Portegies, M. L. P., Koudstaal, P. J., Hofman, A., Van Der Lugt, A., Ikram, M. A., et al. (2015). Cerebral microbleeds are associated with an increased risk of stroke: the rotterdam study. *Circulation* 132 (6), 509–516. doi:10.1161/CIRCULATIONAHA.115.016261

Anzai, T., Frey, M. A., and Nogami, A. (2014). Cardiac arrhythmias during long-duration spaceflights. *J. Arrhythmia* 30 (3), 139–149. doi:10.1016/j.joa.2013.07.009

Azzam, E. I., Jay-Gerin, J.-P., and Pain, D. (2012). Ionizing radiation-induced metabolic oxidative stress and prolonged cell injury. *Cancer Lett.* 327 (1–2), 48–60. doi:10.1016/j.canlet.2011.12.012

Barisano, G., Sepehrband, F., Collins, H. R., Jillings, S., Jeurissen, B., Taylor, J. A., et al. (2022). The effect of prolonged spaceflight on cerebrospinal fluid and perivascular spaces of astronauts and cosmonauts. *Proc. Natl. Acad. Sci.* 119 (17), e2120439119. doi:10.1073/pnas.2120439119

Bian, W., Hess, C. P., Chang, S. M., Nelson, S. J., and Lupo, J. M. (2013). Computer-aided detection of radiation-induced cerebral microbleeds on susceptibility-weighted MR images. *NeuroImage Clin.* 2, 282–290. doi:10.1016/j.nicl.2013.01.012

Charidimou, A., Boulouis, G., Frosch, M. P., Baron, J.-C., Pasi, M., Albucher, J. F., et al. (2022). The Boston criteria version 2.0 for cerebral amyloid angiopathy: a multicentre, retrospective, MRI–neuropathology diagnostic accuracy study. *Lancet Neurology* 21 (8), 714–725. doi:10.1016/S1474-4422(22)00208-3

Comfort, P., McMahon, J. J., Jones, P. A., Cuthbert, M., Kendall, K., Lake, J. P., et al. (2021). Effects of spaceflight on musculoskeletal health: a systematic review and meta-analysis, considerations for interplanetary travel. *Sports Med.* 51 (10), 2097–2114. doi:10.1007/s40279-021-01496-9

Conijn, M. M. A., Geerlings, M. I., Biessels, G.-J., Takahara, T., Witkamp, T. D., Zwanenburg, J. J. M., et al. (2011). Cerebral microbleeds on MR imaging: comparison between 1.5 and 7T. *Am. J. Neuroradiol.* 32 (6), 1043–1049. doi:10.3174/ajnr.A2450

Cozza, M., Amadori, L., and Boccardi, V. (2023). Exploring cerebral amyloid angiopathy: insights into pathogenesis, diagnosis, and treatment. *J. Neurological Sci.* 454, 120866. doi:10.1016/j.jns.2023.120866

Demontis, G. C., Germani, M. M., Caiani, E. G., Barravecchia, I., Passino, C., and Angeloni, D. (2017). Human pathophysiological adaptations to the space environment. *Front. Physiology* 8, 547. doi:10.3389/fphys.2017.00547

Gao, T., Wang, Y., and Zhang, Z. (2008). Silent cerebral microbleeds on susceptibility-weighted imaging of patients with ischemic stroke and leukoaraiosis. *Neurological Res.* 30 (3), 272–276. doi:10.1179/016164107X251556

Goos, J. D. C., Van Der Flier, W. M., Knol, D. L., Pouwels, P. J. W., Scheltens, P., Barkhof, F., et al. (2011). Clinical relevance of improved microbleed detection by susceptibility-weighted magnetic resonance imaging. *Stroke* 42 (7), 1894–1900. doi:10.1161/STROKEAHA.110.599837

Gregoire, S. M., Chaudhary, U. J., Brown, M. M., Yousry, T. A., Kallis, C., Jager, H. R., et al. (2009). The microbleed anatomical rating scale (MARS): reliability of a tool to map brain microbleeds. *Neurology* 73 (21), 1759–1766. doi:10.1212/WNL.0b013e3181c34a7d

Gyanwali, B., Vrooman, H., Venketasubramanian, N., Wong, T. Y., Cheng, C.-Y., Chen, C., et al. (2019). Cerebral small vessel disease and enlarged perivascular spaces-data from memory clinic and population-based settings. *Front. Neurology* 10, 669. doi:10.3389/fneur.2019.00669

Hähnel, S. (2020). Value of advanced MR imaging techniques in mild traumatic brain injury. *Am. J. Neuroradiol.* 41 (7), 1269–1270. doi:10.3174/ajnr.A6629

Haller, S., Bartsch, A., Nguyen, D., Rodriguez, C., Emch, J., Gold, G., et al. (2010). Cerebral microhemorrhage and iron deposition in mild cognitive impairment: susceptibility-weighted MR imaging assessment. *Radiology* 257 (3), 764–773. doi:10.1148/radiol.10100612

Hughson, R. L., Robertson, A. D., Arbeille, P., Shoemaker, J. K., Rush, J. W. E., Fraser, K. S., et al. (2016). Increased postflight carotid artery stiffness and inflight insulin resistance resulting from 6-mo spaceflight in male and female astronauts. *Am. J. Physiology-Heart Circulatory Physiology* 310 (5), H628–H638. doi:10.1152/ajpheart.00802.2015

Hupfeld, K. E., Richmond, S. B., McGregor, H. R., Schwartz, D. L., Luther, M. N., Beltran, N. E., et al. (2022). Longitudinal MRI-visible perivascular space (PVS) changes with long-duration spaceflight. *Sci. Rep.* 12 (1), 7238. doi:10.1038/s41598-022-11593-y

Igase, M., Tabara, Y., Igase, K., Nagai, T., Ochi, N., Kido, T., et al. (2009). Asymptomatic cerebral microbleeds seen in healthy subjects have a strong association with asymptomatic lacunar infarction. *Circulation J.* 73 (3), 530–533. doi:10.1253/circj.CJ-08-0764

Jung, Y. H., Jang, H., Park, S. B., Choe, Y. S., Park, Y., Kang, S. H., et al. (2020). Strictly lobar microbleeds reflect amyloid angiopathy regardless of cerebral and cerebellar compartments. *Stroke* 51 (12), 3600–3607. doi:10.1161/STROKEAHA.119.028487

Kallenberg, K., Dehnert, C., Dörfler, A., Schellinger, P. D., Bailey, D. M., Knauth, M., et al. (2008). Microhemorrhages in nonfatal high-altitude cerebral edema. *J. Cereb. Blood Flow Metabolism* 28 (9), 1635–1642. doi:10.1038/jcbfm.2008.55

Koutroumpakis, E., Deswal, A., Yusuf, S. W., Abe, J., Nead, K. T., Potter, A. S., et al. (2022). Radiation-induced cardiovascular disease: mechanisms, prevention, and treatment. *Curr. Oncol. Rep.* 24 (5), 543–553. doi:10.1007/s11912-022-01238-8

Kuzichkin, D. S., Nichiporuk, I. A., Zhuravleva, O. A., Markin, A. A., Rykova, M. P., Zhuravleva, T. V., et al. (2022). Endothelial dysfunction markers and immune response indices in cosmonauts' blood after long-duration space flights. *Npj Microgravity* 8 (1), 46. doi:10.1038/s41526-022-00237-0

Lawley, J. S., Petersen, L. G., Howden, E. J., Sarma, S., Cornwell, W. K., Zhang, R., et al. (2017). Effect of gravity and microgravity on intracranial pressure. *J. Physiology* 595 (6), 2115–2127. doi:10.1113/JP273557

Lee, A. G., Mader, T. H., Gibson, C. R., Tarver, W., Rabiei, P., Riascos, R. F., et al. (2020). Spaceflight associated neuro-ocular syndrome (SANS) and the neuro-ophthalmologic effects of microgravity: a review and an update. *Npj Microgravity* 6 (1), 7. doi:10.1038/s41526-020-0097-9

Lim, D., Park, J., Choi, W.-H., Bang, D.-H., Jung, O., and Kang, S. (2012). Asymptomatic brain lesions in pilots: a comparative study with non-flying personnel using brain MRI. *Aviat. Space, Environ. Med.* 83 (9), 865–871. doi:10.3357/ASEM.3247.2012

Marshall-Goebel, K., Laurie, S. S., Alferova, I. V., Arbeille, P., Auñón-Chancellor, S. M., Ebert, D. J., et al. (2019). Assessment of jugular venous blood flow stasis and thrombosis during spaceflight. *JAMA Netw. Open* 2 (11), e1915011. doi:10.1001/jamanetworkopen.2019.15011

Miller, K. B., Mi, K. L., Nelson, G. A., Norman, R. B., Patel, Z. S., and Huff, J. L. (2022). Ionizing radiation, cerebrovascular disease, and consequent dementia: a review and proposed framework relevant to space radiation exposure. *Front. Physiology* 13, 1008640. doi:10.3389/fphys.2022.1008640

Morrison, M. A., Hess, C. P., Clarke, J. L., Butowski, N., Chang, S. M., Molinaro, A. M., et al. (2019). Risk factors of radiotherapy-induced cerebral microbleeds and serial analysis of their size compared with white matter changes: a 7T MRI study in 113 adult patients with brain tumors. *J. Magnetic Reson. Imaging JMRI* 50 (3), 868–877. doi:10.1002/jmri.26651

Morrison, M. A., Payabvash, S., Chen, Y., Avadiappan, S., Shah, M., Zou, X., et al. (2018). A user-guided tool for semi-automated cerebral microbleed detection and volume segmentation: evaluating vascular injury and data labelling for machine learning. *NeuroImage Clin.* 20, 498–505. doi:10.1016/j.nicl.2018.08.002

Poels, M. M. F., Ikram, M. A., Van Der Lugt, A., Hofman, A., Niessen, W. J., Krestin, G. P., et al. (2012). Cerebral microbleeds are associated with worse cognitive function: the Rotterdam Scan Study. *Neurology* 78 (5), 326–333. doi:10.1212/WNL.0b013e3182452928

Poels, M. M. F., Vernooij, M. W., Ikram, M. A., Hofman, A., Krestin, G. P., Van Der Lugt, A., et al. (2010). Prevalence and risk factors of cerebral microbleeds: an update of the rotterdam scan study. *Stroke* 41 (10_Suppl. l_1), S103–S106. doi:10.1161/STROKEAHA.110.595181

Puy, L., Pasi, M., Rodrigues, M., van Veluw, S. J., Tsivgoulis, G., Shoamanesh, A., et al. (2021). Cerebral microbleeds: from depiction to interpretation. *J. Neurology, Neurosurg. Psychiatry* 92 (6), 598–607. doi:10.1136/jnnp-2020-323951

Reynolds, R. J., and Day, S. M. (2019). Mortality of US astronauts: comparisons with professional athletes. *Occup. Environ. Med.* 76 (2), 114–117. doi:10.1136/oemed-2018-105304

Reynolds, R. J., Little, M. P., Day, S. M., Charvat, J., Blattnig, S., Huff, J., et al. (2021). Cancer incidence and mortality in the USA astronaut corps, 1959–2017. *Occup. Environ. Med.* 78 (12), 869–875. doi:10.1136/oemed-2020-107143

Shams, S., Martola, J., Cavallin, L., Granberg, T., Shams, M., Aspelin, P., et al. (2015). SWI or T2*: which MRI sequence to use in the detection of cerebral microbleeds? The karolinska imaging dementia study. *Am. J. Neuroradiol.* 36 (6), 1089–1095. doi:10.3174/ajnr.A4248

Stavnichuk, M., Mikolajewicz, N., Corlett, T., Morris, M., and Komarova, S. V. (2020). A systematic review and meta-analysis of bone loss in space travelers. *Npj Microgravity* 6 (1), 13. doi:10.1038/s41526-020-0103-2

Stehling, C., Wersching, H., Kloska, S. P., Kirchhof, P., Ring, J., Nassenstein, I., et al. (2008). Detection of asymptomatic cerebral microbleeds: a comparative study at 1.5 and 3.0 T. *Acad. Radiol.* 15 (7), 895–900. doi:10.1016/j.acra.2008.01.013

Sun, H., Cleary, J. O., Glarin, R., Kolbe, S. C., Ordidge, R. J., Moffat, B. A., et al. (2020). Extracting more for less: multi-echo MP2RAGE for simultaneous T1-weighted imaging, T1 mapping, R2* mapping, SWI, and QSM from a single acquisition. *Magnetic Reson. Med.* 83 (4), 1178–1191. doi:10.1002/mrm.27975

Vernikos, J., and Schneider, V. S. (2010). Space, gravity and the physiology of aging: parallel or convergent disciplines? A mini-review. *Gerontology* 56 (2), 157–166. doi:10.1159/000252852

Wardlaw, J. M., Benveniste, H., Nedergaard, M., Zlokovic, B. V., Mestre, H., Lee, H., et al. (2020). Perivascular spaces in the brain: anatomy, physiology and pathology. *Nat. Rev. Neurol.* 16 (3), 137–153. doi:10.1038/s41582-020-0312-z

Yates, P. A., Sirisriro, R., Villemagne, V. L., Farquharson, S., Masters, C. L., Rowe, C. C., and For the AIBL Research Group (2011). Cerebral microhemorrhage and brain β-amyloid in aging and Alzheimer disease. *Neurology* 77 (1), 48–54. doi:10.1212/WNL.0b013e318221ad36

Yates, P. A., Villemagne, V. L., Ellis, K. A., Desmond, P. M., Masters, C. L., and Rowe, C. C. (2014). Cerebral microbleeds: a review of clinical, genetic, and neuroimaging associations. *Front. Neurology* 4, 205. doi:10.3389/fneur.2013.00205

Zu Eulenburg, P., Buchheim, J.-I., Ashton, N. J., Vassilieva, G., Blennow, K., Zetterberg, H., et al. (2021). Changes in blood biomarkers of brain injury and degeneration following long-duration spaceflight. *JAMA Neurol.* 78 (12), 1525–1527. doi:10.1001/jamaneurol.2021.3589

Appendix

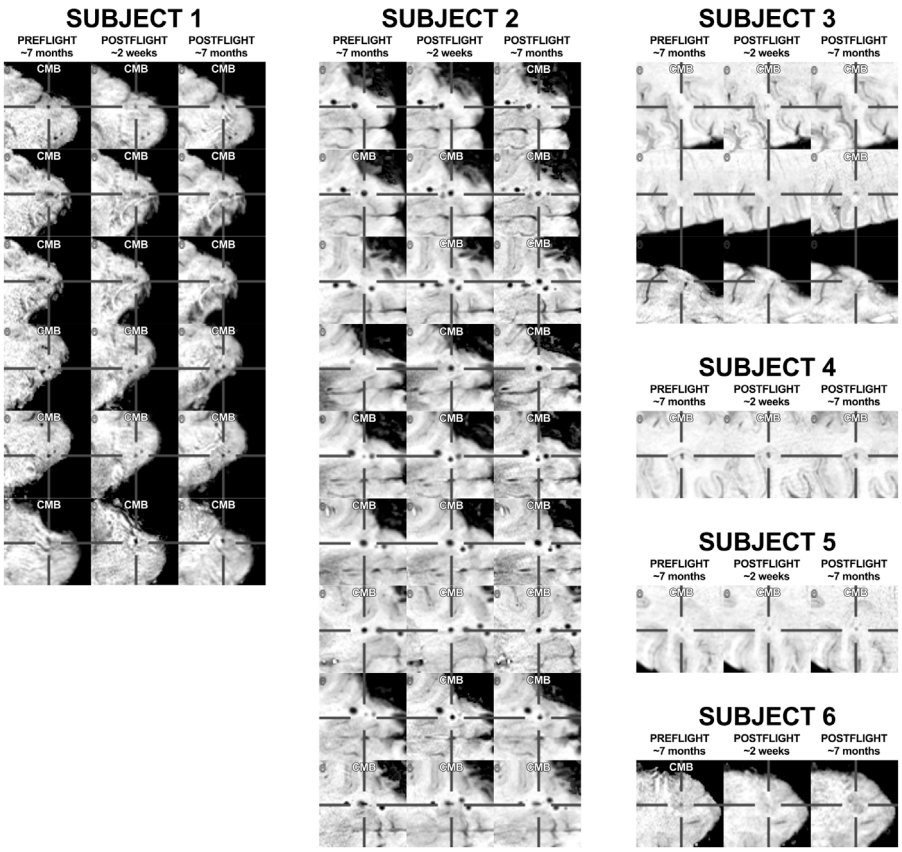

FIGURE A1
All positively identified microbleeds. Subject numbers correspond to those presented in Figure 1.

frontiers | Frontiers in Physiology

TYPE Data Report
PUBLISHED 20 June 2024
DOI 10.3389/fphys.2024.1375929

OPEN ACCESS

EDITED BY
Marc-Antoine Custaud,
Université d'Angers, France

REVIEWED BY
Felice Strollo,
IRCCS San Raffaele Pisana, Italy
Ronan Padraic Murphy,
Dublin City University, Ireland

*CORRESPONDENCE
Daria N. Kashirina,
daryakudryavtseva@mail.ru

RECEIVED 24 January 2024
ACCEPTED 01 May 2024
PUBLISHED 20 June 2024

CITATION
Kashirina DN, Pastushkova LK, Goncharova AG and Larina IM (2024), Assessment of the effect of 21-day head-down bed rest on the cardiovascular system by blood protein composition.
Front. Physiol. 15:1375929.
doi: 10.3389/fphys.2024.1375929

Assessment of the effect of 21-day head-down bed rest on the cardiovascular system by blood protein composition

Daria N. Kashirina*, Ludmila Kh. Pastushkova, Anna G. Goncharova and Irina M. Larina

SSC RF–Institute of Biomedical Problems of the Russian Academy of Sciences, Moscow, Russia

Head-down bed rest (HDBR) is one of the models of the physiological effects of weightlessness used, among other things, to assess the effect of hypokinesia on the physiological systems of the human body and, first of all, on the cardiovascular system. The aim of the work was to study the effect of 21 days of HDBR factors on the cardiovascular system based on blood proteomic profile data. It was revealed that HDBR conditions led to an increase in the levels of proteins of the complement and the coagulation cascade systems, platelet degranulation, fibrinolysis, acute phase proteins, post-translational modification of proteins, retinol-binding protein 4 (RBP4), apolipoprotein B, which are associated with cardiovascular diseases, and other proteins that affect the functions of endothelial cells. Blood levels of proteins involved in cytoskeletal remodelling, oxygen transport, heme catabolism, etc. have been shown to decrease during HDBR.

KEYWORDS

head-down bed rest, mass spectrometry, blood, cardiovascular system, retinol-binding protein 4

1 Introduction

Head-down bed rest (HDBR) is not only one of the models of the physiological effects for weightlessness, but also for hypodynamia, which can be considered as an inevitable companion of scientific and technological progress, accompanied both by a significant reduction in the amount of physical labour and by a characteristic lifestyle that has become more and more widespread in recent times. The modern lifestyle leads to metabolic changes and a deterioration in vascular function, which can ultimately have a negative impact on health. As noted, hypokinesia (a sharp reduction in motor activity, a decrease in muscle work), along with the spread of a Western diet, is one of the most serious causes of the emergence and threateningly rapid spread of cardiovascular and neurological diseases, as well as diseases associated with disorders of the gastrointestinal tract, endocrine glands and other organs and systems (Davies et al., 2017).

It is known that exposure to HDBR is associated with the development of compensatory adaptive responses involving the cardiovascular, endocrine, central, and peripheral nervous systems (Boutouyrie et al., 2022; Buoite et al., 2021; Blanc et al., 2000). During the acute phase of HDBR, participants experience a decrease in circulating plasma volume and a movement of extracellular fluid and blood volumes in

a cranial direction (Millet et al., 2001). The responses of the cardiovascular system to blood redistribution are currently being actively investigated. In a 21-day HDBR experiment, a decrease in left ventricular mass and diastolic volume was observed (Greaves et al., 2019). A decrease in the heart volume leads to lower cardiac output (decrease in systolic and minute blood volume). In this case, the heart rate increases both at rest and during exercise. The redistribution of vasoconstrictor and pressor influences in the vessels of different regions of the body observed during HDBR (Baranov et al., 2016) also affects systemic hemodynamics and cardiovascular system (CVS) function. It has recently been shown that HDBR causes a significant increase in aortic stiffness, the parameters of which did not fully recover 1 month after the end of the experiment, and significant changes in the size of the thoracic aorta and the muscular arteries of the lower body were also revealed (Boutouyrie et al., 2022).

It has been shown that carbohydrate metabolism is also altered in HDBR: insulin secretion increases and glucose tolerance decreases (Blanc et al., 2000; Afonin, 1989). The development of insulin resistance can lead to endothelial dysfunction, which does not allow the vessels to function effectively and is dangerous because of the possibility of developing cardiovascular disease. Therefore, early prevention of insulin resistance and endothelial dysfunction and the search for means and methods to restore vascular function remain the most promising areas in the prevention and treatment of cardiovascular disease.

It is well known that prolonged bed rest causes muscle wasting. Proteomic methods have shown that HDBR leads to changes in the levels and phosphorylation of structural and metabolic muscle proteins (Dillon et al., 2019). Inhibition of muscle focal contact proteins and an increase in the levels of antioxidant response pathway proteins in slow (but not fast) muscle fibres were also observed. HDBR activated markers of neuromuscular damage (Murgia et al., 2022). Proteomic analysis of urine proteins from volunteers participating in HDBR suggested that blood coagulation processes such as fibrinolysis and regulation of cell adhesion were aimed at maintaining homeostasis and were activated in the early period of the experiment. Under the influence of a complex of factors of long-term bed rest, proteolysis and metabolism of oligosaccharides were activated (Pastushkova et al., 2017).

In recent years, proteomics methods based on mass spectrometry have been widely used to study the protein composition of body fluids from healthy individuals in order to analyse biological processes in the body. Understanding protein expression is the key to deciphering the mechanisms of action of various factors and, ultimately, to finding effective countermeasures to prevent adverse changes. The study of the composition of blood proteins functionally associated with the cardiovascular system by proteomic methods will contribute to the understanding of the mechanisms underlying cardiovascular changes under the influence of hypokinesia conditions. This knowledge may also help to understand the pathophysiology of common cardiovascular diseases. In this work, the protein composition of the blood plasma of volunteers was studied using proteomic methods to elucidate the molecular mechanisms of the changes that occurred during the 21-day HDBR.

2 Methods

2.1 Design of HDBR

The 21-day HDBR study involved 6 healthy men aged between 24 and 41 years. Each participant voluntarily signed an Informed Consent form after the potential risks, benefits and nature of the study were explained. All subjects were confirmed by a committee of medical experts to be in good health, free of chronic disease, and with a normal body mass index. All participants in the experiment were placed in a head-down position on a bed with an inclination angle of -6° for 21 days. Venous blood was collected in Vacuette EDTA tubes on an empty stomach 6 days before the start of the experiment and on the 21st day of HDBR.

2.2 Preparation of plasma samples for proteomic analysis

Plasma samples were purified from major proteins using Top 12 columns (Pierce Chemical Co., United States of America) and then standard sample preparation, including the steps of reduction, alkylation, precipitation, and trypsinolysis, was performed (Kashirina et al., 2020). The resulted tryptic peptide mixture was analyzed using liquid chromatography–mass spectrometry method based on a nano-HPLC Dionex Ultimate3000 system (Thermo Fisher Scientific, United States of America) and a timsTOF Pro (Bruker Daltonics, United States of America) mass spectrometer. Peptides were separated using a packed emitter column (C18, 25 cm × 75 µm x 1.6 µm) (Ion Optics, Parkville, Australia) at a flow rate of 400 nL/min by gradient elution with 4%–90% phase B during 40 min. Mobile phase A consisted of 0.1% formic acid in water and mobile phase B consisted of 0.1% formic acid in acetonitrile.

Mass spectrometric analysis was performed using the Parallel Accumulation - Serial Fragmentation (PASEF) acquisition method (Meier et al., 2018). An electrospray ionization (ESI) source was operated at a capillary voltage of 1500 V, an end plate bias of 500 V and 3.0 L/min of dry gas at temperature of 180°C. The measurements were carried out in the m/z range from 100 to 1700 Th. The ion mobility was in the range from 0.60 to 1.60 V s/cm^2. The total cycle time was 1.88 s and the number of PASEF MS/MS scans was set to 10.

2.3 Data analysis

The resulting LC-MS/MS data were analyzed using PEAKS Studio 8.5. Only proteins identified by at least 2 peptides, one of which was specific for a particular protein, were subjected to further analysis. The given limiting parameters were as follows: parent mass error tolerance - 20 ppm; fragment mass error tolerance - 0.03 Da; enzyme - trypsin; the maximum number of missed cleavages - 3; fixed modifications - carbamidomethyl C); variable modifications - oxidation M), acetylation (N-terminus). The false positive rate (FDR) threshold was set to 0.01.

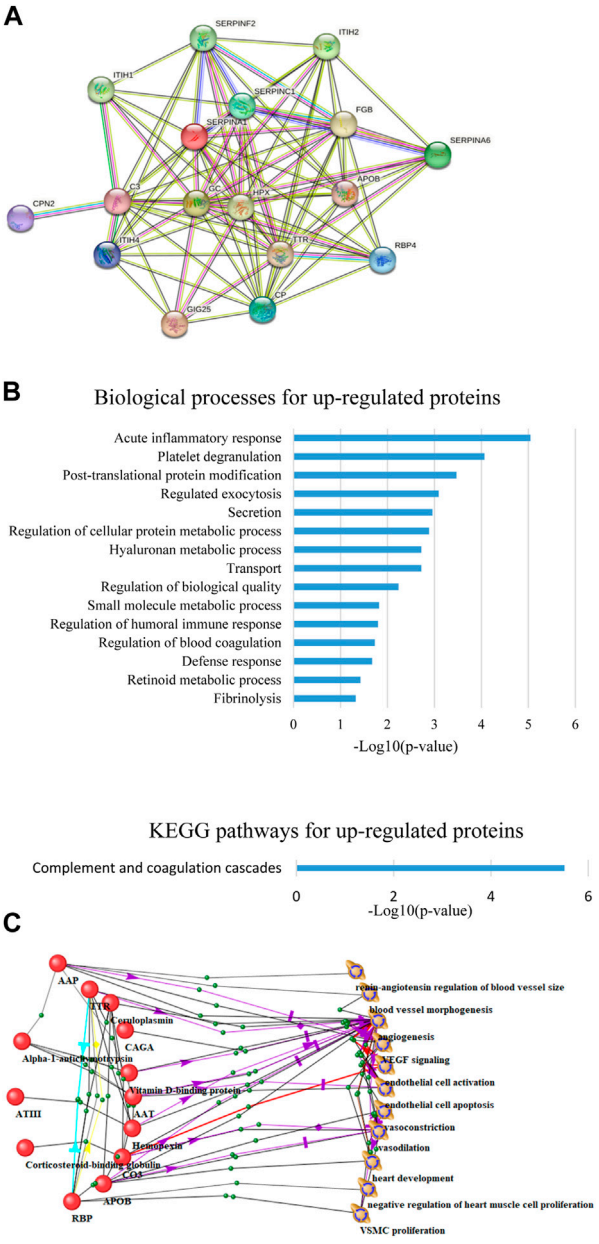

FIGURE 1
(A) Upregulated protein interaction network constructed using the STRING web resource. **(B)** Biological processes and KEGG pathways involving overexpressed proteins. **(C)** Connections of proteins significantly changed by the end of HDBR with the processes occurring in the cardiovascular system.

All the LC-MS/MS results have been deposited to the ProteomeXchange Consortium via the PRIDE (Vizcaino et al., 2016) partner repository with the dataset identifier PXD053149.

2.4 Statistical and bioinformatic methods of data processing

Statistical analysis was carried out using the Statistica 12 program. The homogeneity of sample variances was assessed using the Levene test. The normality of data distribution in each group was determined using the Shapiro-Wilk test. In the absence of normal distribution and equal variances, the Mann-Whitney test was used, which is a nonparametric alternative to the *t*-test.

Molecular functions and biological processes enriched with the identified proteins were determined using the STRING web resource (https://string-db.org), and the search for links with processes associated with the cardiovascular system was performed using the ANDSystem program (http://www-bionet.sscc.ru/and/cell).

3 Results

As a result of proteomic analysis, 533 different proteins were identified in plasma samples. Based on statistical analysis using the Mann-Whitney test (p-value <0.05), 25 proteins were identified whose levels changed significantly by the end of HDBR. Among the 17 proteins whose concentration increased by the end of the experiment (Figure 1A), there were proteins involved in the complement and coagulation cascade (C3, FGB, SERPINF2, SERPINC1, SERPINA1), acute phase response (ITIH4, SERPINF2, SERPINC1, GIG25, SERPINA1), platelet degranulation (ITIH4, FGB, SERPINF2, GIG25, SERPINA1), blood coagulation (FGB, SERPINF2, SERPINC1), fibrinolysis (FGB, SERPINF2), transport (APOB, TTR, C3, CP, HPX, ITIH4, FGB, SERPINF2, SERPINC1, RBP4, GIG25, SERPINA1, GC), retinoid metabolic processes (APOB, TTR, RBP4), etc. (Figure 1B).

It was found that eight proteins, the concentration of which significantly decreased by the end of HDBR, had various functions from mRNA splicing and cell cytoskeleton remodeling, to heme catabolism and oxygen transport (Table 1). However, processes and pathways connecting these proteins have not been identified.

4 Discussion

4.1 Comparison of results with literature data

Our data are confirmed by previous studies of HDBR. Thus, it has been shown that there is an increase in the concentration of FGB (fibrinogen), ITIH2 and ITIH4 (inter-alpha-trypsin inhibitor heavy chains 2 and 4), and SerpinF2 (α2-antiplasmin) in HDBR (Kashirina et al., 2020). Although microgravity simulation experiments did not reveal activation of the coagulation cascade during the experiments (Haider et al., 2013; Cvirn et al., 2015). However, after 21 days of HDBR in the recovery period, there was an increase in the peak and rate of thrombin formation (Waha et al., 2015), which indicated an increased risk of thrombosis after the end of the experiment (Cvirn et al., 2015; Waha et al., 2015). Apparently, at the end of the experiment, increased hydrostatic pressure and shear stress in unadapted lower body vessels cause activation of blood coagulation mediated by the endothelial cell secretome (Cvirn et al., 2015). Therefore, the study of the proteomic composition of blood, which is in direct contact with endothelial cells, can shed light on the functional state of endothelial cells or reveal blood proteins that contributed to the balance shift toward procoagulation properties of the endothelium.

TABLE 1 Functions of downregulated proteins.

Gene	Protein	Function
BPGM	Bisphosphoglycerate mutase	Regulates the affinity of hemoglobin to O2
SLU7	Pre-mRNA-splicing factor SLU7	mRNA splicing
CAPNS1	Calpain small subunit 1	Remodeling of the cytoskeleton
HBD	Hemoglobin subunit delta	Oxygen transport
S100A8	Protein S100-A8	Regulation of inflammatory responses
BLVRB	Flavin reductase	NADPH-dependent reduction of various flavins, heme catabolism
MYO1C	Unconventional myosin-Ic	Provides intracellular movement, including glucose transporters GLUT4 to the plasma membrane
UBE2V1	Ubiquitin-conjugating enzyme E2 variant 1	Plays a role in cell cycle control and differentiation

In this experiment, one of the possible reasons for the decrease of bisphosphoglycerate mutase (BPGM) and hemoglobin subunit delta (HBD) levels could be a decrease in red blood cell mass (RBCM), however, studies show that RBCM does not decrease in short bed rests (Branch et al., 1998) or decreases only after the end of the experiment (Leach and Johnson, 1984). Although there is evidence of a significant decrease in erythropoietin during HDBR (Gunga et al., 1996), which was observed in HDBR as early as the first few days, the effect of erythropoietin on RBCM could not have occurred in such a short time. Regarding long-duration spaceflight, the phenomenon of hemolysis is widely documented (Trudel et al., 2022), but no hemolysis was detected under conditions of short HDBR. On the contrary, HDBR caused hemoconcentration, and circulating parameters of hemolysis remained unchanged throughout bed rest (Trudel et al., 2017).

4.2 Association of up- and downregulated proteins with processes occurring in the CVS

Within the framework of this study, the relationships between significantly changed proteins and processes occurring in the CVS were analyzed using the ANDSystem program. This approach identified proteins directly or indirectly related to processes such as activation and apoptosis of endothelial cells, VEGF signaling, vasoconstriction, vasodilation, and angiogenesis (Figure 1C).

One of the proteins, RBP, retinol-binding protein 4, has been associated with processes directly related to the heart: negative regulation of heart muscle cell proliferation, heart muscle development (Figure 1C). RBP4 is an adipokine whose main function is retinol transport, but its association with cardiovascular disease (CVD) is now widely known: it correlates with increased thickness of the carotid intima-media complex, early onset of cardiovascular disease [Li et al., 2019 RBP4 is thought to mediate insulin-induced VSMC proliferation and contribute to the development of atherosclerosis (Li et al., 2014). The effect of RBP4 on the cardiovascular system may be mediated by endothelial cells, as carbachol-induced endothelium-dependent vasodilation of carotid arteries *ex vivo* was enhanced in RBP4 knockout mice and, conversely, reduced in RBP4 overexpressing mice (Kraus et al., 2015). Elevated levels of RBP4 attract macrophages to adipose tissue and promote local inflammation by causing macrophages to secrete pro-inflammatory cytokines: nuclear factor κ-B (NFκB), c-Jun N-terminal kinases (JNK), and interleukin 1β, leading to insulin resistance (Yang et al., 2005). The level of this protein decreased during exercise (60 min of bicycling and running per day for at least 3 days per week) (Graham et al., 2006). Moreover, serum RBP4 levels decreased in people in whom exercise improved insulin sensitivity, but not in those people in whom this effect was not achieved (Graham et al., 2006), indicating an RBP4-mediated link between a physically inactive lifestyle and insulin resistance. Moreover, studies in mice have shown that elevated serum levels of RBP4 can induce insulin resistance (Yang et al., 2005). Thus, accurate measurements of serum RBP4 levels can provide a quantitative measure of disease severity and guide the development of drugs to improve insulin sensitivity. In addition, since RBP4 levels are elevated in the serum of thin, non-diabetic but insulin-resistant individuals with a high genetic risk of developing type 2 diabetes (Graham et al., 2006), RBP4 may be useful as an early marker of diabetes risk.

Among other things, GLUT4 protein (the main insulin-stimulated glucose transporter) in adipocytes and serum RBP4 levels have been shown to be inversely correlated (Graham et al., 2006). Although we did not detect GLUT4 in the samples, nevertheless, by day 21 of HDBR, a significant decrease in the concentration of actin-associated molecular motor protein (MYO1C) was detected, which, as shown in the article (Toyoda et al., 2011), is able to regulate glucose uptake and improve insulin sensitivity. It is known, that HDBR conditions affect carbohydrate metabolism - insulin secretion increases and impaired glucose tolerance develops (Afonin, 1989). Insulin resistance can cause endothelial dysfunction, which is dangerous for the development of cardiovascular diseases. Thus, during HDBR the level of RBP4 increased, altering insulin sensitivity and modulating the molecular interrelations of other cardiovascular risk factors.

Apolipoprotein B (APOB), which is the only apolipoprotein of low-density lipoproteins that causes cholesterol accumulation in vessel walls, also plays an important role in the regulation of endothelial function. It has been demonstrated that apolipoprotein B impairs endothelium-dependent vasodilation with attenuation of NO-mediated pathway efficiency (Zhang et al., 2014). This agrees well with the results of a large cohort study of 1,016 subjects which showed that the level of apolipoprotein

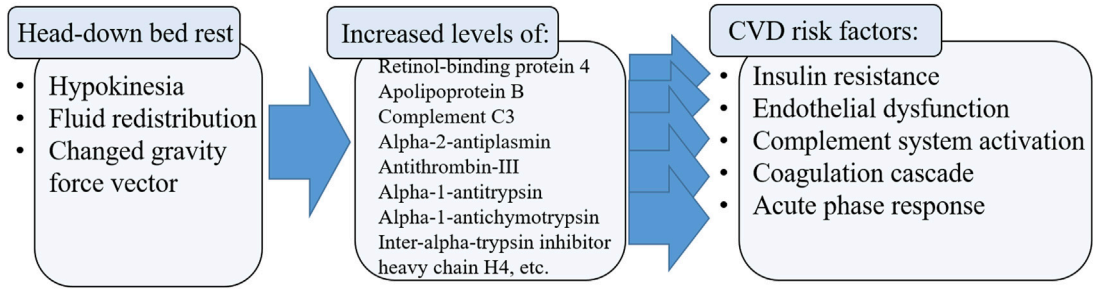

FIGURE 2
Schematic presentation of results in the context of human health.

B is inversely correlated with endothelium-dependent vasodilation (Lind, 2007).

The link with cardiovascular processes is also demonstrated by complement component C3, which plays a central role in all three pathways of complement system activation: classical, alternative and lectin. The endothelial monolayer of all blood vessels, due to its location, is in close contact with the circulating complement components. Some of the complement factors can directly or indirectly affect the endothelium (Hertle et al., 2014). Endothelial cells express anaphylatoxin receptors and complement regulators on their surface, suggesting that they are a direct target of complement molecules (Propson et al., 2021; Schraufstatter et al., 2002). C3a, C5a, and C5b have been shown to induce the expression of adhesion molecules and pro-inflammatory cytokines in endothelial cells *in vitro* (Bossi et al., 2011), which initiates and promotes the development of atherosclerosis. It should be noted that proteins of the complement system had the highest representation among the proteins specific for 21 days of HDBR, confirming the involvement of the complement system in response to bed rest conditions.

5 Conclusion

HDBR conditions led to an increase in the levels of proteins involved in the complement system and the coagulation cascade, platelet degranulation, fibrinolysis, acute phase proteins, post-translational modification of proteins and other proteins that affect the functions of endothelial cells (Figure 2). At the same time, the levels of proteins involved in amino acid biosynthesis, glycolysis, oxygen transport, heme catabolism, etc., decreased in the blood of healthy volunteers.

Thus, on day 21 of HDBR, the levels of RBP4, APOB and C3 proteins increased, each of which plays an important role in one way or another in modulating the properties of the endothelium and contributing to the development of atherosclerosis, which is a precursor of many cardiovascular diseases. Identification of the molecular mechanisms of changes in vascular endothelial function may help to develop preventive measures to counteract the negative effects of prolonged hypokinesia. And although 21 days of HDBR is not enough for the development of serious clinically significant changes in the activity of the cardiovascular system, we can still capture the first molecular reactants to the conditions of hypodynamia and hypokinesia, which may trigger subsequent processes associated with deterioration in the activity of blood vessels and the heart, which can no longer be reversed. It is therefore particularly important to identify early signs of changes in vascular function that can still be compensated for.

6 Limitations

Finally, the limitations of this work should be noted. The main physiological mechanisms that trigger changes in the blood proteomic profile are associated with thoracocranial redistribution of blood (Millet et al., 2001), changes in the regulation of vascular tone (Rusanov et al., 2020), a decrease in cardiac output under conditions of HDBR (Greaves et al., 2019). However, this study did not include an instrumental study of the above indicators. Another limitation of the work is the study of a small sample of subjects, but such complex human studies are mostly carried out on a small sample and provide unique results of theoretical and practical importance.

Data availability statement

The datasets presented in this study can be found in online repositories. The names of the repository/repositories and accession number(s) can be found below: http://www.proteomexchange.org/, identifier PXD053149.

Ethics statement

The studies involving humans were approved by Commission on Biomedical Ethics of the State Scientific Center of the Russian Federation–Institute of Biomedical Problems RAS. The studies were conducted in accordance with the local legislation and institutional requirements. The participants provided their written informed consent to participate in this study.

Author contributions

DK: Funding acquisition, Investigation, Methodology, Validation, Visualization, Writing–original draft, Writing–review and editing. LP: Formal Analysis, Investigation, Writing–original draft. AG: Conceptualization, Data curation, Writing–review and

editing. IL: Conceptualization, Methodology, Writing–review and editing.

Funding

The author(s) declare that financial support was received for the research, authorship, and/or publication of this article. This research was funded by the Russian Science Foundation grant No. 22-74-00069, https://rscf.ru/project/22-74-00069/.

Acknowledgments

The team of authors expresses gratitude to Dr. Alexey V. Shpakov for the opportunity to participate in the HDBR experiment.

Conflict of interest

The authors declare that the research was conducted in the absence of any commercial or financial relationships that could be construed as a potential conflict of interest.

Publisher's note

References

Afonin, B. V. (1989). Effect of space flight antiorthostatic hypokinesia of various durations on blood insulin level. *Biol. Aviakosm. Med.* 23 (3), 77–79.

Baranov, M. V., Katuntsev, V. P., Shpakov, A. V., and Baranov, V. M. (2016). A method of ground simulation of physiological effects of hypogravity on humans. *Bull. Exp. Biol. Med.* 160 (3), 401–405. doi:10.1007/s10517-016-3181-0

Blanc, S., Normand, S., Pachiaudi, C., Duvareille, M., and Gharib, C. (2000). Leptin responses to physical inactivity induced by simulated weightlessness. *Am. J. Physiol. Regul. Integr. Comp. Physiol.* 279 (3), R891–R898. doi:10.1152/ajpregu.2000.279.3.R891

Bossi, F., Peerschke, E. I., Ghebrehiwet, B., and Tedesco, F. (2011). Cross-talk between the complement and the kinin system in vascular permeability. *Immunol. Lett.* 140, 7–13. doi:10.1016/j.imlet.2011.06.006

Boutouyrie, P., Fayol, A., Fortier, C., Khettab, H., Cristian, C., Gencer, U., et al. (2022). Impact of 60 days of head-down bed rest on large arteries. *J. Hypertens.* 40 (10), 2058–2067. doi:10.1097/HJH.0000000000003235

Branch, J. D., Bodary, P. F., and Convertino, V. A. (1998). Red cell volume and (erythropoietin) responses during exposure to simulated microgravity. *Aviat. Space Environ. Med.* 69, 347–351.

Buoite, S. A., Ajčević, M., Furlanis, G., and Manganotti, P. (2021). Neurophysiological adaptations to spaceflight and simulated microgravity. *Clin. Neurophysiol.* 132 (2), 498–504. doi:10.1016/j.clinph.2020.11.033

Cvirn, G., Waha, J. E., Ledinski, G., Schlagenhauf, A., Leschnik, B., Koestenberger, M., et al. (2015). Bed rest does not induce hypercoagulability. *Eur. J. Clin. Invest.* 45 (1), 63–69. doi:10.1111/eci.12383

Davies, J. M. S., Cillard, J., Friguet, B., Cadenas, E., Cadet, J., Cayce, R., et al. (2017). The oxygen paradox, the French paradox, and age-related diseases. *Geroscience* 39 (5-6), 499–550. doi:10.1007/s11357-017-0002-y

Dillon, E. L., Soman, K. V., Wiktorowicz, J. E., Sur, R., Jupiter, D., Danesi, C. P., et al. (2019). Proteomic investigation of human skeletal muscle before and after 70 days of head down bed rest with or without exercise and testosterone countermeasures. *PLoS One* 14 (6), e0217690. doi:10.1371/journal.pone.0217690

Graham, T. E., Yang, Q., Bluher, M., Hammarstedt, A., Ciaraldi, T. P., Henry, R. R., et al. (2006). Retinol-binding protein 4 and insulin resistance in lean, obese, and diabetic subjects. *N. Engl. J. Med.* 354 (24), 2552–2563. doi:10.1056/NEJMoa054862

Greaves, D., Arbeille, P., Guillon, L., Zuj, K., and Caiani, E. G. (2019). Effects of exercise countermeasure on myocardial contractility measured by 4D speckle tracking during a 21-day head-down bed rest. *Eur. J. Appl. Physiol.* 119 (11-12), 2477–2486. doi:10.1007/s00421-019-04228-0

Gunga, H.-C., Kirsch, K., Baartz, F., Maillet, A., Gharib, C., Nalishiti, W., et al. (1996). Erythropoietin under real and simulated microgravity conditions in humans. *J. Appl. Physiol.* 81, 761–773. doi:10.1152/jappl.1996.81.2.761

Haider, T., Gunga, H. C., Matteucci-Gothe, R., Sottara, E., Griesmacher, A., Belavý, D. L., et al. (2013). Effects of long-term head-down-tilt bed rest and different training regimes on the coagulation system of healthy men. *Physiol. Rep.* 1 (6), e00135. doi:10.1002/phy2.135

Hertle, E., Stehouwer, C. D., and Van Greevenbroek, M. M. (2014). The complement system in human cardiometabolic disease. *Mol. Immunol.* 61, 135–148. doi:10.1016/j.molimm.2014.06.031

Kashirina, D. N., Brzhozovskiy, A. G., Pastushkova, L.Kh., Kononikhin, A. S., Nikolaev, E. N., Larina, I. M., et al. (2020). Semi-quantitative proteomic research of protein plasma profile of volunteers in 21-day head down bed rest. *Front. Physiol.* 11, 678. doi:10.3389/fphys.2020.00678

Kraus, B. J., Sartoretto, J. L., Polak, P., Hosooka, T., Shiroto, T., Eskurza, I., et al. (2015). Novel role for retinol-binding protein 4 in the regulation of blood pressure. *FASEB J.* 29, 3133–3140. doi:10.1096/fj.14-266064

Leach, C. S., and Johnson, P. C. (1984). Influence of space flight on erythrokinetics in man. *Science* 225, 216–218. doi:10.1126/science.6729477

Li, F., Xia, K., Sheikh, M. S., Cheng, J., Li, C., and Yang, T. (2014). Retinol binding protein 4 promotes hyperinsulinism-induced proliferation of rat aortic smooth muscle cells. *Mol. Med. Rep.* 9 (5), 1634–1640. doi:10.3892/mmr.2014.2028

Li, X., Zhu, S., Song, G., Zhang, K., Gao, W., Huang, J., et al. (2019). Retinol-binding protein 4 is closely correlated to blood pressure level and E/A in untreated essential hypertension patients. *Ann. Palliat. Med.* 8, 645–650. doi:10.21037/apm.2019.11.07

Lind, L. (2007). Vasodilation in resistance arteries is related to the apolipoprotein B/A1 ratio in the elderly – the Prospective Investigation of the Vasculature in Uppsala Seniors (PIVUS) study. *Atherosclerosis* 190 (2), 378–384. doi:10.1016/j.atherosclerosis.2006.02.027

Meier, F., Brunner, A. D., Koch, S., Koch, H., Lubeck, M., Krause, M., et al. (2018). Online Parallel Accumulation–Serial Fragmentation (PASEF) with a novel trapped ion mobility mass spectrometer. *Mol. Cell. Proteomics.* 17 (12), 2534–2545. doi:10.1074/mcp.TIR118.000900

Millet, C., Custaud, M. A., Allevard, A. M., Zaouali-Ajina, M., Monk, T. H., Arnaud, S. B., et al. (2001). Effects of 17 days of head-down bed rest on hydro-electrolytic regulation in men. *J. Gravit. Physiol.* 8 (1), P121–P122.

Murgia, M., Ciciliot, S., Nagaraj, N., Reggiani, C., Schiaffino, S., Franchi, M. V., et al. (2022). Signatures of muscle disuse in spaceflight and bed rest revealed by single muscle fiber proteomics. *PNAS Nexus* 1 (3), pgac086. doi:10.1093/pnasnexus/pgac086

Pastushkova, L. K., Custaud, M. A., Kononikhin, A. S., Brzhozovsky, A. G., Dmitrieva, L. E., Dobrokhotov, I. V., et al. (2017). Modification of the urine proteome in healthy human during 21-day bed rest. *Hum. Physiol.* 43, 813–817. doi:10.1134/S0362119717070155

Propson, N. E., Roy, E. R., Litvinchuk, A., Kohl, J., and Zheng, H. (2021). Endothelial C3a receptor mediates vascular inflammation and blood-brain barrier permeability during aging. *J. Clin. Invest.* 131, e140966. doi:10.1172/JCI140966

Rusanov, V. B., Pastushkova, L. K., Larina, I. M., Chernikova, A. G., Goncharova, A. G., Nosovsky, A. M., et al. (2020). The effect of five-day dry immersion on the nervous and metabolic mechanisms of the circulatory system. *Front. Physiol.* 11, 692. doi:10.3389/fphys.2020.00692

Schraufstatter, I. U., Trieu, K., Sikora, L., Sriramarao, P., and Discipio, R. (2002). Complement c3a and c5a induce different signal transduction cascades in endothelial cells. *J. Immunol.* 169, 2102–2110. doi:10.4049/jimmunol.169.4.2102

Toyoda, T., An, D., Witczak, C. A., Koh, H. J., Hirshman, M. F., Fujii, N., et al. (2011). Myo1c regulates glucose uptake in mouse skeletal muscle. *J. Biol. Chem.* 286 (6), 4133–4140. doi:10.1074/jbc.M110.174938

Trudel, G., Shahin, N., Ramsay, T., Laneuville, O., and Louati, H. (2022). Hemolysis contributes to anemia during long-duration space flight. *Nat. Med.* 28 (1), 59–62. doi:10.1038/s41591-021-01637-7

Trudel, G., Uhthoff, H. K., and Laneuville, O. (2017). Hemolysis during and after 21 days of head-down-tilt bed rest. *Physiol. Rep.* 5 (24), e13469. doi:10.14814/phy2.13469

Vizcaino, J. A., Csordas, A., del-Toro, N., Dianes, J. A., Griss, J., Lavidas, I., et al. (2016). 2016 update of the PRIDE database and its related tools. *Nucleic Acids Res.* 44, 447–456. doi:10.1093/nar/gkv1145

Waha, J. E., Goswami, N., Schlagenhauf, A., Leschnik, B., Koestenberger, M., Reibnegger, G., et al. (2015). Effects of exercise and nutrition on the coagulation system during bedrest immobilization. *Med. Baltim.* 94 (38), e1555. doi:10.1097/MD.0000000000001555

Yang, Q., Graham, T. E., Mody, N., Preitner, F., Peroni, O. D., Zabolotny, J. M., et al. (2005). Serum retinol binding protein 4 contributes to insulin resistance in obesity and type 2 diabetes. *Nature* 436, 356–362. doi:10.1038/nature03711

Zhang, Y., Zhang, W., Edvinsson, L., and Xu, C.-B. (2014). Apolipoprotein B of low-density lipoprotein impairs nitric oxide-mediated endothelium-dependent relaxation in rat mesenteric arteries. *Eur. J. Pharmacol.* 725, 10–17. doi:10.1016/j.ejphar.2014.01.008

frontiers | Frontiers in Physiology

TYPE Original Research
PUBLISHED 26 June 2024
DOI 10.3389/fphys.2024.1417719

OPEN ACCESS

EDITED BY
Kunihiko Tanaka,
Gifu University of Medical Science, Japan

REVIEWED BY
Ke Lv,
China Astronaut Research and Training Center, China
David Giovannucci,
University of Toledo, United States

*CORRESPONDENCE
Yoshiyuki Shibukawa,
yshibuka@tdc.ac.jp

†These authors have contributed equally to this work

RECEIVED 15 April 2024
ACCEPTED 04 June 2024
PUBLISHED 26 June 2024

CITATION
Ouchi T, Kono K, Satou R, Kurashima R, Yamaguchi K, Kimura M and Shibukawa Y (2024), Upregulation of *Amy1* in the salivary glands of mice exposed to a lunar gravity environment using the multiple artificial gravity research system.
Front. Physiol. 15:1417719.
doi: 10.3389/fphys.2024.1417719

Upregulation of *Amy1* in the salivary glands of mice exposed to a lunar gravity environment using the multiple artificial gravity research system

Takehito Ouchi[1†], Kyosuke Kono[1], Ryouichi Satou[2†], Ryuya Kurashima[1†], Koji Yamaguchi[3], Maki Kimura[1] and Yoshiyuki Shibukawa[1*]

[1]Department of Physiology, Tokyo Dental College, Tokyo, Japan, [2]Department of Epidemiology and Public Health, Tokyo Dental College, Tokyo, Japan, [3]NeSTRA (Next-Generation Space System Technology Research Association), Yokohama, Japan

Introduction: Space is a unique environment characterized by isolation from community life and exposure to circadian misalignment, microgravity, and space radiation. These multiple differences from those experienced on the earth may cause systemic and local tissue stress. Autonomic nerves, including sympathetic and parasympathetic nerves, regulate functions in multiple organs. Saliva is secreted from the salivary gland, which is regulated by autonomic nerves, and plays several important roles in the oral cavity and digestive processes. The balance of the autonomic nervous system in the seromucous glands, such as the submandibular glands, precisely controls serous and mucous saliva. Psychological stress, radiation damage, and other triggers can cause an imbalance in salivary secretion systems. A previous study reported that amylase is a stress marker in behavioral medicine and space flight crews; however, the detailed mechanisms underlying amylase regulation in the space environment are still unknown.

Methods: In this study, we aimed to elucidate how lunar gravity (1/6 *g*) changes mRNA expression patterns in the salivary gland. Using a multiple artificial gravity research system during space flight in the International Space Station, we studied the effects of two different gravitational levels, lunar and Earth gravity, on the submandibular glands of mice. All mice survived, returned to Earth from space, and their submandibular glands were collected 2 days after landing.

Results: We found that lunar gravity induced the expression of the salivary amylase gene *Amy1*; however, no increase in *Aqp5* and *Ano1*, which regulate water secretion, was observed. In addition, genes involved in the exocrine system, such as vesicle-associated membrane protein 8 (*Vamp8*) and small G proteins, including *Rap1* and *Rab* families, were upregulated under lunar gravity.

Conclusion: These results imply that lunar gravity upregulates salivary amylase secretion via *Rap*/*Rab* signaling and exocytosis via *Vamp8*. Our study highlights *Amy1* as a potential candidate marker for stress regulation in salivary glands in the lunar gravity environment.

KEYWORDS

lunar gravity, salivary gland, small G protein, amy1, microarray

1 Introduction

The transition from 1 *g* to the space environment changes not only gravity but also various other conditions such as the circadian rhythm (Otsuka et al., 2018) and exposure to cosmic rays (Zeitlin et al., 2013). It is important to elucidate the medical risks that humans face when living in a space environment, such as the oxidative stress caused by cosmic radiation (Overbey et al., 2019) and mechanical stress caused by microgravity (Dadwal et al., 2019). Artificial imitation of these environments may provide an understanding of gravitational physiology and determine how to avoid space stress.

A previous study showed that the gravitational threshold in the space environment provides a platform for exploring the mechanisms controlling the skeletal muscle response to alterations in gravity (Hayashi et al., 2023). Elucidation of the functional changes and molecular mechanisms involved may lead to the development of strategies to maintain human health during future long-term space travel. The musculoskeletal system and muscle movement controlled by somatic nerves have been studied previously in space and artificial gravitational environments (Juhl et al., 2021; Hayashi et al., 2023). Although studies on the heart rate and activity rhythms controlled by the autonomic nervous system in space are addressed (Blaber et al., 2004; Liu et al., 2015), research on the salivary glands, which are representative of local fluid balance regulation by the system, are limited. Saliva maintains the moist environment of oral tissues and is essential not only for feeding, mastication, and swallowing food but also for oral functions such as digestion, and articulation. In addition, saliva has antibacterial properties that help control the growth of harmful bacteria in the mouth, contributing to oral hygiene and prevention of dental issues such as cavities and gum disease. Saliva helps maintain pH balance in the mouth and neutralizes the acids produced by bacteria, thereby reducing the risk of tooth decay and erosion. It plays a role in taste perception by dissolving food particles and allowing them to interact with the taste buds in the tongue. Therefore, saliva is a multifunctional fluid that contributes significantly to oral and digestive health. Insufficient saliva production, known as dry mouth or xerostomia, can lead to various oral health problems and difficulties chewing, swallowing, and speaking. However, little is known about the regulatory mechanisms of salivary secretion during spaceflights.

In this study, we collected submandibular glands from mice exposed to artificial lunar gravity.

Among the major salivary glands, the large amount of saliva secretion comes from the submandibular gland. Therefore, we thought that changes in salivary gland mRNA due to environmental changes might be more clearly observed in the submandibular gland compared to other salivary glands. In addition, the submandibular gland is a mixed gland, and we considered that it would be a good model to observe the control mechanism and balance of protein secretion and water secretion by the sympathetic and parasympathetic nerves, i.e., under autonomic regulation.

Artificial lunar gravity was developed using multiple artificial gravity research systems (MARS) that use a centrifuge to create artificial gravity, enabling comparative studies between the effects of gravity and microgravity in space (Shimbo et al., 2016; Shiba et al., 2017; Okada et al., 2021). This system has contributed to analysis of sulfur metabolomic and transcriptomic changes in the liver (Kurosawa et al., 2021), metabolic effects in adipose tissues (Suzuki et al., 2020; Uruno et al., 2021), blood parameters changes (Shimizu et al., 2023), bone mineralization, blood pressure, and lipid metabolism in mouse kidneys (Suzuki et al., 2022) during space travel. This study investigated the basic foundations for oral clinical medicine under lunar gravity. We sought to understand whether lunar gravity (1/6 *g*) influence the mRNA expression in salivary glands during space flight. Using the developed MARS, two independent missions (MHU-4 and MHU-5) were conducted in the space. Using the MARS system, we analyzed the mRNA expression of the whole submandibular gland tissue of mice raised under lunar (1/6 *g*) and Earth gravity (1 *g*).

2 Materials and methods

2.1 Animals

C57BL/6 J male mice (Stock #000664) obtained from Jackson Laboratories (Bar Harbor, ME, United States) and Charles River Laboratories (Wilmington, MA, United States) were used for the MHU-4 and -5 missions. All experiments were approved by the Institutional Animal Care and Use Committee of the Japan Aerospace Exploration Agency (JAXA) (Protocol Number: No. 018-011D for MHU-4 and No. 018-036D for MHU-5), Explora Biolabs (Study Number: No. EB19-003 for MHU-4 and No. SP19-003 for MHU-5), and the National Aeronautics and Space Administration (NASA) (Protocol Number: No. FLT-18-118 for MHU-4 and No. JAXA MHU-5/FLT-19-121 for MHU-5). All experiments were conducted in accordance with the guidelines and applicable laws of Japan and the United States.

2.2 MHU missions

The ground control group (GC) comprised of six age-matched (9-week-old) male C57BL/6 J mice per mission, maintained on Earth under the same conditions as those aboard the International Space

Station (ISS). A detailed description of the space flight experiments has been previously reported (Hayashi et al., 2023).

In the MHU-4 mission, six 9-week-old male C57BL/6 J mice in a transportation cage unit were launched aboard SpX-17 on 7 May 2019, from the NASA Kennedy Space Center and were then transported to the ISS. The MHU-4 partial gravity (PG) group was maintained in an artificial gravity environment of 1/6 *g* on the bottom floor of the habitat cage unit by centrifugation at 31 rpm in MARS using a short-radius (15 cm) centrifuge (MARS-S).

In the MHU-5 mission, six 9-week-old male C57BL/6 J mice in a transportation cage unit were launched aboard SpX-20 on 10 March 2020, from the NASA Kennedy Space Center and were then transported to the ISS. The MHU-5_PG group was maintained in an artificial gravity environment of 1/6 *g* on the bottom floor of the habitat cage unit by centrifugation at 21 rpm in MARS using a long-radius (35 cm) centrifuge (MARS-L).

The lighting in the mouse habitat cage considered the circadian rhythm and used a 12-h cycle according to the ISS and GMT (standard) time, with a light period of 7:00 to 19:00 and a dark period from 19:00 to 7:00 the next day.

Cage unit was equipped with a water dispenser and a feeder that can automatically supply water and food. The crew only needed to periodically refill the water and replenish the food, reducing the workload of the crew. The water dispenser was based on a balloon for injecting medicines, and drinking water was supplied by pressurizing the water using the elasticity of the balloon. The amount of water in the balloon was able to be detected by a sensor when it was full and when a certain amount of water had been consumed from full. For feeding, a spring was used to push out integrally molded food to the feeding surface. Food needed to be replenished once a week, but the food in this device was in cartridge form, making it easy for the crew to replace the cartridges.

All the mice from each mission were sacrificed on the second day after returning to the Earth.

2.3 Sample collection and preparation

Submandibular glands were fixed with 4% paraformaldehyde (Wako, Osaka, Japan) for 1–2 d at 4 °C before replacing the paraformaldehyde with phosphate-buffered saline (PBS). The MHU-4 mission samples were processed in the United States in June 2019, and the MHU-5 mission samples were processed in the United States in April 2020. After approximately 40 d, the samples were treated with different concentrations of methanol, 25%, 50%, 75%, and 100%, for 30 min each and then maintained in 100% methanol. The MHU-4 mission samples were processed in Japan in July 2019, and the MHU-5 mission samples were processed in Japan in May 2020.

Samples from the ground control experiments were treated using the same method as those from the space experiments. The MHU-4 mission, samples were processed in December 2019; and the MHU-5 samples were processed in October 2020.

2.4 Total RNA isolation

Total RNA from whole submandibular gland in each group (the MHU-4 GC, the MHU-4 PG, the MHU-5 GC, the MHU-5 PG); n = 1 for each was isolated from the cells using the RNeasy Mini Kit (QIAGEN, Germany), according to the manufacturer's instructions. RNA samples were quantified using a Nanodrop ND-1000 spectrophotometer (Thermo Fisher Scientific, Waltham, MA, United States), and their quality was confirmed using a 2,200 TapeStation (Agilent Technologies, Santa Clara, CA, United States).

2.5 Gene expression microarrays

The total RNA from whole submandibular gland in each group was amplified using GeneChip® WT Pico Kit (Thermo Fisher Scientific) and hybridized to the Clariom™ S Assay, mouse (Thermo Fisher Scientific), according to the manufacturer's instructions. All hybridized microarrays were scanned using an Affymetrix scanner (Thermo Fisher Scientific). Relative hybridization intensities and background hybridization values were calculated using Affymetrix Expression Console™. Gene set enrichment analysis (GSEA) was conducted according to methods previously described (Mootha et al., 2003; Subramanian et al., 2005).

2.6 Data analysis and filter criteria

The raw signal intensities of all samples were normalized by a quantile algorithm using Affymetrix® Power Tools version 1.15.0 software. To identify up- or downregulated genes, we calculated Z-scores [Z] and ratios (non-log scaled fold-change) from the normalized signal intensities of each probe for comparison between the control and experimental samples. The criteria for upregulated genes was Z-score ≥2.0 and ratio ≥1.5-fold and for downregulated genes was Z-score ≤ −2.0 and ratio ≤0.66. Since there were no replicate samples in this analysis, it was impossible to evaluate the data using *p*-values. We used intensity-based Z-scores and fold changes to extract differentially expressed mRNAs. This is expected to reduce noise compared to extracting variable mRNAs based only on fold change values (Quackenbush, 2002).

2.7 Immunofluorescence analysis

We conducted immunofluorescence staining by using the whole submandibular gland in each group (the MHU-4 GC, the MHU-4 PG, the MHU-5 GC, the MHU-5 PG); n = 1 for each. The fixed submandibular glands were embedded in paraffin, and 2 μm sections were prepared using a microtome (Leica Biosystems, Wetzlar, Germany). The sections were deparaffinized by immersing in xylene (Wako) for 10 min three times. The sections were then rehydrated using sequential immersion in 100%, 95%, and 70% ethanol for 10 min. After ethanol treatment, the sections were washed three times with PBS. For immunofluorescence analysis, the samples were permeabilized with Triton X-100 (Sigma Aldrich, St. Louis, MO, United States) for 5 min before incubating with blocking buffer (Nacalai Tesque, Kyoto, Japan) at room temperature for 15 min. To evaluate the protein expression patterns, the samples were then

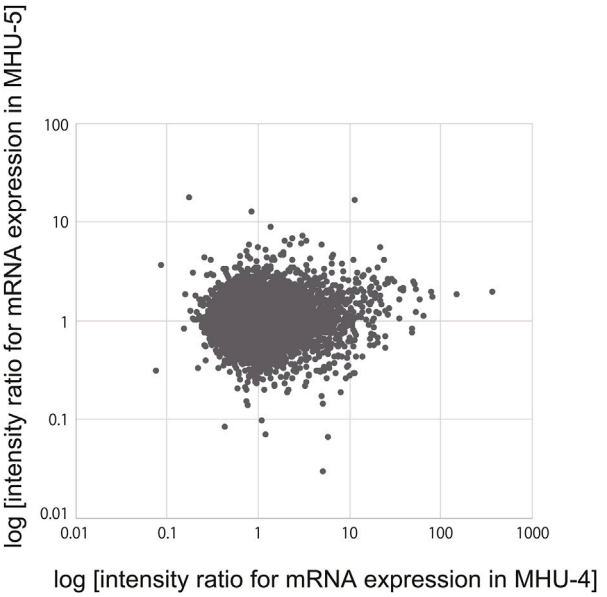

FIGURE 1
No correlation of salivary gene expression was observed between the MHU-4 and -5 missions. Microarray analysis revealed no correlation between changes in the mRNA expression of 22,206 genes (correlation coefficient: 0.077052) between the MHU-4 and -5 missions.

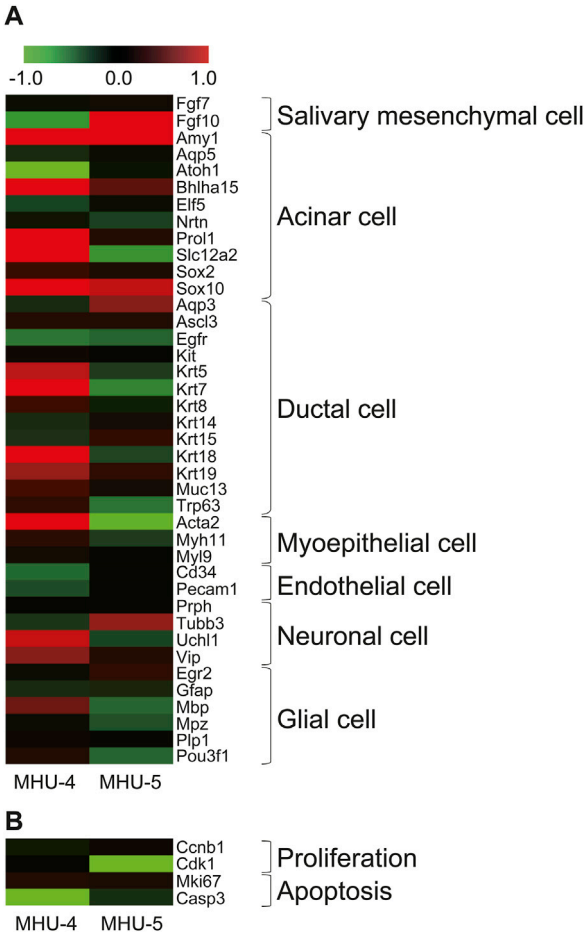

FIGURE 2
Increases of gene expression in acinar cells in lunar gravity environment. **(A)** Heat map shows representative mRNAs, encoding marker protein for the cells comprising submandibular gland. The map represents the ratio calculated from the signal intensity of 1/6 *g*–1 *g*. Microarray analysis revealed that the expression increases with significance were more seen in acinar cells. Gene expression increases were more observed in MHU-4 compared with those in MHU-5. **(B)** Genes relating to cell proliferation and apoptosis showed no upregulation. Red in heat map indicates upregulated mRNA at 1/6 *g* and green in heat map indicates downregulated mRNA at 1/6 *g* compared to the 1 *g* group.

incubated overnight at 4 °C with the following primary antibodies: mouse monoclonal anti-Amylase (sc-46657; 1:200; Santa Cruz Biotechnology, Inc., Dallas, TX, United States), rabbit polyclonal anti-Aquaporin5 (ab53212; 1:200; Abcam, Cambridge, United Kingdom), mouse monoclonal anti-Rap1 (sc-398755; 1:200; Santa Cruz Biotechnology, Inc.), mouse monoclonal anti-Rab2a (67501-1-Ig; 1:200; Proteintech, Rosemont, IL, United States), rabbit polyclonal anti-Rab10 (11808-1-AP; 1:200; Proteintech), rabbit polyclonal anti-Rab27b (13412-1-AP; 1:200; Proteintech), and rabbit polyclonal anti-Vamp8 (15546-1-AP; 1:200; Proteintech).

After washing with PBS, the following secondary antibodies were then incubated for 1 h at room temperature: Alexa Fluor® 568 donkey anti-mouse (#A10037; Thermo Fisher Scientific), Alexa Fluor® 488 donkey anti-rabbit (#A21206, Thermo Fisher Scientific). After washing with PBS, the stained samples were mounted in a mounting reagent with 4,6-diamidino-2-phenylindole (ab104139; Abcam) and analyzed using a fluorescence microscope (X710, X800; Keyence, Osaka, Japan).

3 Results

Microarray analysis to examine the changes in mRNA expression of the 22,206 genes found no correlation (correlation coefficient: 0.077052) between the submandibular gland samples obtained from the MHU-4 and -5 missions, even though both missions were conducted under the same lunar surface gravity environments (Figure 1). This may be due to differences in the centrifugal gradient caused by the radius of each MARS and circadian fluctuation between the time points for collecting samples in two missions.

We then investigated the cells comprising the submandibular glands and surrounding cell populations, based on specific marker, to identify which cell components showed specific mRNA expression changes in the lunar gravity environment in MHU-4 and -5. The heat map in Figure 2A shows signal intensity ratio of mRNA expression in samples at 1 *g* and 1/6 *g* environment in both MHU-4 and MHU-5 missions. Red indicates upregulated genes at 1/6 *g* and green indicates downregulated genes at 1/6 *g* compared to the 1 *g* group. Microarray analysis of whole submandibular glands samples from both MHU-4 and -5 revealed that the overall variation in mRNA expression was more pronounced in the MHU-4 mission than in the MHU-5 mission. Expression of mRNA relating the acinar cells, characterized by *Amy1*, *Bhlha15*, *Sox10* were more pronounced than those from other cell populations (Figure 2A). The expression of mRNA related to proliferation and apoptosis did not significantly increase at 1/6 *g* compared to the 1 *g* group

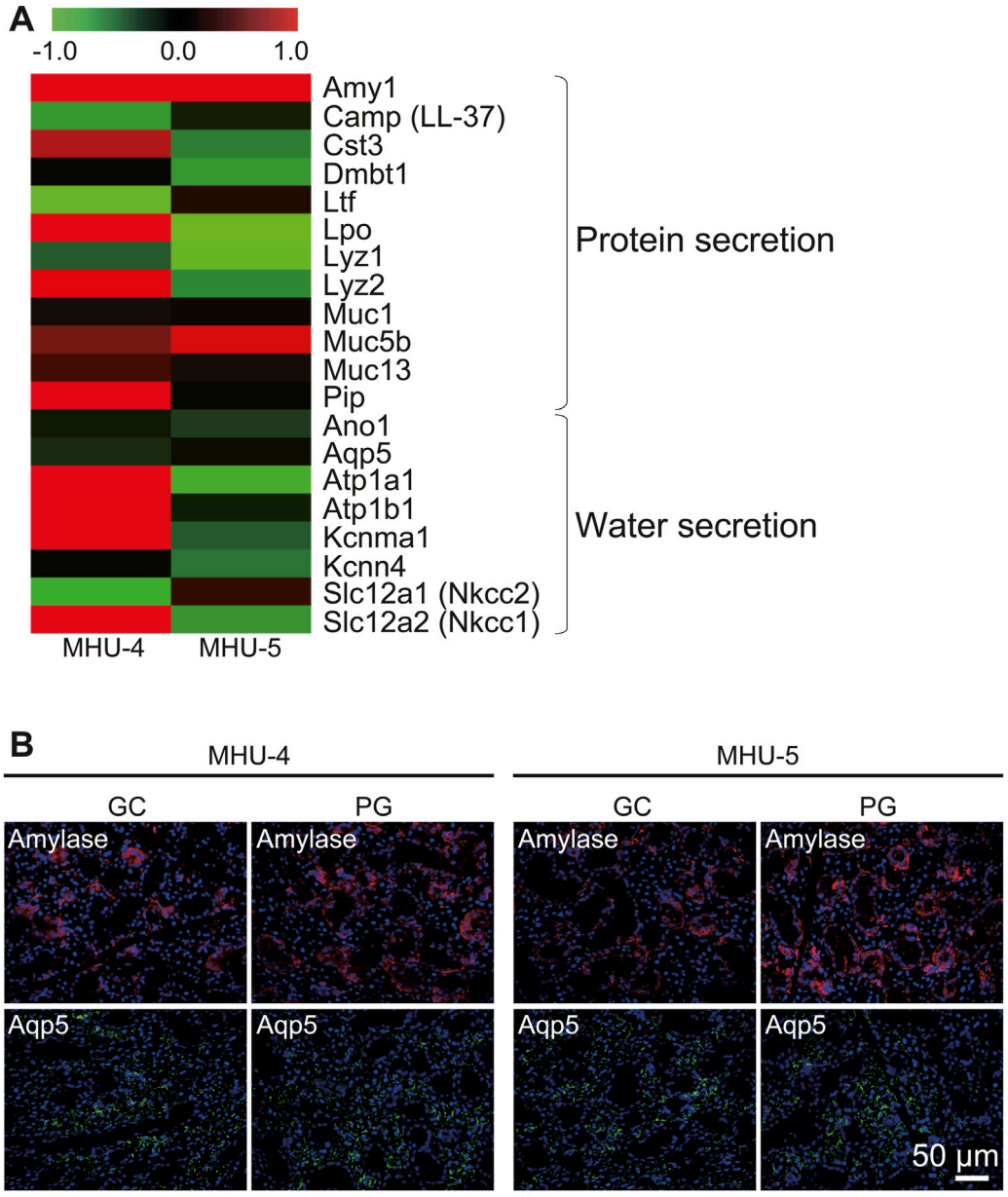

FIGURE 3
Upregulation of salivary *Amy1* in 1/6 *g* lunar gravity environment in both MHU-4 and MHU-5 missions. **(A)** Heat map showing the ratio calculated from the signal intensity of 1/6 *g*–1 *g*. Microarray analysis revealed that salivary protein gene *Amy1* was upregulated in 1/6 *g* lunar gravity in both MHU-4 and -5 missions. No significant increases of *Aqp5* were observed. Red in heat map indicates upregulated mRNA at 1/6 *g* and green in heat map indicates downregulated mRNA at 1/6 *g* compared to the 1 *g* group. **(B)** Immunofluorescence staining confirmed the increased expression of amylase in 1/6 *g* lunar gravity in both MHU-4 and -5 but no increase of Aqp5 even though the salivary cells were highly immunopositive for Aqp5. Scale bar: 50 μm.

(Figure 2B). Therefore, we focused on mature acinar cells that have physiological functions such as protein and water secretion.

Amy1 encodes salivary amylase secreted by acinar cells, which is an organic component involved in serous saliva. *Amy1* showed significant upregulation in the samples in the 1/6 *g* environment during both MHU missions (Figure 3A). In contrast, *Aqp5*, which is involved in water secretion in acinar cells, was highly expressed (data not shown), but no significant changes in the mRNA expression were observed between lunar gravity and ground controls in either mission (Figure 3A). Immunofluorescence staining showed that the amylase protein was expressed at a higher level in lunar gravity than in the ground control, which was consistent with the microarray results. Aqp5 protein expression was also consistent with the microarray data (Figure 3B).

We further examined signal intensity ratio of mRNA for membrane proteins with cytosolic coiled-coil domains, termed SNAREs, which are found in vesicles (v-SNAREs) and organelles (t-SNAREs) in whole submandibular glands. Vesicle-associated membrane protein 8 (*Vamp8*) is a v-SNARE gene involved in protein vesicle secretion mainly by acinar cells and was highly expressed under lunar gravity in both MHU missions; however, there was no increase in t-SNARE (Figure 4A). Based on these

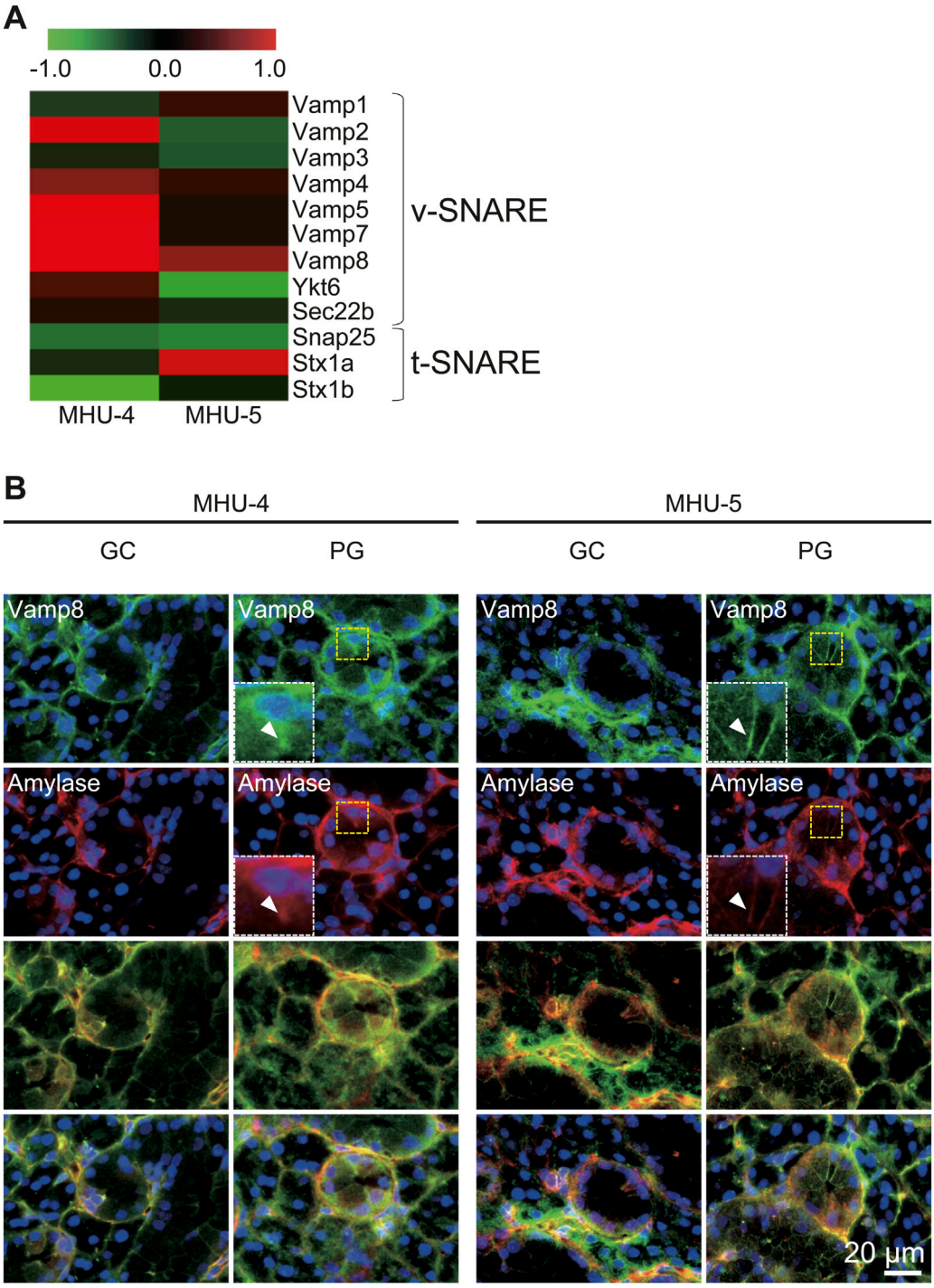

FIGURE 4
Upregulation of *Vamp8* in the lunar gravity group in both MHU-4 and MHU-5. **(A)** Heat map showing the ratio calculated from the signal intensity of 1/6 *g*–1 *g*. Microarray analysis revealed changes in expression of the v-SNARE gene, *Vamp8*. Other v-SNARE genes such as *Vamp2, 5,* and *7* were upregulated at 1/6 *g* compared to the 1 *g* in MHU-4. Upregulation of the t-SNARE gene in lunar gravity was not observed. Red in heat map indicates upregulated mRNA at 1/6 *g* and green in heat map indicates downregulated mRNA at 1/6 *g* compared to the 1 *g* group. **(B)** Immunofluorescence staining confirmed the co-localization of amylase and Vamp8 in acinar cells. Co-localized expression of amylase and Vamp8 was higher in lunar gravity compared with ground control for MHU-4 and MHU-5 missions. Insets (white dotted rectangles) were enlarged from the yellow dotted rectangles. Arrowheads indicate strong expression of Vamp8 protein and amylase at apical side of cell membrane in acinar cells. Scale bar: 20 μm.

results, it was assumed that amylase secretion was promoted through Vamp8 in the 1/6 *g* lunar gravity environment compared to 1 *g*. In samples from the both MHU-4 and MHU-5 missions, immunostaining revealed that amylase and Vamp8 protein expression was co-localized within acinar cells. We also observed strong expression of Vamp8 protein at apical side of cell membrane

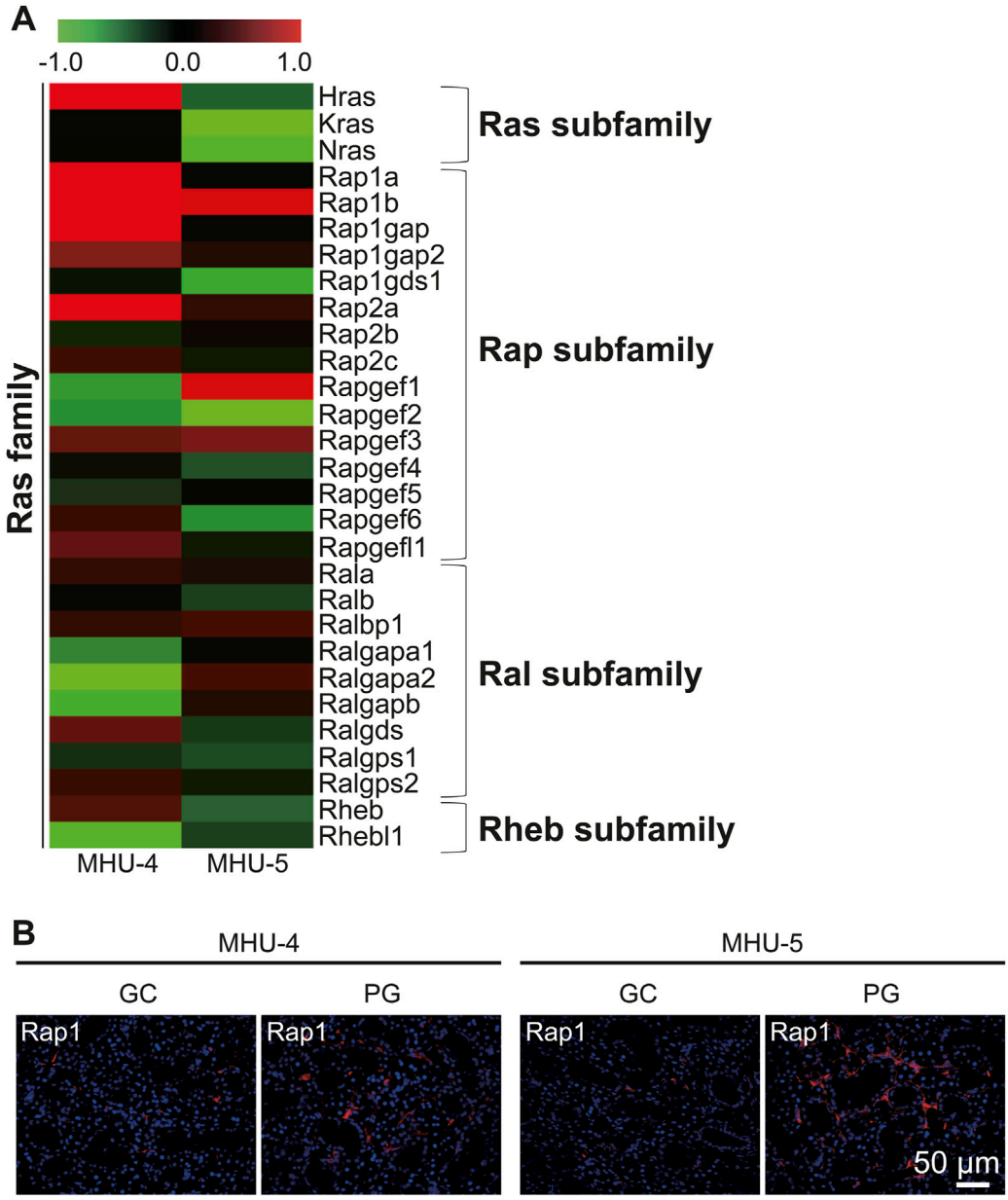

FIGURE 5
Upregulation of *Rap1* in lunar gravity in both MHU-4 and MHU-5. **(A)** Heat map showing the ratio calculated from the signal intensity of 1/6 *g*–1 *g*. Microarray analysis revealed changes in expression of *Rap1* in 1/6 *g* in both MHU-4 and MHU-5. Red in heat map indicates upregulated mRNA at 1/6 *g* and green in heat map indicates downregulated mRNA at 1/6 *g* compared to the 1 *g* group. **(B)** Immunofluorescence staining confirmed the upregulation of Rap1 in lunar gravity compared with ground control for both MHU-4 and MHU-5 missions. Scale bar: 50 μm.

in acinar cells at 1/6 *g* environment, implying enhancement of vesicle-membrane docking to secrete salivary proteins (Figure 4B).

Microarray analysis showed an increase in the mRNA expression of *Rap1b*, a subfamily of the *Ras* family in the 1/6 *g* lunar gravity of both MHU-4 and -5 groups (Figure 5A). The immunofluorescence staining results showed the upregulation of Rap1 protein, which were similar with the microarray data (Figure 5B). Increases of mRNA expression in samples from PG in both MHU-4 and MHU-5 missions were also observed for *Rab1*, *Rab2a*, *Rab10*, and *Rab27*, which are members of the *Rab* family (Figure 6A). Immunofluorescence staining showed upregulation of Rab2a, Rab10, and Rab27 protein which were similar with the microarray data (Figure 6B). Upregulation of some mRNAs from the *Rho* (Figure 7A), *Sar/Arf* (Figure 7B), and *Ran* (Figure 7C) families was observed at 1/6 *g* samples but did not show common expression patterns between MHU-4 and -5 missions, except for GEF/GAP (Figures 7A–C).

We explored upstream signaling pathways, including G_s, G_i, or G_q protein-coupled receptors and their respective second messengers and enzyme-related factors, as well as mRNA related to adrenergic receptors in the sympathetic nervous system and acetylcholine receptors in the parasympathetic nervous system. We observed no significant differences in mRNA expression of them between the samples of GC and PG

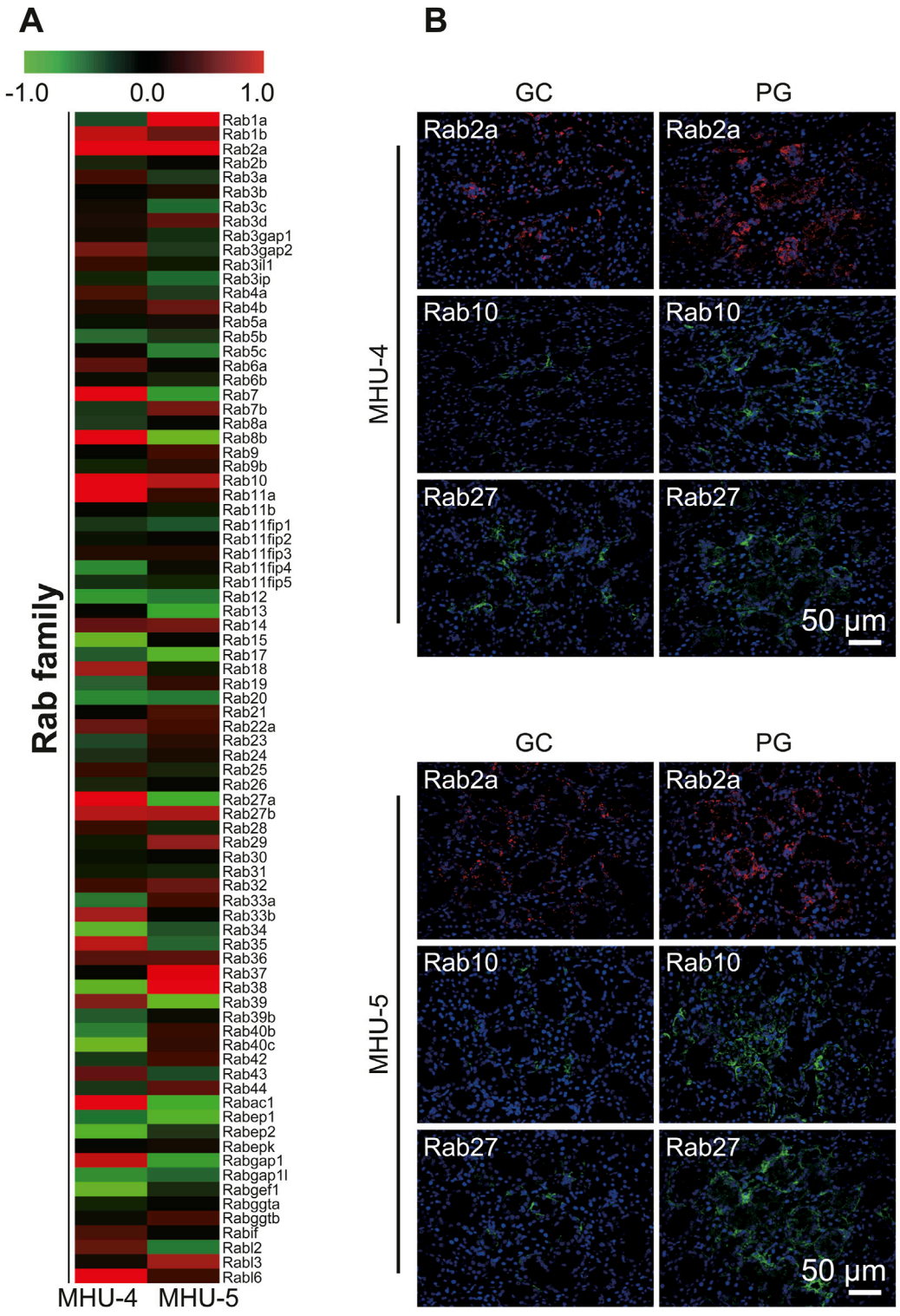

FIGURE 6
Upregulation of *Rab2a*, *Rab10*, and *Rab27* in lunar gravity in both MHU-4 and MHU-5. **(A)** Heat map showing the ratio calculated from the signal intensity of 1/6 *g*–1 *g*. Microarray analysis revealed that changes in the expression *Rab2a*, *Rab10*, and *Rab27* in 1/6 *g* in both MHU-4 and MHU-5. Red in heat map indicates upregulated mRNA at 1/6 *g* and green in heat map indicates downregulated mRNA at 1/6 *g* compared to the 1 *g* group. **(B)** Immunofluorescence staining confirmed the upregulation of Rab2a, Rab10, and Rab27 in lunar gravity compared with ground control for both MHU-4 and MHU-5 missions. Scale bar: 50 μm.

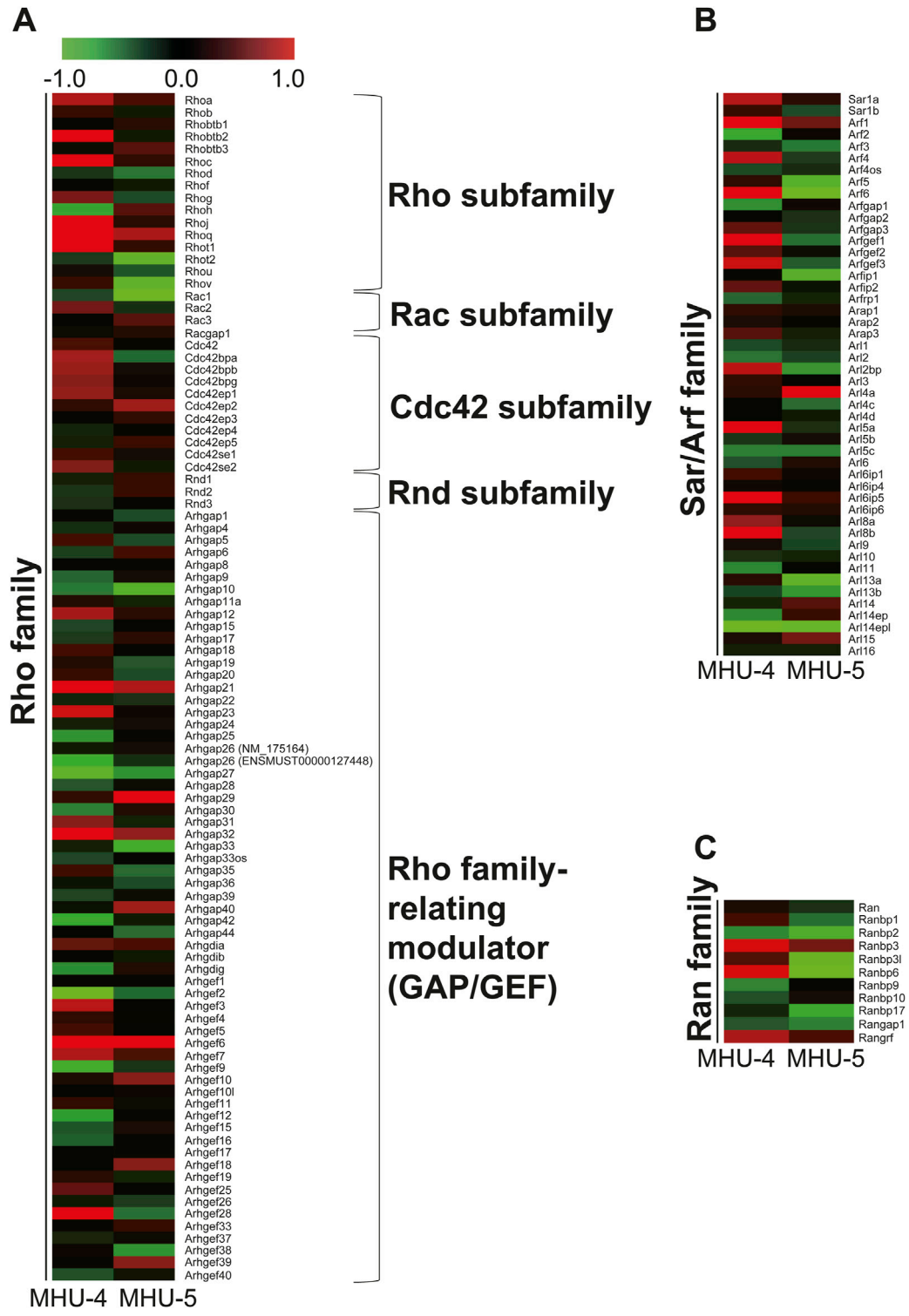

FIGURE 7
No common upregulation of *Rho*, *Sar/Arf*, and *Ran* family genes was observed in the lunar gravity groups of the MHU-4 and MHU-5 missions. **(A–C)** Heat map showing the ratio calculated from the signal intensity on small G protein, *Rho*, *Sar/Arf*, and *Ran* family of 1/6 *g*–1 *g*. Microarray analysis revealed no common upregulation of *Rho*, *Sar/Arf*, and *Ran* family except for *GEF/GAP* in lunar gravity for both MHU-4 and MHU-5 missions. Red in heat map indicates upregulated mRNA at 1/6 *g* and green in heat map indicates downregulated mRNA at 1/6 *g* compared to the 1 *g* group.

in both the MHU-4 and MHU-5 missions (Figure 8A). In sympathetic and parasympathetic nerve functions, genes related to adrenergic and cholinergic receptors in the submandibular glands were not significantly upregulated in 1/6 *g* lunar gravity in both the MHU-4 and -5 groups (Figure 8B). Therefore, changes in mRNA expression may occur downstream signals of salivary

10.3389/fphys.2024.1417719

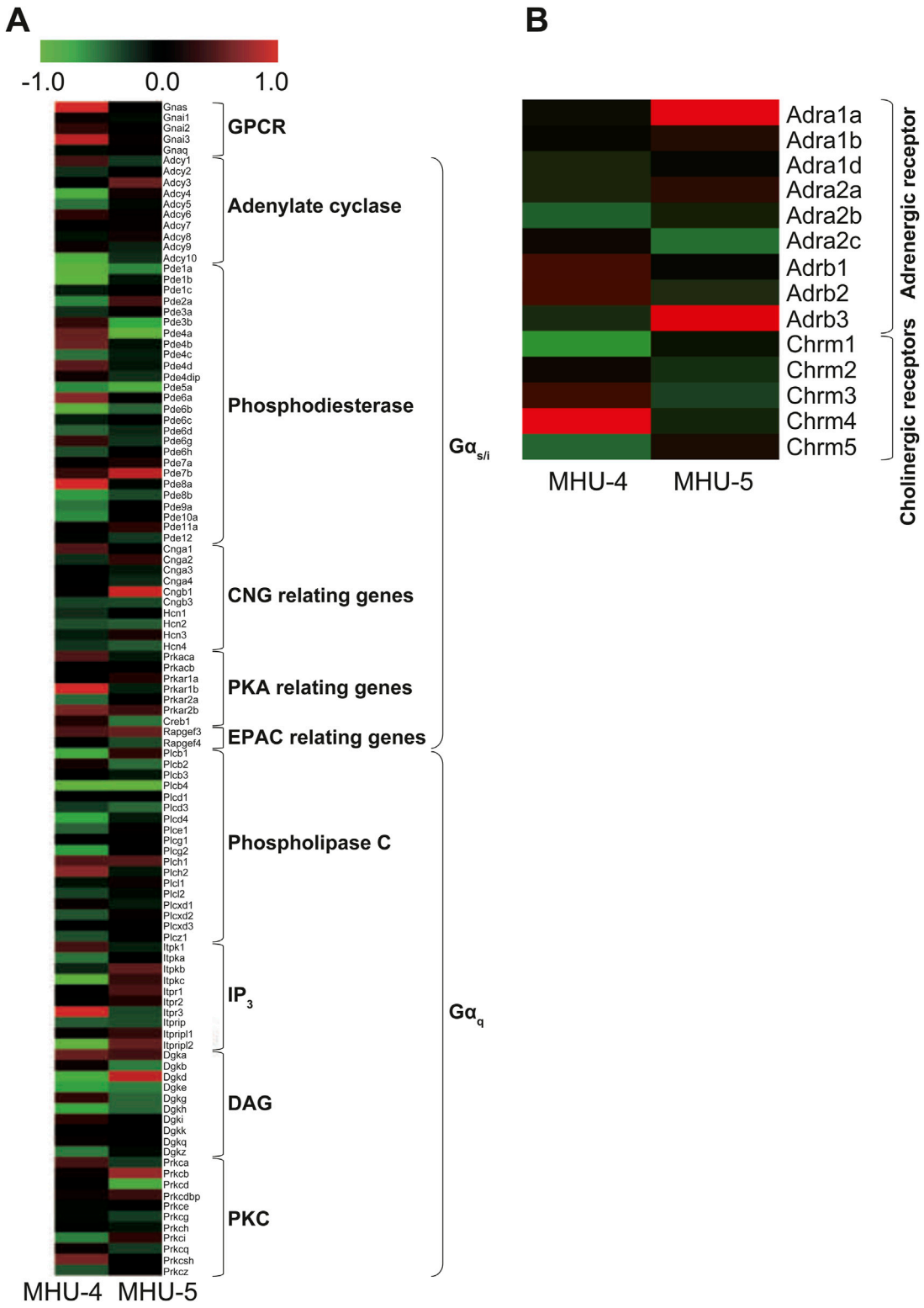

FIGURE 8
No common upregulation of GPCR, including G_s, G_i, or G_q proteins involved in salivary secretion, was observed. **(A)** Heat map showing the ratio calculated from the signal intensity of 1/6 *g*–1 *g*. Microarray analysis revealed no common upregulation of GPCR, including G_s, G_i, or G_q, involved in salivary secretion under the lunar gravity environment in MHU-4 and -5 missions. **(B)** There were no significant upregulation of autonomic nerve related receptor genes, including adrenergic and cholinergic receptors. Red in heat map indicates upregulated mRNA at 1/6 *g* and green in heat map indicates downregulated mRNA at 1/6 *g* compared to the 1 *g* group.

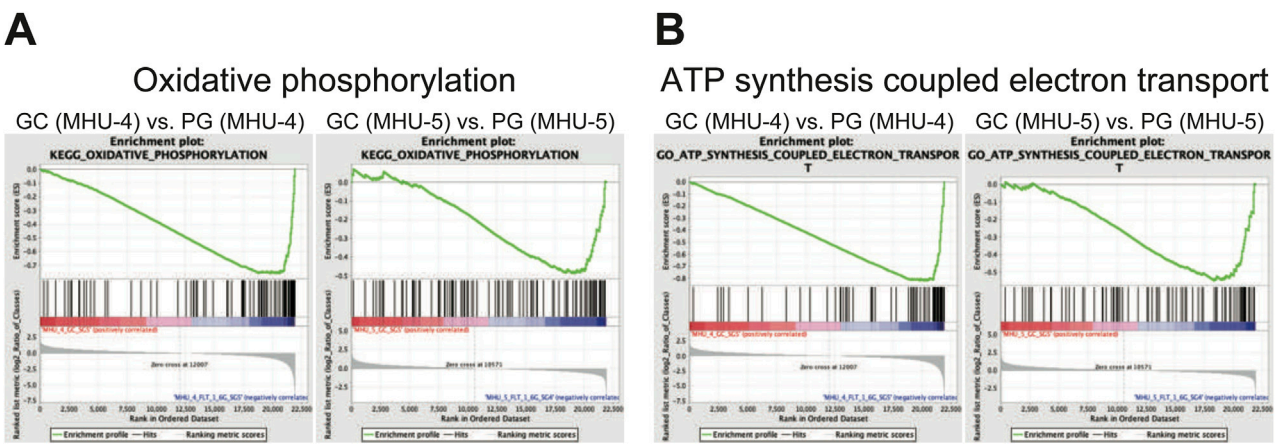

FIGURE 9
Enrichment in a set of mRNAs relating oxidative phosphorylation and ATP synthesis coupled electron transport was observed in lunar gravity in both MHU-4 and -5 missions. **(A)** Gene set enriched analysis (GSEA) revealed the activation of oxidative phosphorylation in lunar gravity for both MHU-4 and -5 missions. **(B)** GSEA also revealed the activation of ATP synthesis coupled electron transport in lunar gravity for both MHU-4 and -5 missions.

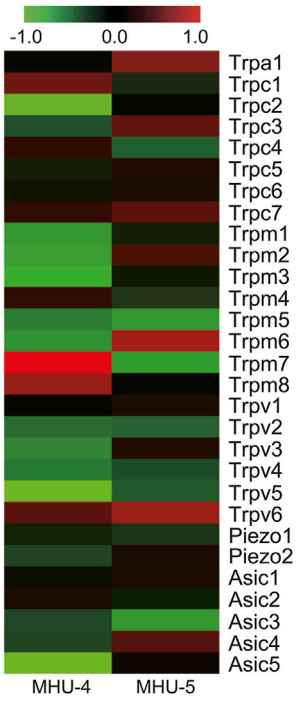

FIGURE 10
Downregulation of mechanosensitive ion channels in lunar gravity. Heat map showing the ratio calculated from the signal intensity of 1/6 *g*–1 *g*. Microarray analysis revealed downregulation of mechanosensitive ion channels, such as *Trpv2*, *Trpv4*, *Piezo1*, *Piezo2*, and *Asic3*, in lunar gravity for both the MHU-4 and MHU-5 missions. Red in heat map indicates upregulated mRNA at 1/6 *g* and green in heat map indicates downregulated mRNA at 1/6 *g* compared to the 1 *g* group.

secretion system involved in vesicular transport and secretion at apical side of acinar cells.

GSEA results revealed that the gene set involved in oxidative phosphorylation were highly upregulated in submandibular gland samples under 1/6 *g* lunar gravity in MHU-4 and -5 (Figure 9A). In addition, the gene set involved in ion exchange associated with ATP synthesis was also upregulated at 1/6 *g* lunar gravity compared to that under 1 *g* in the MHU-4 and -5 missions (Figure 9B).

We then investigated whether mechanosensitive ion channels in the submandibular glands sense gravity-induced fluid changes. The heat map shows ratio in changes in the mRNA expression of cation channels, especially transient receptor potential (TRP), Piezo, and acid-sensing ion (ASIC) channels. We revealed mechanosensitive ion channel genes, such as *Trpv2*, *Trpv4*, *Piezo1*, *Piezo2*, and *Asic3* were downregulated in the 1/6 *g* group compared with the 1 *g* group in MHU-4 and -5 (Figure 10).

4 Discussion

In the 1/6 *g* lunar gravitational environment, *Amy1* was upregulated in the submandibular glands, as were *Vamp8* and the small G protein *Rap1* (*Ras* family)/*Rab2a*, *Rab10*, and *Rab27* (Rab family) which are involved in vesicle secretion. Amylase has been identified as a stress marker in behavioral medicine and space flight crews (Ali and Nater, 2020; Ghasemi et al., 2021). *Vamp8* acts as a v-SNARE that regulates the secretion of the entire exocrine system (Wang et al., 2007). Salivary proteins are synthesized in acinar cells. Based on the genetic information in acinar cells, salivary proteins are synthesized in ribosomes, pass through the rough endoplasmic reticulum, become vesicles, and are transported to the Golgi apparatus. Intravesicular proteins that undergo modifications, such as glycosylation, in the Golgi apparatus are concentrated and stored in secretory granules. Small G proteins such as Ras and Rab families function salivary secretion, as guanosine triphosphate (GTP)-binding proteins with a molecular weight of 20–30 kDa. This hydrolysis results in inactive guanosine diphosphate (GDP). Small G proteins act as molecular switches that bind specific target molecules and transmit intracellular signals. GDP/GTP exchange proteins (GEF) are regulated by GTPase-activating proteins (GAPs). The combined GTP and GDP states

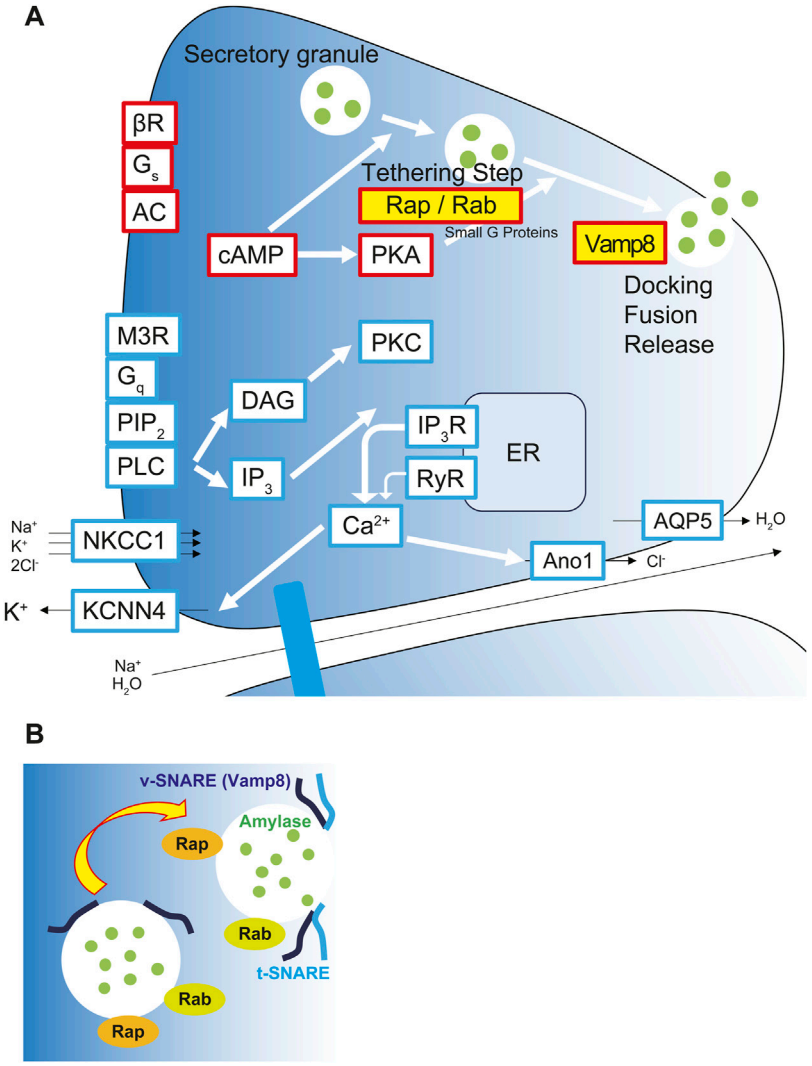

FIGURE 11
Upregulation of salivary amylase secretion via Rap/Rab signaling and exocytosis via Vamp8 under the lunar gravity. **(A)** Graphical scheme shows signaling pathway for salivary secretion in acinar cells. Yellow labeled Rap-, Rab-, and Vamp8-encoding mRNAs and their proteins were upregulated and localized at apical membrane in acinar cells at the 1/6 *g* lunar gravity. Red boxes represent proteins and molecules for salivary protein secretion. Blue boxes represent proteins and molecules for the water/ion secretion. **(B)** Rap and Rab small G proteins modulate the processivity of vesicles to apical side of cell membrane. Apical side of cell membrane showed upregulation of Vamp8 protein and vesicle-membrane docking to secrete salivary amylase at 1/6 *g* environment. AC, adenylyl cyclase; Ano1, anoctamin1; AQP5, aquaporin 5; βR, β-adrenergic receptor; cAMP, cyclic adenosine monophosphate; Ca^{2+}, calcium ion; DAG, diacylglycerol; ER, endoplasmic reticulum; G_q, G_q protein-coupled receptor; G_s, G_s protein-coupled receptor; IP_3, inositol trisphosphate; IP_3R, inositol trisphosphate receptor; KCNN4, potassium calcium-activated channel subfamily N member 4; M3R, muscarinic acetylcholine receptor M_3; NKCC1, sodium, potassium, chloride cotransporter 1; PIP_2, phosphatidylinositol 4,5-bisphosphate; PKA, protein kinase A; PKC, protein kinase C; PLC, phospholipase C; Rab, small G protein Rab; Rap, small G protein Rap; RyR, ryanodine receptor; t-SNARE, target membrane-associated T-soluble *N*-ethylmaleimide-sensitive factor attachment protein receptor; Vamp8, vesicle-associated membrane protein 8; v-SNARE, vesicle-associated V-soluble *N*-ethylmaleimide-sensitive factor attachment protein receptor.

function as molecular switches corresponding to the on/off states. Activity regulation is temporally and spatially controlled and functions as a biotimer. Small G proteins are classified into five families, and regulate various cellular functions. *Rap*/*Rab* signaling plays an important role in saliva and amylase secretion (D'Silva et al., 1998; Sabbatini et al., 2008; Gomi et al., 2017). Our study showed no increase in the expression of mRNA related to receptors for noradrenaline secreted from sympathetic nerves involved in protein secretion, where is the upstream of salivary secretion system, while upregulations of Rap/Rab signaling for transporting intracellular vesicles and v-SNARE (Vamp8) to secrete amylase via exocytosis at apical side of acinar cells were observed in the 1/6 *g* environment.

In addition, salivary secretion requires high levels of adenosine triphosphate (ATP) not only for salivary secretion by maintaining intracellular K^+ concentration in acinar cells, but also for modification of saliva by reabsorption and secretion in ductal cells of submandibular gland. Our GSEA data show that a set of mRNAs involved in oxidative phosphorylation was highly upregulated under 1/6 *g* lunar gravity in MHU-4 and -5. Plus, mRNAs in association of ionic transport coupled with ATP synthesis or hydrolysis were also upregulated at 1/6 *g* lunar

gravity compared to that under 1 *g* in the MHU-4 and -5 missions. We also hypothesized that changes in gravity may induce changes in body fluids, resulting in excessive fluid inflow into the submandibular gland. Our data shows downregulation of mechanosensitive ion channels such as *TRP*, *Piezo*, and *ASIC* channels, however. Fluid balance fluctuates when gravity changes, shifting fluid to the upper body and creating a situation where the astronauts have edema around the salivary glands, which causes mechanical stress. It is possible that the mRNA levels of these mechanosensitive ion channels in the submandibular gland decrease because of a function that restores them to their normal state.

In conclusion, our results indicate that changes in the gravitational environment induce qualitative changes in salivary secretion function and that multiple genes may be involved in maintaining salivary secretion homeostasis in the space environment. Overall, our data suggested that lunar gravity upregulates salivary amylase secretion via vesicular transport and exocytosis mediated by Rap/Rab signaling and Vamp8 at apical side of acinar cells (Figure 11). However, we have not shown the functional assay as amylase secretion in this study. To clarify the correlation mechanisms between these mRNAs and amylase secretion, it will need to be verified whether any effect on amylase secretion is caused by both gain-of-function and loss-of-function experiments in acinar cells. Further research on salivary secretion signal and gene regulation may contribute to the future monitoring of the physical and mental health of humans living in space as well as the improvement of oral medicine.

Data availability statement

The original contributions presented in the study are included in the article/Supplementary Material, further inquiries can be directed to the corresponding author.

Ethics statement

The animal studies were approved by the Institutional Animal Care and Use Committee of the Japan Aerospace Exploration Agency (JAXA) (Protocol Number: No. 018-011D for MHU-4 and No. 018-036D for MHU-5), Explora Biolabs (Study Number: No. EB19-003 for MHU-4 and No. SP19-003 for MHU-5), and the National Aeronautics and Space Administration (NASA) (Protocol Number: No. FLT-18-118 for MHU-4 and No. JAXA MHU-5/FLT-19-121 for MHU-5). All experiments were conducted in accordance with the guidelines and applicable laws of Japan and the United States. The studies were conducted in accordance with the local legislation and institutional requirements. Written informed consent was obtained from the owners for the participation of their animals in this study.

Author contributions

TO: Conceptualization, Data curation, Formal Analysis, Investigation, Methodology, Validation, Writing–original draft, Writing–review and editing, Funding acquisition, Project administration. KK: Conceptualization, Writing–original draft, Writing–review and editing. RS: Conceptualization, Data curation, Investigation, Methodology, Validation, Writing–original draft, Writing–review and editing. RK: Conceptualization, Methodology, Validation, Writing–review and editing, Writing–original draft. KY: Conceptualization, Validation, Writing–original draft, Writing–review and editing. MK: Conceptualization, Validation, Writing–original draft, Writing–review and editing. YS: Conceptualization, Investigation, Supervision, Validation, Writing–original draft, Writing–review and editing, Project administration.

Funding

The author(s) declare that financial support was received for the research, authorship, and/or publication of this article. Tokyo Dental College Research Grant (Wellbeing Project).

Acknowledgments

Biospecimens used in this study were provided by tissue sharing solicitation for JAXA mouse missions in space.

Conflict of interest

The authors declare that the research was conducted in the absence of any commercial or financial relationships that could be construed as a potential conflict of interest.

The author(s) declared that they were an editorial board member of Frontiers, at the time of submission. This had no impact on the peer review process and the final decision.

Publisher's note

References

Ali, N., and Nater, U. M. (2020). Salivary alpha-amylase as a biomarker of stress in behavioral medicine. *Int. J. Behav. Med.* 27, 337–342. doi:10.1007/s12529-019-09843-x

Blaber, A. P., Bondar, R. L., and Kassam, M. S. (2004). Heart rate variability and short duration spaceflight: relationship to post-flight orthostatic intolerance. *BMC Physiol.* 4, 6. doi:10.1186/1472-6793-4-6

Dadwal, U. C., Maupin, K. A., Zamarioli, A., Tucker, A., Harris, J. S., Fischer, J. P., et al. (2019). The effects of spaceflight and fracture healing on distant skeletal sites. *Sci. Rep.* 9, 11419. doi:10.1038/s41598-019-47695-3

D'Silva, N. J., Jacobson, K. L., Ott, S. M., and Watson, E. L. (1998). Beta-adrenergic-induced cytosolic redistribution of Rap1 in rat parotid acini: role in secretion. *Am. J. Physiol.* 274, C1667–C1673. doi:10.1152/ajpcell.1998.274.6.C1667

Ghasemi, S., Dashti, M., and Akbarboojar, F. M. (2021). Salivary stress biomarkers in flight crew during space missions to assess stress levels: a systematic review. *Int. J. Microgravity Sci. Appl.* 38, 380305. doi:10.15011/jasma.38.380305

Gomi, H., Osawa, H., Uno, R., Yasui, T., Hosaka, M., Torii, S., et al. (2017). Canine salivary glands: analysis of Rab and SNARE protein expression and SNARE complex formation with diverse tissue properties. *J. Histochem. Cytochem.* 65, 637–653. doi:10.1369/0022155417732527

Hayashi, T., Fujita, R., Okada, R., Hamada, M., Suzuki, R., Fuseya, S., et al. (2023). Lunar gravity prevents skeletal muscle atrophy but not myofiber type shift in mice. *Commun. Biol.* 6, 424. doi:10.1038/s42003-023-04769-3

Juhl, O. J. 4th, Buettmann, E. G., Friedman, M. A., DeNapoli, R. C., Hoppock, G. A., and Donahue, H. J. (2021). Update on the effects of microgravity on the musculoskeletal system. *Microgravity* 7, 28. doi:10.1038/s41526-021-00158-4

Kurosawa, R., Sugimoto, R., Imai, H., Atsuji, K., Yamada, K., Kawano, Y., et al. (2021). Impact of spaceflight and artificial gravity on sulfur metabolism in mouse liver: sulfur metabolomic and transcriptomic analysis. *Sci. Rep.* 11, 21786. doi:10.1038/s41598-021-01129-1

Liu, Z., Wan, Y., Zhang, L., Tian, Y., Lv, K., Li, Y., et al. (2015). Alterations in the heart rate and activity rhythms of three orbital astronauts on a space mission. *Life Sci. Space Res. (Amst)* 4, 62–66. doi:10.1016/j.lssr.2015.01.001

Mootha, V. K., Lindgren, C. M., Eriksson, K. F., Subramanian, A., Sihag, S., Lehar, J., et al. (2003). PGC-1alpha-responsive genes involved in oxidative phosphorylation are coordinately downregulated in human diabetes. *Nat. Genet.* 34, 267–273. doi:10.1038/ng1180

Okada, R., Fujita, S. I., Suzuki, R., Hayashi, T., Tsubouchi, H., Kato, C., et al. (2021). Transcriptome analysis of gravitational effects on mouse skeletal muscles under microgravity and artificial 1 *g* onboard environment. *Sci. Rep.* 11, 9168. doi:10.1038/s41598-021-88392-4

Otsuka, K., Cornelissen, G., Kubo, Y., Shibata, K., Hayashi, M., Mizuno, K., et al. (2018). Circadian challenge of astronauts' unconscious mind adapting to microgravity in space, estimated by heart rate variability. *Sci. Rep.* 8, 10381. doi:10.1038/s41598-018-28740-z

Overbey, E. G., da Silveira, W. A., Stanbouly, S., Nishiyama, N. C., Roque-Torres, G. D., Pecaut, M. J., et al. (2019). Spaceflight influences gene expression, photoreceptor integrity, and oxidative stress-related damage in the murine retina. *Sci. Rep.* 9, 13304. doi:10.1038/s41598-019-49453-x

Quackenbush, J. (2002). Microarray data normalization and transformation. *Nat. Genet.* 32 (Suppl. l), 496–501. doi:10.1038/ng1032

Sabbatini, M. E., Chen, X., Ernst, S. A., and Williams, J. A. (2008). Rap1 activation plays a regulatory role in pancreatic amylase secretion. *J. Biol. Chem.* 283, 23884–23894. doi:10.1074/jbc.M800754200

Shiba, D., Mizuno, H., Yumoto, A., Shimomura, M., Kobayashi, H., Morita, H., et al. (2017). Development of new experimental platform 'MARS'—multiple Artificial-gravity Research System—to elucidate the impacts of micro/partial gravity on mice. *Sci. Rep.* 7, 10837. doi:10.1038/s41598-017-10998-4

Shimbo, M., Kudo, T., Hamada, M., Jeon, H., Imamura, Y., Asano, K., et al. (2016). Ground-based assessment of JAXA mouse habitat cage unit by mouse phenotypic studies. *Exp. Anim.* 65, 175–187. doi:10.1538/expanim.15-0077

Shimizu, R., Hirano, I., Hasegawa, A., Suzuki, M., Otsuki, A., Taguchi, K., et al. (2023). Nrf2 alleviates spaceflight-induced immunosuppression and thrombotic microangiopathy in mice. *Commun. Biol.* 6, 875. doi:10.1038/s42003-023-05251-w

Subramanian, A., Tamayo, P., Mootha, V. K., Mukherjee, S., Ebert, B. L., Gillette, M. A., et al. (2005). Gene set enrichment analysis: a knowledge-based approach for interpreting genome-wide expression profiles. *Proc. Natl. Acad. Sci. U. S. A.* 102, 15545–15550. doi:10.1073/pnas.0506580102

Suzuki, N., Iwamura, Y., Nakai, T., Kato, K., Otsuki, A., Uruno, A., et al. (2022). Gene expression changes related to bone mineralization, blood pressure and lipid metabolism in mouse kidneys after space travel. *Kidney Int.* 101, P92–P105. doi:10.1016/j.kint.2021.09.031

Suzuki, T., Uruno, A., Yumoto, A., Taguchi, K., Suzuki, M., Harada, N., et al. (2020). Nrf2 contributes to the weight gain of mice during space travel. *Commun. Biol.* 3, 496. doi:10.1038/s42003-020-01227-2

Uruno, A., Saigusa, D., Suzuki, T., Yumoto, A., Nakamura, T., Matsukawa, N., et al. (2021). Nrf2 plays a critical role in the metabolic response during and after spaceflight. *Commun. Biol.* 4, 1381. doi:10.1038/s42003-021-02904-6

Wang, C. C., Shi, H., Guo, K., Ng, C. P., Li, J., Gan, B. Q., et al. (2007). VAMP8/endobrevin as a general vesicular SNARE for regulated exocytosis of the exocrine system. *Mol. Biol. Cell.* 18, 1056–1063. doi:10.1091/mbc.e06-10-0974

Zeitlin, C., Hassler, D. M., Cucinotta, F. A., Ehresmann, B., Wimmer-Schweingruber, R. F., Brinza, D. E., et al. (2013). Measurements of energetic particle radiation in transit to mars on the mars science laboratory. *Science* 340, 1080–1084. doi:10.1126/science.1235989

frontiers | Frontiers in Physiology

TYPE Original Research
PUBLISHED 30 September 2024
DOI 10.3389/fphys.2024.1460131

OPEN ACCESS

EDITED BY
Marc-Antoine Custaud,
Université d'Angers, France

REVIEWED BY
Dieter Blottner,
Charité University Medicine Berlin, Germany
Felice Strollo,
IRCCS San Raffaele Pisana, Italy

*CORRESPONDENCE
Philippe Arbeille,
arbeille@med.univ-tours.fr

RECEIVED 05 July 2024
ACCEPTED 13 August 2024
PUBLISHED 30 September 2024

CITATION
Arbeille P, Zuj K and Guillon L (2024) Liver tissue changes during and post 6-month spaceflight as measured by ultrasound radio frequency signal processing.
Front. Physiol. 15:1460131.
doi: 10.3389/fphys.2024.1460131

Liver tissue changes during and post 6-month spaceflight as measured by ultrasound radio frequency signal processing

Philippe Arbeille*, Kathryn Zuj and Laurent Guillon

UMPS-CERCOM (Space Physiology and Medicine) School of Medicine University of Tours, Tours, France

Background: Analysis of ultrasound radio frequency (RF) signals allows for the determination of the index of reflectivity (IR), which is a new measure that is dependent on tissue properties. Previous work has shown differences in the IR of the carotid artery wall with long-duration spaceflight; therefore, it was hypothesized that liver tissue would also show differences in this measure with spaceflight.

Methods: The RF signal of a liver tissue region of interest (ROI) was displayed and processed along six different lines covering a surface of approximately 2 cm × 2 cm. The IR was calculated as the energy backscattered by the liver ROI divided by the total energy returned to the ultrasound probe.

Results: Seven astronauts were investigated preflight, inflight on day 150, and postflight 4 days and 6 months after rerunning to Earth. Compared to preflight (63% ± 18%), the liver tissue ROI IR was significantly lower on flight day 150 (46% ± 14%; p = 0.027) and 4 days postflight (46% ± 19%; p = 0.025). At 6 months postflight, the IR returned to preflight values (59% ± 13%; p = 0.919).

Conclusion: The significant decrease in the coefficient of reflectivity inflight and 4 days postflight indicates an alteration in the liver tissue that reduces the reflection of ultrasound waves. This change in tissue properties could either be due to the addition of particles that do not reflect ultrasound waves or structural or cellular changes that alter the reflectivity of the tissue.

KEYWORDS

liver, radio frequency signal, RF, echography, spaceflight

Introduction

Previous studies have shown a connection between insulin resistance and liver steatosis (Genazzani et al., 2024; Anousin et al., 2024). Elevation of an insulin resistance index has also been found after 6 months of spaceflight (Hughson et al., 2016). This suggests that liver structure may also be altered with long-duration spaceflight on the International Space Station (ISS).

Measurement of the index of reflectivity (IR), determined from analysis of the ultrasound radio frequency (RF) signal, has shown changes in the carotid artery wall with long-duration spaceflight (Arbeille et al., 2021). As this new ultrasound measurement was able to detect changes in tissue properties of the arterial wall, it is possible that similar measures of liver tissue will also identify changes in liver tissue properties with long-duration spaceflight on the ISS. Therefore, the objective of the present research was to

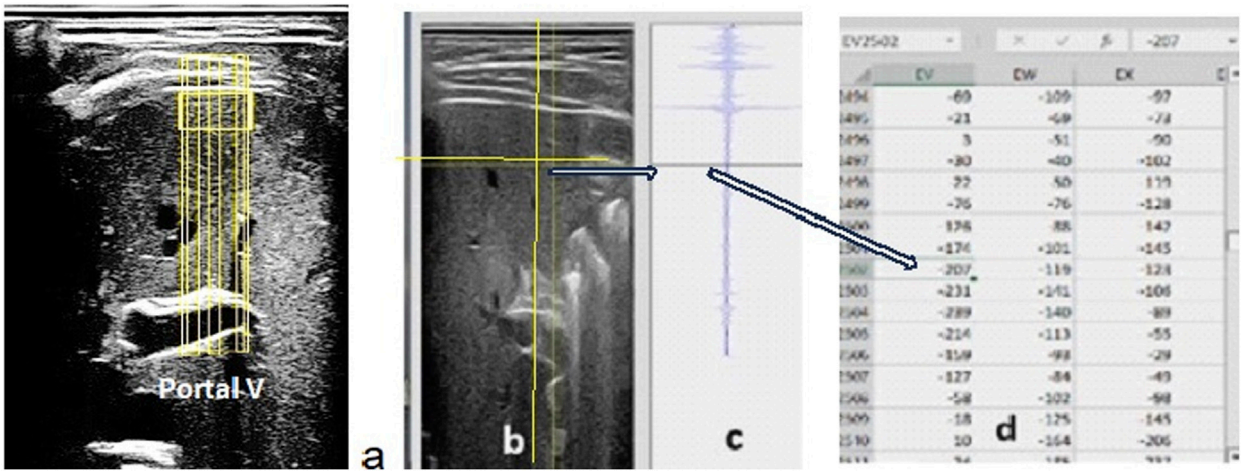

FIGURE 1
(A) B-mode liver view with the portal vein as a reference at the bottom of the image. The RF data are collected over the entire image but processed only along the six vertical lines passing through the liver region of interest. **(B)** Vertical and horizontal lines that the sonographer moves to determine the value of the energy reflected by the point at the intersection of these lines. Using this tool, the operator can identify the right and left and upper and lower limits of the ROI values and sum the values of the energy reflected along each vertical segment of the ROI on the six lines selected in the data table. **(C)** The RF signal presented corresponds to one full vertical ultrasound line crossing the sample. **(D)** The tabulated data display the values of the amplitude of the ultrasound signal reflected at any point in the image. The square of the amplitude values (minus the background noise estimated at the bottom of the ultrasound image) was used to estimate the energy reflected at each point.

determine whether the IR, determined by ultrasound RF signal processing, was altered for liver tissue during long-duration spaceflight and postflight recovery.

The RF signal is the native ultrasound signal that is processed by the ultrasound system manufacturer's software (i.e., filtered, smoothed, and amplified) to construct B-mode (black and white) ultrasound images. During operation, ultrasound probes emit hundreds of ultrasound beams in the plane below the probe head. As the beams reflect off successive interfaces along linear paths, changes in the reflected waves are captured by the probe as the radio frequency signal (RF) (Figure 1C).

The native RF signal is recognized in ultrasound science with applications designed to accurately track tissue displacement in the carotid artery walls (Palombo et al., 2012) or brain tissue (Jurkonis et al., 2020) and to study tissue characteristics. Tissue microstructure has been examined (Maleke and Konofagou, 2008), as have changes in tissue properties after being heated by focused ultrasound, with reports of a relationship between an increased stiffness and the reduction in micro-displacement inside the tissue (Maleke and Konofagou, 2008). RF recording and processing were also used in studies of carotid artery stenosis to evaluate the average blood integrated-back scattered energy within the lumen at proximal and distal segments to gain an estimate of a functional ischemia parameter (Okada et al., 2019). At the abdominal level, the processing of the ultrasound image content or the RF signal was applied to identify tissue aspect changes such as liver steatosis or fibrosis (Byeong Geun et al., 2024; Moradi et al., 2006) and detection/characterization of prostate malignant tumors (Schmitz et al., 1999). Lastly, RF signal processing has been used to investigate membranes of tumors of the inner eye (Trier, 1983).

The present study was based on the use of the index of reflectivity (IR), as defined previously for the evaluation of carotid wall changes during spaceflight and dry immersion (Arbeille et al., 2021; 2022). Using the same method, the RF signal of a liver tissue region of interest (ROI) was collected and analyzed preflight, inflight, and postflight, and the IRs of these ROIs were calculated. We hypothesized that the morphological and/or mechanical properties of the liver tissue structure and or content would be affected by spaceflight and detected as a change in the corresponding IR.

Research design and methods

Population investigated

Approximately 1 month before a 6-month spaceflight, after 150 days of flight, and 4 days and 6 months after return to Earth, seven astronauts (five men and two women; age: 44 ± 3 years; height: 177 ± 5 cm; weight: 76 ± 11 kg) underwent an ultrasound investigation where liver B-mode images and RF signals were acquired. The protocol was approved by the University of Waterloo Office of Research Ethics, the Johnson Space Center Committee for the Protection of Human Subjects, the NASA Human Research Medical Review Board, the European Space Agency Medical Review Board, and the Japanese Space Agency Research Ethics Board (Study Protocol #Pro1222; NASA MPA116301606HR; FWA00019876) in accordance with the Declaration of Helsinki. Each participant was informed in detail about the experiment and gave informed consent before participating.

Data acquisition

A 2D, B-mode ultrasound image of the liver with the portal vein at the bottom of the image was acquired, and the RF signal of the

entire image was recorded. The RF signal was displayed and processed along each ultrasound line selected by the sonographer (Figure 1). The RF signal was processed along six different lines covering a liver ROI of approximately 2 cm × 2 cm on the 2D image of the liver, close to the upper limit of the right lobe. The index of reflectivity was calculated from the RF signal as the quotient of the energy back scattered by the liver tissue ROI along each of the six vertical RF lines and the total energy returned to the ultrasound probe along the same selected lines. Therefore, the index of reflectivity represented the percentage of the total energy returned along the selected line by the liver ROI to the ultrasound probe.

The IR of one ROI segment (IRseg) was expressed as the sum of the energy reflected by this vertical segment (Eseg) divided by the sum of the total energy reflected along the line (Etot) minus the sum of the energy reflected by the portion of the line between the upper limit of the segment and the skin (Esup) with IRseg = Eseg/(Etot − Esup). The IR value (expressed in %) for each sample was the average value of the six IRseg calculated along the six segments inside the liver ROI. Caution was taken with the selection of the ultrasound view from which the RF signal was processed to optimize the reproducibility and accuracy of the ultrasound measurements. During spaceflight, the astronauts were guided (vocally) from the ground to locate the ultrasound probe on the portal vein acoustic window. The trained sonographer on the ground then teleoperated the ultrasound probe sensor orientation (tilt and rotation) to obtain a clear image of the portal vein. The radiofrequency signal capture (internal software) was then activated, and the recording was stored on the ISS device hard disc for later downlink.

The index of reflectivity was calculated on an ROI located at the upper part of the liver's right lobe on an image showing the portal vein trunk at the bottom. This condition was required to confirm that the liver ROI was in the same area for each of the imaging sessions. Additionally, as the accuracy of any ultrasound measurement depends mostly on the quality of the B-mode image and that image quality is partially operator-dependent, the same two operators performed the assessments pre, during, and postflight.

The astronauts remained supine during the pre and postflight assessments and were free floating inside the ISS for the inflight measurement. The same ultrasound device (Sonoscanner, Paris, France) with the same probe (curved array 3.5 Mhz) and ultrasound presets (frequency, depth, and gain) was used for each data collection.

Each index of reflectivity value was a mean of six IR segments placed on the B-mode image. For one crew member, only one RF line was available for one of the images, and it was still included in the analysis. As the ultrasound was teleoperated, the time to find the appropriate liver view and the RF signal on astronauts on board the ISS did not exceed 2 min.

Statistical analysis

The effects of spaceflight were determined using a one-way, repeated measures analysis of variance (SigmaPlot, 12.5; Systat Software, San Jose, CA) with Tukey *post hoc* testing performed to assess all pairwise comparisons. Significance was set at $p < 0.05$, with all results reported as mean ± SD.

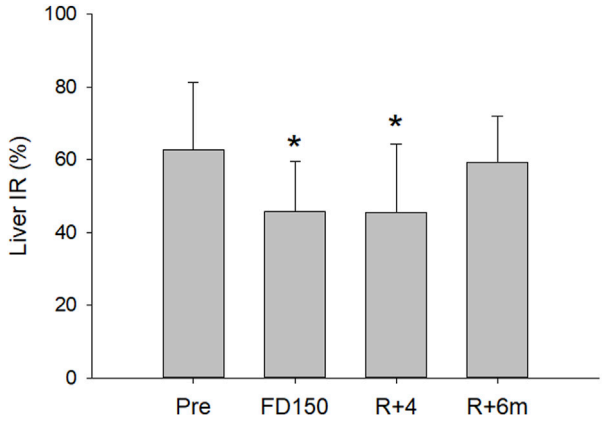

FIGURE 2
Mean (±SD) liver IR values preflight (pre), after 150 days of spaceflight (FD150), 4 days after returning to Earth (R+4), and 6 months after returning to Earth (R+6 m). The liver IR was decreased both inflight (FD150) and postflight (R+4), while at R+6 m, the value returned to preflight levels (statistically different from Pre indicated by *, $p < 0.05$)

Our ROI size is based on our previous work on reflectance changes with fluid shift analogs on seven subjects exposed to microgravity for 6 months and 12 people exposed to dry immersion for 4 days (Arbeille et al., 2021; 2022), indicating a large effect (d = 1.3) to increase reflectance. Based on a one-tailed dependent t-test of alpha = 0.05, n = 5 participants is sufficient to have 80% power to detect differences over time (G*Power v 3.1.9.7).

Results

Ultrasound images of the liver with the portal vein at the bottom of the image as a landmark to confirm the upper part of the right liver lobe were successfully recorded for all astronauts. The RF signal over the entire part of this image was recorded during spaceflight and downlinked to the ground for processing. Processing on the ground consisted of displaying the RF data for the entire B-mode image (tabulated data) and then moving two lines on the B-mode image to identify the liver tissue ROI to be investigated. The data columns corresponding to the sample segment limits were identified, and the different segment energy values were calculated (Figure 1). The liver RF data were collected for seven astronauts preflight, inflight (day 150), and postflight 4 days (R + 4) and 6 months after returning to Earth.

The analysis found a significant effect of time on the IR ($p = 0.007$). Compared to preflight levels (63% ± 18%), the IR of the liver tissue ROI was significantly lower inflight after 150 days (46% ± 15%; $p = 0.022$) and on day R + 4 postflight (46% ± 19%; $p = 0.023$), with no difference found between flight day 150 and R+4 ($p = 0.999$). Assessment of the liver IR 6 months postflight found that IR had returned to preflight levels (59% ± 13%; $p = 0.941$) (Figures 2, 3).

Discussion

The current study utilized analysis of the ultrasound radio frequency signal to evaluate liver tissue properties during and

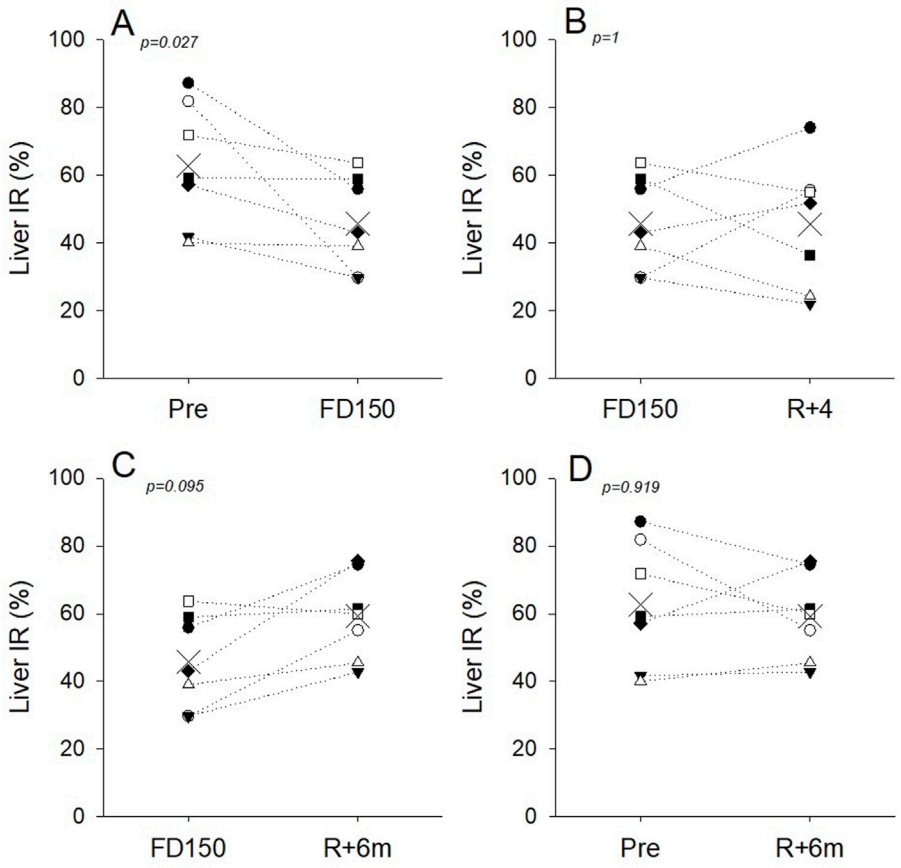

FIGURE 3
Individual liver IR values and group means (X symbol) preflight (Pre), during spaceflight (FD150), 4 days (R+4), and 6 months (R+6m) after returning to Earth. Dotted lines are included to visualize individual responses and do not indicate a linear time course. **(A)** Liver IR was decreased in all astronauts on FD150 compared to pre; **(B)** at R+4, IR tended to increase in three astronauts and decreased further in the other four; **(C)** IR tended to recover in five of the seven astronauts at R+6m; **(D)** at 6 months, postflight IR has recovered to preflight values for five of the seven astronauts.

after long-duration spaceflight. After 150 days of spaceflight, the IR of the liver was found to be significantly reduced, suggesting alterations in tissue content or structure with spaceflight. This study confirmed that the RF signal processing technique to assess IR provides an additional, noninvasive measure for assessing adaptations to spaceflight.

The ultrasound B-mode images from which the RF signal was recorded during spaceflight were of high quality, as the probe transducer orientation and device setting were successfully teleoperated (controlled) in real-time by an expert sonographer in the ground space center. The teleoperation mode allowed the sonographer on the ground to optimize the view of the liver and trigger the RF capture at the most appropriate moment. Additionally, the expert evaluated the echo image and the corresponding RF traces recorded and could repeat the capture if necessary to acquire the best RF data. It was not possible to verify that the ultrasound probe's position over the portal vein acoustic window during spaceflight was exactly the same as it was on the ground. However, the astronauts were able to locate this acoustic window easily from the basic anatomical references used on the ground. Additionally, even if the liver had moved by 1 cm, changed its volume from fluid shifts, or was structurally modified, the astronaut and the sonographer on the ground found the same portal vein image inflight and on the ground, indicating that the RF signal was collected on the same liver area (ROI) during spaceflight as on the ground.

The alteration in the index of reflectivity measured inside the liver tissue suggests changes in the physical properties of the tissue in response to spaceflight. While these changes persisted 4 days after returning to Earth, the index returned to preflight values after 6 months. The decrease in the index of reflectivity means that the liver tissue reflected less of the ultrasound waves during flight than preflight. A reduction in liver IR could be due to particles that do not reflect ultrasound entering this organ (change in water/tissue composition including fat content), potential structural or cellular changes (more collagen and more glycation in the organ), higher superficial tissue absorption, or any combination of these three processes.

During spaceflight, the decrease in the index of reflectivity could be related to fluid shifts toward the upper part of the body. Exposure to microgravity shifts fluid toward the head and neck with potential storage as increased blood pooling in the neck and abdominal vessels and organs, as indicated by the increase in jugular and portal vein volume during spaceflight (Arbeille et al., 2015). Returning to

Earth's surface, fluid shifts away from the head and neck with rapid recovery of blood vessels. However, with the decreased liver IR found to persist 4 days post-flight, recovery of the liver tissue liquid content may take much longer. On the other hand, the decrease in the index of reflectivity may also be the result of structural changes inside the organ, which would require more than several days to recover and should also be considered a possible second process not related to the fluid shifts.

Individual variability was also noted in IR measurements. While on average, liver IR values were not different on FD150 and R+4, values for four astronauts were lower on R+4 than on FD150, and values for the other three astronauts had increased toward preflight levels on R+4. (Figure 3B). The hypothesis of liver tissue structural modifications is supported by the fact that the decrease in IR was still present in four of the seven astronauts investigated at R+4 and in two of the seven astronauts after 6 months (Figures 3C, D). Conversely, for the other three astronauts who recovered at R+4, changes in liver IR with spaceflight may be primarily due to inflight fluid shifts that may disappear during the 4 first days postflight. In the absence of histological confirmation, both processes must be considered potentially contributing to the observed liver IR changes.

Changes in liver position or morphology may also contribute to the altered liver IR with spaceflight. Microgravity may result in changes in liver position, or liver tissue may be compressed with increased thoracic or abdominal pressure with spaceflight. However, the hypothesis of possible liver compression by surrounding organs or in relation to fluid shifts does not look likely as there was no difference in the density of the hepatic vein (subjectively evaluated) between pre and inflight ultrasound images. Increased portal vein size with spaceflight does indicate fluid retention and blood pooling at the level of the liver, but it is unknown if this has a compression effect on liver tissue.

The index of reflectivity provides an easily acquired, noninvasive index characterizing changes in tissue properties with spaceflight. Several other studies used the RF signal or the image brightness distribution to characterize the tissue structure or content of various organs. A liver ultrasound image scan showed signs of fat storage in the liver (steatosis), inflammation and swelling (hepatitis), and scar tissue (fibrosis or cirrhosis) (Byeong Geun et al., 2024). At the prostatic level, a method based on processing radio frequency ultrasonic echo signals in humans was used for the detection of prostatic carcinoma and estimating the probability of malignancy (Schmitz et al., 1999). Another RF-based study reported encouraging results on animal studies designed to analyze the capability of the fractal dimension of RF time series (AHDRFT) in characterizing, *in vitro*, different tissue types (Moradi et al., 2006; 2007). At the eye, a technique for radio frequency tissue characterization with a hand-held transducer in the 5–25 MHz frequency range was successfully tested on ocular tissues, especially on membranes and tumors of the inner eye (Tiers, 1983). Lastly, ultrasound-guided percutaneous RF ablation has been widely used for tumors (HCCs) and metastases in the liver and could improve overall and disease-free survival rates (Jin Woong et al., 2015).

However, none of the above studies used the very simple quantification of the RF signal energy backscattered from a volume of an organ as we do in the present study. The RF signal, being the native ultrasound signal, is present in every ultrasound machine but is not necessarily displayed. An option for this measurement can be installed on every ultrasound device with the appropriate software to process the RF data. Moreover, the RF signal collection is performed with a 2D, B-mode image, which is used to easily locate the tissue ROI to record the RF signal. The RF signal of the entire image was recorded in the ultrasound device used for the current study, allowing the sonographer to choose any sample area in the image, and the corresponding tabulated data of the tissue sample was immediately displayed.

The analysis of the RF signal in different areas of organs provides an additional metric to conventional parameters based on the quantification of the ultrasound image brightness. In many cases, assessment of the IR is more sensitive, as alterations in this variable have been found for images of the walls of the common carotid artery and superficial muscles despite traditional ultrasound image assessments finding limited or no changes in the carotid wall or neck muscles (Arbeille et al., 2021). Similar observations can also be made with the liver, as previous assessments have not identified any alterations in the organ despite the portal vein being increased in a majority of astronauts and liver IR reduced in the current study with similar conditions.

Nevertheless, in the absence of anatomical analysis of the organ structure investigated by optical or electron microscopy, we cannot identify the tissue- or cellular-level mechanism responsible for the change in the index of reflectivity, although the ultrasound image can be enough to suggest steatosis as a possible diagnostic clue. Presently, similar studies analyzing liver tissue by RF measures are being conducted using microgravity analogs, such as long-term bed rest, associated with MRI investigations. In the future, the presence of an MRI modality onboard the space station will probably help clarify this question.

Conclusion

The liver index of reflectivity, as evaluated from the RF signal, provides additional information on the structure or content of the liver tissue beyond the traditional B-mode image. The results support the hypothesis of liver tissue remodeling, a change in liver tissue content, or liver positioning change or compression due to increased thoracic or abdominal pressure during and after spaceflight.

Data availability statement

The raw data supporting the conclusions of this article will be made available by the authors, without undue reservation.

Ethics statement

The studies involving humans were approved and the protocol was approved by the University of Waterloo Office of Research Ethics, the Johnson Space Center Committee for the Protection of Human Subjects, the NASA Human Research Medical Review Board, the European Space Agency Medical Review Board, and the Japanese Space Agency Research Ethics Board (Study Protocol #Pro1222; NASA MPA116301606HR; FWA00019876) in

accordance with the Declaration of Helsinki. Each participant was informed in detail about the experiment and gave informed consent before participating. The studies were conducted in accordance with the local legislation and institutional requirements. The participants provided their written informed consent to participate in this study. Written informed consent was obtained from the individual(s) for the publication of any potentially identifiable images or data included in this article.

Author contributions

PA: Conceptualization, Data curation, Funding acquisition, Investigation, Methodology, Resources, Supervision, Writing–original draft. KZ: Formal Analysis, Writing–review and editing. LG: Data curation, Investigation, Writing–review and editing.

Funding

The author(s) declare financial support was received for the research, authorship, and/or publication of this article. The project was supported by CNES (French Space Agency) grants to PA (4800001115).

Acknowledgments

The authors would like to acknowledge Maryannick Gaveau-Porcher and Roselyne Claveau for their assistance in the echographic data collection and processing pre, during, and postflight.

Conflict of interest

The authors declare that the research was conducted in the absence of any commercial or financial relationships that could be construed as a potential conflict of interest.

The author(s) declared that they were an editorial board member of Frontiers, at the time of submission. This had no impact on the peer review process and the final decision.

Publisher's note

References

Anousin, H., Southisavath, P., Kling, K., Hattendorf, J., Vorasane, S., Paris, D. H., et al. (2024). Steatotic liver disease among lean and non-lean individuals in Southern Lao PDR: a cross-sectional study of risk factors. *Ann. Med.* 56 (1), 2329133. doi:10.1080/07853890.2024.2329133

Arbeille, P., Greaves, D., Chaput, D., Maillet, A., and Hughson, R. (2021). Index of reflectivity of ultrasound radiofrequency signal from the carotid artery wall increases in astronauts after a 6-month spaceflight. *Ultrasound Med. Biol.* (21), S0301–S5629. doi:10.1016/j.ultrasmedbio.2021.03.028

Arbeille, P., Greaves, D., Guillon, L., and Hughson, R. (2022). 4 Days in dry immersion increases arterial wall response to ultrasound wave as measured using radio-frequency signal. (comparison with spaceflight data). *Front. Physiol. 08* 13, 983837. doi:10.3389/fphys.2022.983837

Arbeille, P., Provost, R., Zuj, K., and Vincent, N. (2015). Measurements of jugular, portal, femoral, and calf vein cross-sectional area for the assessment of venous blood redistribution with long duration spaceflight (Vessel Imaging Experiment). *Eur. J. Appl. Physiol. Oct.* 115 (10), 2099–2106. doi:10.1007/s00421-015-3189-6

Byeong Geun, S., Kang, T. W., Sinn, D. H., Kim, Y.-Y., Ji, H. M., and Hwang, J.Ah, Jaeseung Shin Ultrasonographic findings of metabolic dysfunction-associated fatty liver disease: a comparative study with non-alcoholic fatty liver disease and clinical characteristics 2024:108:110097. doi:10.1016/j.clinimag.2024.110097

Genazzani, A. D., Battipaglia, C., Rusce, L., Prampolini, G., Aio, C., Ricciardiello, F., et al. (2024). Alpha lipoic acid administration improved both peripheral sensitivity to insulin and liver clearance of insulin reducing potential risk of diabetes and nonalcoholic fatty liver disease in overweight/obese PCOS patients. *Gynecol. Endocrinol.* 40 (1), 2341701. doi:10.1080/09513590.2024.2341701

Hughson, R. L., Robertso, A., Arbeille, P., Shoemaker, K., Rush, J., Frazer, K., et al. (2016). Increased post-flight carotid artery stiffness and inflight insulin resistance resulting from six-months spaceflight in male and female astronauts. *Am. J. Physiol. Heart Circ. Physiol.* 310 (5), H628–H638. doi:10.1152/ajpheart.00802

Jin Woong, K., Shin, S. S., Heo, S. H., Hong, J. H., Lim, H. S., Ju Seon, H., et al. (2015). Ultrasound-guided percutaneous radiofrequency ablation of liver tumors: how we do it safely and completely. *Korean J. Radiol.* 16 (6), 1226–1239. doi:10.3348/kjr.2015.16.6.1226

Jurkonis, R., Makūnaitė, M., Baranauskas, M., Lukoševičius, A., Sakalauskas, A., Matijošaitis, V., et al. (2020). Quantification of endogenous brain tissue displacement imaging by radiofrequency ultrasound. *Diagn. (Basel)* 10 (2), 57. doi:10.3390/diagnostics10020057

Maleke, C., and Konofagou, E. E. (2008). Harmonic motion imaging for focused ultrasound (HMIFU): a fully integrated technique for sonication and monitoring of thermal ablation in tissues. *Phys. Med. Biol.* 53 (6), 1773–1793. doi:10.1088/0031-9155/53/6/018

Moradi, M., Mousavi, P., and Abolmaesumi, P. (2007). "Tissue characterization using fractal dimension of high frequency ultrasound RF time series," in Miccai *2007, Part II, lncs 4792*. Editors N. Ayache, S. Ourselin, and A. Maeder (Springer-Verlag Berlin Heidelberg), 900–908.

Moradi, P. A., P., I., Siemens, D., Sauerbrei, E., and Mousavi, P. (2006). "Detection of prostate cancer from RF ultrasound echo signals using fractal analysis," in *Proceedings of IEEE EMBC2006*, 2400–2403.

Okada, K., Hibi, K., Matsushita, K., Yagami, H., Tamura, K., Honda, Y., et al. (2019). Intravascular ultrasound radiofrequency signal analysis of blood speckles: physiological assessment of intermediate coronary artery stenosis. *Catheter Cardiovasc Interv.* 28, E155-E164. doi:10.1002/ccd.28612

Palombo, C., Kozakova, M., Guraschi, N., Bini, G., Cesana, F., Castoldi, G., et al. (2012). Radiofrequency-based carotid wall tracking: a comparison between two different systems. *J. Hypertens.* 30 (8), 1614–1619. doi:10.1097/HJH.0b013e328354dd44

Schmitz, G., Ermert, H., and Senge, T. (1999). Tissue-characterization of the prostate using radio frequency ultrasonic signals. *IEEE Trans. Ultrasonics, Ferroelectr. Freq. Control* 46, 126–138. doi:10.1109/58.741523

Trier, H. G. (1983). Ocular tissue characterization by RF-signal analysis: results and experience of a 4 year *in vivo*-study. *Ultrasound Med. Biol.* Suppl 2 (Suppl. 2), 157–161.

frontiers | Frontiers in Physiology

TYPE Original Research
PUBLISHED 20 November 2024
DOI 10.3389/fphys.2024.1451269

OPEN ACCESS

EDITED BY
Marc-Antoine Custaud,
Université d'Angers, France

REVIEWED BY
Allison Paige Anderson,
University of Colorado Boulder, United States
Benoît Bolmont,
Université de Lorraine, France

*CORRESPONDENCE
Suzanne T. Bell,
✉ Suzanne.t.bell@nasa.gov

RECEIVED 18 June 2024
ACCEPTED 20 September 2024
PUBLISHED 20 November 2024

CITATION
Dev SI, Khader AM, Begerowski SR, Anderson SR, Clément G and Bell ST (2024) Cognitive performance in ISS astronauts on 6-month low earth orbit missions.
Front. Physiol. 15:1451269.
doi: 10.3389/fphys.2024.1451269

Cognitive performance in ISS astronauts on 6-month low earth orbit missions

Sheena I. Dev[1], Alaa M. Khader[2], Sydney R. Begerowski[1], Steven R. Anderson[1], Gilles Clément[1] and Suzanne T. Bell[3]*

[1]NASA Behavioral Health and Performance Laboratory, KBR, Inc., Houston, TX, United States, [2]NASA Behavioral Health and Performance Laboratory, JES Tech, Houston, TX, United States, [3]NASA Behavioral Health and Performance Laboratory, NASA Johnson Space Center, Houston, TX, United States

Introduction: Current and future astronauts will endure prolonged exposure to spaceflight hazards and environmental stressors that could compromise cognitive functioning, yet cognitive performance in current missions to the International Space Station remains critically under-characterized. We systematically assessed cognitive performance across 10 cognitive domains in astronauts on 6-month missions to the ISS.

Methods: Twenty-five professional astronauts were administered the Cognition Battery as part of National Aeronautics and Space Administration (NASA) Human Research Program Standard Measures Cross-Cutting Project. Cognitive performance data were collected at five mission phases: pre-flight, early flight, late flight, early post-flight, and late post-flight. We calculated speed and accuracy scores, corrected for practice effects, and derived z-scores to represent deviations in cognitive performance across mission phases from the sample's mean baseline (i.e., pre-flight) performance. Linear mixed models with random subject intercepts and pairwise comparisons examined the relationships between mission phase and cognitive performance.

Results: Cognitive performance was generally stable over time with some differences observed across mission phases for specific subtests. There was slowed performance observed in early flight on tasks of processing speed, visual working memory, and sustained attention. We observed a decrease in risk-taking propensity during late flight and post-flight mission phases. Beyond examining group differences, we inspected scores that represented a significant shift from the sample's mean baseline score, revealing that 11.8% of all flight and post-flight scores were at or below 1.5 standard deviations below the sample's baseline mean. Finally, exploratory analyses yielded no clear pattern of associations between cognitive performance and either sleep or ratings of alertness.

Conclusion: There was no evidence for a systematic decline in cognitive performance for astronauts on a 6-month missions to the ISS. Some differences were observed for specific subtests at specific mission phases, suggesting that processing speed, visual working memory, sustained attention, and risk-taking propensity may be the cognitive domains most susceptible to change in Low Earth Orbit for high performing, professional astronauts. We

provide descriptive statistics of pre-flight cognitive performance from 25 astronauts, the largest published preliminary normative database of its kind to date, to help identify significant performance decrements in future samples.

KEYWORDS

Cognitive performance, astronauts, low earth orbit, spaceflight, cognition, ISS

1 Introduction

Astronauts on current and future spaceflight missions are required to execute complex tasks in which even minor errors could have devastating consequences. Intact cognitive functioning is critical to maintain exceptional performance standards during long duration spaceflight missions. However, astronauts are exposed to spaceflight environmental stressors that include spaceflight hazards (i.e., radiation, altered gravity, isolation and confinement, hostile/closed environment, and distance from Earth) as well as operational challenges (e.g., work overload, circadian shifts, communication delays) that could compromise cognitive functioning (Slack et al., 2016). Some of these challenges are experienced by astronauts living and working on the International Space Station (ISS), yet the extent to which cognitive performance decrements are observed on ISS missions remains critically under-characterized.

Anecdotal and self-report evidence suggest some astronauts experience subjective cognitive difficulties inflight (Stuster, 2010; Stuster, 2016; Schroeder and Tuttle, 1992; Clément et al., 2020), particularly for tasks requiring sustained attention and speed of processing. However, objective assessments of cognitive performance in spaceflight have yielded mixed findings (For review see Thoolen and Strangman (2023)). Early studies assessing dual tasking performance in short duration shuttle missions suggest that attention may be adversely impacted during tasks that include a primary sensorimotor component (Heuer et al., 2003; Manzey et al., 1995; Manzey et al., 2000). More recent studies examining cognitive performance during 6-month ISS missions have largely focused on specific cognitive domains. For example, Jones et al. (2022) recently reported that astronauts who obtained 5 h or less of sleep on the ISS performed worse on a task of sustained attention. Relative to pre-flight, slowed reaction time on a task of spatial working memory post-flight but not during flight (Tays et al., 2021), decrements in visuospatial line orientation inflight and early post-flight (Takács et al., 2021), and increased error on a dual tasking paradigm on landing day (Moore et al., 2019) have been reported. The post-flight decrements observed in these studies returned to pre-flight levels over 30 days follow up. In contrast, no differences were reported in spatial working memory accuracy, processing speed, cognitive-dual tasking, and visual memory (Burles and Iaria, 2023; Moore et al., 2019; Tays et al., 2021). This body of literature is limited by small samples, lack of measurement standardization across studies, limited sensitivity of measures to detect change in high performing populations, and inconsistent timepoints within mission (Strangman et al., 2014). Further, the scope of cognitive domains assessed is restricted and there is an overall paucity of data documenting other cognitive functions that may impact mission relevant tasks, such as memory, executive functions, and emotional processing. Nevertheless, current evidence suggests at most mild and reversible decrements in aspects of cognition among astronaut crew on ISS missions of 6-month duration or shorter.

Only one published study to date has comprehensively assessed a wide range of cognitive domains across multiple mission phases in spaceflight. The well-known NASA Twin study (Garrett-Bakelman et al., 2019) conducted cognitive testing using the Cognition Battery (Basner et al., 2015) in a pair of monozygotic twins, one of which spent approximately 1 year (340 days) on the ISS while the other remained on Earth. Early inflight improvements were documented in speed and accuracy, with the exception of accuracy decrements in specific domains of visual memory and abstract reasoning (>1 standard deviation [SD] decline). Relative to early flight, late flight performance was slower in emotion recognition (>1SD) and less accurate in abstract reasoning (>2 SD). However, the most notable decrements were observed in the post-flight mission phase across most cognitive domains that persisted up to 6 months. Though a single case study, findings underscore the relevance of assessing a breadth of cognitive domains in spaceflight, support previous studies indicating that cognitive performance may be differentially impacted at different mission phases, and suggest that longer duration missions may induce more persistent decrements.

Terrestrial analogs that simulate spaceflight conditions offer a unique opportunity to study singular or combined spaceflight hazards and stressors on relevant behavioral health and performance outcomes. Group level changes in cognitive performance were not present in several long duration European, Russian, and Antarctic analog missions (Lorenz et al., 1996; Gemignani et al., 2014; Mairesse et al., 2019; Connaboy et al., 2020). However, a subset of individuals in these settings appear to be more vulnerable to decrements in aspects of attention, memory, or visuospatial abilities, including those who report depressive symptoms (Premkumar et al., 2013), heightened stress and sleep loss (Basner et al., 2014), and greater hippocampal volume loss (Stahn et al., 2019). Indeed, sleep restriction protocols implemented in one- and 2-week isolation and confinement spaceflight analogs were associated with worse emotion recognition, slower and less accurate sustained attention, and slower cognitive and psychomotor processing speed (Nasrini et al., 2020). Other studies also have examined the effects of altered gravity on cognition. Parabolic flight studies assessing impacts of acute gravitational alterations have documented decrements on tasks of spatial cognition (Stahn et al., 2020) and attention (Friedl-Werner et al., 2021). Head Down Bed Rest (HDBR) studies, designed to simulate cephalic fluid shift in microgravity, report that prolonged HDBR can induce early but mild reductions in overall cognitive speed that remain consistent for the duration of the protocol (Basner et al., 2021a) and more specific decrements on tasks of executive functioning (Yuan et al., 2016), emotional processing

(Basner et al., 2021a; Brauns et al., 2019; Benvenuti et al., 2013; Liu et al., 2012), and aspects of memory (Chen et al., 2013). Decrements resolve soon after returning to normal daily activities and were only exacerbated by a combined HDBR and CO_2 protocol in isolated tasks of executive function and sustained attention (Basner et al., 2021b; Lee et al., 2019; Mahadevan et al., 2021). Thus, analog studies have identified mild, possibly reversible, decrements in cognitive performance across several domains in the context of spaceflight stressors. Even among those that did not report significant group level differences, observed individual variability in performance suggests that some individuals are more at risk for cognitive decrements than others.

Taken together, the extant literature documenting cognitive performance in spaceflight or spaceflight analogs suggests possible mild decrements in some, but not necessarily all, cognitive domains and that these decrements may be singularly or synergistically influenced by multiple spaceflight hazards (e.g., altered gravity) and stressors (e.g., sleep restriction). Given the dynamic nature of spaceflight missions and thus the potential for hazards and stressors to interact in varying degrees within a mission, it is also possible that there are specific mission phases in which performance is more vulnerable to decrements. However, we were unable to locate a published study that has described the neuropsychological profile expected in low earth orbit spaceflight by systematically assessing cognitive performance across a wide range of cognitive domains in a cohort of astronauts aboard the ISS for 6-month missions.

The primary aims of the current study were to 1) provide a descriptive summary of performance across several cognitive domains in a sample of professional astronauts on 6-month ISS missions, 2) characterize cognitive performance over time and between distinct mission phases of a 6-month ISS mission, and 3) examine the prevalence of low scores across subtests. While we generally expected stable cognitive performance across time, we predicted that performance would be most vulnerable during mission phases that require greater adaptation to and from spaceflight conditions. Further, processing speed, attention, and working memory are cognitive domains which are more susceptible to state-like alterations due to internal or external distractions (Eysenck and Calvo, 1992; Robert and Hockey, 1997). Thus, we hypothesized that 1) there would be mild decrements in early flight and early post-flight mission phases relative to pre-flight; and 2) the subtests with the greatest frequency of low scores would be those assessing processing speed, attention, and working memory. Finally, given previous studies identifying individual differences predicting variability in cognitive performance, we also explored the relationship between self-reported sleep and ratings of alertness.

2 Materials and methods

2.1 Participants

A total of 25 professional astronauts aged 33 to 61 (mean (SD) = 45.12 (7.25); 32% Female) participated in the NASA Spaceflight Standard Measures study. All US orbital segment astronauts assigned to a mission to the ISS were eligible to participate in the study; no additional exclusion or inclusion criteria were applied. Ten crew members had previous flight experience that ranged from 12 to 199 days inflight (mean (SD) = 129.9 (85.6)) prior to the current mission. Cognitive performance was assessed once pre-mission, twice in-mission (within 30 days of launch and return, respectively), and twice post-mission (within 10 and 30 days of landing, respectively). All crew members completed an approximately 6-month ISS mission. See Figure 1 for data collection timeline.

2.2 The Cognition Battery

The Cognition Battery is a computerized test that was developed to assess a range of cognitive domains in high performing individuals over successive administrations (Basner et al., 2015; Lee et al., 2020). There are 10 subtests that are modeled after well-known neuropsychological tests. The battery has 15 alternate versions and published corrections to minimize practice effects with successive administrations (Basner et al., 2020a). The Cognition Battery was installed and administered to crew on Hewlett Packard Z-Book 15 G^2 laptops for all sessions. The average to complete a full session was 37.10 min (*SD* = 25.16). Performance metrics were calculated consistent with previous studies using the Cognition Battery in spaceflight or spaceflight analogs to facilitate comparison across studies. Metrics across most subtests are broadly characterized with speed (i.e., reaction time recorded to nearest millisecond) and accuracy scores. A familiarization and practice session preceded all pre-flight data collection session to introduce participants to the battery.

The Visual Object Learning Task (VOLT) is a task of visual learning and memory. Participants are directed to memorize three-dimensional figures and are later instructed to select those targets from a set that includes both old and new figures.

The Fractal 2-Back (F2B) is a task of nonverbal working memory. The task presents sequential figures that have the potential to repeat multiple times. Participants must respond when the current stimulus matches the one displayed two figures prior.

Abstract Matching (AM) is a difficult executive functioning task that assesses abstraction, problem-solving, and concept formation. Participants are presented with object pairs and are required to match target items to one of the two pairs based on abstract rules not explicitly provided to them.

The Line Orientation Task (LOT) is a measure of visuospatial orientation. Participants are presented with two lines and are required to rotate one until it is parallel to its counterpart. The presented lines vary in length and orientation.

The Emotion Recognition Task (ERT) assess facial emotion recognition. Participants are shown photographs of people portraying a range of facial emotions and are required to select one of five labels that most accurately describes the expressed emotion. The possible labels are “happy”, “sad”, “angry”, “fearful”, and “no emotion”.

The Matrix Reasoning Task (MRT) is a task of nonverbal abstract reasoning and pattern recognition and is analogous to a well-known paradigm often utilized for assessing general intelligence. A pattern series is presented on a grid and one item

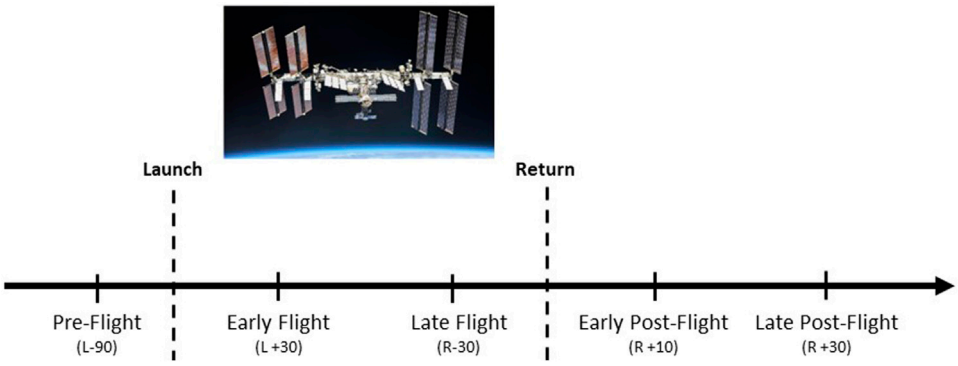

FIGURE 1
Administration Protocol of the Cognition Battery on 6-month ISS missions. Note: Pre-flight assessment occurred approximately 90 (*M* = 116.44, *SD* = 65.42) days before launch (L). The early flight assessment occurred approximately 30 (*M* = 28.88, *SD* = 10.01) days after launch and late flight occurred approximately 30 days before return (R). Early post-flight occurred approximately 10 (*M* = 9, *SD* = 1.85) days after return and late post-flight was approximately 30 (*M* = 29.8, *SD* = 5.6) days after return. Photography Credit: NASA.

in the pattern is missing. The participant is directed to select the item that fits the pattern from a set of potential options.

The Digit Symbol Substitution Task (DSST) measures complex scanning, visual tracking, and speed of processing. Participants are provided with a legend linking single digits to unique symbols. One of the nine symbols appear on the screen and participants select the corresponding number as quickly as possible. The entire task has a fixed duration of 90 s.

The Balloon Analog Risk Test (BART) is a measure of risk-taking behavior. Participants either inflate an animated balloon or choose to collect a reward. However, the balloon will pop after an unknown number of pumps that changes from trial to trial, which requires the participant to judge the behavior of balloons and adjust their strategy. Rewards are given as a function of when it was collected relative to the balloon's final possible size.

The Psychomotor Vigilance Test (PVT) is a task of vigilant and sustained attention that assesses response times to visual stimuli that are seen at random intervals. Crew members are asked to press the space bar as quickly as possible when they see a millisecond counter appear on the screen. They are instructed to inhibit responses when the number counter is not present. The current implementation utilized a validated 3-min version with 2–5 s interstimulus intervals and a 355-m lapse threshold.

The Motor Praxis Task (MPT) assesses sensorimotor speed. Participants click randomly generated squares on the screen that become successively smaller over the trial. Speed is assessed by time to click the squares.

2.3 Cognitive performance

Speed and accuracy scores were calculated for each subtest in the Cognition Battery (Basner et al., 2015; Basner et al., 2021a; Basner et al., 2020a; Basner et al., 2021b; Lee et al., 2020). Speed outcomes for each task are represented as the average response time (in milliseconds), except for the PVT, which was calculated as 10 minus the reciprocal of the response time. Accuracy is measured as the proportion correct to total stimuli for five of the subtests (VOLT, AM, ERT, MRT, DSST). For F2B, the accuracy score was a proportion that accounts for the number of matches (i.e., correct hits) and non-matches (i.e., correct rejection). The LOT accuracy score is a proportion that accounts for the number of clicks the participant was off from the correct orientation. The PVT accuracy score is a proportion that accounts for lapses, false starts, and the total number of stimuli presented. The BART risk score is a proportion that considers the maximum pumps possible and the total pumps taken. Scores range from 0 to 1 with higher values indicating greater risk tolerance. In other words, higher scores suggest that the individual is more willing to risk popping the balloon in return for a higher reward. No accuracy score was calculated for the MPT as directions for this task does not emphasize accurate performance. Published corrections to account for stimulus set and practice effects due to repeated administrations over an average of 12 days were applied (Basner et al., 2020a). Descriptive information and figures of raw scores at each mission phase can be found in Supplementary Material.

All individual outcome scores were z-transformed using the mean and standard deviation of the full sample's baseline test session, after excluding the individual, that occurred during the pre-fight mission phase. Z-scores for speed were multiplied by (−1), such that higher z-scores indicate better (i.e., faster) performance. Higher z-scores for the BART Risk score indicates greater risk tolerance. Finally, summary speed and accuracy z-scores were calculated by averaging all subtest speed and accuracy z scores (Basner et al., 2021a; Basner et al., 2021b). While the BART speed score was included in the overall speed score, the BART risk score was not included in the overall accuracy score as it is not a measure of accuracy.

2.4 Surveys

Immediately prior to the first subtest, crew members were asked to self-report the number of hours of sleep they obtained the previous evening. They also provided subjective ratings of alertness from 0 (Tired) to 10 (Alert) in the moment in which they submitted their ratings (Basner et al., 2015).

TABLE 1 Descriptive Characteristics of pre-flight baseline raw subtest scores at pre-flight mission phase.

Subtest	N	Mean	Median	SD	Min	Max
VOLT Speed	25	1627.96	1506	617.83	712.20	3097.40
VOLT Accuracy	25	.95	.95	.06	.78	1.0
F2B Speed	24	552.94	530.80	60.95	469.40	670.0
F2B Accuracy	24	.92	.93	.07	.77	1.0
AM Speed	25	2353.32	2179.6	877.69	1028.0	4587.1
AM Accuracy	25	.81	.84	.11	.60	1.0
LOT Speed	24	4691.30	4455.30	1183.95	2874.20	7026.1
LOT Accuracy	24	.78	.81	.08	.58	.97
ERT Speed	25	2645.30	2631.82	886.40	1439.60	4720.38
ERT Accuracy	25	.72	.72	.11	.47	.92
MRT Speed	25	8546.15	8021.43	2340.55	5114.22	13,908.73
MRT Accuracy	25	.79	.83	.14	.49	0.99
DSST Speed	25	1209.38	1184.2	145.95	932.9	1485.1
DSST Accuracy	25	.98	.98	.02	.95	1
BART Speed	25	637.83	575.44	429.65	0	1702.88
BART Risk	25	.72	.74	.11	.43	.93
PVT Speed	24	5.25	5.21	.24	4.75	5.73
PVT Accuracy	24	.97	.97	.04	.81	1
MPT Speed	25	1061.18	1040.5	153.53	855.5	1434.3

Note: BART Accuracy score reflects risk taking propensity. N represents number of unique data points in pre-flight baseline sample. Data points removed for F2B, PVT, and LOT, as described in Results section; SD, standard deviation.

2.5 Analytical approach

Descriptive statistics for speed and accuracy metrics for each subtest were generated for baseline (i.e., pre-flight) raw scores and for z scores at each mission phase (aim 1). A series of linear mixed model (LMM) analyses with random subject intercepts were used to assess the relationship between mission phases and each speed and accuracy performance outcome variable (aim 2). Age, gender, and previous flight experience were included as fixed effects to statistically control for reported associations with cognitive performance (Lee et al., 2020) and possible differences in the magnitude of structural brain alterations (Hupfeld et al., 2022) between novice and repeat flyers. For each LMM, residuals were plotted and normality was assessed using the Shapiro-Wilk test. Robust LMMs were utilized when violations of normality were detected (Koller, 2016). The False Discovery Rate method was applied to adjust for 21 multiple comparisons. Trimmed models with adjusted *p*-values for each measure are reported in text and tables; unadjusted *p*-values can be found in Supplementary Table S1. Follow up LMMs with random subject intercepts to facilitate pairwise comparisons included timepoint as a categorical variable to examine differences between mission phases. Tukey's HSD was applied to adjust for Type I error and adjusted *p*-values are reported. To examine the frequency of low scores during flight and post-flight performance (aim 3), the percent frequency of data points representing performance 1.5 standard deviations at or below the baseline (i.e., pre-flight) sample mean ($z \leq -1.5$) was calculated for each subtest. This cutoff was utilized because it is commonly used to detect impairment in clinical populations (Petersen et al., 2001; Petersen and Morris, 2005; Petersen et al., 1999; Jak et al., 2009). For exploratory analyses, LMMs with random subject intercepts were utilized to assess the relationships between survey items and all speed and accuracy measures for each subtest across all mission phases. Statistical significance was set to $\alpha = 0.05$ and all analyses were performed using R 4.2.1.

3 Results

Data were downloaded, processed, visualized, and inspected for quality. Data from four subtests were excluded from data analysis, not necessarily from the same individual: one was excluded due to technical difficulties that interfered with task performance, two were excluded due to suspected non-adherence (i.e., pattern of accuracy and speed outliers indicative of rapid responding rapid and/or careless responding and elevated false positives; (Basner et al., 2015)), and one was excluded due to a participant comment indicating confusion with subtest instructions. Table 1 displays raw baseline (i.e., pre-flight) scores used to generate z-scores for the present analysis and can be used as a preliminary normative

10.3389/fphys.2024.1451269

TABLE 2 Descriptive Characteristics of Z-scores by subtest and mission phase.

Subtest	Pre-flight M (SD) range	Early flight M (SD) range	Late flight M (SD) range	Early post-flight M (SD) range	Late post-flight M (SD) range
Summary Speed	−.02 (.59) −1.53–1.37	−.33 (.54) −1.38–1.25	−.18 (.61) −1.07–1.38	−.13 (.64) −1.84–.95	−.04 (.5) -.86–1.15
Summary Accuracy	−.03 (.43) −.98–.76	−.07 (.41) −1.21–.34	−.06 (.37) −1.09–.57	−.20 (.44) −1.56–.56	−.22 (.44) −1.34–.48
VOLT Speed	−.02 (1.09) −2.79–1.59	−.10 (1.17) −3.74–1.60	.09 (.79) −1.71–1.43	.07 (.91) −3.12–1.42	.004 (.77) −2.14–1.27
VOLT Accuracy	−.04 (1.14) −3.19–.80	−.13 (1.04) −3.07–.80	−.21 (.85) −2.03–.80	.03 (.86) −1.55–.80	−.52 (1.10) −2.80–.80
F2B Speed	−.01 (1.07) −2.15–1.46	−1.24 (1.64) −4.87–1.46	−1.06 (1.59) −4.23–1.40	−.82 (1.4) −3.94–1.40	−1.24 (1.41) −5.25–.57
F2B Accuracy	−.02 (1.08) −2.55–1.18	.24 (.76) −1.03–1.18	.01 (.97) −2.23–1.18	−.15 (.95) −1.94–1.18	−.16 (.96) −2.29–1.18
AM Speed	−.02 (1.10) −3.06–1.62	.10 (.87) −1.83–1.31	.38 (.79) −1.12–1.59	.45 (.71) −1.19–1.76	.50 (.52) -.95–1.37
AM Accuracy	−.01 (1.07) −2.17–1.87	−.42 (1.38) −3.56–1.69	−.09 (1.01) −2.07–1.87	−.38 (1.4) −4.03–1.41	−.55 (1.27) −3.03–1.39
LOT Speed	−.01 (1.07) −2.22–1.66	−.15 (1.06) −3.11–1.96	−.24 (.97) −2.15–1.48	−.11 (.95) −1.95–1.50	−.14 (.87) −2.11–1.24
LOT Accuracy	−.01 (1.13) −2.78–2.74	.29 (.9) −1.64–1.34	.14 (.87) −2–2.33	−.13 (1.0) −2.36–1.61	.06 (1.09) −2.69–1.67
ERT Speed	−.02 (1.10) −2.73–1.45	.03 (.88) −2.12–1.06	.12 (.92) −1.73–1.44	.40 (.74) −1.15–1.72	.39 (.69) −1.69–1.45
ERT Accuracy	−.01 (1.08) −2.50–2.08	−.23 (.70) −1.41–.85	−.04 (1.15) −2.10–1.96	−.10 (1.13) −2.83–2.07	.31 (.99) −1.79–1.81
MRT Speed	−.01 (1.08) −2.66–1.57	−.33 (1.09) −2.65–1.49	−.19 (1.18) −2.79–2.03	.13 (1.20) −2.16–2.02	.41 (1.07) −2.24–2.29
MRT Accuracy	−.02 (1.09) −2.47–1.63	−.29 (.85) −2.07–1.52	−.45 (1.03) −3.31–1.52	−.40 (1.17) −3.03–1.55	−.38 (1.01) −2.48–.93
DSST Speed	−.01 (1.08) −2.10–2.10	−.79 (1.54) −5.58–1.71	−.73 (1.48) −3.72–2.72	−.75 (1.72) −6.44–1.62	−.33 (1.39) −4.30–2.34
DSST Accuracy	−.01 (1.07) −2.19–.97	.04 (1.17) −.341–.97	.22 (1.11) −2.80–.97	−.20 (1.38) −3.77–.97	−.30 (1.58) −4.96–.97
BART Speed	−.01 (1.09) −2.95–1.59	−.11 (.95) −2.44–1.59	.01 (.90) −1.72–1.22	−.19 (.75) −2.09–1.24	.02 (.80) −1.94–1.59
BART Risk	−.02 (1.12) −3.35–2.13	−.20 (1.19) −3.57–1.80	−.88 (.95) −3.08–.47	−.72 (1.02) −3.81–.99	−.96 (1.05) −3.27–1.09
PVT Speed	−.003 (1.08) −2.22–2.28	−.53 (1.04) −2.76–1.08	−.23 (1.43) −4.12–2.01	−.39 (1.45) −4.37–2.03	−.40 (1.73) −4.64–2.71
PVT Accuracy	−.11 (1.48) −6.36–.76	−.09 (.68) −1.52–.75	−.06 (.61) −1.38–.75	−.29 (1.06) −3.56–.76	−.19 (1.03) −4.12–.73
MPT Speed	−0.02 (1.09) −2.87–1.42	−.16 (.99) −2.95–1.46	.02 (.87) −2.06–1.53	.12 (1.18) −3.79–1.34	.41 (.89) −1.76–1.94

Note: Z-scores calculated with current samples pre-flight baseline raw scores. BART Accuracy score reflects risk taking propensity; SD, standard deviation.

database for future studies. Descriptive information for each subtest's z-scores by mission phase is presented in Table 2.

3.1 Cognitive performance over mission phases

Hypothesis 1. suggested that there would be mild decrements in early flight and early post-flight mission phases relative to pre-flight. For each outcome we first present results assessing linear relationships of performance over mission phases (see Supplementary Table S1) followed by direct pairwise comparisons between mission phases. Linear mixed models revealed no linear relationship between mission phase and the summary speed score. In support of Hypothesis 1, pairwise analysis characterizing differences in summary speed between mission phases (Figure 2, Panel A) revealed significant, but small, differences between pre-mission and early flight (β = .35, adjusted p = .002, Δz = .31) as well as early flight and late post-flight (β = −.33, adjusted p = .004, Δz = .29). There was no significant difference between pre-flight and early post-flight. Summary accuracy declined over time (β = −.05, adjusted p = .03) but no pairwise comparisons were significantly different (Figure 2, Panel A) and the effect sizes of the mean differences between mission phases were negligible.

Support for Hypothesis 1 across the 10 subtests in the Cognition battery varied by domain. Differences between mission phases were observed in several subtests, even among those with no linear associations with time (Figures 2, 3). VOLT speed and accuracy remained stable over time and between mission phases. No pairwise comparisons between mission phases survived multiple comparisons and the effect sizes of the mean differences in VOLT accuracy (Δz's = .07 to .55) and speed (Δz's = .02 to .11) between mission phases ranged from negligible to medium. See Figure 2, Panel B.

F2B speed declined over time (β = −.23, 95% CI [-.35–.1], adjusted p < .001). Pairwise contrasts revealed faster performance during pre-mission compared to all other mission phases (β's range .8–1.29; adjusted p's range .01 to < .001). The effect sizes of the significant mean differences between mission phases were large (Δz's = .81 to 1.23). F2B accuracy remained stable over time and between mission phases. See Figure 2, Panel C.

AM speed improved over time (β = .12, 95% CI [.07 – .17], adjusted p < .001). Pre-flight performance was slower than late in-flight (β = −.35, adjusted p = .03, Δz = .40) and both post-flight phases (vs early: β = −.39, adjusted p = .01, Δz = .47; vs. late: β = −.43,

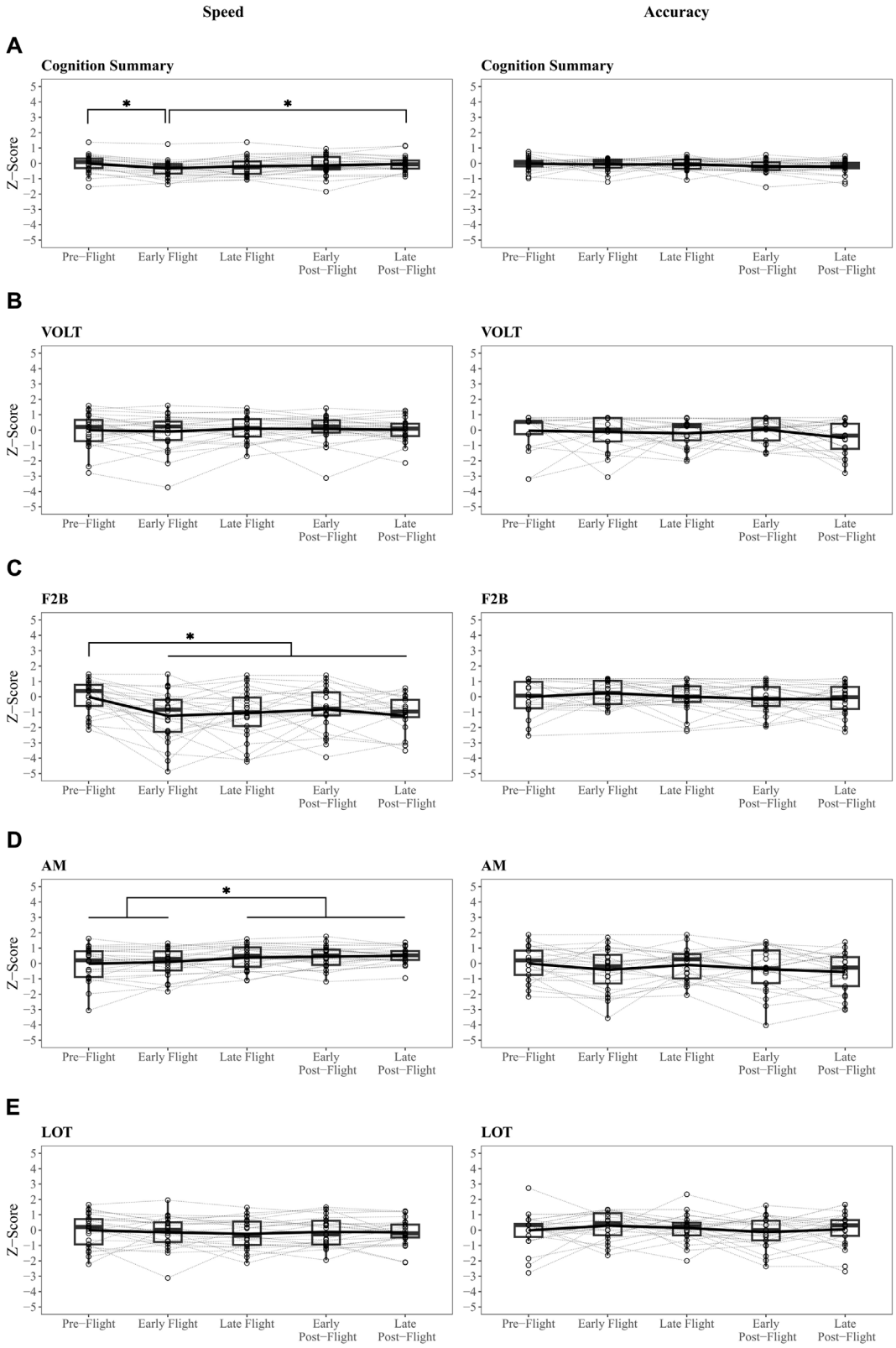

FIGURE 2
Speed and Accuracy Scores Over Mission Phase. Adjusted pairwise comparisons of speed and accuracy scores between mission phases in a subset of Cognition Battery subtests. **(A)** Summary speed and accuracy scores remained stable. **(C)** Speed was slower on the Fractal 2 Back (F2B) task at the early flight mission phase and persisted through post-flight phases. **(D)** Performance on Abstract Matching (AM) was faster over time, likely reflecting residual practice effects. **(B)** and **(E)** Stable scores across mission phases were observed on the Visual Object Learning (VOLT) and Line Orientation Task (LOT). *adjusted $p < .05$.

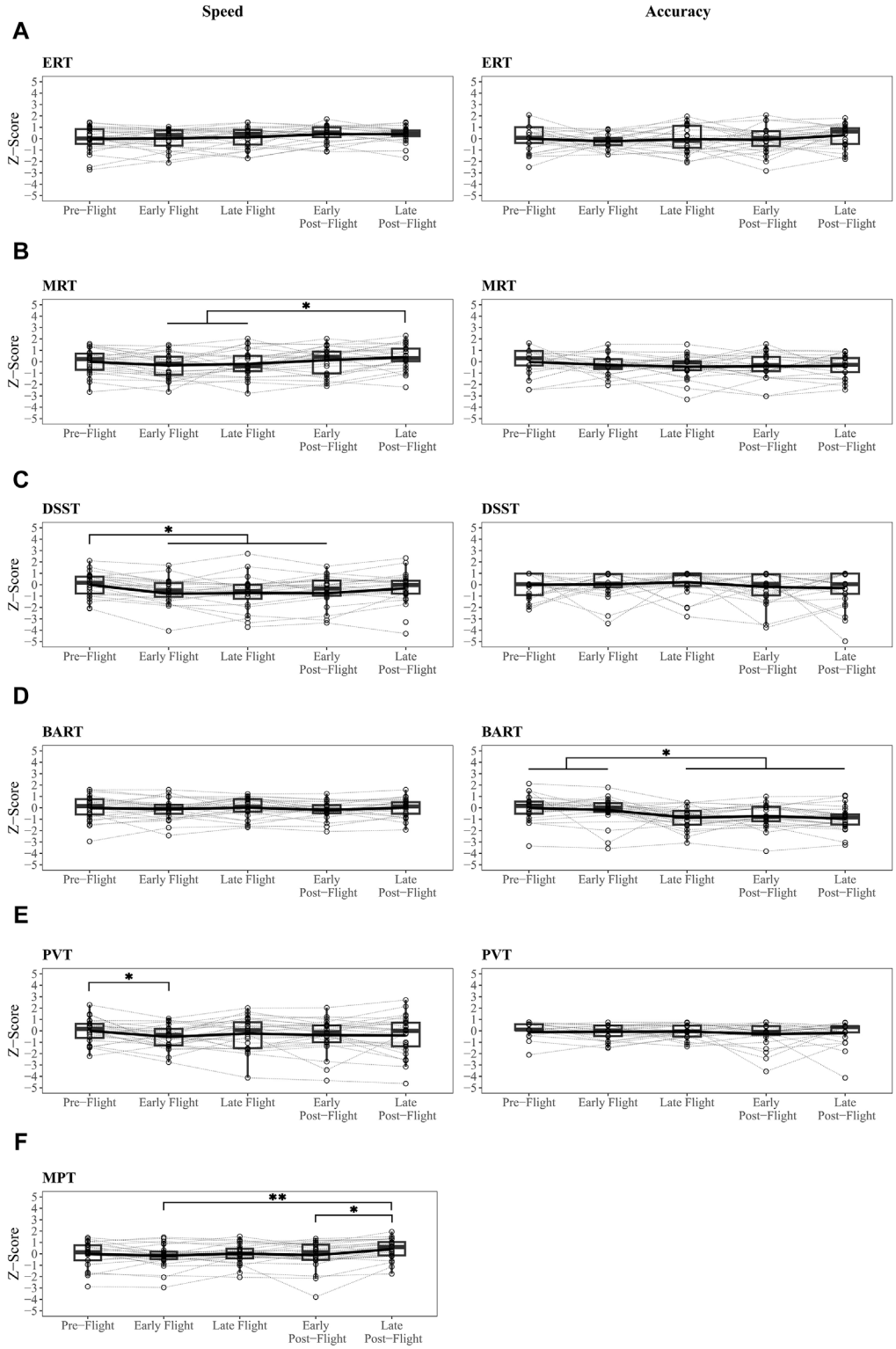

FIGURE 3
Speed and Accuracy Scores Over Mission Phase Continued. Adjusted pairwise comparisons of speed and accuracy scores between mission phases in a subset of Cognition Battery subtests. **(A)** Stable scores across mission phases on the Emotion Recognition Task (ERT). **(B)** Performance on Matrix Reasoning Task (MRT) was faster over time, likely reflecting residual practice effects. **(C)** Speed was slower on the Digit Symbol Substitution Task (DSST) at the early flight mission phase and persisted through the early post-flight phase. **(D)** Reduced risk taking propensity on the Balloon Analog Risk Test (BART) task after the early flight phase. **(E)** Reduced speed the Psychomotor Vigilance Test (PVT) during the early flight phase only. **(F)** Faster performance on Motor Praxis Task (MPT) during the late post mission phase. *adjusted $p < .05$.

adjusted p = .004; Δz = .52). Early in-flight performance was also slower than both post-flight phases (vs early: β = −.36, adjusted p = .03; Δz = .35; vs late: β = −.41, p = .009; Δz = .40). The effect sizes of the significant mean differences ranged from small to medium. AM accuracy remained stable over time and between mission phases. See Figure 2, Panel D.

LOT speed and accuracy remained stable over time and between mission phases. See Figure 2, Panel E.

ERT speed improved over time (β = .1, 95% CI [.03 – .17], adjusted p = .02). No pairwise comparisons between mission phases were significant and the effect sizes of the mean differences for ERT speed between mission phases ranged from negligible to small (Δz's = .05 to .41). ERT accuracy remained stable over time and between mission phases. See Figure 3, Panel A.

MRT speed improved over time (β = .13, 95% CI [.04 – .23], adjusted p = .02). Late post-flight performance was faster relative to both in flight mission phases (vs early: β = −.81, adjusted p = .002, Δz = .74; vs late: β = −.6, p = .04, Δz = .60); effect sizes of the significant mean differences between mission phases ranged from medium to large. MRT accuracy remained stable over time and between mission phases. See Figure 3, Panel B.

There was no significant linear association between time and DSST speed (β = −.05, 95% CI [-.13–.04], adjusted p = .42). However, comparison of discrete mission phases revealed slowed performance during both in flight (vs early: β = .78, adjusted p = .0001, Δz = .78; vs late: β = .73, adjusted p = .0002, Δz = .72) and early post-flight (β = −.61, adjusted p = .003, Δz = .74) compared to pre-flight performance. Effect sizes of the significant mean differences between mission phases were large. DSST accuracy remained stable over time and between mission phases. See Figure 3, Panel C.

BART speed remained stable over time and between mission phases. The BART Risk Score declined over time (β = −.23, 95% CI [-.31 to −.15], adjusted p < .001). Pairwise comparisons between mission phases revealed greater risk tolerance during pre-flight and early flight phases compared to late flight (vs pre-flight: β = .78, adjusted p = .0002, Δz = .86; vs early flight: β = .70, adjusted p = .001, Δz = .68), early post-flight (vs pre-flight: β = .61, adjusted p = .007, Δz = .70; vs early flight: β = .53, adjusted p = .03, Δz = .52) and late post-flight (vs pre-flight: β = .9, adjusted p < .0001, Δz = .94; vs early flight: β = .82, adjusted p = .0001, Δz = .77) mission phases. The effect sizes of the significant mean differences between mission phase ranged from medium to large. See Figure 3, Panel D.

There was no significant relationship between time and PVT speed (β = −.07, 95% CI [-.17–.03], adjusted p = .27). However, comparison of discrete mission phases revealed slowed performance during early flight compared to pre-flight mission phases (β = .62, adjusted p = .05, Δz = .5); the effect size of the mean difference was medium. PVT accuracy remained stable over time and between mission phases. See Figure 3, Panel E.

MPT speed improved over time (β = .09, 95% CI [.02 – .17], adjusted p = .03). Pairwise comparisons of mission phases revealed that MRT speed was faster in the late post-flight mission phase compared to early in-flight (β = −.63, adjusted p = .0005, Δz = .57) and early post-flight (β = −.48, adjusted p = .02, Δz = .29) and marginally faster than late flight (β = −.4, adjusted p = .06, Δz = .39). Corresponding effect sizes for the significant mean differences between mission phases were small to moderate. See Figure 3, Panel F.

3.2 Frequency of low scores

Overall, 11.8% of all individual test scores were at or below 1.5 standard deviations of the full sample baseline mean (i.e., z-score ≤ −1.5). Consistent with Hypothesis 2, the subtests with the greatest frequency of low scores were on tasks of working memory (F2B; 18.7%), processing speed (DSST; 16.7%), and sustained attention (PVT; 13.6%). The frequency of low scores on the BART risk score (19.2%) was also higher than speed and accuracy scores on other subtests; these scores represent individual observations indicating substantially decreased risk taking propensity compared to pre-flight baseline. See Table 3. Figure 4 selects the three subtests with the highest frequencies of low scores, respectively, and presents data across mission phases.

3.3 Sleep duration and alertness over mission phases

Across all mission phases, there were no relationships between hours of sleep reported and performance on any subtest of the Cognition battery. Alertness was inversely related to DSST accuracy (β = −.1, p = .05) only. See Table 4.

4 Discussion

This investigation characterized performance across a wide breadth of cognitive domains in a sample of 25 astronauts on 6-month ISS missions. We were unable to locate any published studies with a more comprehensive or larger dataset on a sample of astronauts; thus, we believe this study makes a substantial contribution in characterizing astronaut cognitive performance in spaceflight. We have reported pre-flight baseline descriptive information characterizing cognitive performance across all subtests that can be utilized as a preliminary normative database for future research. As a group, astronaut crew demonstrated generally stable performance on summary measures of cognition and only mild changes in isolated cognitive domains during specific mission phases. Specifically, slowed performance was observed early in flight on tasks of processing speed (i.e., DSST), visual working memory (i.e., F2B), and sustained attention (i.e., PVT); slowed processing speed and working memory persisted into post-flight. Risk taking propensity also reduced after the early flight mission phases. A total of 11.8% of all flight and post-flight scores were classified as low, such that they fell at or below 1.5 standard deviations below the sample's pre-flight baseline mean. Finally, exploratory analysis found no consistent relationships between cognitive performance and either self-reported amount of sleep or ratings of alertness. This study makes three important contributions which are discussed next.

First, we report no systematic decline in cognitive performance during 6-month low earth orbit missions among the largest sample of professional astronauts published to date. This is in contrast to some of the previous research that observed declines across several cognitive domains during flight and post-flight mission phases (Garrett-Bakelman et al., 2019; Takács et al., 2021). Our results

TABLE 3 Percent frequency of low scores during flight and post-flight.

Subtest	Speed	Accuracy	Subtest total
VOLT	5.1	13.1	9.1
F2B	28.3	9.1	18.7
AM	1.01	20.2	10.6
LOT	7.1	7.1	7.1
ERT	5.1	8.1	6.6
MRT	11.1	13.1	12.1
DSST	19.4	14.3	16.7
BART	7.1	19.2	13.3
PVT	20.2	7.1	13.6
MPT	8.1	--	8.1
Total	11.2	12.4	11.8

Note: Low scores were identified as scores at or below 1.5 standard deviations below average baseline (i.e., pre-flight) performance ($z \leq -1.5$). BART accuracy score reflects risk taking propensity.

do not necessarily contradict these findings as we also observed interindividual variability in our sample and it is possible that longer duration missions elicit greater decrements at later mission phases. However, we did not find support for group level impacts of spaceflight conditions on cognitive performance in low earth orbit.

Next, by using a comprehensive assessment of cognitive functions we identified cognitive domains that were more variable across phases of a 6-month low earth orbit missions. This suggests that these cognitive domains are more vulnerable to spaceflight conditions than other domains. Specifically, we observed early flight slowed performance, but stable accuracy, on tasks of processing speed and visual working memory that persisted through the duration of the mission. Visual working memory speed did not return to pre-flight levels at 30 days post mission. Slower performance on the PVT was observed during early flight only. Notably, these decrements were present despite generally preserved, or even improved, sensorimotor functioning. These findings are consistent with astronaut self-report of "brain fog" (Clément et al., 2020; Stuster, 2010; Stuster, 2016), the NASA Twin Study (Garrett-Bakelman et al., 2019), and analog studies simulating prolonged microgravity (Basner et al., 2021a; Basner et al., 2021b; Liu et al., 2012; Lipnicki and Gunga, 2009) and sleep restriction (Wang et al., 2014). This is also consistent with documented pre to post mission alterations in brain structure and function (Roy-O'Reilly et al., 2021; Doroshin et al., 2022; Jillings et al., 2023) that can contribute to cognitive inefficiency. Our results also revealed decreases in the BART risk taking score after the early flight mission phase, suggesting that astronauts were less likely to take risks in late mission and post mission phases. Greater comfort with risk taking at early flight may reflect the novel and inherently hazardous nature of operational activities that require crew to accept risk in order to complete. Risk taking is relatively understudied in spaceflight despite the hazardous environment, though others have reported increases in flight (Garrett-Bakelman et al., 2019), no changes during simulated prolonged microgravity (Basner et al., 2021a; Basner et al., 2021b), and decreases during social isolation (Erskine-Shaw et al., 2017; Zivi et al., 2023) and fatigue (Hisler and Krizan, 2019). This finding warrants further study as the ability to modulate risk taking propensity across the mission may be an adaptive skill that enables the astronaut to appropriately approach mission demands. Finally, we observed no decrements in concept formation, abstract reasoning, or visuospatial learning and memory, though other studies indicate there may be individual differences in vulnerability to decrements in these domains (Premkumar et al., 2013; Garrett-Bakelman et al., 2019). Indeed, frontal and hippocampal structures that support these functions are sensitive to radiation exposure (Desai et al., 2022), stress (Mandrick et al., 2016; Wingenfeld and Wolf, 2014), isolation and confinement (Stahn et al., 2019), and microgravity (Koppelmans et al., 2016; Lee et al., 2021; Li et al., 2015). Thus, it is possible that longer duration missions with greater exposure to spaceflight hazards or individual vulnerabilities to stressors will exacerbate decrements in future exploration missions.

Finally, we present the first published professional astronaut preliminary normative dataset for the Cognition Battery that can be used to derive standard scores to identify significant deviations from pre-flight baseline functioning. For example, despite modest group level differences in cognitive performance across most subtests, 11.8% of observations across all tasks during flight or post-flight fell at or below 1.5 standard deviations of the samples pre-flight baseline mean. The greatest number of observations below cut off were on tasks assessing working memory, processing speed, and sustained attention, which are domains vulnerable to state-like alterations related to acute changes in sleep (Jones et al., 2022; Lim and Dinges, 2010), stress (Eysenck and Calvo, 1992), workload (Ghalenoei et al., 2022), and dehydration (Wittbrodt and Millard-Stafford, 2018). Though there is no evidence of an increased frequency of low scores in this sample compared to other cognitively healthy populations (Crawford et al., 2007; Binder et al., 2009), even highly infrequent or temporary barriers to adequately engaging cognitive functions required to perform complex operational

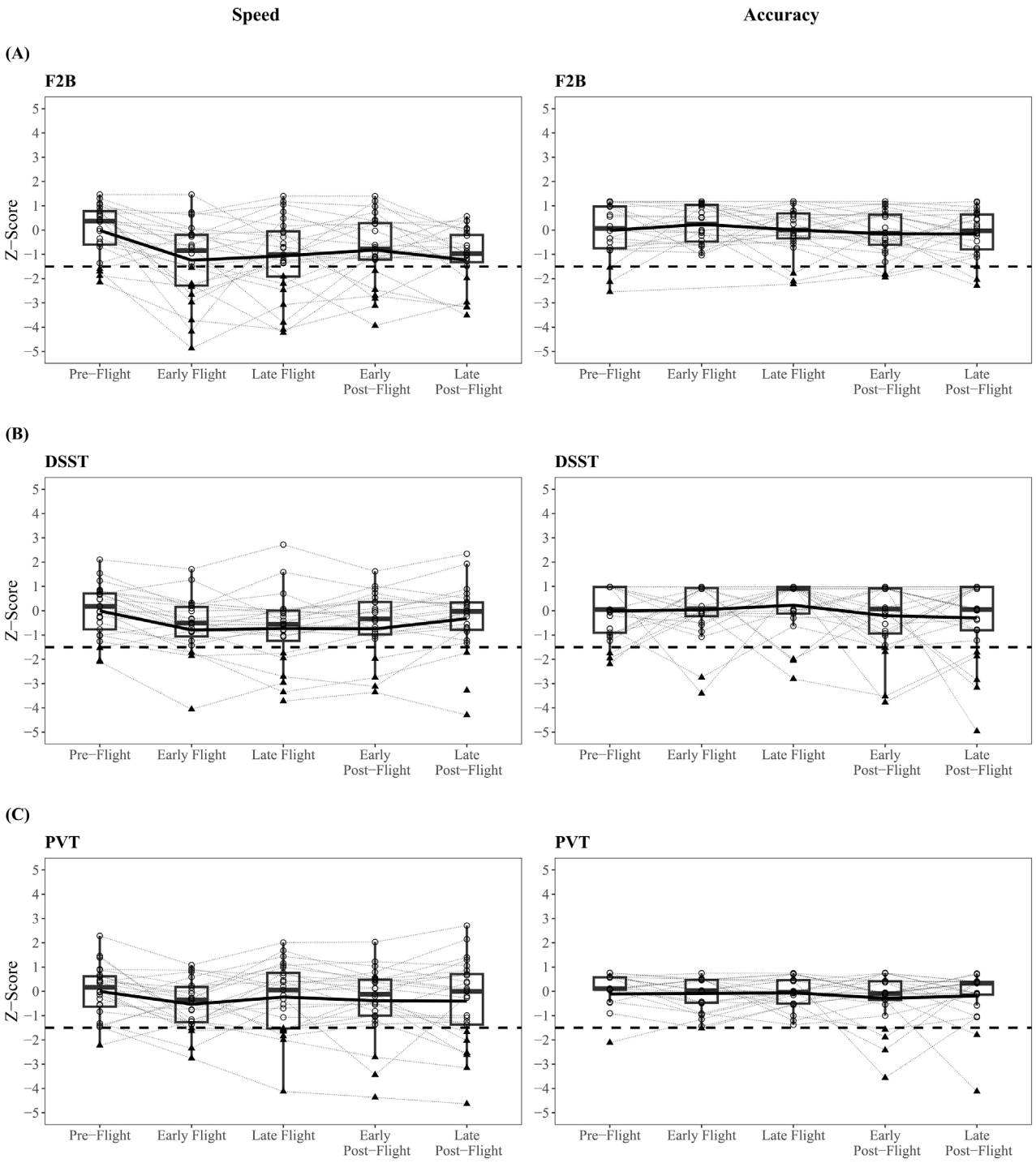

FIGURE 4
Frequency of Low Scores Low scores were defined as any individual test score that was at or below 1.5 standard deviations of the samples pre-flight baseline performance (z-score ≤ –1.5). The Fractal 2-Back (F2B; **(A)**), Digit Symbol Substitution Task (DSST; **(B)**), and Psychomotor Vigilance Test (PVT; **(C)**) subtests had greater than 13% of flight and post-flight data that were classified as a low score. All low scores that were below our pre-determined cut-off (dotted line) are represented in solid triangles.

task may result in catastrophic consequences in spaceflight. This preliminary normative dataset provides operational support with the ability to identify low scores during flight, elucidate effective in mission support to enhance performance (i.e., stress reduction, timeline alterations), or inform concept-of-operations during mission critical tasks. This dataset can also be utilized in future research to compare performance against future astronauts on extended duration missions or those that venture beyond low earth orbit and include more extreme stressors.

TABLE 4 Self-reported hours of sleep and alertness.

	Pre-flight M (SD) range	Early flight M (SD) range	Late flight M (SD) range	Early post-flight M (SD) range	Late post-flight M (SD) range
Sleep	6.53 (1.56) .75–8.5	6.42 (.94) 4–8	6.38 (1.21) 3–8	7.24 (1.23) 3.5–9	6.98 (.7) 6–8
Alert	6.56 (2.02) 2–9	6.46 (1.89) 3–10	5.96 (2.46) 2–9	5.92 (2.25) 2–9	6.32 (2.1) 3–10

Note: Self-reported number of hours slept during the night prior to cognitive performance testing. Subjective ratings of alertness assessed on a 10-point scale, from (0) Tired to 10 (Alert), per (Basner et al., 2014). SD, standard deviation.

These significant contributions underscore critical knowledge gaps that should be prioritized for future research. First, there are likely individual differences in susceptibility to spaceflight environmental stressors. The current sample size was too small to stratify our normative baseline by age. Although we did not find clear associations between cognitive performance and self-reported hours of sleep or ratings of alertness, there are several other stressors that are not accounted for in the current dataset such as workload, stress and fatigue specific to extravehicular activities, nutrition/exercise, and individual behavioral health. These may become more impactful during future space exploration missions as conditions of greater radiation exposure, extra-vehicular surface activities, and earth independent operations deplete individual cognitive reserve to unmask larger decrements. The operational consequences to observed changes in cognitive performance also remains unknown. The everyday demands required of spaceflight are more complex, dangerous, and uncertain than those of terrestrial life suggesting that current clinical thresholds to define impairment may not be appropriate. Basner et al. (2020b) reported associations between a spaceflight docking task and processing speed, sustained attention, visuospatial orientation, and abstract reasoning, suggesting that this mission critical task is vulnerable to some of the decrements we observed in this investigation. Future studies investigating the relationship between cognitive performance and other operationally activities are required to determine appropriate decrement thresholds beyond which performance is most at risk. Further development of earth independent operational supports to maintain optimal cognitive performance will further reduce the risk to individual cognitive health and performance on operational tasks.

The reported results should be interpreted in the context of some limitations. Despite applying corrections for practice effects, the reported data suggests continued improvement over time in a subset of the Cognition Battery subtests. This likely due to small sizes and key differences between our study design and that of the published corrections, including administration intervals (i.e., 10–28 days vs > 60 days) and population (i.e., university vs. operational settings). Updates to the practice corrections may be warranted now that the Cognition Battery has become more commonly used among several high performing operational environments. Cognitive performance assessed during the early flight and early post-flight stages were collected on average 28.88 (*SD* = 10.01) days after launch and 9 (*SD* = 1.85) days after landing. Thus, performance was not characterized during what may be the most acute transitional phases of a mission or during long term follow up. Nevertheless, the pre-flight data published here is the first preliminary astronaut normative dataset that can be used in future studies to derive standard scores for independent samples.

In summary, we observed no evidence for systematic widespread declines in cognitive performance suggestive of damage to the central nervous system during 6-month ISS missions. Our results revealed early mildly slowed performance in isolated tasks of processing speed, working memory, and attention that persisted to varying degrees through the mission, reduced risk taking after early flight mission phases, and stable performance on tasks of memory and executive functions. This investigation makes a substantial contribution by providing a pre-flight normative sample of professional astronauts that can be used to characterize individual or group level deviations from baseline functioning, characterizes cognitive performance under conditions of spaceflight in low earth orbit, and substantially shapes a growing body of literature towards a future that best positions humans to thrive in space.

Data availability statement

The data presented in the study are deposited in the NASA Life Science Portal at https://nlsp.nasa.gov/view/lsdapub/lsda_experiment/ea3997a6-1093-5e0f-8f54-47684d4f1e73.

Ethics statement

The studies involving humans were approved by NASA Institutional Review Board. The studies were conducted in accordance with the local legislation and institutional requirements. The participants provided their written informed consent to participate in this study.

Author contributions

SD: Conceptualization, Data curation, Formal Analysis, Investigation, Methodology, Project administration, Supervision, Visualization, Writing–original draft, Writing–review and editing. AK: Data curation, Project administration, Visualization, Writing–review and editing. SB: Data curation, Project administration, Writing–review and editing. SA: Investigation, Project administration, Writing–review and editing. GC: Funding acquisition, Project administration, Resources, Writing–review and editing. SB: Conceptualization, Data curation, Investigation, Methodology, Resources, Writing–review and editing.

Funding

The author(s) declare that financial support was received for the research, authorship, and/or publication of this article. Research was funded by the National Aeronautics and Space Administration (NASA) Human Research Program Standard Measures Cross-Cutting Project. SID, AMK, SRG, SRA, and GC were supported by KBR's Human Health and Performance Contract NNJ15HK11B through NASA.

Acknowledgments

We thank Mathias Basner for data processing and analysis consultation, Millennia Young for statistical consultation, the NASA Spaceflight Standard Measures and Research Operation and Integration teams for facilitating this research, and the ISS astronaut crew for their dedicated time and efforts to support behavioral health research in spaceflight. The authors of this report are entirely responsible for its content. Any opinions, findings, and conclusions or recommendations expressed in this material are those of the authors and do not necessarily reflect the views of the US Government, NASA, KBR, or JES Tech. The authors have no interests that may be perceived as conflicting with the work described or proposed here.

Conflict of interest

Authors SD, SB, SA, and GC were employed by KBR, Inc.

Author AK was employed by JES Tech.

The remaining authors declare that the research was conducted in the absence of any commercial or financial relationships that could be construed as a potential conflict of interest.

Publisher's note

Supplementary material

The Supplementary Material for this article can be found online at: https://www.frontiersin.org/articles/10.3389/fphys.2024.1451269/full#supplementary-material

References

Basner, M., Dinges, D. F., Howard, K., Moore, T. M., Gur, R. C., Mühl, C., et al. (2021a). Continuous and intermittent artificial gravity as a countermeasure to the cognitive effects of 60 Days of head-down tilt bed rest. *Front. Physiol.* 12, 643854. doi:10.3389/fphys.2021.643854

Basner, M., Dinges, D. F., Mollicone, D. J., Savelev, I., Ecker, A. J., DI Antonio, A., et al. (2014). Psychological and behavioral changes during confinement in a 520-day simulated interplanetary mission to mars. *PloS one* 9, e93298. doi:10.1371/journal.pone.0093298

Basner, M., Hermosillo, E., Nasrini, J., Saxena, S., Dinges, D. F., Moore, T. M., et al. (2020a). Cognition test battery: adjusting for practice and stimulus set effects for varying administration intervals in high performing individuals. *J. Clin. Exp. Neuropsychol.* 42, 516–529. doi:10.1080/13803395.2020.1773765

Basner, M., Moore, T. M., Hermosillo, E., Nasrini, J., Dinges, D. F., Gur, R. C., et al. (2020b). Cognition test battery performance is associated with simulated 6df spacecraft docking performance. *Aerosp. Med. Hum. Perform.* 91, 861–867. doi:10.3357/AMHP.5602.2020

Basner, M., Savitt, A., Moore, T. M., Port, A. M., Mcguire, S., Ecker, A. J., et al. (2015). Development and validation of the cognition test battery for spaceflight. *Aerosp. Med. Hum. Perform.* 86, 942–952. doi:10.3357/AMHP.4343.2015

Basner, M., Stahn, A. C., Nasrini, J., Dinges, D. F., Moore, T. M., Gur, R. C., et al. (2021b). Effects of head-down tilt bed rest plus elevated CO(2) on cognitive performance. *J. Appl. Physiol.* 130, 1235–1246. doi:10.1152/japplphysiol.00865.2020

Benvenuti, S. M., Bianchin, M., and Angrilli, A. (2013). Posture affects emotional responses: a head down bed rest and ERP study. *Brain cognition* 82, 313–318. doi:10.1016/j.bandc.2013.05.006

Binder, L. M., Iverson, G. L., and Brooks, B. L. (2009). To err is human: "abnormal" neuropsychological scores and variability are common in healthy adults. *Arch. Clin. Neuropsychol.* 24, 31–46. doi:10.1093/arclin/acn001

Brauns, K., Werner, A., Gunga, H. C., Maggioni, M. A., Dinges, D. F., and Stahn, A. (2019). Electrocortical evidence for impaired affective picture processing after long-term immobilization. *Sci. Rep.* 9, 16610. doi:10.1038/s41598-019-52555-1

Burles, F., and Iaria, G. (2023). Neurocognitive adaptations for spatial orientation and navigation in astronauts. *Brain Sci.* 13, 1592. doi:10.3390/brainsci13111592

Chen, S., Zhou, R., Xiu, L., Chen, S., Chen, X., and Tan, C. (2013). Effects of 45-day -6° head-down bed rest on the time-based prospective memory. *Acta Astronaut.* 84, 81–87. doi:10.1016/j.actaastro.2012.10.040

Clément, G. R., Boyle, R. D., George, K. A., Nelson, G. A., Reschke, M. F., Williams, T. J., et al. (2020). Challenges to the central nervous system during human spaceflight missions to Mars. *J. neurophysiology* 123, 2037–2063. doi:10.1152/jn.00476.2019

Connaboy, C., Sinnott, A. M., Lagoy, A. D., Krajewski, K. T., Johnson, C. D., Pepping, G.-J., et al. (2020). Cognitive performance during prolonged periods in isolated, confined, and extreme environments. *Acta Astronaut.* 177, 545–551. doi:10.1016/j.actaastro.2020.08.018

Crawford, J. R., Garthwaite, P. H., and Gault, C. B. (2007). Estimating the percentage of the population with abnormally low scores (or abnormally large score differences) on standardized neuropsychological test batteries: a generic method with applications. *Neuropsychology* 21, 419–430. doi:10.1037/0894-4105.21.4.419

Desai, R. I., Limoli, C. L., Stark, C. E. L., and Stark, S. M. (2022). Impact of spaceflight stressors on behavior and cognition: a molecular, neurochemical, and neurobiological perspective. *Neurosci. Biobehav Rev.* 138, 104676. doi:10.1016/j.neubiorev.2022.104676

Doroshin, A., Jillings, S., Jeurissen, B., Tomilovskaya, E., Pechenkova, E., Nosikova, I., et al. (2022). Brain connectometry changes in space travelers after long-duration spaceflight. *Front. Neural Circuits* 16, 815838. doi:10.3389/fncir.2022.815838

Erskine-Shaw, M., Monk, R. L., Qureshi, A. W., and Heim, D. (2017). The influence of groups and alcohol consumption on individual risk-taking. *Drug Alcohol Depend.* 179, 341–346. doi:10.1016/j.drugalcdep.2017.07.032

Eysenck, M. W., and Calvo, M. G. (1992). Anxiety and performance: the processing efficiency theory. *Cognition Emot.* 6, 409–434. doi:10.1080/02699939208409696

Friedl-Werner, A., Machado, M. L., Balestra, C., Liegard, Y., Philoxene, B., Brauns, K., et al. (2021). Impaired attentional processing during parabolic flight. *Front. Physiol.* 12, 675426. doi:10.3389/fphys.2021.675426

Garrett-Bakelman, F. E., Darshi, M., Green, S. J., Gur, R. C., Lin, L., Macias, B. R., et al. (2019). The NASA Twins Study: a multidimensional analysis of a year-long human spaceflight. *Science* 364, eaau8650. doi:10.1126/science.aau8650

Gemignani, A., Piarulli, A., Menicucci, D., Laurino, M., Rota, G., Mastorci, F., et al. (2014). How stressful are 105 days of isolation? Sleep EEG patterns and tonic cortisol in healthy volunteers simulating manned flight to Mars. *Int. J. Psychophysiol.* 93, 211–219. doi:10.1016/j.ijpsycho.2014.04.008

Ghalenoei, M., Mortazavi, S. B., Mazloumi, A., and Pakpour, A. H. (2022). Impact of workload on cognitive performance of control room operators. *Cognition, Technol. & Work* 24, 195–207. doi:10.1007/s10111-021-00679-8

Heuer, H., Manzey, D., Lorenz, B., and Sangals, J. (2003). Impairments of manual tracking performance during spaceflight are associated with specific effects of microgravity on visuomotor transformations. *Ergonomics* 46, 920–934. doi:10.1080/0014013031000107559

Hisler, G., and Krizan, Z. (2019). Sleepiness and behavioral risk-taking: do sleepy people take more or less risk? *Behav. Sleep. Med.* 17, 364–377. doi:10.1080/15402002.2017.1357122

Hupfeld, K. E., Richmond, S. B., Mcgregor, H. R., Schwartz, D. L., Luther, M. N., Beltran, N. E., et al. (2022). Longitudinal MRI-visible perivascular space (PVS) changes with long-duration spaceflight. *Sci. Rep.* 12, 7238. doi:10.1038/s41598-022-11593-y

Jak, A. J., Bondi, M. W., Delano-Wood, L., Wierenga, C., Corey-Bloom, J., Salmon, D. P., et al. (2009). Quantification of five neuropsychological approaches to defining mild cognitive impairment. *Am. J. Geriatr. Psychiatry* 17, 368–375. doi:10.1097/JGP.0b013e31819431d5

Jillings, S., Pechenkova, E., Tomilovskaya, E., Rukavishnikov, I., Jeurissen, B., VAN Ombergen, A., et al. (2023). Prolonged microgravity induces reversible and persistent changes on human cerebral connectivity. *Commun. Biol.* 6, 46. doi:10.1038/s42003-022-04382-w

Jones, C. W., Basner, M., Mollicone, D. J., Mott, C. M., and Dinges, D. F. (2022). Sleep deficiency in spaceflight is associated with degraded neurobehavioral functions and elevated stress in astronauts on six-month missions aboard the International Space Station. *Sleep* 45, zsac006. doi:10.1093/sleep/zsac006

Koller, M. (2016). robustlmm: an R package for robust estimation of linear mixed-effects models. *J. Stat. Softw.* 75, 1–24. doi:10.18637/jss.v075.i06

Koppelmans, V., Bloomberg, J. J., Mulavara, A. P., and Seidler, R. D. (2016). Brain structural plasticity with spaceflight. *NPJ Microgravity* 2, 2. doi:10.1038/s41526-016-0001-9

Lee, J. K., DE Dios, Y., Kofman, I., Mulavara, A. P., Bloomberg, J. J., and Seidler, R. D. (2019). Head down tilt bed rest plus elevated CO(2) as a spaceflight analog: effects on cognitive and sensorimotor performance. *Front. Hum. Neurosci.* 13, 355. doi:10.3389/fnhum.2019.00355

Lee, J. K., Koppelmans, V., Pasternak, O., Beltran, N. E., Kofman, I. S., DE Dios, Y. E., et al. (2021). Effects of spaceflight stressors on brain volume, microstructure, and intracranial fluid distribution. *Cereb. Cortex Commun.* 2, tgab022. doi:10.1093/texcom/tgab022

Lee, G., Moore, T. M., Basner, M., Nasrini, J., Roalf, D. R., Ruparel, K., et al. (2020). Age, sex, and repeated measures effects on NASA's "cognition" test battery in STEM educated adults. *Aerosp. Med. Hum. Perform.* 91, 18–25. doi:10.3357/AMHP.5485.2020

Li, K., Guo, X., Jin, Z., Ouyang, X., Zeng, Y., Feng, J., et al. (2015). Effect of simulated microgravity on human brain gray matter and white matter--evidence from MRI. *PLoS One* 10, e0135835. doi:10.1371/journal.pone.0135835

Lim, J., and Dinges, D. F. (2010). A meta-analysis of the impact of short-term sleep deprivation on cognitive variables. *Psychol. Bull.* 136, 375–389. doi:10.1037/a0018883

Lipnicki, D. M., and Gunga, H. C. (2009). Physical inactivity and cognitive functioning: results from bed rest studies. *Eur. J. Appl. Physiol.* 105, 27–35. doi:10.1007/s00421-008-0869-5

Liu, Q., Zhou, R., Chen, S., and Tan, C. (2012). Effects of head-down bed rest on the executive functions and emotional response. *PLoS One* 7, e52160. doi:10.1371/journal.pone.0052160

Lorenz, B., Lorenz, J., and Manzey, D. (1996). Performance and brain electrical activity during prolonged confinement. *Adv. Space Biol. Med.* 5, 157–181. doi:10.1016/s1569-2574(08)60058-1

Mahadevan, A. D., Hupfeld, K. E., Lee, J. K., DE Dios, Y. E., Kofman, I. S., Beltran, N. E., et al. (2021). Head-Down-Tilt bed rest with elevated CO(2): effects of a pilot spaceflight analog on neural function and performance during a cognitive-motor dual task. *Front. Physiol.* 12, 654906. doi:10.3389/fphys.2021.654906

Mairesse, O., Macdonald-Nethercott, E., Neu, D., Tellez, H. F., Dessy, E., Neyt, X., et al. (2019). Preparing for Mars: human sleep and performance during a 13 month stay in Antarctica. *Sleep* 42. doi:10.1093/sleep/zsy206

Mandrick, K., Peysakhovich, V., Rémy, F., Lepron, E., and Causse, M. (2016). Neural and psychophysiological correlates of human performance under stress and high mental workload. *Biol. Psychol.* 121, 62–73. doi:10.1016/j.biopsycho.2016.10.002

Manzey, D., Lorenz, T. B., Heuers, H., and Sangals, J. (2000). Impairments of manual tracking performance during spaceflight: more converging evidence from a 20-day space mission. *Ergonomics* 43, 589–609. doi:10.1080/001401300184279

Manzey, D., Lorenz, B., Schiewe, A., Finell, G., and Thiele, G. (1995). Dual-task performance in space: results from a single-case study during a short-term space mission. *Hum. Factors* 37, 667–681. doi:10.1518/001872095778995599

Moore, S. T., Dilda, V., Morris, T. R., Yungher, D. A., Macdougall, H. G., and Wood, S. J. (2019). Long-duration spaceflight adversely affects post-landing operator proficiency. *Sci. Rep.* 9, 2677. doi:10.1038/s41598-019-39058-9

Nasrini, J., Hermosillo, E., Dinges, D. F., Moore, T. M., Gur, R. C., and Basner, M. (2020). Cognitive performance during confinement and sleep restriction in NASA's Human Exploration Research Analog (HERA). *Front. physiology* 11, 394. doi:10.3389/fphys.2020.00394

Petersen, R. C., Doody, R., Kurz, A., Mohs, R. C., Morris, J. C., Rabins, P. V., et al. (2001). Current concepts in mild cognitive impairment. *Arch. Neurol.* 58, 1985–1992. doi:10.1001/archneur.58.12.1985

Petersen, R. C., and Morris, J. C. (2005). Mild cognitive impairment as a clinical entity and treatment target. *Arch. Neurol.* 62, 1160–1163. ; discussion 1167. doi:10.1001/archneur.62.7.1160

Petersen, R. C., Smith, G. E., Waring, S. C., Ivnik, R. J., Tangalos, E. G., and Kokmen, E. (1999). Mild cognitive impairment: clinical characterization and outcome. *Arch. Neurol.* 56, 303–308. doi:10.1001/archneur.56.3.303

Premkumar, M., Sable, T., Dhanwal, D., and Dewan, R. (2013). Circadian levels of serum melatonin and cortisol in relation to changes in mood, sleep, and neurocognitive performance, spanning a year of residence in Antarctica. *Neurosci. J.* 2013, 254090. doi:10.1155/2013/254090

Robert, J., and Hockey, G. (1997). Compensatory control in the regulation of human performance under stress and high workload: a cognitive-energetical framework. *Biol. Psychol.* 45, 73–93. doi:10.1016/s0301-0511(96)05223-4

Roy-O'Reilly, M., Mulavara, A., and Williams, T. (2021). A review of alterations to the brain during spaceflight and the potential relevance to crew in long-duration space exploration. *npj Microgravity* 7, 5. doi:10.1038/s41526-021-00133-z

Schroeder, J. E., and Tuttle, M. L. 1992. Investigation of possible causes for human-performance degradation during microgravity flight.

Slack, K. J., Williams, T. J., Schneiderman, J. S., Whitmire, A. M., Picano, J. J., Leveton, L. B., et al. 2016. Risk of Adverse cognitive or behavioral conditions and psychiatric disorders: evidence report.

Stahn, A. C., Gunga, H. C., Kohlberg, E., Gallinat, J., Dinges, D. F., and Kühn, S. (2019). Brain changes in response to long antarctic expeditions. *N. Engl. J. Med.* 381, 2273–2275. doi:10.1056/NEJMc1904905

Stahn, A. C., Riemer, M., Wolbers, T., Werner, A., Brauns, K., Besnard, S., et al. (2020). Spatial updating depends on gravity. *Front. Neural Circuits* 14, 20. doi:10.3389/fncir.2020.00020

Strangman, G. E., Sipes, W., and Beven, G. (2014). Human cognitive performance in spaceflight and analogue environments. *Aviat. space, Environ. Med.* 85, 1033–1048. doi:10.3357/ASEM.3961.2014

Stuster, J. (2010). *Behavioral issues associated with long-duration space expeditions: review and analysis of astronaut journals: experiment 01-E104 (Journals)*. Johnson Space Center Houston, TX: National Aeronautics and Space Administration.

Stuster, J. 2016. Behavioral issues associated with long duration space expeditions: review and analysis of astronaut journals experiment 01-E104 (Journals) phase 2 final report. *NASA/TM-2016- 2181603.*

Takács, E., Barkaszi, I., Czigler, I., Pató, L. G., Altbäcker, A., Mcintyre, J., et al. (2021). Persistent deterioration of visuospatial performance in spaceflight. *Sci. Rep.* 11, 9590. doi:10.1038/s41598-021-88938-6

Tays, G. D., Hupfeld, K. E., Mcgregor, H. R., Salazar, A. P., DE Dios, Y. E., Beltran, N. E., et al. (2021). The effects of long duration spaceflight on sensorimotor control and cognition. *Front. Neural Circuits* 15, 723504. doi:10.3389/fncir.2021.723504

Thoolen, S., and Strangman, G. (2023). "Cognitive performance and neuromapping," in *Spaceflight and the central nervous system: clinical and scientific aspects*. Springer.

Wang, Y., Jing, X., Lv, K., Wu, B., Bai, Y., Luo, Y., et al. (2014). During the long way to Mars: effects of 520 days of confinement (Mars500) on the assessment of affective stimuli and stage alteration in mood and plasma hormone levels. *PLoS One* 9, e87087. doi:10.1371/journal.pone.0087087

Wingenfeld, K., and Wolf, O. T. (2014). Stress, memory, and the hippocampus. *Front. Neurol. Neurosci.* 34, 109–120. doi:10.1159/000356423

Wittbrodt, M. T., and Millard-Stafford, M. (2018). Dehydration impairs cognitive performance: a meta-analysis. *Med. Sci. Sports Exerc* 50, 2360–2368. doi:10.1249/MSS.0000000000001682

Yuan, P., Koppelmans, V., Reuter-Lorenz, P. A., DE Dios, Y. E., Gadd, N. E., Wood, S. J., et al. (2016). Increased brain activation for dual tasking with 70-days head-down bed rest. *Front. Syst. Neurosci.* 10, 71. doi:10.3389/fnsys.2016.00071

Zivi, P., Sdoia, S., Alfonsi, V., Gorgoni, M., Mari, E., Quaglieri, A., et al. (2023). Decision-making and risk-propensity changes during and after the COVID-19 pandemic lockdown. *Brain Sci.* 13, 793. doi:10.3390/brainsci13050793

frontiers | Frontiers in Physiology

TYPE Original Research
PUBLISHED 02 May 2025
DOI 10.3389/fphys.2025.1464028

OPEN ACCESS

EDITED BY
Olga Vinogradova,
Russian Academy of Sciences (RAS), Russia

REVIEWED BY
Pierre Denise,
INSERM U1075 Mobilités Vieillissement, Pathologie, Santé, France
Rich Whittle,
University of California, Davis, United States

*CORRESPONDENCE
N. Goswami,
nandu.goswami@medunigraz.at,
nandu.goswami@dubaihealth.ae

†These authors share first authorship

RECEIVED 13 July 2024
ACCEPTED 16 April 2025
PUBLISHED 02 May 2025

CITATION
Stead T, Blaber AP, Divsalar DN, Xu D, Tavakolian K, Evans J, Billette de Villemeur R, Bareille M-P, Saloň A, Steuber B and Goswami N (2025) Repeatability of artificial gravity tolerance times.
Front. Physiol. 16:1464028.
doi: 10.3389/fphys.2025.1464028

Repeatability of artificial gravity tolerance times

T. Stead[1†], A. P. Blaber[1,2†], D. N. Divsalar[1], D. Xu[1], K. Tavakolian[1,2], J. Evans[3], R. Billette de Villemeur[4], M-P Bareille[4], A. Saloň[5], B. Steuber[5] and N. Goswami[5,6,7*]

[1]Department of Biomedical Physiology and Kinesiology, Simon Fraser University, Burnaby, BC, Canada, [2]Biomedical Engineering Program, University of North Dakota, Grand Forks, ND, United States, [3]Biomedical Engineering, Retired, University of Kentucky, Lexington, KY, United States, [4]Institut de Médecine et de Physiologie Spatiales, Toulouse, France, [5]Gravitational Physiology and Aging Research Unit, Division of Physiology and Pathophysiology, Otto Löwi Research Center of Vascular Biology, Immunity and Inflammation, Medical University of Graz, Graz, Austria, [6]Center for Space and Aviation Health, Mohammed Bin Rashid University of Medicine and Health Sciences, Dubai, United Arab Emirates, [7]Health Sciences Division, Innlandet University College, Innlandet, Norway

Introduction: Exposure to microgravity results in physiological deconditioning, including orthostatic intolerance. Artificial gravity (AG) from short-arm centrifuges is being tested in ground-based studies to counter these effects. Orthostatic tolerance testing with centrifuges before and after these spaceflight analogs could determine the efficacy of an AG countermeasure to orthostatic tolerance. However, there has not been an investigation on how long before analog testing AG orthostatic tolerance data would remain valid for such a study.

Methods: A secondary analysis of two experiments involving AG orthostatic tolerance testing (starting at 0.6 for females and 0.8 Gz for males and increased by 0.1 Gz every 3 minutes until presyncope) conducted 7 months apart at MEDES revealed 4 male and 3 female participants who had taken part in both.

Results: Comparisons of participants' time to presyncope between the two tests using Lin's concordance correlation coefficient (LCCC) showed a significant relationship in time to presyncope between the two test dates (LCCC = 0.98) for males but not for females (LCCC = −0.64). While the cardiovascular data from one female was unusable, the mean heart rate responses to increasing artificial gravity during the orthostatic tolerance procedure showed a strong linear correlation between the two tests for all other participants (all $p < 0.008$). The LCCC heart rate changes with centrifuge level varied across male participants from 0.61 to 0.97, suggesting that the high LCCC for time to presyncope was achieved with varied HR baselines between the two test dates.

Discussion: These findings indicate that time-to-presyncope tests may remain valid up to 7 months after the testing date for males. We highly recommend further study with larger numbers of male and female participants.

KEYWORDS

short-arm human centrifuge, presyncope, cardiovascular, heart rate, blood pressure

Introduction

Long-term spaceflight, such as that seen with crewed missions on the International Space Station (ISS), introduces the challenge of physiological deconditioning within the

human body which has been shaped by life on Earth. This deconditioning takes place across multiple body systems and includes the loss of muscle and bone mass, increased risk of thrombo-embolism, and the development of orthostatic intolerance (Blaber et al., 2011; Goswami et al., 2012; Goswami et al., 2013; Goswami, 2017; Goswami et al., 2019c; Harris K. et al., 2022; Harris K. M. et al., 2022; Rittweger et al., 2015). Orthostatic tolerance refers to the ability to maintain cerebral perfusion while standing, thereby maintaining oxygen delivery via blood flow to the brain. These adaptations that occur in the microgravity environment present as disadvantages and have disabling effects upon the subsequent return to Earth's gravity. Since the establishment of a permanent presence in space with the ISS, scientists have spent much time in developing and perfecting countermeasures such as pharmaceuticals, nutrition, exercise prescription, lower body negative pressure (LBNP) (Goswami et al., 2019a; Goswami et al., 2019b; Goswami, 2023), and artificial gravity (AG) (Evans et al., 2018; Laing et al., 2020; Tanaka et al., 2017; Winter et al., 2018).

When conducting AG studies using a short-arm human centrifuge (SAHC), typically the research team conducts a time-to-presyncope test to determine the gravitational-load tolerance limit of the individual (Evans et al., 2015; Goswami et al., 2015). This test is primarily conducted to find the upper limit of gravitational forces the person will experience before losing consciousness. The prescription of AG used afterward is usually based on this time-to-presyncope test. As such, the presyncope test is conducted first, normally a few weeks before the targeted study intervention is to be carried out. For this reason, it is important to understand how long the time-to-presyncope test remains valid for screening participants. The repeatability of presyncope tests has been explored in other spaceflight countermeasures, such as LBNP (Goswami et al., 2009), which did not show a difference in heart rate, mean arterial pressure, total peripheral resistance, cerebral artery blood flow velocities, and cerebral oxygen saturation between exposures separated by 4 weeks (Kay and Rickards, 2015). Therefore, the purpose of this study was to investigate the repeatability of SAHC time-to-presyncope test protocols based on heart rate responses for healthy males and females spaced 7 months between exposure to the same presyncope protocol.

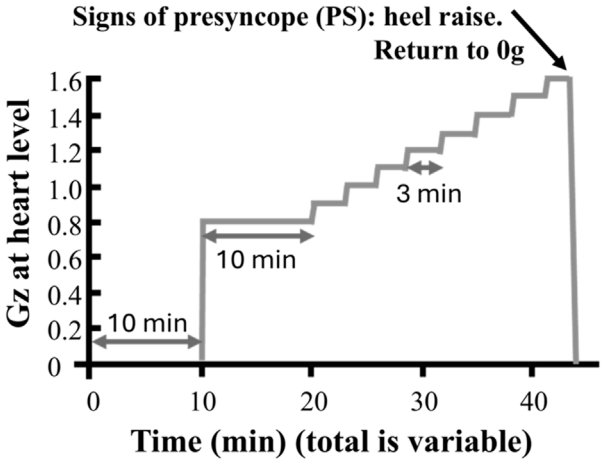

FIGURE 1
Example of a time to presyncope protocol. Participants were instrumented for heart rate and blood pressure monitoring while supine in the nacelle of the short-arm centrifuge. Following a 10-min rest period while systems were checked, centrifugation started with a 10-min baseline at 0.8 g (0.6 g for female participants) at the level of the heart after which a ramped of 3-min 0.1 g increments was applied until onset of presyncope (based on Goswami et al., 2015). At the onset of presyncope, participants were told to do a heel raise to activate venous return via the skeletal muscle pump, while the centrifuge was slowed to 0 g through a controlled stop.

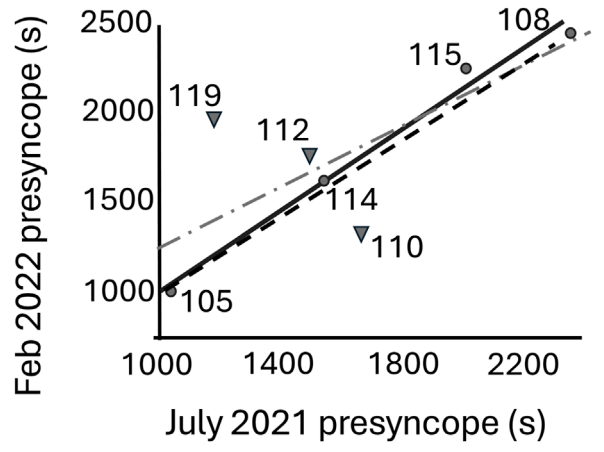

FIGURE 2
Linear regression fit line of time-to-presyncope test (s) for July 2021 and February 2022 for only the four male participants (circles, solid line) and with all the participants (addition of three females (triangles, dash-dot line). The line of concordance is shown as a dashed line.

Methods

Participants

Secondary analysis of data from volunteers who took part in two independent centrifuge research projects with the same presyncope protocol were used. In both projects, the presyncope test was used to determine participants' orthostatic tolerance before implementation of any test procedures. A review of participants from the two studies found four males and three females who took part in both AG studies. They ranged in age from 27 to 34 (31 ± 2.9, mean ± SD) years with an average height of 170 ± 7.1 cm and an average weight of 70.2 ± 5.0 kg.

Selection criteria for both projects were the same. The recruited participants were healthy, un-trained, non-obese, non-smoking individuals free of chronic illness or acute infectious disease, ENT, orthopedic, cardiovascular, and neurological disorders, particularly orthostatic hypotension, and vestibular disorders. They were also free of alcohol or substance dependence and did not require medical treatment. Participants also underwent medical examination, including screening by a physician, urinalysis, and an exercise stress test. If all medical criteria were met, the participants underwent an orientation session with the SAHC, where they were centrifuged at 1.0G at the foot for 10 minutes. Those participants without vestibular or cardiovascular disturbances were then enrolled in the study.

TABLE 1 Individual regression results (Figure 4) from the comparison of average HR of February 2022 with July 2021 and Lin's concordance correlation coefficient (LCCC, Lin et al., 2002).

Sex	Participant	Intercept	HR slope	HR r^2 adj	HR p-value	LCCC
Male	105	−6.0	1.09	0.99	0.003	0.97
	108	6.5	1.11	0.99	0.0001	0.61
	114	13.7	1.03	0.93	0.0003	0.77
	115	−10.9	1.13	0.95	0.0001	0.95
Female	112	−0.8	1.03	0.99	0.0001	0.99
	119	20.4	0.77	0.91	0.008	0.87

Presyncope data were collected from two separate sessions using the same protocol in July 2021 and February 2022, using the SAHC at the MEDES Space Clinic in Toulouse, France.

Ethical approval for all research was obtained from the *Comité de Protection des Personnes/CPP Sud-Ouest Outre-Mer I* and the *Agence Française de Sécurité Sanitaire des Produits de Santé* for each aspect of the study and scientific protocols. Research associated with our analysis was approved by the Office of Research Ethics at Simon Fraser University. A written informed consent was signed by each participant.

Equipment for AG and data collection

The device used to collect heart rate (HR) during both protocols was a three-lead ECG (Philips Monitor IntelliVue) using the Lead II configuration of electrode placement. Blood pressure was recorded from a non-invasive photoplethysmograph (BMEYE, Amsterdam, Netherlands) placed on the index finger of the participant's right hand. The SAHC device used in both the July and February protocols was located at the MEDES Space Clinic in Toulouse, France (European Space Agency).

Protocol

The protocol for the time-to-presyncope test (Figure 1) in both studies had the participants lie supine in the centrifuge with baseline level 0 G for 10 minutes, followed by 10 minutes 0.6 G for the female participants and 0.8 G for the male participants at the level of the heart (detailed in Goswami et al., 2015; Evans et al., 2015). The acceleration of the SAHC was increased by 0.1 G every 3 minutes, continuing until the participants showed signs or symptoms of presyncope—defined using any of the following criteria: i) a drop in systolic blood pressure (SBP) below 80 mmHg or by a drop ≥20 mmHg/min, ii) a drop in diastolic blood pressure (DBP) ≥10 mmHg/min, iii) a drop in heart rate ≥15 bpm, iv) the occurrence of light-headedness, visual disturbances, nausea, clammy skin, or pallor skin, and/or v) at the request of the participant (Gao et al., 2008; Hinghofer-Szalkay et al., 2011)—or until the cardiac output dropped to half of the outset value. Real-time interpretation of the ECG for heart rate, and the blood pressure signal for systolic, diastolic, and mean arterial blood pressure along with Windkessel model (Wesseling et al., 1993) derived cardiac output were displayed solely for medical monitoring during the operation of the SAHC and not recorded. Participants did not change lifestyle habits between the two studies.

Data analysis and interpretation

The ECG and blood pressure waveforms were exported from their respective devices and recorded simultaneously at 1,000 Hz using a National Instruments USB-6218 16-bit data capture equipment and LabVIEW 2013 software (National Instruments Inc, TX, United States). Beat-by-beat analysis of these data was performed off-line. Unusable data (raw data from beats in which the mean could not be reliably calculated, either due to noise or lack of signal) were removed and the time series adjusted by interpolating new values from the two valid points surrounding the excluded segment.

Statistical analysis of cardiovascular responses was performed using JMP® Version 16 (SAS Institute Inc., Cary, NC, United States). Baseline cardiovascular measurements were compared between the two test dates using paired Wilcoxon on ranks method.

The Lin's concordance correlation coefficient (Lin et al., 2002) analysis was performed in Microsoft Excel to determine the repeatability of time to presyncope using the eight participants as well as for each sex. This procedure was also used to determine the repeatability of heart rate responses to changes in centrifuge g levels between the two dates. The mean HR at each g-level stage of the centrifuge protocol in both time-to-presyncope tests was determined from the ECG using MATLAB (MathWorks Inc., United States).

Secondary comparisons of time to presyncope and individual heart rate changes with g level were conducted using a linear regression function (JMP® Version 16).

Results

The ECG and blood pressure signals from participant 110 were not usable. As a group, excluding participant 110, there

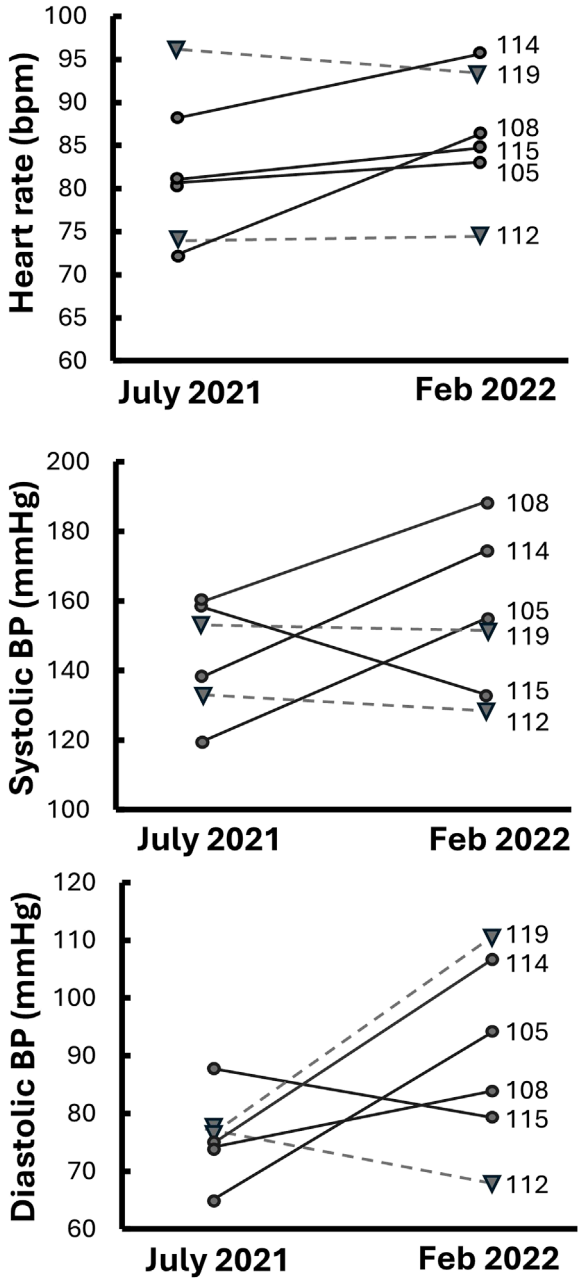

FIGURE 3
Individual cardiovascular changes for participants between July 2021 and February 2022. Solid lines and circles are male participants and dashed lines with triangles are female participants.

were no significant and consistent differences in cardiovascular measurements between the two test dates (July 2021 vs. February 2022) in baseline HR (82 ± 4 vs. 86 ± 3 bpm, p = 0.38), SBP (143 ± 7 vs. 156 ± 9 mmHg, p = 0.58), or DBP (76 ± 3 vs. 90 ± 7 mmHg, p = 0.093), although there were varied individual responses with some showing large changes either increasing or decreasing from July 2021 (Figure 3).

A comparison of the time to presyncope from July 2021 and February 2022 gave an LCCC of 0.73 using the eight participants. This value increased when only male participants were included (LCCC = 0.98) and reduced with only female participants (LCCC = −0.64). The line of concordance is shown in Figure 2.

A comparison of the time to presyncope between the two study dates had a linear relationship for the group of men and women (n = 8) (Figure 2, dashed line) (Equation 1).

$$\mathrm{Feb}_{2022} = (394 \pm 518) + (0.84 \pm 0.31) \cdot \mathrm{July}_{2021};\ (r^2 = 0.51, p = 0.043) \quad (1)$$

However, the female participants (n = 3) did not show any significant relationship (r^2 = 0.78, p = 0.22), whereas the male participants exhibited a strong linear relationship (Figure 2, solid line) between the two dates (Equation 2).

$$\mathrm{Feb}_{2022} = (-114 \pm 179) + (1.11 \pm 0.11) \cdot \mathrm{July}_{2021};\ (r^2 = 0.98, p = 0.008) \quad (2)$$

The concordance (LCCC) between the average HR at each level of centrifugation until presyncope was compared between the two test dates for each participant (Table 1) with individual lines of concordance lines provided in Figure 4. Three of the six participants had LCCC values greater than 0.95.

The linear relationship between the average HR at each level of centrifugation until presyncope was compared between the two test dates (Figure 4) using regression analysis. The HR over the two separate tests were found to be highly correlated with the minimum r^2 of 0.91 (Table 1). All slopes were significantly greater than 0 (all p < 0.008). The average slope of the regressions was not significantly different from 1 and the average intercept not different from 0.

Five of the eight selected participants had their tests runs at the same time of day (morning or afternoon) on the two test dates. However, three participants (115, 112, and 119) did not. Initially, participants 115 and 119 underwent their tests in the afternoon, while participant 112 had their first test in the morning.

Discussion

We examined the repeatability of the time-to-presyncope testing for SAHC which had not previously been studied. Our analysis revealed that the time-to-presyncope between the two test dates had a high degree of concordance (LCCC>0.95) and were highly linearly correlated in the males. Female participants' times to presyncope, however, had a low LCCC (>0.7) and were not significantly linearly correlated between the two test dates. HR changes with Gz regressions were highly correlated in both males and females, with the slopes not different from one and intercepts not different from zero. However, the LCCC values ranged dramatically between male participants with two showing low concordance (<0.8), but not the females (LCCC>0.85). This may indicate that differences in cardiovascular baseline did not affect male presyncope time outcomes.

Overall, the SAHC presyncope test with males was repeatable after 7 months. While this observation may not be conclusive in the light of the limited number of male (n = 4) and female participants (n = 3), several factors could contribute, including sex and seasonal differences.

Previous literature has shown significant differences in the regulation of blood pressure and autonomic responses to orthostatic

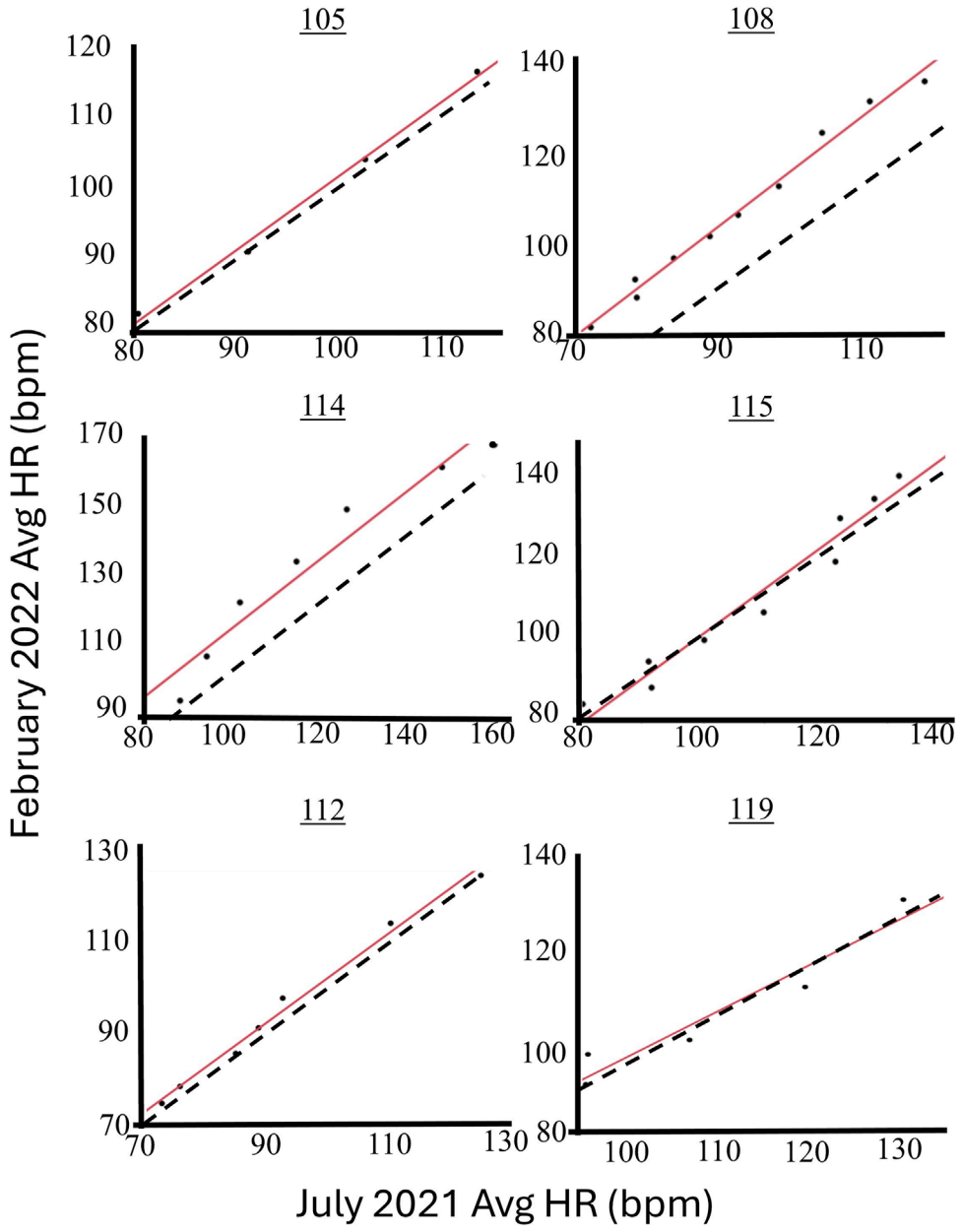

FIGURE 4
Linear regression fit lines (solid) for the HR responses of four male and two female participants where each data point represents the average HR for each increment of AG during the presyncope test for comparison of the July 2021 and February 2022 tests. The line of concordance is shown as a dashed line.

stress between the sexes, especially during hypovolemia, a major result of true space flight as well as models of spaceflight, like bedrest, immersion and hypovolemia (Evans et al., 2018; Goswami et al., 2019b; Patel et al., 2016; Shankhwar et al., 2023). In particular, participant 119 exhibited a much higher baseline DBP in February 2022 compared to July 2021 (110.57 vs. 74.73 mmHg)—and participant 105 displayed a similar pattern (Figure 3)—which suggests enhanced vasoconstriction in February 2022. This participant's HR also increased slower in February 2022 than in July 2021 in response to increments of AG (Table 1; Figure 4), which could be attributed to greater vasoconstriction. As a result, participant 119 may have achieved longer presyncopal time in February 2022 compared to July 2021 (1927 vs. 1,201 s). While women typically respond to orthostatic stress with elevated HR (Arzeno et al., 2013; Mark et al., 2014), changes in the involvement of vasoconstriction of participant 119 across two test sessions could be a seasonal factor with reduced vascular function in the winter (Gordon et al., 2024). Menstrual phase has also been shown to affect hemodynamic responses (Shankhwar et al., 2024). Three of the participants were tested at a different time of the day, including 119, but the other two, one male and the other female, had no discernable difference in presyncope time. However, since the sample size is

small, future studies on the reliability of presyncope testing should maintain consistent timing of tests and include factors like sex and environment.

Like LBNP and tilt testing (Ector et al., 1998; Güell et al., 1990; Benditt et al., 1996), human centrifugation can be used to determine and improve an individual's orthostatic tolerance, (Goswami et al., 2015; Evans et al., 2015; Evans et al., 2004; Stenger et al., 2007). For comparison's sake, LBNP tolerance has been shown to be repeatable up to 1 year for stepwise tests, and anywhere from one to 4 months for continuous ramp tests (Convertino, 2001; Kay and Rickards, 2015). Further, 90% reproducibility in tilt table testing has been shown for up to a week between tilt tests in a study using adult men and women (Grubb et al., 1992). Our results indicate that stepped centrifuge time-to-presyncope test can also be a valid screening tool for AG investigations that occur within 7 months from the test date.

Repeated human centrifugation has been shown to be an effective tool for increasing orthostatic tolerance in both men and women (Goswami et al., 2015; Evans et al., 2015; Evans et al., 2004; Stenger et al., 2007) but more effective in men than women (Stenger et al., 2007; Evans et al., 2015). This difference has only barely been studied and may provide information concerning basic sex differences in response to gravity. The repeatability of g tolerance in individuals implies a genetic influence on this variable, while the increase in g tolerance with repeated AG exposure indicates that the genetic influence can be modified. Establishing criteria to define a clear g tolerance limit will therefore be necessary to: 1) Distinguish individual tolerance levels to classify subjects' performance, 2) determine effects of repeated AG exposures, 3) determine effects of other countermeasures (exercise, for example), 4) determine effects of deconditioning (space flight, bed rest, immersion, hypovolemia), and 5) determine gender, aging and inactivity effects.

Limitations

Limitations of this study mainly lay in the small sample size of 4 male and 3 female participants that qualified for this investigation. However, we believe that this exploratory pilot study lays the foundation for carrying out bigger epidemiological studies in larger populations. These novel data also advance the literature related to AG-induced presyncopal times.

Conclusions and future directions

As AG-induced presyncopal times were highly repeatable over 7 months in five of the seven participants tested, our results suggest that presyncope tests completed using SAHC-induced AG can be used to compare orthostatic tolerance pre- and post-exposure to interventions looking to improve orthostatic intolerance. However, with the small sample size and possible effects of sex and environmental factors, caution is required.

Tolerance for gravity diminishes during exposure to weightlessness, whether that be exposure to bedrest, water immersion or to spaceflight and a clear test for this tolerance needs to be developed. The criteria for this test will be how long its effects will last and how often it can be administered without significantly influencing the results. The present study indicates that AG tolerance time is a promising candidate for such a test in men that can be spaced as much as 7 months apart. Results from women, however, indicate that this test does not appear to be valid for women and that women's response to AG exposure may be different from men's. An effect that needs to be explored in future studies.

Finally, results of this study advance the literature related to orthostatic intolerance. Our results show the feasibility of stepped SAHC presyncope testing to determine an individual's orthostatic tolerance limit. Upon further validation, this test will provide a gravity-based tool to assess orthostatic intolerance, itself a measure of a prospective astronaut's fitness for spaceflight. Additionally, the presyncope test plays a crucial role in individualized centrifugation training which can be used as a countermeasure against orthostatic intolerance. In this training, the AG limit is determined from the maximum AG level at presyncope (Goswami et al., 2015). With orthostatic intolerance being a growing problem in geriatrics (Goswami, 2017; Goswami et al., 2017; Sachse et al., 2019; Trozic et al., 2019), an individualized training protocol could be an effective diagnostic tool considering the large, individual differences in the cardiovascular tolerance limits of seniors, but those studies are yet to be done.

Data availability statement

Data will be shared upon request if it conforms to the original conditions of ethical approval. Requests to access the datasets should be directed to Andrew Blaber, andrew_blaber@sfu.ca.

Ethics statement

The studies involving humans were approved by Comité de Protection des Personnes/CPP Sud-Ouest Outre-Mer I, Agence Française de Sécurité Sanitaire des Produits de Santé, and the Office of Research Ethics at Simon Fraser University. The studies were conducted in accordance with the local legislation and institutional requirements. The participants provided their written informed consent to participate in this study.

Author contributions

TS: Data curation, Formal Analysis, Investigation, Validation, Writing – original draft, Writing – review and editing. AB: Conceptualization, Data curation, Formal Analysis, Funding acquisition, Investigation, Methodology, Project administration, Resources, Software, Supervision, Validation, Visualization, Writing – review and editing. DD: Investigation, Writing – review and editing. DX: Data curation, Investigation, Methodology, Project administration, Software, Supervision, Validation, Writing – review and editing. KT: Investigation, Supervision, Writing – review and editing. JE: Conceptualization, Writing – review and editing. RB: Data curation, Investigation, Project administration, Resources, Supervision,

Writing – review and editing. M-PB: Data curation, Investigation, Project administration, Resources, Supervision, Writing – review and editing. AS: Investigation, Writing – review and editing. BS: Investigation, Writing – review and editing. NG: Conceptualization, Data curation, Formal Analysis, Funding acquisition, Investigation, Methodology, Project administration, Resources, Supervision, Validation, Visualization, Writing – review and editing.

Funding

The author(s) declare that financial support was received for the research and/or publication of this article. Nandu Goswami was the PI of an ESA approved GBF-CORA project. The study was supported by European Space Agency and MEDES, Toulouse. Andrew Blaber received support from the Canadian Space Agency. The funders had no role in study planning, results, data analysis, or interpretation.

Conflict of interest

The authors declare that the research was conducted in the absence of any commercial or financial relationships that could be construed as a potential conflict of interest.

The author(s) declared that they were an editorial board member of Frontiers, at the time of submission. This had no impact on the peer review process and the final decision.

Publisher's note

References

Arzeno, N. M., Stenger, M. B., Lee, S. M. C., Ploutz-Snyder, R., and Platts, S. H. (2013). Sex differences in blood pressure control during 6° head-down tilt bed rest. *Am. J. Physiol. Heart Circ. Physiol.* 304, H1114–H1123. doi:10.1152/ajpheart.00391.2012

Benditt, D. G., Ferguson, D. W., Grubb, B. P., Kapoor, W. N., Kugler, J., Lerman, B. B., et al. (1996). Tilt table testing for assessing syncope. American College of Cardiology. *J. Am. Coll. Cardiol.* 28 (1), 263–275. doi:10.1016/0735-1097(96)00236-7

Blaber, A. P., Goswami, N., Bondar, R. L., and Kassam, M. S. (2011). Impairment of cerebral blood flow regulation in astronauts with orthostatic intolerance after flight. *Stroke* 42, 1844–1850. doi:10.1161/STROKEAHA.110.610576

Convertino, V. A. (2001). Lower body negative pressure as a tool for research in aerospace physiology and military medicine. *J. Gravitational Physiology* 8 (2), 1–14. doi:10.3390/bioengineering10101226

Ector, H., Reybrouck, T., Heidbüchel, H., Gewillig, M., and Van De Werf, F. (1998). Tilt training: a new treatment for recurrent neurocardiogenic syncope and severe orthostatic intolerance. *Pacing Clin. Electrophysiol.* 21 (1), 193–196. doi:10.1111/j.1540-8159.1998.tb01087.x

Evans, J. M., Knapp, C. F., and Goswami, N. (2018). Artificial gravity as a countermeasure to the cardiovascular deconditioning of spaceflight: gender perspectives. *Front. Physiol.* 9, 716. doi:10.3389/fphys.2018.00716

Evans, J. M., Ribeiro, L. C., Moore, F. B., Wang, S., Zhang, Q., Kostas, V., et al. (2015). Hypovolemic men and women regulate blood pressure differently following exposure to artificial gravity. *Eur. J. Appl. Physiol.* 115 (12), 2631–2640. doi:10.1007/s00421-015-3261-2

Evans, J. M., Stenger, M. B., Moore, F. B., Hinghofer-Szalkay, H., Rössler, A., Patwardhan, A. R., et al. (2004). Centrifuge training increases presyncopal orthostatic tolerance in ambulatory men. *Aviat. Space, Environ. Med.* 75 (10), 850–858.

Gao, Y., Goswami, N., Grasser, E., Rössler, A., Stöger, E., Schwaberger, G., et al. (2008). Radix astragali and orthostatic response: a double-masked crossover study. *Aviat. Space Environ. Med.* 79, 94–98. doi:10.3357/asem.2193.2008

Gordon, A., Ross, M., Weston, K., Neubeck, L., and Muggeridge, D. J. (2024). Seasonal variation in vascular function: a systematic review and recommendations for future research. *Int. J. Environ. Health Res.*, 1–17. doi:10.1080/09603123.2024.2432562

Goswami, N. (2017). Falls and fall-prevention in older persons: geriatrics meets spaceflight. *Front. Physiol.* 8, 603. doi:10.3389/fphys.2017.00603

Goswami, N. (2023). Compensatory hemodynamic changes in response to central hypovolemia in humans: lower body negative pressure: updates and perspectives. *J. Muscle Res. Cell Motil.* 44, 89–94. doi:10.1007/s10974-022-09635-z

Goswami, N., Batzel, J. J., Clément, G., Stein, T. P., Hargens, A. R., Sharp, M. K., et al. (2013). Maximizing information from space data resources: a case for expanding integration across research disciplines. *Eur. J. Appl. Physiol.* 113, 1645–1654. doi:10.1007/s00421-012-2507-5

Goswami, N., Blaber, A. P., Hinghofer-Szalkay, H., and Convertino, V. A. (2019a). Lower body negative pressure: physiological effects, applications, and implementation. *Physiol. Rev.* 99, 807–851. doi:10.1152/physrev.00006.2018

Goswami, N., Blaber, A. P., Hinghofer-Szalkay, H., and Montani, J. P. (2017). Orthostatic intolerance in older persons: etiology and countermeasures. *Front. Physiol.* 8, 803. doi:10.3389/fphys.2017.00803

Goswami, N., Evans, J., Schneider, S., Wiesche, M. von der, Mulder, E., Rössler, A., et al. (2015). Effects of individualized centrifugation training on orthostatic tolerance in men and women. *PLOS ONE* 10 (5), e0125780. doi:10.1371/journal.pone.0125780

Goswami, N., Lackner, H., Grasser, E., and Hinghofer-Szalkay, H. (2009). Individual stability of orthostatic tolerance response. *Acta Physiol. Hung* 96, 157–166. doi:10.1556/APhysiol.96.2009.2.2

Goswami, N., Reichmuth, J., Di Mise, A., Brix, B., Roessler, A., Centrone, M., et al. (2019b). Comparison between men and women of volume regulating hormones and aquaporin-2 excretion following graded central hypovolemia. *Eur. J. Appl. Physiol.* 119, 633–643. doi:10.1007/s00421-018-4053-2

Goswami, N., Roma, P. G., De Boever, P., Clement, G., Hargens, A. R., Loeppky, J. A., et al. (2012). Using the Moon as a high-fidelity analogue environment to study biological and behavioral effects of long-duration space exploration. *Planet. Space Sci.* 74, 111–120. doi:10.1016/j.pss.2012.07.030

Goswami, N., van Loon, J., Roessler, A., Blaber, A. P., and White, O. (2019c). Editorial: gravitational physiology, aging and medicine. *Front. Physiol.* 10, 1338. doi:10.3389/fphys.2019.01338

Grubb, B. P., Wolfe, D., Temesy-Armos, P., Hahn, H., and Elliott, L. (1992). Reproducibility of head upright tilt table test results in patients with syncope. *Pacing Clin. Electrophysiol. PACE* 15 (10 Pt 1), 1477–1481. doi:10.1111/j.1540-8159.1992.tb02921.x

Güell, A., Braak, L., le Traon, A. P., and Gharib, C. (1990). Cardiovascular deconditioning during weightlessness simulation and the use of Lower Body Negative Pressure as a countermeasure to orthostatic intolerance. *Acta Astronaut.* 21 (9), 667–672. doi:10.1016/0094-5765(90)90078-Y

Harris, K., Laws, J. M., Elias, A., Green, D. A., Goswami, N., Jordan, J., et al. (2022a). Search for venous endothelial biomarkers heralding venous thromboembolism in space: a qualitative systematic review of terrestrial studies. *Front. Physiol.* 13, 885183. doi:10.3389/fphys.2022.885183

Harris, K. M., Weber, T., Greaves, D., Green, D. A., Goswami, N., and Petersen, L. G. (2022b). Going against the flow: are venous thromboembolism and impaired cerebral drainage critical risks for spaceflight? *J. Appl. Physiol.* 132, 270–273. doi:10.1152/japplphysiol.00425.2021

Hinghofer-Szalkay, H., Lackner, H. K., Rössler, A., Narath, B., Jantscher, A., and Goswami, N. (2011). Hormonal and plasma volume changes after presyncope. *Eur. J. Clin. Invest* 41, 1180–1185. doi:10.1111/j.1365-2362.2011.02523.x

Kay, V. L., and Rickards, C. A. (2015). Reproducibility of a continuous ramp lower body negative pressure protocol for simulating hemorrhage. *Physiol. Rep.* 3 (11), e12640. doi:10.14814/phy2.12640

Laing, C., Green, D. A., Mulder, E., Hinghofer-Szalkay, H., Blaber, A. P., Rittweger, J., et al. (2020). Effect of novel short-arm human centrifugation-induced gravitational gradients upon cardiovascular responses, cerebral perfusion and g-tolerance. *J. Physiol.* 598, 4237–4249. doi:10.1113/JP273615

Lin, L., Hedayat, A. S., Sinha, B., and Yang, M. (2002). Statistical methods in assessing agreement: models, issues, and tools. *J. Am. Stat. Assoc.* 97 (457), 257–270. doi:10.1198/016214502753479392

Mark, S., Scott, G. B. I., Donoviel, D. B., Leveton, L. B., Mahoney, E., Charles, J. B., et al. (2014). The impact of sex and gender on adaptation to space: executive summary. *J. Womens Health (Larchmt)* 23, 941–947. doi:10.1089/JWH.2014.4914

Patel, K., Rössler, A., Lackner, H. K., Trozic, I., Laing, C., Lorr, D., et al. (2016). Effect of postural changes on cardiovascular parameters across gender. *Med. Baltim.* 95, e4149. doi:10.1097/MD.0000000000004149

Rittweger, J., Bareille, M.-P., Clément, G., Linnarsson, D., Paloski, W. H., Wuyts, F., et al. (2015). Short-arm centrifugation as a partially effective musculoskeletal countermeasure during 5-day head-down tilt bed rest—results from the BRAG1 study. *Eur. J. Appl. Physiology* 115 (6), 1233–1244. doi:10.1007/s00421-015-3120-1

Sachse, C., Trozic, I., Brix, B., Roessler, A., and Goswami, N. (2019). Sex differences in cardiovascular responses to orthostatic challenge in healthy older persons: a pilot study. *Physiol. Int.* 106 (3), 236–249. doi:10.1556/2060.106.2019.16

Shankhwar, V., Urvec, J., Steuber, B., Schmid Zalaudek, K., Bergauer, A., Alsuwaidi, H., et al. (2023). Association of gender with cardiovascular and autonomic responses to central hypovolemia. *Front. Cardiovasc Med.* 10, 1211774. doi:10.3389/fcvm.2023.1211774

Shankhwar, V., Urvec, J., Steuber, B., Schmid Zalaudek, K., Salon, A., Hawliczek, A., et al. (2024). Effects of menstrual cycle on hemodynamic and autonomic responses to central hypovolemia. *Front. Cardiovasc Med.* 11, 1290703. doi:10.3389/fcvm.2024.1290703

Stenger, M. B., Evans, J. M., Patwardhan, A. R., Moore, F. B., Hinghofer-Szalkay, H., Rossler, A., et al. (2007). Artificial gravity training improves orthostatic tolerance in ambulatory men and women. *Acta Astronaut.* 60, 267–272. doi:10.1016/j.actaastro.2006.08.008

Tanaka, K., Nishimura, N., and Kawai, Y. (2017). Adaptation to microgravity, deconditioning, and countermeasures. *J. Physiological Sci.* 67 (2), 271–281. Article 2. doi:10.1007/s12576-016-0514-8

Trozic, I., Platzer, D., Fazekas, F., Bondarenko, A. I., Brix, B., Rossler, A., et al. (2019). Postural hemodynamic parameters in older persons have a seasonal dependency: a pilot study. *Z Gerontol. Geriatr.* 53 (2), 145–155. doi:10.1007/s00391-019-01525-3

Wesseling, kH., Jansen, J. R. C., Settels, J. J., and Schrueder, J. J. (1993). Computation of aortic flow from pressure in humans using a nonlinear, three-element model. *J. Appl. Physiol.* 74 (5), 2566–2573. doi:10.1152/jappl.1993.74.5.2566

Winter, J., Laing, C., Johannes, B., Mulder, E., Brix, B., Roessler, A., et al. (2018). Galanin and adrenomedullin plasma responses during artificial gravity on a human short-arm centrifuge. *Front. Physiol.* 9, 1956. doi:10.3389/fphys.2018.01956

Frontiers in Physiology

Understanding how an organism's components work together to maintain a healthy state

The second most-cited physiology journal, promoting a multidisciplinary approach to the physiology of living systems - from the subcellular and molecular domains to the intact organism and its interaction with the environment.

Discover the latest Research Topics

See more →

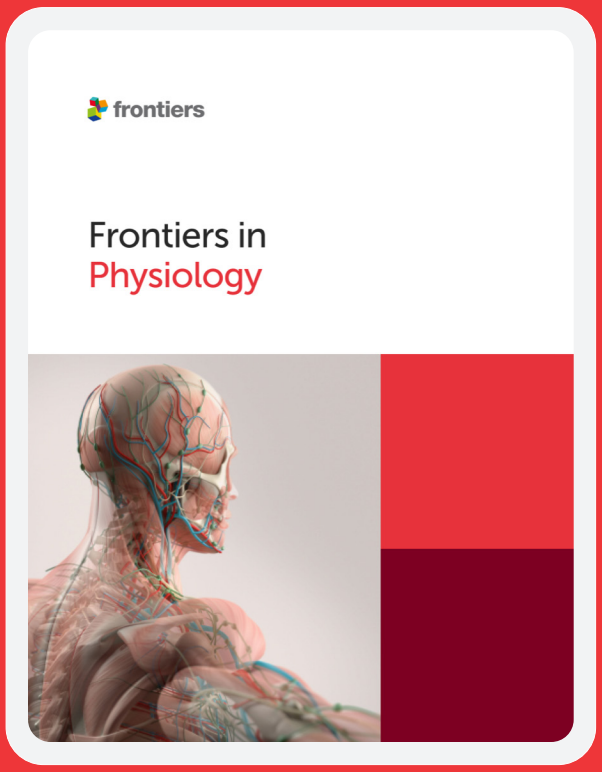

Frontiers

Avenue du Tribunal-Fédéral 34
1005 Lausanne, Switzerland
frontiersin.org

Contact us

+41 (0)21 510 17 00
frontiersin.org/about/contact